CUMULATIVE FATIGUE DAMAGE

OF

PLAIN CONCRETE IN COMPRESSION

A Thesis presented for the

Degree of Doctor of Philosophy

by

Pibul Jinawath, B.Eng., M.Sc., A.M.I.E.(Thailand)

89 ROSSUKON LANE,
LARD PRAO ROAD,
BANGGAPI, BANGKOK 10,
THAILAND. Tel. 775894

The Department of Civil Engineering

The University of Leeds

December, 1974

ORIGINAL COPY IS TIGHTLY BOUND AND TEXT IS CLOSE TO THE EDGE OF THE PAGE

ABSTRACT

The thesis reports an investigation carried out on more than two hundred and fifty prismatic specimens to study the cumulative fatigue damage of plain concrete subjected to constant and variable amplitude cyclic compressive stresses.

Pulse velocity measurements and strain charecteristics were used to indicate the extent of progressive fatigue damage. At a given percentage of the life the amount of damage of a specimen is dependent on the stress level.

Prismatic specimens were also subjected to repeated compressive stresses according to various load programmes in which the maximum load was varied between two limits the minimum load being kept constant throughout. The results were interpreted according to the pulse velocity measurements, the physical appearance of fractered specimens together with the phenomenon of progressive fracture itself.

Palmgren-Miner hypothesis was found to give conservative or unsafe predictions of the fatigue life depending on the load programme. Factors affecting the accuracy of the hypothesis are discussed and an empirical design chart is presented.

ACKNOWLEDGEMENTS

The writer wishes to record his gratitude to Dr. E.W. Bennett, M.Sc., Ph.D., M.I.C.E., F.I.Struct.E., Reader in Civil Engineering, under whose supervision the work was carried out, for his valuable advice, continuous guidance, constructive criticisms and his kindness.

The writer is grateful to Professor A.M.Neville, M.C.,T.D., D.Sc.(Eng.), Ph.D., M.Sc., C.Eng., F.I.C.E., F.I.Struct.E., F.Am.Soc.C.E., Head of the Department of Civil Engineering,Leeds University, for providing him the facilities needed in this investigation.

Thanks are due to Messrs J.S.Higgins, and the technical staff of the Civil Engineering Department for their help and co-operation during the experimental work.

The writer is greatly indepted to his parents for their love and encouragement. He is also indepted to his wife for her part in sharing the difficulties and her understanding during their university lives. Thanks are due to his two friends Messrs S. Sirirangkamanont and S. Siwasaranond for their assistance in the preparation of the thesis.

The writer also wishes to acknowledge gratefully the British Council for the financial support provided throughout the period of this work under the Colombo Plan Scholarship.

ABBREVIATIONS

A.C.I.	American Concrete Institute.
A.S.C.E.	American Society of Civil Engineers.
A.S.M.E.	American Society of Mechanical Engineers.
A.S.T.M.	American Society for Testing Materials.
A.R.C.	Aeronautical Research Council.
B.R.S.	Building Research Station.
B.S.	British Standard.
C & C.A.	Cement and Concrete Association.
C.E.B.	European Concrete Committee.
F.I.P.	International Prestressing Federation.
H.R.B.	Highway Research Board.
I.C.E.	Institution of Civil Engineers.
M.C.R.	Magazine of Concrete Research.
P.C.A.	Portland Cement Association.
RILEM	The International Union of Testing and Research Laboratories for Materials and Structures.
R.R.L.	Road Research Laboratory.
T.R.R.L.	Transport and Road Research Laboratory

NOMENCLATURE AND SYMBOLS

As far as possible the notations used in this thesis are in conformity with the recommendations of B.S.3518:1962 and the International Organization for Standardization and the following definitions apply for the terms used:

Stress cycle =A stress cycle is the smallest section of the stress time function which is repeated periodically and identically.

Stress level,(S) =Percentage of ultimate static prism strength.

Maximum stress level,(S_{max}) =Highest algebraic value of stress level in the stress cycle.

Minimum stress level,(S_{min}) =Lowest algebraic value of stress level in the stress cycle

Range of stress level,(S_r) =Algebraic difference between the maximum and minimum stress levels in one cycle.

n =Number of loading cycles

N =Fatigue life or number of cycles at failure for a given test condition.

Cycle ratio, (n/N) =The ratio of the number of applied loading cycles to the number of cycles causing failure at the same constant amplitude stress level.

Fatigue limit =The limiting value of the stress level below which a material can presumably endure an infinite number of stress cycles.

Fatigue strength or Endurance,S_N =The greatest stress level which can be sustained for a given number of stress cycles without failure.

S -N diagram =A semilog plot of stress level against number of cycles at failure.

S-N-P diagram =A semilog plot of stress level against number of cycles at failure for different probabilities of failure,P.

a, b, c, d =Constants for empirical relationships, their specific use are explained as they occur.

CONTENTS

CHAPTER ONE

INTRODUCTION

1.1 General

Most structures are subjected to fluctuating and repetitive loads, such as those caused by the wind, occupants, mobile equipment, or moving vehicles (live loads). When a structural member is subjected to a sufficiently large number of loading cycles, failure may occur even though the stress due to loading is lower than the ultimate static strength (determined by a single loading) of a similar member. This phenomenon, termed fatigue failure, is found to exist in concrete as in most structural materials and has been under investigation by various research organizations since the beginning of the present century. There are, nevertheless, many aspects of the behaviour of concrete under repetitive loading that need further investigation, among them the problem of cumulative fatigue damage.

1.2 Cumulative fatigue damage

As the stress induced by repeated loading fluctuates in the material of a structure, physical changes occur. If the variation of stress is sufficiently great, permanent damage may result although this damage is not normally discernible. The progressive increase of this damage under repeated cycles of stress is termed fatigue damage and eventually leads to visible deterioration and fatigue failure.

There are three main problems in designing any structure subjected to complex live loads so that the accumulation of fatigue damage does not threaten safety:-

(1) Predicting and describing the fatigue producing stress variations that the structure will experience.

(2) Evaluation of cumulative damage.

(3) Accounting for the wide scatter in fatigue life that is observed for seemingly identical test specimens and structures.

The evaluation of cumulative damage is a problem because the stress cycles in actual structures vary so greatly in magnitude, number and order that it is practically impossible to perform enough experiments to cover all variations. Therefore, the total fatigue damage has to be evaluated by summation of the effects of individual cycles. If the progressive damage mechanism during each stress cycle was fully understood, this summation to determine the cumulative effect, would present no problem. The other alternative is to employ one of the proposed cumulative fatigue damage hypotheses (to be examined in chapter 8), however, none of them has been experimentally proved to be sufficiently reliable when applied to concrete.

An investigation of how a concrete element is progressively damaged under both uniform and repetitive loadings of varying amplitude, leading to fatigue failure, is therefore of considerable value. The practical application of the resulting knowledge would be advantageous not only in the safe and serviceable design of structures such as bridge girders, slabs, pavements, machine foundation, off-shore structures subject to heavy wave action, or prestressed railway sleepers, but also for the economical use of structural materials.

1.3 Levels of approach in studying concrete

There are three levels of approach in studying any deformable body of a composite material, i.e. the phenomenological or large scale level, the fundamental or structural level, and the molecular or atomic level.[1] For the study of fatigue in concrete, two levels of approach, the fundamental and the phenomenological have been suggested.[2]

The fundamental level is concerned with the behaviour and interaction of the contituent parts of concrete with the purpose of explaining the

observed characteristics such as strength or fatigue behaviour in terms of phase interaction. This type of research adds to the basic knowledge of the mechanism of behaviour of concrete, but does not necessarily find an immediate application to any specific problem.

The phenomenological level is concerned with the behaviour of concrete as a whole such as, for example, its stress level-fatigue life relationship. The results of this type of research may find direct application in practical problems, mostly in the form of empirical information. Indeed most fatigue tests of concrete to date have been carried out in order to give practical information to engineers. However, this kind of information alone cannot give satisfactory explanation of the mechanism of the behaviour of concrete. It is from the combination of information obtained from these two levels of study that a real understanding of the nature of fatigue in concrete begins to emerge, as has occurred in the study of metal fatigue.

1.4 Proposal for present investigation

Since the available information regarding cumulative fatigue damage in concrete in compression is very scarce the approach to this investigation will be at both levels though predominantly phenomenological. In this way it is hoped that, besides producing some empirical data of practical application, the knowledge gained from the more fundamental observations may help towards an improved understanding of the nature of fatigue in concrete.

1.5 Objective of investigation

The purpose and scope of the investigation is to examine the cumulative fatigue damage of high strength concrete under a cycling compressive load between a constant lower stress level and both constant and systematically varied upper stress levels. The work consists of three parts as follows:-

Part 1 : Review and description of tests.

Part 2 : Tests under loading of constant amplitude.

The objective of this part of the work are as follows:

1. To study the effect upon the gross behaviour of a particular concrete of various constant amplitude cyclic loadings with a view to correlating the parameters, namely maximum stress level; number of cycles to failure; and probability of failure.

2. To investigate the effects of the cyclic loadings on various properties, namely shape of stress-strain curve; elastic and inelastic strain; Modulus of elasticity, etc.

3. To study by ultrasonic pulse velocity technique, the mechanism of static and fatigue crack initation and propagation which can indicate the extent of damage and the relative rates of accumulation of fatigue damage and to examine the relationship between pulse velocity and number of cycles of stress in the relation to the total fatigue life.

Part 3 : Tests under loading of variable amplitude.

The objective of this part of the work are as follows:

1. To investigate possible alternative damage concepts of cumulative damage and cumulative fatigue damage theories with particular reference to the Palmgren-Miner cumulative damage hypothesis.

2. To investigate the limitations of the Palmgren-Miner hypothesis in order that engineers may have a better appreciation of the circumstances in which the hypothesis is unsafe, or safe, and to suggest and investigate possible modifications in order to improve the accuracy.

A practical cumulative fatigue concept is put forward and the validity of the concept is verified in the light of the conclusions drawn from the present investigation.

1.6 Limitations of the investigation

In order to investigate as many variations of repeated loading as possible the following variables were maintained constant throughout the programme of tests.

1. Mix proportions, range of age of concrete and environmental conditions.
2. Wave form of loading cycle (sinusoidal).
3. Frequency of loading.
4. Minimum stress level.
5. Maximum stress level (Between 65% and 85% of the ultimate static strength of concrete).

The effects that variations in mix, age of concrete, type and rate of loading, etc. will have on the cumulative fatigue damage in concrete in compression are beyond the scope of this study, and must be left until more is known about the nature of cumulative fatigue damage under the above simplified conditions.

CHAPTER TWO

REVIEW OF CURRENT KNOWLEDGE ON THE FAILURE OF PLAIN CONCRETE UNDER COMPRESSIVE FATIGUE LOADING

2.1 General Reviews

Studies of the fatigue behaviour of concrete under repeated loading now extend over more than 70 years. However, the majority of them, being exploratory investigations, have been fragmentary and of limited scope and it is difficult to draw many firm conclusions from the available information which is based on the results of tests conducted on different types of specimens subjected to various loading conditions.

The information concerning fatigue properties of concrete may be divided into the three categories of plain, reinforced, and prestressed concrete. The current knowledge of the fatigue properties of concrete, reinforcing bars, welded reinforcing mats, prestressing tendons is now published by the A.C.I. Committee 215[3] and will not be covered here. The purpose of this chapter is to summarise the relevant important work and to indicate its limitations and requirements for further research, with particular reference to the fatigue behaviour of plain concrete under axial compressive fatigue loading.

Reviews of the earlier work were published by Mills and Dawson[4] in 1927, by Cassie[5] in 1939 and in more detail, by Nordby,[6] and by Bate[7] in 1958. In 1960, the A.C.I. produced an exhaustive annotated bibliography[8] covering the period up to the end of 1958. In February 1965, Murdock[9] published a comprehensive and critical review of fatigue research on plain concrete in which he summarised the state of knowledge at that time and suggested some recommendations for future research. Neal and Kesler,[10] later in the same year, published a report on the fatigue of plain concrete in which they summarised the state of knowledge with particular reference to the extensive investigations at the University of Illinois. In 1968, as a

preliminary part of a comprehensive research programme on plain concrete to be undertaken by the Transport and Road Research Laboratory, Raithby and Whiffin[11] published an extensive literature review and outlined some recommendations for future research. In March 1974, the A.C.I. committee 215 published a report[3] which provided the most updated information concerning the fatigue properties of component materials, namely, concrete, reinforcing bars, etc. More recently, the A.C.I. published a special publication[12] (ACI-SP41) in which 15 papers presented at the Abdes symposium 'Fatigue of Concrete' in November 1972, were included. A concise review of the current state of knowledge on fatigue in concrete was also published by Bennett[13] in May, 1974.

2.2 Fatigue of plain concrete under repeated axial compressive loads

In reviewing the work that has been done on concrete it is convenient to use the following broad headings:

(1) Constant amplitude tests.

(2) Time dependent effects (i.e., specimen age, rate of loading rest periods, etc).

(3) Effect of Material properties.

(4) Mechanism of fatigue failure.

(5) Effect of previous stress history.

(6) Stress interaction and cumulative damage.

2.2.1 Constant amplitude tests

Some of the earliest work on fatigue was reported by Van Ornum[14] in 1903, mainly on 51mm neat portland cement cubes four weeks old but also including some concrete cubes, tested in repeated compression at four cycles per minute. In 1907,[15] tests on 127x127x305mm prisms aged both one month and one year at frequencies of two to four cycles per minute were described. The scope of the tests was limited to lives of less than about 10^4 cycles. Van Ornum's work merits attention because it established the existence of

the fatigue phenomenon for concrete and recorded the observation of progressive failure. The slope of the stress-strain relationship varied with the number of load cycles applied, initially being convex but later changeing to linear and to concave, with a progressive decrease in stiffness, and finally near failure it became S-shaped. His tests indicated that concrete has no fatigue limit as in the case of metal but he concluded that the fatigue strength under repeated loading could be stated to be about 55 percent of the static ultimate strength for a fatigue life of 7000 cycles. He appeared also to be the first to have expressed the fatigue strength of cement mortar and concrete in form of an S-N diagram (Fig2.1).[8]

Williams,[16] in 1920, tested cylinders at six to eight cycles per day. Limited data indicated a slight increase in the modulus of elasticity of concrete with repetitions of load.

In the thirty years following Van Ornum's tests, there were several investigations which followed similar lines, notably by Probst and his students[17,18] and by Ban[19] and Graf and Brenner[20,21] at Karlsruhe, Germany. These investigations were mainly concerned with progressive deformation under fatigue loading and particular attention has been paid to recording stress-strain diagrams at various stages of the tests. Although the number of specimens was small, it was possible to extend the observations to longer lives than those of Van Ornum. Consideration was also given at this time to the interrelation between fatigue strain and creep, following earlier observations by Berry,[22] and to the implications of partial strain recovery on the removal of the load.

The investigation by Graf and Brenner[20] was significant because it introduced a modified Goodman diagram for the first time into concrete study, describing the effect of rangeofstress on the fatigue behaviour of concrete. Only a limited number of points was covered but some typical results are given in Fig 2.2.

These German investigations, although more detailed and meticulous than Van Ornum, did relatively little more than substantiate his results. However, they do provide a firm basis for continued work which may provide a better understanding of the mechanism of fatigue failure. The work of Graf and Brenner,[20,21] in particular, included the effect of a number of variables, namely, cross-section, speed of testing, mix proportions, curing, range of stress and specimen age.

For almost a quarter of a century from 1936 to 1959, no further reports of fatigue tests under direct compression appeared. In 1959, Antrim and McLaughlin[23] reported a study of fatigue behaviour of air-entrained and non-air-entrained concrete. Tests were made on 76x152mm cylinders subjected to repeated axial compression at a frequency of loading of 1000 cycles per minute. The data indicated when extrapolated, a fatigue strength of about 55 percent of the static ultimate strength at 10 million cycles without any significant differences between the fatigue strength of the two types of concrete; and no evidence of a fatigue limit was found (see Fig. 2.3.). In a subsequent study carried out in 1961, Gray, McLaughlin and Antrim[24] extended the investigation to include lightweight aggregate concretes at frequencies of 500 and 1000 cycles per minute and again the specimens where 76x152mm cyclinders. No fatigue limit was found and no effect of speed of testing was discernible. There was no significant difference between the fatigue strength between lightweight concrete and that of conventional concrete (see Fig. 2.4). Although the results were limited in scope, and the number of tests was relatively small, the main contribution of these tests was in the extension of fatigue knowledge to a different type of concrete and to higher frequencies of loading used.

In 1965, Linger and Gillespie [25] reported a study in which axial load tests were performed on cylinders both in direct compression and in split-cylinder indirect tension. The results obtained were very similar to those

of Van Ornum, although covering a much wider range of lives. No significant difference in fatigue life was found between tensile and compressive loading when the applied load was expressed in terms of percentage of the ultimate static strength and there also appeared to be slightly less scatter in the results for the tensile splitting tests (see Fig 2.5). The Goodman diagrams were also used to show the results, which although were limited by the small number of relevant test points, indicated a consistency in fatigue strength between compressive and indirect tensile loading, therefore, suggesting a similarity in the mechanism of failure.

At the university of Leeds, Muir[26] conducted a programme of fatigue tests on high strength concrete 76x76x203mm prisms loaded in compression at frequencies between 190 to 340 c.p.m. and the published test results[27] indicated a fatigue strength at one million cycles of between 66 and 71 percent of the static ultimate strength, when the lower load limit was maintained at 8.62 N/mm^2. When corrected by the modified Goodman diagram, this corresponds to 60 percent at 1 million cycles and when extrapolated, 61 and 57 percent at 2 million and 10 million cycles respectively. The results were generally in good agreement with the previous investigators of the 1930's and established a definite trend of a slightly lower value for the high strength concrete.

Raju[28] in 1968, of the same university, conducted an extensive programme of tests, on high strength concrete 76x76x203mm prisms with the main objective of studying the mechanism of fatigue failure of plain concrete and the published test results[29] indicated a fatigue strength of concrete of about 62 percent of static ultimate strength at 2 million cycles when the lower load limit was maintained at 1.4-1.7 N/mm^2. The results were in agreement of the previous investigations except the average static strength of the concrete used was 40 N/mm^2 compared to 39-63 N/mm^2 of Bennett and Muir.[27] The test data also has been analysed on a statistical basis using McCall's[30] model introducing the probability of failure to the conventional S-N diagram.

The main contribution of these tests by Bennett and his students lies in the extension of fatigue knowledge to high strength concrete (>60 N/mm^2), and to provide a better understanding of the mechanism of fatigue in compression. The work of Muir[26] also included the effects of the maximum size of coarse aggregates between 3/8 in. (9mm) and 3/4 in. (18mm) and the results indicated no significant difference of the fatigue strength of the two type of specimens. The work of Raju[28] included the effects of understressing, the introduction of cylindrical inclusion at the middle of the prismatic specimens, the comparisons of the fatigue behaviour of cement pastes and mortars, and the study of microcrack formation by both optical and ultrasonic pulse velocity techniques .

The work by Ople and Hulsbos[31] at Lehigh University in 1966, merits attention because although most investigators have used either direct axially compressive loading or pure flexure, in these tests the behaviour of concrete prisms with a compressive stress gradient has been studied. The specimens were loaded eccentrically to produce the required stress gradient across the section. Marked differences were found in fatigue life between uniformly stressed and non-uniformly stressed specimens, the fatigue strength of the latter being higher than the former. For specimens having the same maximum compressive stress, an increase in fatigue strength of about 15 to 18 percent of static ultimate strength wasachieved on specimens having a zero to maximum strain distribution, when compared with uniformly stressed specimens for a fatigue life of 40,000 to 1,000,000 cycles. The test data was analysed on a statistical basis using the McCalls's[27] mathematical model.

More recently, in 1972 Awad and Hilsdorf[32] published a study on the strength and deformation characteristics of plain concrete subjected to high repeated and sustained compressive loads. Particular emphasis was placed on studies of effect of the time during which the concrete was subjected to high stresses. Tests were made on 102x102x305mm prisms aged 3,7, and 90 days subjected to repeated or sustained compressive loads with maximum stresses rang-

ing from 80 to 95 percent of the static ultimate strength and rates of loading of 4.14,41.36 and 413.68 $N/mm^2/min$. The results indicated that the response of concrete to high repeated loads was to a large extent controlled by the duration of time during which the concrete had to resist stresses higher than its sustained load strength. Therefore, the speed of testing had a substantial influence on the fatigue life of concrete, this is discussed further in Section 2.2.2.2 p. 13. An analytical procedure was also developed to predict the number of cycles to failure for concrete subjected to various stress ranges at various rates of loading.

2.2.2 Time dependent effects.

2.2.2.1 Effect of age of specimen

Little work appears to have been done hitherto on the effects of age on compressive fatigue performance of concrete. The sole systematic research appears to be that of Linger and Gillespie[25] who conducted tests on cylindrical specimens in repeated compression. The limited results indicated that for specimens less than 3 months old, fatigue strength increased with age, theincrease being approximately linear over an age of 40 to 84 days. The results showed the fatigue strength at one million cycles to be 0·64 of the static strength at 40 days increasing to 0,82 at 84 days. No data was available for ages greater than 84 days.

The only other attempt to investigate the effects of age on the fatigue strength of concrete was by Raithby and Galloway[33] of the T.R.R.L. who conducted flexural fatigue tests on small concrete beams with the objectives of studying the effects of moisture state, age in terms of curing time and rate of loading on the fatigue performance of three types of concrete used in highway construction. The results of these flexural tests are not directly relevant but it is of interest that they indicated the fatigue performance to be strongly dependent on the age of the concrete. They also suggested that a reasonably good prediction of long term performance of concrete of ages up to 3 years might be obtained by extrapolation from the results of short term tests under

appropriate conditions.

A sustained load test may be considered as a limiting case of fatigue loading where the stress range R=0. Awad and Hilsdorf[32] conducted sustained load tests on prisms aged 7,28 and 90 days at maximum sustained stress levels σ_{sus} of 85, 90 and 95 percent of the static ultimate strength; the results indicated that for high stress levels causing failure after less than 500 min (σ_{sus}=0.90), old concrete was more resistant to sustained loading than young concrete. However, this trend was reversed at lower stress levels causing failure after more than 1000 min, the time to failure for concrete loaded at an age of 7days was larger than for older concrete. This was explained as probably due to continued hydration while the specimen was under load which may have partially or completely offset the damage caused by the load. Hydration under load was particularly significant at low stress levels when the time to failure was sometimes several days.

2.2.2.2 Rate of loading

As the static strength of concrete depends greatly on the rate of loading, it might be expected that fatigue performance would also be affected by the speed of testing. Results from several tests indicate, however, that the effect is not great. Tests by Mehmel[17] over the range 30 to 90 cycles/min (0.5-1.5Hz), and Graf and Brenner[20,21] in the range of 260 to 450 cycles/min (4.33-7.5Hz), showed that frequency of loading had no effect on the fatigue life provided the maximum stress level was less than 75 percent of the static strength. This conclusion was supported by Antrim and McLaughlin,[23] and Gray, McLaughlin and Antrim[24] for tests at 500 and 1000 cycles/min (8.33-16.7Hz). Comparative tests at 500 and 9000 cycles/min (8.33-150Hz) were conducted on 51x102mm cylinders in 1959 by Assimacopoulos, Warner and Ekberg[34] of Lehigh University in an effort to develop satisfactory methods of accelerated fatigue testing. The limited test data (9 specimens at 500 cycles/min and 25 at 9000 cycles/min) indicated a fatigue strength of 63 percent of static strength at 2 million cycles for a minimum stress level of 10 percent of the static strength. The two rates of loading were found

to have no significant effect on the fatigue life despite the fact that at 9000 cycles/min a considerable temperature rise (in some cases from room temperature of 78°F to 175°F) occurred due to internal friction in the specimen.

However, the conclusions drawn from the above investigations cannot be regarded as being very reliable due to the fact that the number of specimens tested, and the range of frequencies covered were too small. The individual results were somewhat inconclusive and showed enormous scatter (as much as 1000 to 1 of Max/Min life at particular stress levels).

For higher stress levels (80 to 95 percent of static strength) a significant influence of rate of loading has been observed by Awad and Hilsdorf.[32] Under such conditions, creep effects became more important, leading to a reduction in fatigue strength with decreasing rate of loading. It was found that a decrease of rate of loading by one order of magnitude resulted in a decrease of the fatigue life by almost one order of magnitude (rate of loading V.S log N).

Work has recently been completed by Sparks and Menzies[35] in which compressive fatigue tests were performed on 102x102x203mm prisms with maximum load levels between 70% and 90% of the static strength in a triangular wave form at rate of 0.5 and 50 N/mm^2/sec and the minimum load level was maintained constant at one third of the static strength tested at the rate of loading specified in BS 1881: 1970 (0.25 N/mm^2/sec). The results indicated that the rate of loading did infact affect the fatigue strength of plain concrete in compression. The degree to which the fatigue life was enhanced in the tests by the more rapid application of loading was dependent upon the level of the maximum load. Although it was not possible to put an exact figure on the improvement of life, it was generally of lower order than the increase in the rate of loading. The typical result showed that a hundred-fold increase in the rate of loading produced a tenfold improvement in fatigue life. The conclusions drawn from this work together with those of Awad and Hilsdorf are of importance because it means that accelerated fatigue testing of concrete in compression may

produce an overestimate of their true fatigue strength if the actual rate of loading is very low. It is interesting to note that this reduction in fatigue strength with lower rates of loading was in fact observed as early as 1934-6 by Graf and Brenner[20,21] when they noticed a slight decrease in endurance at a slow rate of 10 cycles/min (o.167Hz).

2.2.2.3 Deformation

In general, the strain of concrete during repeated loading increased substantially beyond the value observed after the first load application.[29] The deformation is greater at lower rates of loading.[3,11,13]

2.2.2.4. Rest Periods

The effect of rest periods on the fatigue behaviour of concrete in compression has not been sufficiently explored. Early investigators (during 1923-1930)observed that rest periods appeared to have a beneficial effect on the fatigue strength of concrete.[11] No other data is available concerning the effect of rest periods in compressive fatigue tests.

In flexural fatigue tests, however, a few investigations have been conducted to study the effect of rest periods, namely by Hilsdrof and Kesler[36] and more recently by Raithby and Galloway.[33] The test results of the former indicated that rest periods of up to 5 minutes increased the fatigue strength but that periods longer than 5 minutes had no further effect and the frequency of the rest periods appeared to be more important than their duration (see Fig. 2.6). In contrast, the results of the latter indicated that the rest periods appeared to give a slight reduction in life but the differences were not statistically significant at the 5% level. The contradiction in these two conclusions is probably due to the difference in the testing programmes, Hilsdorf and Kesler[35] introduced rest periods of 1 to 27 minutes at the end of blocks of about 4500 cycles whereas in the tests of Raithby and Galloway[33] rest periods of 0.5 and 2.0 sec were applied after each cycle of loading.

2.2.3 Effect of material properties

Test reports as early as 1936 indicated that the fatigue strength decreased slightly with an increase in the static strength; however, the reduction with an increase in static strength appeared to be too small to be of practical importance.[13] It has also been found that cement paste and cement-sand mortar specimens, of the same proportions as in concrete specimens did not differ significantly from the concrete in fatigue strength.[29]

Fatigue testing has been extended to include air-entrained concrete[23] and light-weight aggregate concretes of high and low strength.[24] In each case the fatigue characteristics were similar to thoseof normal concrete; no fatigue limit was found under 10 million cycles, at which duration the extrapolated fatigue strength was about 55 percent of the static ultimate strength when the minimum stress is zero.

2.2.4 Mechanism of fatigue failure.

The fatigue of concrete is a process of progressive permanent internal cracks of microscopic width at the cement matrix/aggregate interface and the matrix itself when subjected to repeated stresses. Fatigue fracture of concrete is more extensive and characterised by considerably larger strains and microcracking as compared to the somewhat similar cracking accompanying concrete under static compressive loading.[13] The internal cracking of the concrete could be detected by the decrease in the pulse velocity of an ultrasonic pulse in lateral direction. Another effect of fatigue on the properties of concrete is the concavity of the stress-strain curves prior to failure, this could be the result of some of the cracks at right angles to the direction of loading, tending to close under increasing stress.[29]

2.2.5 Effect of previous stress history

The application of repeated compressive stresses at a level below the fatigue strength at 10 million cycles i.e., less than 55 percent of the static strength, which is known as 'Understressing', has been found to have a margin-

-ally beneficial effect on the subsequent static strength. This amount varied from 5 percent to as much as 15 percent increase in static strength in early investigation.[11] More recently, the results from tests by Bennett and his students[27,29] showed the same trend on concrete of much higher strength (40-60 N/mm^2), the average increase in static strength was about 11 percent[27] and 5 percent.[29] This phenomenon has also been observed in beams subjected to understressing in flexural tests.[11]

2.3 Work on stress interaction and cumulative damage

In the majority of fatigue testing programmes, the range of cyclic stresses has remained the same throughout each individual test (Constant amplitude tests). In contrast, concrete may in practice be subjected to a whole spectrum of stresses in random order and to assess the fatigue strength in such cases it is necessary to know the accumulation of fatigue damage under cyclic stresses of varying amplitude and order. Currently, no data is available concerning the fatigue performance of concrete under compressive cyclic loads of varying magnitude.

2.4 Limitations of previous investigations.

Review of the published investigations to date shows that, with a few exceptions, the scope of each investigation has been rather limited and the methods of testing have varied considerably. Loading arrangement, form and rate of loading, type and size of specimens, and age of specimens are a few of the variables which have differed in each investigation. However, the obvious significant limitation of the investigations is the lack of information on stress interaction and cumulative fatigue damage in plain concrete in compression. In view of their importance it is rather surprising that these problems have scarcely been touched upon. Although the compressive fatigue problem is not likely to be critical in structural reinforced and prestressed concrete members under the load and stress conditions governed by present practice, this position may change due to the introduction of

advanced design procedures and increasing use of high strength material, for example, more slender columns, piles, more flexible machine bases and off-shore structures etc.

Furthermore, precise information is needed to enable a reliable evaluation to be made of fatigue damage in an actual structure. It is doubtful whether the present practice in estimating the fatigue performance from the limited knowledge gained from constant amplitude tests will always result in a safe and serviceable structure.

2.5 Requirements for further investigation

Since the fatigue behaviour of concrete subjected to compressive cyclic loading of varying amplitude appears to be practically unknown, it would seem that the initial requirement is a thorough systematic study of the effects of varying loading programmes. This should probably begin by establishing an S-N diagram or more precisely an S-N-P diagram of a particular concrete by constant amplitude tests, under one set of environmental conditions and with strict control of the many variables to permit qualitative and quantitative assessment of the results. The progressive changes in the properties of concrete under fatigue loading which could define the degree of fatigue damage i.e. the strain data, hysteresis curves etc. will be monitored. However, these changes are only useful for laboratory specimens and are of little use in the field. Particular attention will, therefore, be paid to ultrasonic non-destructive testing techniques which may offer an indirect method of measuring the fatigue damage sustained by a structural member in situ.

When the S-N-P diagram has been established, the concrete specimens will be subjected to several loading programmes designed to yield as much information as possible on the cumulative fatigue damage, and the physical changes in the concrete specimens will simultaneously be monitored by ultrasonic methods. The results of such systematic tests may outline characteristics of the cumulative fatigue damage and check the validity of any proposed cumulative damage theory.

CHAPTER 3

TEST SPECIMENS: DESIGN, PREPARATION

3.1 Materials, mix proportions

3.1.1. Materials

The cement used for all tests came from a single consignment of a rapid hardening type ("Ferrocrete" of the Blue Circle Cement Group) conforming to B.S.12:1971. An analysis is shown in Table 3.1.* The aggregates were well graded North Nottinghamshire quartzitic gravels. The coarse aggregates (irregular shape) had a maximum nominal size of 10mm (3/8 in.) and the fine aggregate was 5mm (3/16 in.) graded sand. The fineness moduli, defined as the sum of the cumulative percentages retained on the sieves of the standard series: 150, 300, 600 μm, 1.20, 2.40, 4.76mm (nos. 100, 52, 25, 14, 7, 3/16 in.) and up to the largest sieve size present, of both coarse and fine aggregates were 5.90 and 2.62 respectively. Both aggregates conformed to the limits set out in B.S.882& 1201:1965, the fine aggregate following within zone 2. The typical grading curves of coarse aggregate, fine aggregate, and the combined aggregates in the ratio of 2:1 corresponding approximately to the curve no.2 of McIntosh and Erntroy's type grading curves[37] are shown in Fig. 3.1.

3.1.2. Mix Proportions

After several preliminary mix trials consisting of aggregate cement ratios of 5:1, 6:1, 7:1, and water cement ratios of 0.5, 0.55, 0.6, 0.65. Mix proportions of 1:2:4 with a water cement ratio of 0.6 was standardised for the tests. The mix was adopted on the basis that it gave a minimum characteristic cube strength of 40 N/mm^2 at 28 days, and an average prism strength of 36 N/mm^2 at 35 days (after air drying in the laboratory for at least 3days). A typical gain of strength with time of the mix is shown in Fig. 3.2 and a histogram of all batches is shown in Fig. 3.3. The workability of the mix was measured by

---

* Private communication: C.M. Gibson, Technical Dept., The Cement Marketing Co. Ltd.

Slump, Compacting Factor, and Vebe tests. The average values for the first 5 batches were: Slump, 12.7mm (1/2 inch); C.F., 0.92; and Vebe time, 4 seconds.

3.2 Specimen shape and size

The effect of cross-sectional shape and height to width ratio of the specimen on the mode of progressive damage and failure were two factors considered in selecting the final shape and size of the specimens for this investigation. A critical study of the influence of these two parameters is not intended in this work because it has been under investigation by various international research organizations[38-44] at least as far as the influence on the static compressive strength of concrete is concerned. The conclusion reached in these works could be summarised as follows:

There is little variation in the crushing strength of specimens having similar dimensions but different cross-sectional shapes.[43,44] Also, the apparent strength of concrete specimens with the same cross-section increases with decrease of the ratio of height to width or diameter. The effect is very marked below a ratio of 1.5 and less marked above 2.5. The former is due to increased frictional lateral restraining effect of the loading platens of the test machine on the ends of the specimens and the latter to the tendency towards instability in slender specimens.[38,39] However, for research investigations, a ratio of height to width or diameter greater than 2.5 has been proposed[45] on the basis that the middle third of the specimen could be regarded as an undisturbed compression for measurement in the elastic range and up to failure.

Based on these facts, it was decided to use 76x76x203mm (3x3x8 in.) concrete prisms which were convenient size for the testing rigs and more suitable for ultra pulse velocity measurements than those of circular cross-section. This size had been used previously for both fatigue and creep investigations in this laboratory,[27,29,46] and would therefore enable comparisons to be made.

For quality control tests, 102mm (4in.) cubes were used throughout the investigation.

3.3 Casting, Curing and Quality Control

The specimens were cast vertically into steel moulds conforming to B.S. 1881:1970. A pan mixer of 2 cubic feet (0.863 m^3) capacity was used for mixing with a constant mixing time of 2 minutes and 8 prisms and 12 control cubes were cast in each batch. The pan of the mixer was thoroughly hosed down and excess water tipped away before use, to ensure even wetting of the pan and kept the variation of the water cement ratio of the mix to minimum as possible for each batch. Good compaction of the specimens was achieved by the use of an Allam vibrating table and a constant compaction time of 30 seconds was observed for each casting layer. After compaction excess concrete was removed, and the top surface was trowelled off to a smooth finish. The specimens were allowed to set partially before covered with wet hessian and polythene sheet. They were removed from their moulds after 24 hours and stored in the controlled conditions of the curing room at a temperature of 18°C ± 1°C (65°F) and a relative humidity of 95-100% for a period of 28 days before testing.

In order to ensure that all of the specimens used in the tests were fairly uniform in strength, each step in preparation was standardised and closely supervised. The sieve analysis of aggregates was performed at regular intervals in order to detect any irregularity in the grading curves. The whole consignment of R.H.P. cement (1 Tonne) along with the high alumina cement employed in capping the prisms were delivered in double paper bags which were carefully wrapped and stored at uniform temperature (20°C) and humidity (50-60%) throughout the test period. The effort was justified and resulted in a fairly uniform strength (Fig. 3.3). The relationship between the standard deviation and ultimate cube strength at 28 days is shown in Fig. 3.5. The average within-batch standard deviation* of the control cubes at 28 days (33 batches) is

*Average within-batch standard deviation, $\hat{S}_M$ computed from:

$$\hat{S}_M = \sqrt{\frac{S_1^2 + S_2^2 + \ldots S_N^2}{N}}$$

where; $S_1, S_2, \ldots$ etc., = Standard deviations within batch.
N = Number of batches.

1.26 N/mm^2 (coefficient of variation is 2.93%) which is well below the value recommended by the working group1 set up by a joint CEB/CIB/FIP/RILEM committee[47] (Fig. 3.4).

3.4 Preparation of ends of specimens

The ends of the specimens were required to be perfectly plane and at right angles to the sides. As the tops of the specimens could not be adequately smoothed off before the concrete had set, the resulting surfaces were somewhat rough and not truly plane. When testing in uniaxial compression, stress concentrations resulted and the apparent strength of the concrete was greatly reduced. At the same time, the scatter of strength was increased because of the influence of the defects in planeness. A lack of planeness of 0.25mm (0.01 in.) can lower the strength as much as by one-third, the loss in strength being particularly large in high-strength concrete.[48]

In fatigue tests where the specimens are stressed to various stress levels based on the average static strength of the control specimens, it is obviously essential that the specimens should give reliable and consistent strength results. In order to achieve this not only must the quality of the concrete be closely controlled but also the ill-effects of uneven end surfaces of the specimens must be eliminated.

There are three means of overcoming the problem of a rough end surface of the specimen: packing with a bedding material, grinding, and capping.

The test results from several investigations (49 - 51) indicate that packing, usually of softboard, cardboard, rubber, lead or polyethylene can appreciably reduce the scatter of strength, but at the same time it can also lead to an appreciable lowering of the apparent mean strength of the concrete compared with capped or even with smooth-trowelled specimens. The reduction in strength arises from lateral strains induced in the specimen by Poisson's ratio effect in the packing material which is generally higher than that of the concrete so that splitting is induced. This effect is usually greater than,

that of lubricating the ends of the specimen in order to eliminate the restraining influence of the friction between the specimen and the platen on lateral spread of the concrete, which has been found to reduce the strength of the specimen.[52]

The grinding of a plane, square bearing surface is another alternative, but is rather expensive. The writer 's attempts to eliminate the defects by grinding both top and bottom surfaces of the specimens were unsuccessful. The resulting scatter of the strength, indicated by the coefficient of variation, was 7.5% (3 batches: 24 prisms). This value is,however,less than the test results of "as-cast" prisms which had a coefficient of variation of 10%. The average relative strengths of the ground specimens and the "as-cast" specimens were 70% and 59% of the control cubes respectively. These values are in agreement with those of Muir.[26]

The use of high alumina cement caps (1.5-3mm thick) in conjunction with mild steel loading plates (13-19mm thick), having the same cross-section as the prisms (76x76mm) was found by Muir[26] to give the least coefficient of variation (6%) to gether with a high relative strength of 77% of the cube strength. The relative strength in Raju's tests[28] was 79%. It was found by Raju that the premature splitting of the ends under high repeated loads observed by Muir could be prevented by good compaction of the caps and a slight modification of the capping method.

The possibility of using a "brush platen"[53,54] which allows the free lateral deformation of concrete to develop hence eliminating the friction and providing a uniform compressive stress was also considered. However, when compared with the advantages of using the well proven capping method of Raju[28] and Whaley,[46] and the useful comparison with previous results, the delay which would have arisen in manufacturing brush platens was concluded to be uneconomical. It was therefore decided to use the capping method which had previously been employed in this laboratory.

The previously used capping jigs shown in plate 1 (a), consisted of two vertical machined steel plates 76x50x22mm (3x2x7/8 in.) and 102x50x22mm (4x2x 7/8 in.) bolted together forming a right angled corner and perpendicularly bolted to a machined base plate 152x152x13mm (6x6x1/2 in.). The capping material consisted of high alumina cement with a water cement ratio of 0.27 and was allowed to set partially before being spread and uniformly compacted on the loading plate to an approximate thickness of 1.5-3mm. The loading plate was then positioned as shown, the prism was held firmly into the right angle, lowered gently onto the cement paste, pressed down and clamped in position. The prism was gently tapped down, the cement paste being squeezed out until the layer was equal to or less than 1.5mm, the excess cement paste removed and the prism was finally clamped tight. In this way all of the eight prisms from a batch could be capped at one time. The operation was repeated on the other end of the specimen 24 hours later, during which they were covered with wet hessian and polythene sheet to maintain the curing condition. The specimens were generally capped when 29-30 days old and cured by keeping in the curing room further for 2 days before they were transferred to the testing laboratory when 32 days old.

Although this method gave accurate alignment of the plates and excellent perpendicularity, it had one disadvantage, namely that the need to repeat the capping operations lengthened the operation and interfered with the testing work. A new design of capping jig, which retained all the good qualities of the previous type but enabled the capping to be performed on both ends in one day, was later developed and brought into use by the end of series-A of the tests.

3.4.1 New Capping Method

The new capping jig was of a similar construction to the original type except that the machined plates forming a right angled corner were wider and taller. It also had an additional detachable top plate. The details of all

component parts are shown in Fig.3.6. Before capping bolt "A" which served to ease the removal of the capped prism, was turned back until the machined end was flush with the exposed inside surface of the vertical plate, after which all the surfaces were thinly coated with mould oil. The same sequence of capping operations was then performed as had been done when using the old jigs. When the lower end had been capped, another loading plate with a layer of cement paste 2mm thick was turned over, placed on the top of the prism and carefully tapped until the top of the loading plate was 2 mm below the top of the adjacent right angled plates. The top plates was then gently placed in position and carefully screwed down by means of 4 bolts "B" thereby squeezing out the excess cement paste which was trowelled off. The complete assembly of the new jig and the capped specimen is shown in Plate 1(b). By this method, all eight of the prisms in one batch could be capped at both ends in one session. The specimens were capped when 29 days old, moist cured for another 2 days and were transferred for air drying in the testing laboratory when 31 days old.

The average value of the coefficient of variation of the strength at the commencement of testing of 24 specimens capped by the new method was 3.8% compared with 4.5% for the old method. Even though the improvement in the control of the scatter of strength was small the practical advantage of the new method was obvious. Every capped prisms had the same standard length of 233mm ($9\frac{11}{64}$in.) with the loading plates and 207.56 mm ($8\frac{11}{64}$in.) without, which was of a great advantage in the study by pulse velocity technique. (Chapter 7).

3.5 Preparation of specimens for testing

As the average temperature of the testing laboratory was $24^{o}\pm1^{o}$C and the relative humidity 50-60% compared with $18^{o}\pm1$C and 95-100% relative humidity of the curing room, the problem of controlling the uniformity of strength again arose since a change of ambient conditions might influence the concrete strength. The effect was studied on the strength of the prisms and control cubes of transfer to the laboratory atmosphere from the moist condition of the curing room, the results of which are shown in Fig. 3.7. It was found that the strength of

both prisms and control cubes increased suddenly when exposed to air drying with reference to the typical strength-time curves for moist curing which were obtained from specimen tested in a saturated condition. There was, however, no significant difference in the above increase of strength whether transfer to the laboratory took place after 28,35,or 42 days. However, one consistent feature of all the specimens under test was that the strength only increased markedly in the first 3 days of air drying, after which the increase in strength was relatively small in up to 14 days. It is probable that the sudden increase of strength after cessation of moist curing is the result of the immediate loss of moisture, since specimens are known to develop a higher strength when tested dry than saturated.[55]

On the basis of this study, the specimens were kept in the testing laboratory for not less than 3-4 days before tests commenced. This practice ensured that the scatter of the strength would be a minimum during the period of testing which lasted up to 3 weeks in some batches although the normal period was 7-9 days per batch.

3.5.1 Protection of caps.

The application of silicone grease, immediately after transfer, to act as a water-retaining membrane around the edges of the caps was found to prevent the occurrence of micro cracks due to drying shrinkage, the latter effect could sometimes lead to the premature splitting of the caps both before and during cyclic load tests.

CHAPTER FOUR

LOADING EQUIPMENT, INSTRUMENTS, AND GENERAL SCHEME OF TESTS

4.1 Testing machines

4.1.1 Losenhausenwerk fatigue testing machine

The Losenhausen Universal Hydraulic System (UHS)-60-type universal fatigue testing machine (Plate 2), with a static load capacity of 60 tonnes (588.42 kN) and a maximum dynamic load capacity of 40 tonnes (392.28kN) was used throughout the investigation for fatigue and static tests of prismatic specimens. The frequencies of loading available were, 190,240,300,380,460,580,720,860, cycles per minute. The stress-time diagram produced by the machine (Fig. 4.1) was nominally a sine wave unless the speed was more than 580 cycles/min. For dynamic tests conducted in this investigation a constant speed of 190 cycles/min (3.167 Hz) was used throughout.

The working principle of this machine is shown diagrammatically in Fig. 4.2. Two opposed pistons each supplied by separate pumps act on a single cross head, the tpp provides tension, the bottom compression. The compression and tension are initially balanced to produce the required minimum specimen load. The pulsator (300 cm cylinder) is switched on and its amplitude of stroke increased gradually. This causes the tension pressure to fluctuate cyclically and hence the corresponding specimen load gradually increases until the maximum load is reached. The compression pressure remains relatively constant due to a large damping reservoir of oil in the circuit. A complete description of the machine may be found elsewhere,[56] and a schematic layout of the hydraulic circuit is shown in Fig. 4.3.

For static tests, the loads were measured by a 12 in. pendulum dynamometer (Pe) which could be read to 500 lbf (2.444 N) and was accurate to 1%. For the measurement of the upper (Pu) and lower loads (Po) under cyclic loading, two 8in. Bourden gauges which could be read to 200 lbs (0.889 N) were used.

These measured, through a system of rotary valves, the difference between compression and tension pressures when the pulsator was at the top and bottom of its stroke. Their accuracy of $\pm$ 3% was maintained by applying an appropriate correction factor obtained from the manufacturer's calibration chart. However, for the plain concrete specimens used in this study, the correction factor was approximately unity.

The machine had built-in automatic load — maintaining devices which kept the load limits constant, automatic safety devices to stop the machine when the specimens failed or the load limits were exceeded and a digital counter reading to 10 indicated the number of loading cycles.

4.1.2 Denison compression testing machine

A 300 ton (2942.1 kN) Denison compression testing machine Avery- Denison Testing Machines Ltd., U.K., was used for all control tests on cubes throughout the investigation. The machine platens consisted of a ball seating for the top platen with a rigid bearing block for the bottom platen. A constant loading of 15 $N/mm^2/min$ (2,200 $lbf/in^2/min$) conforming to B.S. 1881:1970, was used for all the static control tests. The accuracy of the machine was within Grade B classification of B.S. 1610:1964.

4.1.3 Calibration

Prior to testing, the machines were calibrated by means of 25 and 50 T. Johanson dynamometers and the results were in good agreement with those of the manufacturer. Subsequently, the machines were calibrated at regular intervals so that any deviation that might occur due to a change in the oil viscosity resulting from the prolonged running of the UHS machine, could be rectified beforehand.

4.2 Selection of strain measuring devices

The choice of gauges available were

1. Mechanical

2. Electrical Resistance

Preliminary tests were made using demountable mechanical gauges (Demec) developed by Morice and Base;[57] detachable Lamb's 4 in. mirror roller extensometers (A. Macklow-Smith Ltd., London) and electrical resistance strain gauges (e.r.s.) both in static and dynamic tests to study the relative merits of the strain measuring devices.

4.2.1 Method of fixing gauges.

For Demec gauges, stainless steel seating discs were fixed on the specimen at the desired gauge lengths by means of Amco F 88 dental cement using the supplied standard gauge bar. Due to the quick setting action resulting from the evaporation of the solution, the discs were ready for use within 10-15 minutes.

When using Lamb's 4 in. mirror roller extensometer, two gauges were clamped on opposite sides of the specimen, the rollers and the angles of the mirrors were carefully positioned until the reflected images of an illuminated cross from a slide projector were shown on a millimetre scale at a distance of 1·85 m from the prism. The schematic arrangement is shown in Fig. 4.4.

Before fixing the e.r.s. gauges, a selected surface area of the specimen was smoothed by fine emery paper and wiped clean to provide a plain surface which was then coated with a thin layer of the special adhesive supplied by the manufacturers. A second layer of the adhesive was placed on the dried primer layer and the gauge with the leads connected was placed in position and pressed down smoothly under the protective plastic sheet to expel the trapped air bubbles and the surplus adhesive. A minimum of 24 hours was allowed for the adhesive to harden before testing commenced.

4.2.2 Static tests.

It was not possible to measure both longitudinal and lateral strain on the same specimen with the Lamb's extensometers on account of the size of the instrument. When employed for longitudinal measurement, they could give

an accuracy determined by the accuracy of machining of the roller. The mean diameter of the roller was quoted by the manufacturers of the instrument as 0.149755 in., assuming that this is correct to $\pm$ 0.00001 in. This would represent an accuracy of $\pm$ 0.001% although it is doubtful whether such a high standard would be achieved on account of error introduced at the knife-edge and contact surfaces. The resolution was 2.5×10^{-6} strain for a scale distance of 185 cm. In a static test to destruction, it was necessary to remove the instrument in order to avoid costly damage prior to failure. This and the fact that they had to re-mounted on each specimen inturn made them unsuitable for the tests. However, they might have been useful in a test where long-term strain under a non-destructive static load was required i.e. a creep test.

Exploratory tests were conducted on the prismatic specimens by using PL 30 (30 mm) e.r.s. gauges with a resolution of 5×10^{-6} for longitudinal and lateral strains. For comparison 4 in. and 2 in. Demec gauges were also used for strain measurements the former for longitudinal and the latter for lateral strains, these had resolutions of 20 and 25×10^{-6} strain respectively.

For longitudinal compressive strain, the difference between the e.r.s. and Demec gauge reading was about 5%; the difference was probably due to the difference in the gauge lengths employed. A small error of 1-2 divisions in reading the Demec gauges was considered to be insignificant in view of the fact that the longitudinal strain at failure was about 2000 micro-strain.

For lateral tensile strain, the 2 in. Demec gauges were found to be insenitive to small changes in lateral strain which were about one-tenth to one-fifth of that in compression and the error of 1-2 divisions in reading was considerable. In contrast, the e.r.s gauges were more sensitive and gave more consistent results. Hence it was decided to adopt the PL30 e.r.s gauges for static tensile strain measurements.

For longitudinal strain measurements, it was decided to use the 4 in. Demec gauges on the grounds that the e.r.s. gauge length of 30mm is not sufficient

to give accurate, consistent strains when compared with the longer measuring length of 4 in. of the former.

4.2.3 Dynamic tests

Due to the obvious disadvantage of the Lamb's mirror roller Extensometers in the destructive testing, the choice of the gauges was reduced to two. Preliminary tests using e.r.s. and Demec gauges resulted in agreement of the strain values in compression during the early stages of the test; i.e. in the first 1-2 days. However, as the test progressed the readings from the e.r.s. gauges began to drift appreciably from those of the Demec gauges. This could have been due to the effect of an increase in specimen temperature under dynamic loading. Some gauges were even rendered inactive by local cracking across the length of the gauges long before the specimen failed. On the contrary, Demec gauges gave consistent strain readings up to failure so that it was decided to adopt the 4 in. Demec gauges for longitudinal strain measurements in dynamic test, and the PL 30 (30 mm) Japanese e.r.s. gauges for lateral tensile strain measurements in short term dynamic tests (chapter 6).

4.3. Ultrasonic non-destructive testing Equipments

4.3.1 Cawkell Ultrasonic Materials Tester

The ultrasonic non-destructive tester, commercially known as "Materials Tester-Type Ultrasonic Crystal Transducer (UCT)-2", manufactured by A.E. Cawkell Research and Electronics Ltd., U.K. was of an early design developed by Jones and Gatfield[56,59] at the Road Research Laboratory between 1945 and 1949 and also independently in Canada by Leslie and Cheesman[60] at about the same time. The equipment generated a series of pulses of a damped vibration of frequency about 150 kHz at a rate of 50 pulses per second which were transmitted to a specimen by means of a barium titanate transducer 30 mm in diameter. The pulse was received by a receiver-transducer at the other end and amplified to give a visual image trace on a Cathode ray oscilloscope. A built-in electronic time marker system was used to display the time interval for the

measurement of the time in microseconds for the wave to transverse the specimen. Depending on the experience of the operator, it was possible to read the equipment to an accuracy of $\pm$ 0.1 microseconds.

For an efficient transmission of the pulse from the transducer to the specimen, it is essential to provide a proper contact between the transducer faces and the surfaces of the specimen. To achieve this, a small holding frame was developed using two 40x150x12 mm aluminium plates and two 6 mm mild steel bars 300 mm long threaded at the ends. The transducers were held against the opposite faces of the specimen by thumbscrews and washers, and isolated from the frame by 2 rubber washers. An application of thin layers of silicone grease between the transducer faces and the surfaces of the specimen ensured a sharp and steady pulse signal during the tests with minimum loss of energy at the interfaces. A typical arrangement of the Cawkell ultrasonic tester with transducers, holding frame and the specimen is shown in plate 3.

4.3.2 Portable Ultrasonic Non-Destructive Digital Indicating Tester. (PUNDIT)

The PUNDIT non-destructive tester,[61] manufactured by C.N.S. Instruments Ltd., London,U.K. was of a new design employing up-to-date integrated circuits and silicon semiconductors throughout. The equipment consisted of a pulse recurrence generator, set reference delay, receiver amplifier, timing pulse oscillator, gate&decade units, and two piezoelectric crystals. A simplified system diagram is shown in Fig. 4.4 and a typical testing arrangement of the equipment with the transducers is also shown in Plate 2.

Both transducers consisted of lead zirconate titanate (PZT4) ceramic piezoelectric elements mounted in stainless steel case 50 mm in diameter and 42 mm in depth. The pulse generator generated a peak voltage of 800 Volts operating for 2 microsecs to the transmitting transducer which by virtue of its piezoelectric property vibrated mechanically at its resonant frequency equal to 50 KHz with a pulse repetition frequency of 10 pulses per seconds. After trans-

mission through the specimen under test the ultrasonic pulse was converted to an electrical signal in the receiving transducer, amplified and processed through the gate control unit and the transmission time taken by the pulse to pass through the specimen was displayed in the form of 3 digits on three 'in - line' numerical indicator tubes. Two ranges of time measurement were available on the instrument, namely -

a) 0.5 to 499.5 microsecs in units of 0.5 microseconds.

b) 1 to 999 microsecs in units of 1 microsecond.

The accuracy of transit time measurement was generally not less than the direct reading values indicated on the display. When a good transducer coupling was made by means of silicone grease with the surface of the material tested and the pulses were not unduly attenuated, the last digit would either remain at a steady value or would oscillate between two adjacent values. In the latter case, the mean reading was used enabling transmission times to be read to the nearest 0.25 microsecs for the 0.5 microsec range. The manufacturers claimed an accuracy of not less than $\pm$ 1% for very good surface coupling conditions and a minimum path length of 3 in. in testing medium to high strength concrete.

4.3.3 Experimental techniques

With the Cawkell ultrasonic material tester, the recommended method of setting the start of the return pulse to the left hand edge of the appropriate time marker[59] was used to obtain the correct alignment. Much care was needed, however, to read the onset of the return pulse on the cathode ray oscilloscope, as it very much depended on personal judgement.

The Pundit ultrasonic tester was far easier to operate. A one to four microsecond variable delay control was incorporated to set the zero of the instrument each time it was used. The zero was likely to change particularly when different types of transducers were used and the delay control would enable the instrument to be adjusted to read correctly (the design of the receiving

amplifier unit of the Pundit allowed it to be used with transducers over a frequency range from 20kHz to 250kHz; normally a frequency of 50 kHz was used). The variable delay was used in conjunction with a standard reference bar supplied with the instrument and had an accurately known transmission time of about 50 microseconds. This time was affected by the ambient temperature and the correct time was given against a built-in thermometer on the reference bar. Due to the easier reading, the holding frame was discarded and the transducers were held firmly against the opposite faces of the specimen by hands.

Pilot tests were conducted to assess the relative merits of the two testers in measuring the transmission time of a pulse through control cubes and prisms under both static and dynamic loadings. In General, the readings of the transmission time were in agreement, the difference being only 0.5-1%. However, with the Cawkell tester, the initial no-load pulse velocity measurements were generally slightly higher than those indicated by the Pundit. This was probably due to the differing sizes of the transducer crystals, differences in the spread of the pulses, the differences in accuracy, and the higher frequency of the Cawkell crystals. It had been observed by Shah and Chandra[62] that the initial no-load velocity of the ultrasonic pulse increases with an increasing frequency of the crystal. It should be mentioned that Leslie and Chessman[60] concluded that the pulse velocity was independent of the frequency. However, their range of frequencies (10 to 50 kHz) was much smaller than that used by Shah and Chandra (25 to 2250 kHz).

It was not possible to measure the transmission time during the dynamic tests by the Cawkell instrument because it was impossible to read the onset of the return pulse due to its fluctuating patterns. In contrast, the Pundit instrument gave a reliable, accurate, consistent reading during the dynamic tests from the no-load measurement to shortly before failure. It was, therefore, decided to adopt the Pundit tester for the measurements of ultrasonic pulse velocity in static and dynamic tests on the ground that it gave accurate, consistent and most important, reproducable readings. It was easier to operate, independ-

ent of personal judgement, portable, and could be used in continuous monitoring of pulse velocity without interfering with the tests.

4.4 Planning of test programmes

At present, there are no special standards laid down for the fatigue testing of concrete, but it would appear reasonable to adopt the available standards for the fatigue testing of metals[63,64] as a general guild in planning.

As described in Section 1.6 (p.5) a number of variables which were known to affect the fatigue properties of concrete were maintained constant throughout the tests. Even when these conditions are fulfilled, there remain a number of unknown and uncontrollable factors which produce a large scatter in the fatigue life, even of seemingly identical specimens. In the past, this scatter in fatigue life was not regarded as a problem and only a few specimens were used to determine the fatigue life, or the relation between load (stress level) and life, as a result of which the validity of the conclusions was disputable. It is now generally accepted that scatter is an inherent feature of the fatigue characteristics of concrete, so that a large number of specimens is required to obtain correct information on the fatigue life. Tests must, therefore, be planned so that the errors arising from the uncontrollable factors are as small as possible and the data must be statistically interpreted in order to draw correct conclusions.

Findley[(63, section 5)] suggested that at least ten specimens be tested for an S-N diagram, but that a larger number of speciems (20 to 50) would be desirable to establish the S-N diagram accurately and to indicate the variability of the material. Weibull[65,66] experimentally verified that, even if the number of specimens tested had a self-evident influence on the accuracy of the parameters computed from the observations, other factors might be of equal importance. He proposed that at least six specimens should be tested at any stress level or 20-30 specimens altogether in order to establish an acceptable S-N diagram. The efficiency of a test series in this respect depends upon the choice of the stress levels, on the testing machine and possibly on other

factors. Accordingly, in this study, specimens were assigned from each batch at random for control static tests and fatigue test groups, the number depending upon the objective of the test.

4.5 Fatigue testing methods.

The simplest form of fatigue loading is obtained by applying a fluctuating stress of a constant amplitude to the specimen until total failure occurs. Different specimens of the test series may be subjected to different stress amplitudes, but for each individual specimen the amplitude will never be varied. This type of fatigue testing is called a constant-amplitude test.

4.5.1 Constant-amplitude tests

Depending upon the choice of stress levels, constant-amplitude tests may be classified into three categories;[64] providing that the rate of loading is not more than 70 $N/mm^2/s$ which is the case of impact loading.

(1) The routine or normal fatigue test, where applied stresses are chosen in such a way that all specimens are expected to fail after a moderate number of cycles, say 10^3 to 10^7. A few run-outs, although not intended, may occur.

(2) The short-life or low cycling fatigue test, where the maximum stress levels are usually between 85-95% of the static ultimate strength. All specimens are expected to fail at less than 1000 cycles and some may even fail statically on the first application of the load.

(3) The long-life test where stress cycles are near the anticipated fatigue strength for a given number of cycles, usually between 10^6 and 10^7 and a number of the specimens (run-outs) do not fail.

The short-life test and the long-life test were usually performed to supplement the information obtained from the normal fatigue test. For obvious reasons, constant-amplitude, normal fatigue test to failure were used in the second part of this investigation.

4.5.2 Variable-amplitude tests

Complicated forms of loading would be required in order to simulate the stresses to which concrete is subjected in actual service and in order to investigate the laws relating to the accumulation of fatigue damage in a specimen subject to fluctuating stresses of different amplitudes, the programmes of loading must be simplified. These tests termed variable-amplitude tests comprise the third part of the investigation. In these tests only two stress levels were used but with systematically varying sequences of loading. The cumulative damage tests will be dealt with in detail in chapter 8-10.

4.6. General Scheme of tests

It was necessary to set out a general scheme for the investigation, comprising the different series of tests to achieve the different objectives detailed in section 1.5 (p. 3). Table 4.1 presents a summary of each series showing the number of specimens used for control and fatigue tests under both constant and varying amplitude loading together with a short description of the objective of the investigation.

CHAPTER 5

ANALYSIS OF RESULTS: FATIGUE STRENGTH

5.1 General

The experimental programme for the phenomenological studies, consisted of static control tests and normal fatigue tests as defined in Section 4.5.1-(1), p.36 . The former were necessary so that an estimate of the ultimate static compressive strength of the concrete in each batch could be obtained on which basis the specimens were assigned to different stress levels expressed on percentage of the static strength.

5.2 Testing procedures

5.2.1 Static tests.

For each batch, 3 sets of 4 control cubes selected at random were tested respectively at 28 days, at the commencement and at the completion of the test, at the standard rate of loading specified in BS 1881:1970 (0.25 $N/mm^2/sec$) in the 300 Tonne Denison compression testing machine. The results of the static tests made on 102mm cubes are shown in Table 5.1.

For an estimate of the compressive strength of concrete used in each batch, 3 prisms were selected at random and loaded to failure at a uniform rate in the Losenhausenwerk universal testing machine which was also used for the fatigue tests and the mean value of their results was taken as the basis for fixing the stress levels for the specimens to be tested in fatigue. One prism was tested statically at the completion of the fatigue tests as a check on the strength gain during the tests. The results of the static tests on 76x76x - 203mm prisms are shown in Table 5.2

The summary of the average of the ultimate static strength at different ages of the control cubes and the prisms, average of with-in batch standard deviation and coefficient of variation are shown in Table 5.3

The mean ratio of prism to cube strength at the time of the commencement of the tests was 0.72 which was not in agreement with the higher values of 0.77 of Muir [27] and 0.79 of Raju.[29] This was probably due to their method of not breaking the bond between the mild steel loading plates and the high alumina cement caps, whereas in the present tests, the loading plates were detached prior to testing, and placed in position when setting up for the tests.

5.2.2 Fatigue tests

Four prisms from each batch were tested in fatigue at different stress levels. The choice of stress levels depended upon the purpose for which the data were required. In the normal fatigue tests in which concrete specimens were expected to fail at 10^3 to 10^7 cycles, the maximum stress levels employed in the investigation varied from 60-85 percent with an increment of 5 percent. A nominal stress of 1.8 to 2.0 N/mm^2 corresponding to a minimum stress level of 5 to 6 percent was used in the fatigue tests throughout, in order to avoid impact loading on the specimen during cyclic loadings. A typical arrangement for both static and fatigue tests is shown in plate 2.

One preliminary static load cycle was performed on the specimen with the maximum load corresponding to the maximum stress level in the fatigue tests tc determine the modulus and area of the hysteresis loop. Thereafter strain measurements were made at specified intervals during thefatigue test until the end of the test or shortly prior to failure of the specimen. The lower load was then applied and the pulsator was set to the constant frequency of 190 cycles per minute (3.167Hz). Because of the nature of the machine the amplitude of the load cycle could only be gradually increased to the maximum load value, the process taking about 3-400 cycles, the number of cycles was counted from the point at which the maximum load value was reached.

The specimens which did not fail in fatigue after 3×10^6 cycles were considered as 'run-out' and were not included in the analysis. These were subsequently loaded statically to failure. A total of 44 prisms comprising series

A were tested in the first phase of the investigation and the summary of the results of the fatigue tests is shown in Table 5.4.

5.3. Necessity for statistical analysis of fatigue test data

An examination of the results of fatigue tests presented in Table 5.4 clearly indicates the nonreproducable aspects of fatigue. Raju[28] observed that with carefully controlled conditions in fatigue testing of plain concrete in compression, a range of between 3 to 1 and 38 to 1 in the number of cycles to failure at the same stress-level was not unusual. The summary of the range in the number of cycles to failure at each stress level in the work is shown in Table 5.5 below:

TABLE 5.5 SUMMARY OF RANGE OF NŌ. OF CYCLES TO FAILURE

Range of nō of cycles to failure	Stress levels in percent				
	85	80	75	70	65
Minimum	3:1	4.6:1	3.6:1	1.06:1	2.63:1
Maximum	13:1	87:1	31:1	6.14:1	5.37:1

With the exception of a maximum of 87:1 at 80% stress level, the variation was within 30:1 in other stress levels. It was, therefore, obvious that the approach to the scatter of test results was bound to affect seriously the validity of conclusions drawn from the normal fatigue tests.

In view of the widely varying fatigue characterisics observed in the tests, the present fatigue data have been analysed on a statistical basis as recommended by B.S. 3518; Part 5:1966, to improve the validity of the conclusions drawn from them.

5.4 Analysis of test results.

The fatigue strength characteristic of plain concrete subjected to repeated compressive stress of constant amplitude is normally represented by the S-N diagram, in which N the number of cycles to failure is plotted, usually on a logarithmic scale, against S the stress level, and since the relationship

of S to log N is sensibly linear up to at least 10 million cycles, a linear regression analysis may be employed.

One of the fundamental assumptions of linear regression analysis is that the dependent variable, (in this case the fatigue life) has approximately the same (normal) distribution for every value of the independent variable, (the stress level). The shape of the frequency distribution of fatigue life at any stress level cannot be accurately determined from a small number of tests but can only be estimated from the results of previous investigations. No exact data is available for the character of this distribution of concrete mainly due to the great number of specimens required for tests. Weibull[65] argued that even the testing of 100 specimens at each stress level could not yield sufficient information for the distribution to be accurately determined, for which several thousand specimens might be needed.

The cummulative frequency distribution for any particular investigation will approximately reveal the shape of the distribution diagram. Raju [28] found that the distribution of fatigue life of plain concrete specimens at a given stress level was skewed suggesting the log normal relationship. Consequently, in the analysis of the fatigue data in this study, the fit of a log normal distribution for fatigue life was investigated.

The fatigue life of the specimens tested at a give stress level was analysed by ranking the specimens in the order of N and the probability of failure 'P' at a smaller number of cycles than each value of N was calculated by dividing the rank of each specimen 'm' by (n+1), where 'n' was the total number of specimens tested at a given value of S. The calculated value of 'P' with the ranking of the specimens are shown in Table 5.6, In calculating 'P' the reason for dividing by (n+1), rather than by 'n' is to avoid obtaining a probability of failure of 1.0 for the specimen having the greatest fatigue life in the group. The probability that all future specimens will fail at this same number of cycles is not 1.0 however closely it may approach the limit. The ratio of

m/(n+1) appears to give the best estimate of 'P' as proposed by Weibull[66] and Gumbel [67] and had been used by several other investigators.[28,30,65,68]

For each stress level the logarithm of the test value of fatigue life was plotted against the cumulative frequency of the probability of failure. Fig. 5.1 shows the fitted straight lines for different stress levels. From the statistics in Table 5.7 it is evident that the test values of fatigue life at lower stress levels fit the log normal distribution better than those at higher stress levels, and with less scatter.

This analysis clearly shows that the distribution of fatigue life of concrete specimens tested at stress levels from 65 to 85 percent can be reasonably approximated to log normal.

5.4.1 S-N Diagram

The plot of the fatigue life test data suggested a straight line relationship between the two variables which had to be established by a linear regression analysis. In this analysis the stress level S was taken as the independent variable and the logarithm of the fatigue life log N as the dependent variable. The latter may be assumed to be normally distributed as has been discussed in Section 5.3.

The line of regression of the stress level S upon Log N is shown in Fig 5.2. This line had a correlation coefficient of 0.940788 which was significant at a level of 0.1 percent. The statistics of the results of the regression analysis are presented in Table 5.8. Run-out specimens were excluded from these computations.

5.4.1.1 Discussion of results.

The S-N diagram which is statistically reliable only between the stress levels of 65 and 85 percent, indicates a fatigue strength of 62.6 percent for 2×10^6 cycles and, when extrapolated, 58.6 percent for 10^7 cycles. These values are comparable to those of earlier investigations by Muir[27] and Raju[29]

which are summarized in table 5.9.

TABLE 5.9 FATIGUE OF HIGH-STRENGTH CONCRETE IN COMPRESSION

SOURCE	Static Strength [N/mm^2]	Fatigue strength ratio or stress level (S) in percent	
		2×10^6 cycles	10×10^6 cycles
MUIR	39-63	66	63
" (Corrected by Goodman diagram)	39-63	61	57
RAJU	40	62	58
JINAWATH	36	63	59

From Table 5.9, it appears that the fatigue strength ratio slightly decreased as the static strength increased. However, the decrease of the fatigue strength ratio with the increase in static strength appeared to be too small to be of practical importance.

The S-N diagram also indicated the high sensitivity of fatigue life to small changes in the maximum stress levels. A decrease in stress level of only 6 percent resulted in an increase in the fatigue life, from about 95,000 cycles to 1.1×10^6 cycles.

5.4.2 S-N-P diagrams

The S-N diagrams discussed in Section 5.4.1 provide at best an approximate indication of the trend of the relationship between the variables, stress level and fatigue life within an undefined broad range of probability values. This conventional representation of fatigue tests neglected an important characteristic aspect of all fatigue data, namely their scatter. In view of this feature, it is now accepted by investigators[28,30,65] that the S-N diagram should be extended to include the probability of failure P as a third variable, enabling the number of cycles at a given stress level to be determined for a chosen probability of failure.

5.4.2.1 S-N-P diagram from McCall's Model

McCall[30] in 1958 published the first report in which the dimension of

probability was added to the fatigue studies of concrete. The mathematical model proposed to establish a relationship between the Stress level S, the fatigue life N and the probability of failure P can be represented as:

$$L = 10^{-aS^b(\log N)^c} \qquad \text{.....(1)}$$

Where L = Probability of a specimen surviving 'N' repetitions of load.

= (1-P), where p = Probability of failure = m/(n+1)

S= Ratio of the maximum repeated stress to static strength.

a,b,and c are experimental constants

Hence, $\log(-\log L) = \log a + b \log S + c \log\log N$ .....(2)

For ease in computation, this was used in the linear form,

$$Z = A + BX + CY \qquad \text{.....(3)}$$

Where $Z = \log(\log N)$; $X = \log S$; $Y = \log(-\log L)$;

$$A = -\frac{\log a}{c} \; ; \; B = -\frac{b}{c} \text{ and } C = \frac{1}{c}$$

The fit of the present test data to the model was investigated by conducting a multiple regression analysis with 'X' and 'Y' as independent variables and 'Z' as a dependent variable. The constants determined by the regression analysis were,

$$Z = 6.933756 - 3.350850X + 0.119501Y \qquad \text{.....(4)}$$

and $$L = 10^{-9.49 \times 10^{-59} S^{28.04} (\log N)^{8.368}} \qquad \text{.....(5)}$$

These two equations correspond to Eq(3) and (1) respectively. A measure of the degree of correlation of the variables S, N, and L was obtained by calculating the multiple correlation coefficient which had a value of 0.981468 while the standard error of estimate was 0.0293957. The statistics of the results of the regression analysis are presented in Table 5.10.

5.4.2.2 Discussion

The test results are compared with those predicted by the model in Fig.

5.3. While the test results compare favourably with the model prediction for a stress level of 75 percent, there are large deviations for the increasing and decreasing stress levels. In McCalls model dY/dZ is constant so that the graphical representation of Y against Z for discrete values of S results in a series of parallel straight lines representing the various stress levels. The fatigue test data indicate that the range of scatter of log N at higher stress levels is greater than that at the lower stress levels (Table 5.5, p.40). A close examination of the test data plotted in Fig. 5.3 suggests that the slope dY/dZ of the lines representing the various stress levels should decrease with the increase in stress level and vise versa.

5.4.3. S-N-P diagram from Modified McCall's Model[28]

In order to accommodate the phenomenon of scatter associated with any stress level as indicated by the fatigue test data, it was necessary to modify the logarithmic form of the model suggested by McCall. Raju[28] proposed a form as follows:

$$Z = A + BX + CY + DXY \qquad \ldots\ldots\ldots(6)$$

where the symbols had the same meaning as in the previous section with 'D' as an additional constant. The last factor 'DXY' represented the variation in the scatter. The fit of this equation to the present fatigue data was investigated and the constants evaluated by a multiple regression analysis of the fatigue data were found to be :

$$A = 5.637252,\ B = -2.659922,\ C = -2.151478 \text{ and } D = 1.210185$$

The modified form is compared with the test data in Fig 5.4, and is found to give a somewhat better fit to the experimental results as indicated by the multiple correlation coefficient which improved from 0.981468 to 0.989958, while the standard error of estimate decreased from 0.0294 to 0.0220 . The statistics of the multiple regression analysis are shown in Table 5.11.

5.4.4. S-N-P diagram from the cumulative normal distribution function[28]

An alternative approach was made to derive the S-N-P diagrams by using the conventional S-N relation discussed in Section 5.4.1 and the cumulative normal distribution function.[69] The regression equation,

$$\log N = 17.422118 - 0.177616S$$

can be used to predict the fatigue life 'N' for any given stress level 'S' with a 50 percent probability as it is derived from a least square analysis. The relationship of S,N and P is given by the cumulative normal distribution function as :

$$P = \frac{1}{\hat{S}\sqrt{(2\pi)}} \int_{-\infty}^{X} \exp\left[-(x-\mu)^2/2\hat{S}^2\right] dx \qquad \ldots\ldots\ldots(7)$$

Where: P = Probability that failure will occur at a number of cycles equal to or less than N.

$X = \log N$

$\mu = (17.422118 - 0.177616S)$; S = Maximum stress level ;

$\hat{S}$ = Estimate of the standard deviation of the population found to be 0.461153 (Table 5.8)

Eq (7) can be used in the simplified form for computation as follows:

$$\log N = \mu + K\hat{S} \qquad \ldots\ldots\ldots(8)$$

The estimate of fatigue life at a given stress level for the required probability of failure can be made by using suitable values of 'K' from a standard statistical table.[70] The S-N-P diagrams shown in Fig 5.5 were derived in this manner for probabilities ranging from 0.01 to 0.99 and stress levels from 65 to 85 percent using the following values of K:-

P	K
0.01	-2.326
0.05	-1,645
0.10	-1.282
0.30	-0.524
0.50	0.0

0.70	+0.524
0.90	+1.282
0.95	+1.645
0.99	+2.326

5.5 Comparison of S-N-P diagrams and recommendations

The comparisons of the three sets of S-N-P diagrams derived from McCall's model, the modified McCalls's model and from the cumulative normal distribution function representing probabilities of failure range from 0.05 to 0.95 and 0.01 and 0.99 are shown in Fig 5.6 and 5.7 respectively. The selection of any set of diagrams for estimation of fatigue life depends mainly on the exact nature of the variation of scatter associated with the stress level; this cannot be accurately done on the information gained from a small number of tests. Diverse trends had been observed by different investigators but, again, all involved limited number of tests. Venuti[71] in an investigation of fatigue strength of prestressed concrete beams observed that the variability of logarithmic fatigue life increased with the increase of stress level. The results of Raju,[29] Antrim and Mclaughlin[23] showed similar trends in the tests of high strength concrete, ordinary and air-entrained concrete in compression, while the fatigue tests of Ople and Hulsbos[31] indicated the reverse trend of decreasing variability in the fatigue life with the increase in stress level. Little evidence is available from other sources to explain this anomaly; therefore, it is important that the comparison of the results of previous tests carried out under widely different conditions be made with caution. Raju[72] suggested that the S-N-P diagrams derived from the cumulative normal distribution function appeared to be generally valid on the ground that they covered the scatter of test results reasonably well at stress levels between 65 and 85 percent. However, his conclusion came from a graph in which several groups of previous test results were plotted against the probability limits obtained from the analysis of his own test data. Actually every group of test results will have different probability limits, and

should be analysed individually, which is beyond the scope of this investigation. Nevertheless, this work provided a good comparison with the other available evidence and showed clearly the difficult task involved.

As discussed in Section 5.4,p42, the results of the present investigation showed the trend to wider scatter at higher stress levels. In fig. 5.6 and particularly fig. 5.7, this was in agreement with the diagrams derived from the modified McCall's model in which the scatter band at any stress level representing the range of variability of fatigue life increased with an increase in stress level, whereas in McCall's model the scatter band increased with a decrease in stress level. The diagrams derived from the cumulative normal distribution function show a uniform scatter at all stress levels and alone of the three diagrams covered all the test results in the present study.

In view of the high variability of fatigue life and in the absence of any reliable data regarding the scatter, it is recommended that prediction of fatigue life should be made by the S-N-P diagrams derived from the cumulative normal distribution function based on constant scatter at all stress level.

5.6 Conclusions

1) The fatigue life distribution of plain concrete specimens at a given stress level is approximately log normal.

2) A satisfactory relationship between the two variables, predicted fatigue life and maximum stress level can be achieved by a linear regression analysis.

3) In an estimation of the fatigue life, the probability of failure should be included as an additional variable in the light of the high variability inherant in the fatigue test data.

4) Pending the availability of more extensive test results regarding the scatter, the S-N-P diagrams derived from the cumulative normal distribution function using the conventional S-N diagram, may be accepted for stress levels between 65 and 85 percent.

CHAPTER SIX

ANALYSIS OF RESULTS: OTHER EFFECTS

6.1 General

As has been described earlier in Chapter 2, the fatigue behaviour of concrete is related to some of its other characteristics which undergo changes when a stress is applied. The progressive changes of these characteristics with time, under the effect of a repeated cyclic stress, may give some further indication of the degree of accumulation of fatigue damage.

6.2 Test procedure

For a detailed examination of the relationship between these changes and the fatigue life, the first three of the four prisms comprising the series B, were tested at maximum stress levels, of 80, 75 and 70 percent of ultimate static strength with a lower stress of 5 per cent. The last prism in the series was used as a pilot specimen, tested under variable amplitude cyclic loading, (the results of which will be discussed in detail in Chapters 9 - 10). These tests in series B were conducted in addition to the tests in series A with the purpose of gathering more information especially in regard to lateral strains. The average static strength of the batch of concrete is shown in Table 6.1. A static loading cycle was conducted before the start of the fatigue test with strain measurements on all four sides of the specimens for regular increments of load, up to a maximum corresponding to the maximum stress level assigned to the specimens. Thereafter a static load cycle was applied at suitable intervals by interrupting the fatigue test, and the stress-strain curves shown in Figures 6.1 - 6.5 were obtained.

6.3 Shapes of stress-strain curves

The first stress-strain branch on loading in compression is convex

towards the stress axis. This is due to the development of bond cracks between matrix and aggregate oriented at parallel to the direction of application of load and is absent in neat cement paste.[73] The effect is confirmed by the decrease in pulse velocity in the lateral direction perpendicular to the loading axis (Fig. 6.1) to which no corresponding decrease has been observed in neat cement specimens.[62] After a few cycles of loading the loading branch becomes straight and gradually reverses its curvature (i.e. concave towards the stress axis), the slope $(\frac{dS}{d\varepsilon})$ becoming steeper in the upper ranges of stress. (Figs. 6.2 - 6.4). This has been similarly reported by several investigators[27, 29] and indeed these changes were observed in the earliest fatigue studies.[14,15] The reversal of curvature is attributed by Mehmel[17] (confirmed by Bennett and Raju)[29] to the existence and development of bond cracks perpendicular to the direction of loading; their closing leads to a progressive increase in stiffness (termed low-strain stiffness) as the load is increased. At the same time the pulse velocity measurement in the lateral direction which will be discussed in Chapter 7, indicated that during this closing stage of horizontally oriented cracks, the existing vertically oriented cracks were also widening under the influence of the load (Fig. 6.1). When the horizontal cracks were closed this tended to arrest the widening of the vertical cracks hence d S/dε became steeper as the load increased. Provided that the stress level was less than about 85% there was no further cracking in the direction parallel to the load at least not during the static loading. Mehmel also found that there was no low-strain stiffness effect in neat cement. The second reversal of the stress-strain loading branch to become S-shaped when approaching failure, which was first reported by Van Ornum[14,15] was also observed to occur in the present work for the highly-stressed specimens (Figs. 6.1, 6.2). From Fig. 6.1, it can be observed that this is due to the development of more vertically oriented cracks as indirectly indicated by further decrease in pulse velocity in the

lateral direction after the existing vertically oriented cracks have been arrested.

6.4 Hysteresis

The interest in the area enclosed by the loading and unloading branches of the stress-strain curve for a material (hysteresis loop) arises from the fact that it represents the energy absorbed within the material per cycle of load and is manifested by a rise in temperature of the specimen due to the internal friction.[46] Since an application of cyclic stress always leads to some inelastic deformation resulting from the internal structural modification, the change in the area of the subsequent hysteresis loops as compared with the first loop will represent the reduction in the rate of absorption of energy. The irreversible deformation involved may be either in the form of crack initiation or irreversible deformation without a loss of continuity, such as a viscous flow.[52]

Concrete exhibits a large hysteresis area on the first loading cycle due to the high degree of bond microcracking occurring in this cycle (Figs. 6.2 - 6.5). Subsequent cyclic loading results in a reduction in area of the hysteresis loop. The typical changes in the area with cycles of repeated load, expressed as a percentage of the area of the first loop, are shown in Fig. 6.6. The variation of the hysteresis area with the fraction of total fatigue life of the specimens (as denoted by the cycle ratio n/N, where n = number of applied loading cycles, N = number of loading cycles at failure) is also shown in Fig. 6.7. From fig. 6.6, it will be observed that after a few hundred cycles of stress, the hysteresis area was reduced to about 40%of the original area. The study of Fig. 6.7 will reveal that this change occurred at as early as 1 percent of the total life. From the same graph, it can be said that the changes in the hysteresis area consist of 3 stages, namely rapid decrease of the area as early as n/N = 1 to 10% (bond microcracking formation - stage 1), followed by a uniform decrease

from 10 to 85% of the total life (manifested by a rise in temperature coupled with a slow and stable propagation of one or more cracks[74] and some non-elastic deformation without disruption of continuity of the material[52] - stage 2). Finally, when approaching failure, the hysteresis area shows a renewed increase due to the extension of microcracking into the matrix[29] and hence increased the energy absorption (stage 3). It can also be concluded that the lower the maximum stress levels the greater the decrease of the hysteresis area (Fig. 6.7).

6.5 Total strain

Total strain (ε) is defined as the sum of the elastic strain, ε_{el}, (the instantaneously recoverable part of the deformation) and the inelastic strain, ε_{inel}, (the delayed recoverable and the irrecoverable part of the deformation). The variation of the total strain with the number of loading cycles and with the cycle ratio is shown in Figs. 6.8 - 6.11 for specimens tested at 80%, 75%, 70%; and 65% respectively. Generally it can be said that the total strain gradually increased with increased cycles of load, the rapid increase observed as failure approached being exaggerated by the logarithmic scale of the number of cycles (Fig. 6.8 and Fig.6.10). From the study of the curves in Figs. 6.9 and 6.11, it can be observed that the variation of ε with n/N shows the same trend as the changes in the hysteresis area although of a different order, namely a rapid increase from 0 to about 12% of the total life, a uniform increase from 12% to about 90% of the total life and a slight increase in the rate ($d\varepsilon/d(\frac{n}{N})$) from about 90% to failure. One significant observation which can be derived is that the amount of the total strain is larger the lower the stress levels (Fig. 6.9 and 6.11). This is probably due to the smaller number of loading cycles which the highly stressed specimens can sustain before failure as compared with the low stressed specimens.

6.6 Elastic strain

Elastic strain, the instantaneously recoverable part of the deformation, is defined here as the difference between the strain at maximum stress (total strain) and that at zero stress observed on the unloading branch of a stress-strain cycle. The typical changes observed in the elastic strains with the number of loading cycles and with the cycle ratio of specimens subjected to different stress levels are shown in Figs. 6.12 and 6.13 respectively. From Fig. 6.12, it is observed that the elastic strain increased with the number of cycles of load. The strain data plotted against the cycle ratio (Fig. 6.13) again shows the same trend as the changes in the total strain, namely a rapid increase from 0 to 10% of the total life, a uniform increase from 10 to 85% of the total life and a slight increase in the rate $(d\varepsilon_{el}/d(n/N))$ from 85% to failure. However, the specimen which was tested at 65% stress level did not show any sign of rapid increase at as late as 98% of the total life. From Fig. 6.13, the results seem to indicate that the higher the stress level the higher the elastic strain at failure. This observation is contrary to those of Raju[28] who concluded that there seemed to be a limiting value of elastic strain near fatigue failure which was independent of the stress level and hence the number of cycles to failure. It has been shown that there is a slight increase in both the total strain and in the elastic strain at about 90% of the total life to failure. This probably explains the contradiction between the results of Raju and of the present tests. Owing to the limited data available and the absence of an instrument which could record the strain history up to failure without interrupting the tests the difference cannot be explained at present.

6.7 Inelastic strain

The component of strain which is not immediately recoverable at any stage during the course of the fatigue test is here referred to as inelastic

strain. This is normally made up of the strain due to viscous flow and microcracks, which is irrecoverable, and that due to delayed elasticity, recoverable over a period of time.[28,75] Figs. 6.14 and 6.15 show the typical variation of the inelastic strain with the number of loading cycles and with the cycle ratio of specimens subjected to different stress levels. It can be observed that the inelastic strain at the first cycle of loading was larger the greater the stress levels and the strain increased with the number of cycles of load (Fig. 6.14). Plots of the inelastic strain with the cycle ratio (Fig. 6.15) with the exception of the specimen which was tested at 80%, suggested that there was a gradual increase starting from the first cycle of loading rather than a marked increase in the early fraction of the total life. The strain showed a greater rate of increase at about 75 to 85% of the total life to failure. For the specimen which was tested at 65% stress level, the strain showed a marked increase from 0 to about 15% of the total life followed by a uniform increase up to 98% of the total life without showing any sign of rapid increase towards the failure. The plot of the ratio of the inelastic to elastic strain against the cycle ratio indicates that the increase in the inelastic strain component is considerably greater than the elastic component so that the ratio always increases with the total fatigue life which confirms the observations made by Mehmel[17] and Raju.[28] One significant fact emerging from Figs. 6.14 - 6.15 is that in general the lower the stress level the higher the inelastic strain. It is interesting to note that from the measurements of pulse velocity in the lateral direction (which will be discussed in Chapter 7) it will be seen that the lower the stress level the greater the percentage decrease of the original pulse velocity. In all the specimens which were tested at a stress level of less than 60%, almost all the inelastic strain was due to the combined effect of viscous flow and microcracking,[75] but the reduction of pulse velocity is entirely due to microcracking. This,

therefore, indicates that the component of inelastic strain due to micro-cracking is predominant.

6.8 Modulus of elasticity

The secant modulus of elasticity at various stages in the fatigue tests was calculated using the elastic strain data discussed in section 6.6 and the typical results plotted against the number of cycles and the cycle ratio are shown in Figs. 6.17 - 6.18 respectively. A progressive decrease with the number of loading cycles was observed in all specimens which were tested at 80, 75, 70 and 65% stress levels (Fig. 6.17). In Fig. 6.18, with the exception of the specimen tested at 65% stress level, it can be said that the higher the stress level the lower the percentage decrease of the original modulus of the elasticity. The initial decrease is probably due to the development of bond cracks in a load oriented at direction, followed by the uniform decrease from about 10 - 85% of the total fatigue life probably as a result of the progressive propagation of the cracks. Finally a very slight decrease in the modulus prior to failure was observed probably due to the initiation of matrix cracks, the propagation of which rapidly leads to failure.

6.9 Volumetric strain and Poisson's ratio

Figs. 6.19 - 6.21 show the static stress-longitudinal (axial), lateral, volumetric strain (defined as equal to the longitudinal strain - 2 lateral strain)[76] and Poisson's ratio relationships for specimens tested at 80, 75 and 70% stress levels respectively. Generally, it can be said that the higher the stress level the larger the longitudinal, lateral and volumetric strain. The same conclusion can also be applied to Poisson's ratio. The changes of the volumetric strain with time under constant amplitude cyclic loading are shown in Figs. 6.22 - 6.24. The changes in the Poisson's ratio with time are also shown in Fig. 6.25 - 6.27. From Figs. 6.22 - 6.24, it can be observed that the volume of concrete under

cyclic loading at stress levels between 70 - 80% starts to increase rather than decrease after a few hundred cycles of loading (corresponding to about 15% to 25% of the total life) and the lower the stress level the earlier in its fraction of the life that the volume starts to increase. This period corresponds to the marked increase in strain values and the significant decrease in the hysteresis area and modulus of elasticity. The beginning of the volume dilation was observed by Shah and Chandra[75] to be related to the sharp increase in the length of continuous cross-linked microcracks indicating the beginning of slow crack growth. In other words, the beginning of the volume dilation corresponded to the beginning of the uniform increase and decrease of the above characteristics. It is interesting to mention also that the first loading and unloading branches of the stress-volumetric strain curves are convex towards the stress axis and apart from the curve of BF - 3(S_{max} = 70%) the curves showed a slight reversal at the upper range of the stress. This reversal is the point at which under static loading the volume of concrete starts to increase rather than decrease. After a few hundred loading cycles the sign of the volumetric strain changes from contraction to expansion and becomes straight and gradually reverses its curvature to become concave towards the stress axis. Shah and Chandra[74] observed that such behaviour was not found in hardened cement paste specimens; the volume of the paste continued to decrease until failure occurred. It was observed that there was a very rapid increase in the strain value when approaching failure. For example, in Fig. 6.23 the last recorded values of the strain corresponding to about 98% of the total life was about 3 times the magnitude of the strain value at about 84% of the total life.

Figs. 6.25 - 6.27 show that Possion's ratio increases with the number of loading cycles for all specimens which failed in fatigue. This is in contrast to the decrease in the ratio with time under both static and

cyclic stresses found by Whaley[46] and is due to the much lower maximum stress levels used (30 - 60% against 70 - 85% in the present work) as a result of which beneficial effects due to understressing namely, redistribution of stress from matrix to aggregate as a result of viscous flow etc.,[28,46] took place. The low-strain stiffness effects can also be observed from the curves in Fig. 6.26 - 6.28 which show a large decrease in the ratio at low stress with an increase in stiffness at the higher stress as the number of cycles increases. It is observed also that at the first cycle of load the maximum value of the ratio occurs at the maximum point of the increasing load. However as the number of cycles increases towards failure the minimum value of the ratio occurs at the maximum stress level. This is probably due to the closing of the horizontally oriented cracks which causes the marked increase in the longitudinal strain at low load and hence the decrease in the ratio.

6.10 Conclusions

The principal feature to emerge from the observations discussed is that cyclic stresses of constant amplitude have a progressive effect on the properties of concrete each of which is affected to a varying degree depending on the level of stress. These changes may be summarised as follows:

1. The changes in the shape of the stress-strain curves depend on the maximum stress level and the number of loading cycles. These changes qualitatively indicate the phenomenon of progressive damage of fatigue in compression.

2. Generally, the changes in the characteristics affected by the application of cyclic loading consist of 3 stages, firstly a rapid decrease in the area of the hysteresis loop and secant modulus of elasticity and an increase in the total strain, elastic strain, inelastic strain, volumetric strain and Poisson's ratio up to 0 - 10% of the total life. This is followed

by a uniform decrease of the first two and a uniform increase of the other characteristics mentioned above between about 15 - 90% of the total fatigue life. Finally when fatigue failure occurs, there is a slight increase in the hysteresis area, the total strain, elastic and inelastic strain, volumetric strain and Poisson's ratio while the secant modulus of elasticity shows a slight decrease.

3. The lower the maximum stress level the larger the decrease of the hysteresis area. This observation applies to all the three stages of changes.

4. The amount of the total strain is larger the lower the stress level. The same conclusion applies to the inelastic strain.

5. The elastic strain data seemed to indicate that the higher the stress level the larger the value of the elastic strain at failure.

6. For all specimens which failed in fatigue, the secant modulus of elasticity decreased with the increase in the number of loading cycles and the results seemed to indicate that the lower the stress level the larger the decrease.

7. When concrete specimens are subjected to cyclic compressive loading for about 15 - 25% of the total fatigue life the volume of concrete starts to increase rather than continuing to decrease.

8. Poisson's ratio increases with the number of loading cycles for all specimens which failed in fatigue.

CHAPTER SEVEN

STUDY OF FATIGUE DAMAGE BY ULTRASONIC PULSE VELOCITY METHOD

7.1 Introduction

In the previous chapter, certain characteristics of concrete have been shown to be affected by cyclic loading and their relationships with the cycle ratio have been demonstrated. These relationships, may with some reservations be employed as indirect indications of how a specimen undergoes changes (fatigue damage) at a particular constant amplitude cyclic stress level through-out its life. It is obvious that the relationships established are only useful in the determination of the damage-cycle ratio relationship of laboratory specimens and are of little use in actual structures. Furthermore, owing to the limitations of the available strain-measuring instrument it was necessary to interrupt the cyclic loading at intervals to measure strain. This practice introduces rest periods into the loading programme and may hence affect the results. The fatigue damage of concrete has been seen to be a process of progressive permanent internal cracking of microscopic width at the cement matrix/aggregate interface, in the matrix itself and sometimes extending into the coarse aggregate. Thus a method of detecting the initiation and propagation of cracks without interrupting the cyclic loading would be a very useful tool in fatigue research.

Ultrasonic pulse velocity measurements have been successfully related to the incidence of cracks and other voids. With the development by Elvery and others[61] of the PUNDIT (Portable Ultrasonic Non-Destructive Digital Indicating Tester), it is possible for the first time for pulse velocity measurements to be taken continuously during a cyclic loading test. In this chapter, the possibility of using ultrasonic measurements

as external indicators of changes in the internal microstructure of concrete subjected to cyclic loads is investigated.

7.2 General reviews

The ultrasonic pulse velocity technique involves measuring the transit time of an ultrasonic pulse through a path of known length in a concrete specimen. Since the velocity of the ultrasonic pulse in a solid material depends on the density and elastic properties of the material and is also affected by the presence of cracks, the measured pulse velocity can be used to indicate these properties. The technique was first introduced by Long, Kurtz and Sandenaw [77] in 1945 and at that stage was essentially confined to the determination of the elastic properties of a material. An early instrument was also developed by Jones and Gatfield[58,59] in England and independently in Canada by Leslie and Cheesman[60] in 1946-1950 (Soniscope). It was soon realized that the technique, as a non-destructive testing method, had a definite advantage over the alternative method of measuring the resonant frequency[78] in that it could be used on any element irrespective of its size and shape. Many investigators, notably Jones in 1949,[58] and 1952,[79] deduced the presence and development of microcracks from the changes in velocity of an ultrasonic pulse. Jones showed that in a compression test the cracks are mostly parallel to the direction of the load. His technique was later used by several other investigators in the study of the properties of concrete and the initiation and propagation of cracks under both tension and compression. Examples are found in the work of Jones and Gatfield (1955),[59] Rüsch (1959)[80] who unlike Jones measured pulse amplitude instead of velocity, Kaplan (1960),[81] and of Shankar (1963)[82]. More information about extensive work done in Canada and U.S.A. during the period of 1945-1958 was also published in 1959 by the Highway research board.[83] The first authoritative book on the nondestructive testing of concrete and pulse velocity techniques in

particular was published by Jones in 1962[84], and was followed by an ACI Monograph No.2 in 1966.[85] A general review of nondestructive testing by Jones was published posthumously in 1970,[86] in the ICE symposium on nondestructive testing of concrete and timber (1969) in which several interesting papers were also presented. More recent progress in this field was described by Bennett and Raju (1969).[29] Shah and Chandra (1970)[62], Elvery (1971),[61] and Nwokoye (1973).[89] Finally, the British Standard Institution has issued B.S.4408: Recommendations for Nondestructive Methods of testing for Concrete in 1971.[90] These have been published in separate parts and the part concerned with ultrasonic testing is covered by B.S.4408: Part 5: 1971.

7.3 Testing procedure

The equipment and testing technique for the measurements of pulse velocity of concrete specimens under static and cyclic loading is described in Section 4.3, p.31. Since cracks were known to form mostly in the middle part of a specimen and parallel to the direction of the load under uniaxial compression, most of the tests were performed with the transducers on opposite sides at the mid depth of the specimen so as to measure the pulse velocity in the lateral direction perpendicular to the applied load. A study of the percentage decrease of the original pulse velocity in the longitudinal direction parallel to the load was also made on a few specimens subjected to cyclic loads in order to confirm the presence of cracks perpendicular to the direction of the load.

It should be noted that all the work referred to in Section 7.2 was concerned with the properties of concrete and the initiation and propagation of cracks under static loading only. It is the purpose of this part of the present work to study crack initiation and propagation under both static loading and cyclic loading. With regard to the latter, the change in pulse velocity has for the first time been monitored continuously

throughout a fatigue test. By this practice the complication arising from the introduction of rest periods has been eliminated thus improving the accuracy of the test results.

7.4 Analysis of pulse velocity test results

7.4.1 Static tests

The changes in pulse velocity in the lateral direction were measured at intervals during the static control tests and in the first static loading cycle of the fatigue tests on prismatic specimens. Typical curves of stress against percentage decrease of the original pulse velocity for the first few cycles are shown in Figs. 7.1 - 7.4 (also in Fig. 6.1). It will be seen that there is no unique relationship between the stress level and the point where a significant decrease in the pulse velocity occurred. On the contrary the first decrease in the pulse velocity was sometimes observed at a stress as low as 20% and sometimes as high as 70% of the ultimate static strength. The early decrease is probably due to the extension of microcracks induced during setting and subsequently on drying due to local breakdown in the adhesion between the coarse aggregate and the matrix. The greater the amount of decrease which was observed at about 60% of the ultimate is approximately the stage at which the lateral strain, the volumetric strain and Poisson's ratio increased sharply (Figs. 6.19 - 6.21), indicating that microcracks of more significant influence on the elastic properties of concrete are formed and propagate from this stage onwards. This observation is in agreement with the findings of several investigators, namely Newman,[87] Robinson[88] and Jones and Kaplan[91]. According to Newman[87], stable crack initiation and propagation occur at applied stresses below 40% of the ultimate stress, whereas more significant cracking occurs between 40 - 60% of the ultimate. This behaviour was also inferred from acoustic and X-ray techniques.[88]

It was not possible to observe the maximum decrease of the original pulse velocity when failure occurred; however, the average maximum decrease observed when approaching failure was 9 - 10% of the initial pulse velocity which is in agreement with about 9% observed by Raju.[28]

A few measurements of the pulse velocity in the lateral direction were also made on control cubes. It was observed that the first decrease in the velocity was at 30 - 37% of the ultimate and the maximum decrease when approaching failure was about 15% of the initial value. It should be observed that under static loading, the maximum decrease in pulse velocity depends largely on the height to width ratio of the specimen. Jones and Gatfield[59] observed a total decrease of 15% in cubes whereas only half of that was noted for cylinders. The reason for this is that cylinders (or prisms as in the present work) which are more slender than cubes have been observed to undergo lateral deformation, when approaching failure, of only half the value observed in cubes.[45,59] For this reason, together with the above observations, a greater decrease in pulse velocity relates to a larger degree of deformation resulting from a larger degree of cracking both as regard with number and size of the cracks. Therefore, the degree of microcracking (fatigue damage) in both static and fatigue tests can be comparatively assessed by the magnitude of the decrease in pulse velocity.

7.4.2 Fatigue tests

The relationships between the stress and percentage decrease of the original lateral pulse velocity are shown in Figs. 7.1 - 7.4 for specimens tested at 80, 75, 70 and 65% stress levels respectively. Note that these measurements were made at suitable intervals in the course of the fatigue tests in test series A and B in which the need to measure strain compelled the interruption of the tests at intervals. However, the rest of the measurements were made throughout the tests in series C, D and

E continuously without interruption. An important feature to be noted from the figures 7.1 - 7.4 is the progressive growth of microcracks in the material due to fatigue as indicated by the gradual decrease of pulse velocity. A study of the figures also revealed that early in the fatigue life, the decrease of the pulse velocity in each cycle was greater at the maximum stress and the fact that the decrease of pulse velocity was linearly proportional to the stress indicated that there was no opening, closing or propagation of the cracks. After about 25 - 35% of the total life, however, there was an indication that microcracks began to "move", namely to open and close due to the application and removal of the load in each cycle as shown by the loop in the stress-velocity decrease diagram. At the same time there was a transition of the relationship namely, minimum decrease of pulse velocity corresponded to maximum stress as the number of loading cycles increased. It should be noted that this transition corresponds to the stage where low-strain stiffness effects also take place (Figs. 6.2 - 6.5), and corresponds to the convexity and concavity of the stress-strain curves (Figs. 7.1 - 7.4). The similarity between the two relationships implies firstly, that the variation of the stress-strain curves relates to the initiation and propagation of microcracks. Secondly, it indicates that the decrease of pulse velocity is a valid comparative method of monitoring internal changes in a specimen under cyclic loading.

7.5 Pulse velocity-number of cycles and Pulse velocity-cycle ratio relationships

The relationships between the decrease of pulse velocity and the number of loading cycles (n) are shown in Figs. 7.5, 7.7, 7.9 and 7.11 for the specimens tested at 80, 75, 70 and 65% maximum stress level respectively. For comparison, the relationships between the decrease of pulse velocity and the cycle ratio (ratio of the total fatigue life,

n/N) are also shown respectively in Figs. 7.6, 7.8, 7.10 and 7.12. For clarity, all of the relationships except that for the specimen tested at 75% stress level, are shown for the maximum decrease of original pulse velocity. To give a complete record, in Fig. 7.7 and 7.8 the relations for both maximum and minimum decrease of pulse velocity are shown. Generally, it can be said that the decrease of pulse velocity increases with the number of cycles and the cycle ratio. And on the average, the lower the stress level the greater is the decrease of pulse velocity. In Figs. 7.6, 7.8, 7.10 and 7.12, it will be noticed that there are 3 stages in the progress of the decrease of pulse velocity with the cycle ratio. Firstly, there is a sharp decrease of about 15 - 20% of the original velocity at about n/N = 10 - 20% (stage 1), followed by a gradual decrease of pulse velocity from n/N = 20% to 85 - 90% (stage 2). Finally, the rate of decrease of pulse velocity becomes slightly greater when approaching failure. There also seem to be unique relationships between the two pairs of variables represented by the equations:

$$V = a(n)^b \qquad \text{.....(7.1)}$$

and

$$V = a(n/N)^b \qquad \text{.....(7.2)}$$

where; V = maximum percentage decrease of original pulse velocity

n = number of loading cycles in cycles

n/N = the cycle ratio in percent

N = the number of loading cycles where failure occurred

a,b = experimental constants which can be evaluated by a regression analysis.

These equations are used extensively in the analysis of the problem of cumulative damage, both under constant amplitude and variable amplitude tests using the data illustrated in the Figs. 7.1 - 7.11, which will be discussed in detail in Chapters 9 and 10. However, it can be said at this stage that the relationships established can be used to estimate the extent

of fatigue damage suffered by the material, and that the relationships established are significant at the 0.1% level.

In addition to the study of the variation in the pulse velocity in the lateral direction, changes in the pulse velocity in the direction of the load were observed on two prisms in series B, the variation of which is shown in relation to the cycle ratio in Fig. 7.13. It can be seen that there is also a progressive decrease in the pulse velocity in the direction of the load and the decrease is greater as the cycle ratio increases. Note that the magnitude of the decrease of pulse velocity in the longitudinal direction parallel to the load was only about 15 - 23% compared with 40 - 50% of the original in the lateral direction. This proves that the majority of the microcracks formed during cyclic loading in compression are aligned in the direction parallel to the load and have been confirmed by the study of cracks by Bennett and Raju[29]. The frequently observed phenomenon of low-strain stiffness is also explained by the fact that horizontally oriented cracks exist and their closing, together with the opening of the vertically oriented cracks, causes the pronounced downward convexity of the stress-strain curve for low stress levels.

It is of interest also to note that there is a large difference between static and cyclic loading tests in the decrease of pulse velocity when approaching failure. The decrease of pulse velocity in fatigue tests is about 4 to 5 times that observed in static tests. This implies that the degree of cracking under repeated loads is significantly greater than that under static load. This observation is in agreement with those of several investigators[29, 62, 88] and is best confirmed in Plate 6 and Fig. 9.24 in which the cracking mode at failure under a static load and cracking mode under a cyclic loading test are shown respectively. It will be clearly seen that cracking developed under static load is much less extensive than in the fatigued specimens.

7.6 Discussion and conclusions

The study of fatigue damage (microcracking) by ultrasonic pulse velocity method investigated in this chapter has demonstrated that the method can be a very useful tool for detecting the development and growth of microcracks under repeated load as shown by the progressive decrease of original pulse velocity and its analogy to the stress-strain relationships, and from visual observation of the cracks themselves. The method offers far more useful features in the study of microcracking than the other techniques, namely, the use of a powerful microscope[92, 28] together with the assistance of strain gauges and extensometer[92] to locate the SURFACE cracks; slicing of specimens after applying a given number of loading cycles then grinding, dyeing, polishing and inspecting under a microscope[29, 93]. The former method was often very tedious and confined the observation on the surface only whereas in the latter the revelation of the location and length of the cracks were at the expense of loss of continuity of the specimens inherent in a slicing technique. Furthermore, the propagation of microcracks cannot be observed from one stage of test to the next.

There are also several other techniques in the field of logical nondestructive methods of testing in the study of the initiation and propagation of cracks namely, X-rays and fluorescent-dye technique[88] which sometimes required the specimen to be sawn, and therefore, suffered the same draw back in slicing. Another promising approach lies in acoustic methods which work on the principle that the formation or propagation of a microcrack is associated with the release of energy. When a crack forms or spreads, part of the original strain energy is dissipated in the form of heat, mechanical vibrations, and in the creation of new surfaces. The mechanical vibrations component can be detected by acoustic methods and recorded, hence microcracking may be detected by studying sounds emitted

from the concrete. Unfortunately, these methods require expensive equipment, trained personnel, specific size and shape of the material and involve difficult setting up of the equipment. The pulse velocity technique in comparison with the above methods, has considerable advantages in ease of setting up and operation in the laboratory or field; the method permits an assessment of the condition of concrete along the entire path length under both static and cyclic loading continuously through the test.

The use of the suggested relationships determined from tests on small specimens such as those used in the present tests to predict the remaining life of larger structural element requires caution. More tests are needed to study the effects of size, age, mix proportions etc., on pulse velocity in relation to the total fatigue life. The prospect of using the pulse velocity technique in the study of progressive fatigue damage of a brittle material is, however, much more promising and will be used extensively in the next part of the present work involving the study of the cumulative damage under variable loading conditions. It is felt that knowledge thus gained will be of value in assessing the remaining life of a partially fatigued structural element in the field so that the strengthening or replacement could be effected whenever the need arises.

The following conclusions are drawn from the research investigation:

1. Under the usual test conditions, with the specimens in contact with the steel platens, the onset of significant cracks was detected at different proportions of the ultimate load for different shapes of specimen, i.e. about 33% for cubes and about 60% for prisms.

2. When approaching failure, more cracks were developed in cubes than in prisms and were mostly parallel to the direction of the load.

3. A significant decrease in the pulse velocity occurs in both the lateral and longitudinal directions for concrete prisms subjected to

cyclic compressive loads of intensity 65 to 85 percent of the ultimate strength. The decrease becomes greater as the number of cycles increases.

4. Failure in all fatigued specimens is preceded by cracks mostly parallel to the direction of loading, as indicated by the magnitude of the decrease in the pulse velocity in the lateral direction which is nearly four to five times greater than that under static load.

5. The lower the stress level the greater the decrease in pulse velocity.

6. There are unique relations between the decrease of pulse velocity and the number of loading cycles and between the decrease of pulse velocity and the cycle ratio. Empirical relationships established between the parameters were significant at the 0.1% level and can be used in the detailed study of cumulative fatigue damage in compression.

CHAPTER EIGHT

REVIEW OF CURRENT CUMULATIVE FATIGUE DAMAGE HYPOTHESES

8.1 Introduction

As has been described in Chapter 2, the majority of investigations of the fatigue performance of plain concrete have been conducted by means of constant amplitude tests. However, the need to design for the fatigue life at one constant stresss level occurs very rarely in an actual structure, since the stress cycles in service vary greatly in magnitude, number and order. Owing to the complication of the stress variations, it is not practicable to perform enough tests to cover all stress variations, so that the fatigue performance of the actual structure can be accurately evaluated, particularly at the design stage, when the sizes of the structural elements are chosen. Moreover, there will always be some uncertainty in predicting and determining the fatigue-producing stress variations that the structure will experience before the structure has actually been built and put into service.

It is, therefore, necessary to employ a cumulative damage hypothesis for the prediction of the fatigue life of any structure subjected to a spectrum of stresses in random order. Despite the multiplicity of hypotheses available for the design of metal structures the original Palmgren-Miner cumulative damage hypothesis, (Miner's rule)[94] is still generally adopted.[13] There are several reasons for this. Firstly, it is simple to use and is often regarded as giving a conservative (safe) prediction, although this is not necessarily correct and has to be verified experimentally. Secondly, conventional S-N diagrams are commonly available and most of the practical alternative methods of life prediction require additional data which in many cases would be expensive to obtain. Finally none of the subsequent hypotheses has yet been proved sufficiently reliable to outweigh the probable increased complication of their use. For this reason, much of Part 3 of the present work will be devoted to the investigation

of the limitations of Palmgren-Miner hypothesis with particular reference to its application to the problem of cumulative fatigue damage in concrete in compression.

Only a limited amount of work[36] has been done on the problem of cumulative fatigue damage in concrete. Therefore, it is reasonable to review some of the proposed cumulative hypotheses in the more thoroughly studied field of metal fatigue since it may be possible to adapt one or more of these to explain the behaviour of concrete subjected to varying amplitude fatigue loading, In the review of the hypotheses two criteria have been suggested in order to classify them,[95] namely stress dependence and interaction effects.

8.2 Stress dependence

A distinguishing feature of various cumulative-damage hypotheses is the manner in which the course of damage depends on the stress amplitude. This is probably due to the fact that the number of cycles to failure depends on the stress amplitude i.e., the higher the stress amplitude or stress level, the less the number of cycles to failure and vice-versa. However, as will be described below, certain cumulative damage hypotheses can be termed "stress-independent hypotheses". Stress independent, in this case, means that equal amounts of damage are produced at equal fractions of the total life for all stress amplitudes. However, care is required in defining the terms "damage" and "life".

In a simple, constant amplitude test, the specimen is subjected to a constant stress range thoughout each individual test. After undergoing a number of stress cycles, or in some cases even after the first or second repetition of the stress cycle, fatigue damage occurs although it is not usually discernible. This damage is progressive in nature, (see Section 2.2.4.p.16. Mechanism of fatigue failure) and eventually leads to visible deterioration and the disintegation of the specimen (fatigue failure). At this stage, damage may be described as complete, or 100 percent. The process is depicted schematically in Fig. 8.1

Figure 8.2 shows the effect of the stress amplitude on the number of cycles to failure for several levels of stress. On the curves, equal amounts of damage as defined above are not equivalent in an absolute sense, because the damage at failure (indicated either by total strain at failure or by decrease in the ultrasonic pulse velocity in the lateral direction) has been observed to be different for differing stress amplitudes; greater ultimate damage occurs when the stress amplitude is small and the number of cycles to failure is larger.[29] (Chapter 6-7).

The damage measured must, therefore, be revised so that equal ordinates represent the same amount of damage. In the consideration of stress cycles of varying amplitudes in varying order, the amount of damage at failure for the highest stress in the spectrum can be used as a reference so that if the damage at failure for any stress amplitude is divided by the reference value, the resulting relationships between damage and number of cycles (fig. 8.3) will indicate the same true damage at equal values of the ordinate. With the damage measured as shown in Fig. 8.3, the number of cycles to failure in a constant amplitude test; N_i', should be replaced by N_i, the number of cycles that produces an amount of damage equal to the damage at failure at the highest stress amplitude S_1.

If the curves in Fig. 8.3 are adjusted by dividing n, the number of cycles applied, by N_i the number of cycles that produce the selected damage level (damage at failure at the highest stress amplitude), one or other of the two possibilities shown in Fig. 8.4 and Fig. 8.5, will result. The cumulative damage hypotheses that are stress-independent result in Fig. 8.4, while the cumulative damage hypotheses that reduce to the representation of Fig. 8.5 are stress-dependent. Note that the curves in Fig. 8.5 do not necessarily have to be non-intersecting between the origin and point 1,1.

8.3 Interaction effects.

The other important factor to be taken into account in a cumulative-damage hypothesis is interaction. If the relationship between damage and the number of cycles at a specified stress amplitude is assumed to be valid irrespective

of what other stress amplitudes are applied, the cumulative-damage hypotheses is termed an "interaction-free hypothesis". On the other hand, a hypothesis that assumes that the previous application of other stress amplitudes change the course of damage due to the given stress amplitude is an interaction hypothesis.

For example, consider a concrete specimen which has undergone sufficient stress cycles of varying amplitudes to produce a certain amount of damage after which one more stress cycle is applied, e.g. of amplitude S_3. For an interaction-free cumulative damage hypothesis, the increment of damage produced by this additional cycle would be the slope of the damage-cycle ratio curve for the given stress amplitude (S_3) at the level of damage which has already occurred multiplied by the increment of the cycle ratio. For an additional cycle, the increment in the cycle ratio , d(n/N), would be $1/N_3$. In equation form:

$$D = \frac{dD}{d(\frac{n}{N})} \cdot \frac{1}{N_3} \qquad \text{..... (8.1)}$$

where dD/d(n/N) is determined at the appropriate level or the damage curve for the stress ampitude, S_3. The cumulative damage hypotheses in which the above expression is not valid for the incremental damage are interaction hypotheses.

The definition of interaction-free hypotheses applies equally well to either the stress-independent hypotheses of Fig. 8.4 or the stress-dependent hypotheses of Fig. 8.5.

8.4. General comparison of cumulative damage hypotheses

8.4.1. Palmgren-Miner cumulative fatigue damage hypothesis and alliance hypotheses

The most generally known cumulative damage hypothesis, usually attributed to Miner,[94] will be used as a basis comparison. Miner's hypothesis was orginally applied to cumulative damage before the appearance of the first crack. However, there is no fundamental reason why it cannot be applied to life up to any state of damage (but the accuracy of prediction may well depend on the damage state considered).

Actually Palmgren[96] had presented cumulative damage equations identical to Miner's hypothesis some 20 years earlier, apparently as the result of a purely intuitive approach,[95] but it was Miner who made this hypothesis famous by presenting attractively simple cumulative damage equations supported by experimental work.

Palmgren-Miner hypothesis (Fig. 8.6) simply states that, irrespective of the magnitude of the stress, each and every stress cycle has some influence on the ultimate endurance of, and is responsible for a certain amount of fatigue damage to a specimen, component or structure. It specifically assumes that, for each stress amplitude, there is a linear rate of fatigue damage irrespective of the order of load application, and failure occurs when the sum of the damage, increments at each stress level accumulates to unity, i.e. damage is proportional to n/N, the condition for failure being represented by the equation:

$$\sum_{i=1}^{i=m} \frac{n_i}{N_i} = \frac{n_1}{N_1} + \frac{n_2}{N_2} + \frac{n_3}{N_3} + \ldots \frac{n_m}{N_m} = 1 \quad \ldots\ldots\ldots \quad (8.2)$$

where: N_1 to N_m = the number of cycles to failure at stress level S_1 to S_m;

n_1 to n_m = the number of stress cycles actually applied at each stress level in sequence.

Classification and comparison of the cumulative-damage hypotheses can be made by using the two characteristics distinguished in the previous sections namely, stress dependence and interaction effects, as follows:-

1. The cumulative damage hypotheses that reduce to a stress-independent damage-cycle ratio relationship when adjusted in the manner of Fig. 8.4 and are interaction-free are equivalent to the Palmgren-Miner hypothesis.

2. It has been proved [95,97] that the cumulative damage hypotheses that are stress-dependent, reducing to the form shown in Fig. 8.5 when adjusted, and are interaction-free will predict shorter life under random spectrum loading than would be predicted by the Palmgren-Miner hypothesis.

3. In order for a cumulative damage hypothesis to predict longer life than does the Palmgren-Miner hypothesis, it must obviously be an interaction type of cumulative damage hypothesis (and can be either stress-dependent or stress-independent). Interaction-type damage hypotheses can be constructed so as to predict either shorter or longer life than does the Palmgren-Miner hypothesis.

The hypotheses studied were selected as being representative of the breadth of the possibilities, not as being necessarily superior to the others that have been proposed. Those considered and the conclusions drawn from them are as follows:

Under the same classification as the Palmgren-Miner hypotheses of the validity of linear summation of the cycle ratios (stress-independent and interaction free) are those of Langer 1937 [98]; Doland, Richard, and Work 1949. [99] Valluri 1961 [100] in a much more complicated approach, proposed a hypothesis based on dislocation theory and plastic deformation of metal which is not relevent to this work. However, this theory is found to be equivalent to Palmgren-Miner hypothesis if certain restrictions concerning definition of fatigue damage are observed.

8.4.2 Stress-dependent and interaction-free hypotheses

As modified Palmgren-Miner hypotheses, Newmark (1951)[101], and in particular Marco and Starkey (1954)[102] have proposed hypotheses of cummulative damage based on the experimental observations of the fracture appearance of the specimens tested. The following was assumed.[102]

1. Fatigue damage is representable by the term D, and is a variable, beginning from zero when no cyclic-stress history exists in a specimen and becoming unity when the specimen has finally failed (i.e. completly fractured) under the influence of cyclic stressing.

2. Damage may be expressed quantitatively as a function of the cycle ratio number n_i/N_i

Thus, $D = f(n_i/N_i)$ ..... (8.3)

The general equation (8.3) is finally replaced by the exponential relationship:

$$D = (n_i/N_i)^{x_i}, \quad x_i > 1 \qquad \text{.....} \qquad (8.4)$$

The equation (8.4) when shown diagrammatically is similar to Fig. 8.5. These empirical damage-cycle ratio relationships, when used in the prediction of the life of a specimen will predict shorter life in a simple one step test (eg. 2 stages of loading) of high-low sequence namely, tested at S_1 for n_1/N_1 then loaded at S_2 to failure ($S_1 > S_2$) and vice versa. More generally, when applied to variable amplitude loading, this hypothesis will also predict a shorter life than the Palmgren-Miner hypothesis.[94,97]

Grover (1960)[103] has proposed a stress-dependent, interaction-free hypothesis that differs from the Palmgren-Miner hypothesis in that it postulates a two-stage damage process. It is assumed that cracks are initiated during an inital stage of damage as stress cycles are applied. In a single-level or constant amplitude test, this initial stage is completed at some fraction denoted by "a", of the total cycles to failure. In the second stage, propagation of cracks to failure occurs in the course of application of the fraction (1-a) of the total number of cycles

to failure. It is assumed that the value of "a" for any stress amplitude is constant whether or not cycles of other stress amplitudes are applied (i.e. interaction-free). It was pointed out by Kaechele[95] that the essential features of this theory are contained in the method proposed by Langer.

For cumulative-damage calculations under spectrum loading, it is assumed that the Palmgren-Miner hypothesis applies to each stage, which results in two equations:

$$\sum \frac{n_i}{a_i N_i} = 1 \qquad \ldots\ldots\ldots \qquad (8.5)$$

and

$$\sum \frac{m_i}{(1-a_i)N_i} = 1 \qquad \ldots\ldots\ldots \qquad (8.6)$$

where $n = n\bar{o}$ of cycles applied during the initial stage,

$m = n\bar{o}$ of cycles applied during the second stage.

As originally noted[103], if a_i is the same for all stress amplitudes in the spectrum, this theory is equivalent to the Palmgren - Miner hypothesis.

The normalized damage-cycle ratio relationships postulated by this hypothesis are shown in Fig. 8.7. It will be clearly seen that the hypothesis is stress-dependent, since the damage curves in Fig. 8.7 differ for different stress amplitude. Thus, it will predict failure in fewer cycles than will the Palmgren-Miner hypothesis when applied to the well-mixed stress spectrum.

There are insufficient data to provide a meaningful determination of the value of the parameter "a" and how it varies with stress amplitude. However, the hypothesis is still viable in its application in the field of metal fatigue where it has been proposed that the fatigue life of metal consists of several stages.[104]

8.4.3 Stress-dependent and interaction hypotheses

Corten and Dolan (1956)[104] proposed an interaction hypothesis which involves the attractive assumption that interaction effects can be determined from fairly

simple fatigue tests at two stress levels (one-step tests). As originally presented[104], the general form of this hypothesis includes both stress-dependence and interaction effects. Subsequent experimental work[105,106] in connection with the theory, however, led to the formulation of a stress-independent, interaction theory.

In the original presentation, the expression for damage as a function of applied cycles for stress amplitude S_i was given by:

$$D_i = \bar{m}_i r_i n_i^{\bar{a}_i} \qquad \ldots\ldots\ldots\ldots \quad (8.7)$$

where $\bar{m}$ = some number of "damage nuclei"

r_i = a crack-propagation constant,

$\bar{a}_i$ = Constant

These expressions are assumed constant for a specified stress amplitude (in a constant amplitude loading test) but may be different for different stress amplitudes. Damage at failure is prescribed as unity (or 100 per cent), giving

$$D_{fi} = \bar{m}_i\, r_i\, N_i^{\bar{a}_i} = 1 \qquad \ldots\ldots\ldots\ldots \quad (8.8)$$

By dividing $\bar{m}_i\, r_i\, N_i^{\bar{a}_i} = 1$ into Eq (8.7), the following expression for damage is obtained:

$$D_i = \left(\frac{n}{N}\right)_i^{\bar{a}_i} \qquad \ldots\ldots\ldots\ldots \quad (8.9)$$

The damage-cycle ratio relationship derived from this equation can be shown as in Fig. 8.4 or 8.5. As mentioned above, it was concluded that $\bar{a}_i$ was independent of stress for the materials (cold-drawn steel wire) and stress spectra used in the work; thus the case of Fig. 8.4.

Interaction effects are introduced into this theory, leading to the possibility of predictions that differ from the Palmgren-Miner hypothesis. It follows from the assumption that the number of damage nuclei produced by the highest stress in a spectrum will affect the growth at other, lower stress amplitudes.

It is assumed that the damage growth at lower stress amplitudes will be faster after a higher stress amplitude has been applied than when the lower amplitude is applied alone. In other words, $\bar{m}$ is considered to be larger for the higher stress than for the lower stress. With the interaction effect included, the damage Eq. becomes

$$D_i = \frac{\bar{m}_1}{\bar{m}_i} \left(\frac{n}{\bar{N}}\right)_i^{\bar{a}_i} \qquad \ldots\ldots\ldots \qquad (8.10)$$

where $\bar{m}_1$ = the damage - nuclei number for the highest stress in the spectrum (assumed to be applied early in the test)

$\bar{m}_i$ = the damage-nuclei number for the i^{th} (lower) stress amplitude.

By defining a new parameter as

$$M_i = \left[\frac{\bar{m}_i}{\bar{m}_1}\right]^{\frac{1}{\bar{a}_i}} \qquad \ldots\ldots\ldots \qquad (8.11)$$

The damage relationship of Eq. (8.10) can be written as

$$D_i = \left(\frac{n_i}{M_i N_i}\right)^{\bar{a}_i} = \left(\frac{n_i}{N_{I_i}}\right)^{\bar{a}_i} \qquad \ldots\ldots\ldots \qquad (8.12)$$

N_{I_i} which is equal to $M_i N_i$, is a revised (because of interaction) number of cycles to failure at the i^{th} amplitude which should be used in the damage equation when the i^{th} amplitude is mixed together with a higher stress amplitude.

For design purpose, a fictitious S-N diagram for use with spectrum loading can be constructed as a straight line passing through N_1 (the cycles to failure at the highest stress in the spectrum determined from constant amplitude tests) and through a point N_{I_i} at a lower stress amplitude. The value for N_{I_i} is determined from one-step tests containing the two stress levels S_1 and S_i. As

was observed in the original work,[104] $\bar{a}_i$ was independent of stress levels; therefore, cumulative damage could then be assessed for any spectrum by using the Palmgren-Miner hypothesis with the interaction S-N diagram thus obtained.

Apart from the above mentioned work, there are several proposed interaction hypotheses namely, the Freudenthal-Heller hypothesis,[107] Shanley's hypothesis,[108] Henry's hypothesis[109] etc. These hypotheses which in some instances were based on experimental findings and in others were purely theoretical relations introduced interaction effects in a more complex way, and mostly concerned the fatigue behaviour of metal and attempted to relate the cumulative damage to such factors as "Critical crack length", "Mean grain size", "Residual stress due to manufacturing process", etc. which are not very relevant to the study of plain concrete.

More critical reviews and analysis of the cumulative hypotheses as applied to the problem of metal fatigue up to 1971 can be found elsewhere.[95,97,101] Currently, there are at least 22 proposed hypotheses for the metal fatigue problem.[97]

8.5 Conclusions

1) There are two key assumptions with which to determine general trends of the life prediction by cumulative damage hypotheses, namely stress-dependence and interaction effects.

2) Cumulative fatigue damage hypotheses may be stress-dependent or stress-independent. That is the amount of fatigue damage by a certain cycle ratio may be the same for all stress amplitudes (stress-independent) or different (stress-dependent).

3) There may also be interaction or interaction-free hypotheses. The course of damage at one stress amplitude may be changed by other stress amplitudes (interaction), or it may be unaffected (interaction-free).

4) The Palmgren-Miner hypothesis simply states that when a spectrum of stress amplitudes is applied, fatigue failure will occur when the fractions of life expended at each stress amplitude which is the ratio of the number applied

at that amplitude (n_i) to the number that would cause fatigue failure at that amplitude (N_i); add up to one.

5) From the study of the key assumptions, it can be concluded that Palmgren-Miner hypothesis is a stress-independent, interaction-free hypothesis, and other hypotheses that have these assumptions are therefore equivalent to the Palmgren-Miner hypothesis.

6) Stress-dependent, interaction-free cumulative fatigue damage hypotheses when used to predict the life of a concrete specimen subjected to random loading of varying amplitude will predict a shorter life than the Palmgren-Miner hypothesis.

7) Interaction oriented hypotheses can predict a shorter or longer life than the Palmgren-Miner hypothesis and have to be verified experimentally.

CHAPTER NINE

TWO STAGE CUMULATIVE DAMAGE TESTS

9.1 General

At the design stage of engineering structures it is sometimes necessary to obtain a first estimate of fatigue life for any fatigue-sensitive structural elements. In many cases, such as loading in off-shore structures subjected to heavy wave action and loading in machine bases supporting heavy reciprocating metal presses, the service loading is of variable amplitude, and it is here that the need to employ a cumulative damage hypothesis arises.

The design of concrete structures subjected to complex service loading is frequently based on the Palmgren-Miner hypothesis[94,96] which assumes that each cycle in a constant amplitude test consumes the same percentage of the fatigue life of a specimen. If different maximum stress levels are applied within one test, failure occurs when:

$$\sum_{i}^{m} \frac{n_i}{N_i} = 1 \qquad \text{..... (9.1)}$$

$$i = 1,2, \ldots .m$$

Where n_i is the number of loading cycles at a stress level S_i, and N_i is the fatigue life of a specimen tested at S_i.

9.2 Limitation of Palmgren-Miner hypothesis

It is apparent from a study of the literature that the Palmgren-Miner hypothesis can give highly inaccurate estimates of fatigue life under variable amplitude loading. For example, in the only attempt to verify this hypothesis experimentally in flexural fatigue tests of concrete,[36] values of $\sum \frac{n_i}{N_i}$ varying from 0.01 to 2 have been reported. There also are many cases of metal fatigue tests where the values of $\sum n_i/N_i$ have been shown to differ significantly from unity, ranging from 0.01 to over 20.[110] The fact that Miner's data used in support of the hypothesis were derived from tests conducted solely on aluminium-alloy specimens, together with several doubtful basic assumptions in the

hypothesis can explain much of the variation in n_i/N_i as follows:

The basic concept of damage (D) may be expressed in function form as:

$$D = f(n_i/N_i) \qquad \text{.....(9.2)}$$

where n_i/N_i is the cycle ratio

Miner's hypothesis assumes that Eq.(9.2) has the linear form

$$D = n_i/N_i \qquad \text{.....(9.3)}$$

For any stress pattern, Eq (9.3) leads to the conclusion that the amount of damage done is exactly equal to the cycle ratio. Eq. 9.3 is shown graphically in Fig 9.1.

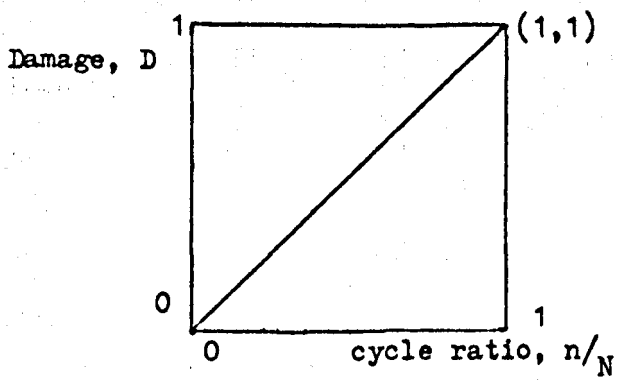

Fig. 9.1 CYCLE RATIO-DAMAGE RELATIONSHIP FOR $D = n_i/N_i$

From Fig. 9.1, it will be clearly seen that if a spectrum of varying amplitude loading is applied to a specimen until failure (D = 1), then

$$\sum_{1}^{m} n_i/N_i = 1$$

$$i = 1,2, \ldots m$$

This concept of damage assumes that if a certain fraction of the life X $= n_i/N_i$ is consumed at stress level S_1, there remains a usable life of $n_2/N_2 = (1-X)$ at any stress level S_2. According to this concept of damage, it makes no difference if S_2 is larger or smaller that S_1. More generally, the remaining usable life depends only on $\sum n_i/N_i$ for all the previous stress levels and is independent of the number of stress levels or the order in which they have occurred.

The hypothesis does not make allowance for the effects of understressing, neither does it take account of the application of an occasional high load which could cause severe damage at a point of stress concentration and the introduction of residual stresses as a consequence.

9.3 Methods of Verification

Many investigations had been carried out to determine the applicability of the hypothesis under a number of loading conditions. In metal fatigue studies, specimens were usually subjected to a sequence of stress cycles in which the amplitude and maximum stress level were maintained constant at one set of values for a fraction of the estimated life, then at another set of values for another fraction of the life, and so on until failure resulted (Step tests). However, in each case a limited number of tests has been run and usually only one specimen has been tested for a given stress pattern. In Miner's work,[94] tests were performed on single specimens for each sequence of loading, consisting of one, two, three, or four steps (VIZ, two, three, four, or five stages) in the sequence and the range of values for $\Sigma n_i/N_i$ was from 0.61 to 1.49, with an average value close to unity. On the basis of the same tests Dolan, Richart, and Work[99] reported a much larger range of values for $\Sigma n_i/N_i$; however, an average value of approximately unity was also indicated by these tests. Marco and Starkey[102] reported, on the basis of tests by Kibbey,[111] in which single specimens were tested with 2,3,4,5,6 and 7 steps, that the average value of $\Sigma n_i/N_i$ was 1.49 for ascending load, and 0.78 decending load. Marco and Starkey also confirmed in their own work[102] that $\Sigma n_i/N_i$ was less than unity in one step tests of decending load and more than unity in onestep tests of ascending load.

In the field of concrete, the results of Hilsdorf and Kesler,[36] quoted above. were obtained from one-step tests performed on single beam specimens for each sequence of loading. The block programme loading similar to the type used by Coten and Dolan[104] was employed in which a test load was applied in repeated

block each of which consisted of n_1 cycles at stress level S_1, n_2 at S_2 (Fig.92) The reported results indicated that $\Sigma n_i/N_i$ was sometimes greater and sometimes less than unity.

In view of the variation and wide range of values of $\Sigma n_i/N_i$ reported in these investigations and the uncertainty regarding the effect of the number of the steps in a sequence of loading and the order in which they are applied, a series of tests was conducted by the writer in an attempt to determine whether these factors would effect the value of $\Sigma n_i/N_i$ thus checking the validity and limitations of the Palmgren-Miner hypothesis.

The tests reported in Chapters 9 and 10 have been of two main types. First reported in this chapter, are the 'Step' tests, where testing commences under constant amplitude loading at one maximum stress level and the level is changed once after a fixed cycle ratio (n_i/N_i) to a second stress level which is maintained until total failure of the specimen has occurred. The minimum stress level is kept constant throughout, the maximum stress level being either decreased or increased from the first to the predetermined second stress level.

The second type of test is the mixed spectrum test ('spectrum' refers to amplitudes), which approximates more closely to service loading conditions. In such tests there are two or more steps, and after the final step repeated loading is continued to failure at the predetermined stress level. The difference between this and the first type of test is that although the stress level (viz. 70% and 80%) are kept constant, they are repeated in "saw-tooth" formation. The results of the writer's tests of this type will be discussed in chapter 10.

The validity of the Palmgren-Miner hypothesis is generally judged by the cumulative cycle ratio , for example, $\sum_{i=1}^{i=m} n_i/N_i$ at failure, and usually written in the abbreviated form Σ n/N.

9.4 Test procedures

All fatigue tests were carried out using two different loading programmes (1 and 2). In Programme 1 (Fig. 9.3a), a fixed cycle ratio (n_1/N_1) of repeated load was applied at a stress level S_1. After n_1 cycles the stress level was decreased to S_2 and the test continued until the specimen failed after an additional n_2 cycles. Programme 2 (Fig. 9.3b) is a reversal of Programme 1 in so far as the lower stress level was applied first, and after n_1 cycles the load was increased from S_1 to S_2. The only two maximum stress levels (S_1 and S_2) used in this part of the work were 80% and 70%. The choice was made on the basis that these represented an intermediate range of stress levels, whereas with a higher stress level (85% or more), excessive deformation resulting from creep can interfere with the tests and may cause premature failure of the test specimens. At the same time, any expected fatigue life of less than about 1600 cycles (which is the expected life at 80% stress level) was considered too short a time for sufficient data to be collected, considering that the speed of loading was 190 cycle/min. On the other hand, a lower stress level (65% or less) may lead to the side effect of understresssing or strengthening of the specimens, hence complicating the interpretation of the results. The minimum stress was kept constant at 5-6% throughout. A summary of the static strength of control cubes and prisms is shown in Table 9.1 and 9.2 respectively. A static loading cycle was conducted before the start of the fatigue test, with strain measurements on all four sides of the specimen for regular increments of load, up to a maximum corresponding to the maximum stress level S_1. This practice, together with continuous monitoring of any internal changes by ultrasonic pulse velocity measurement in the lateral direction was adopted for quality control purposes.

Thereafter, only continuous pulse velocity measurements were made without interruption of the fatigue test. This eliminated the need to introduce rest periods for monitoring purposes, which had been a necessity before the introduction of the digital indicating PUNDIT instrument. It was hoped that the continuous monitoring of any changes to the specimens during the fatigue tests would

improve the accuracy in interpretation of the results since it was known that rest periods can cause a lengthening of the fatigue life of the specimens.[11,36]

9.4.1 Selection Methods for fatigue specimens

Several pilot batches of specimens were tested with the loading programmes 1 and 2, selecting the specimens by the method outlined in section 5.2 chapter 5, p.38 . As was expected, inconsistencies among the results were encountered. Indeed, after a few batches had been tested, the inconsistencies were found to be so great that it was hardly possible to draw any conclusion from the experimental values of $\sum n/N$ and n_2/N_2. It was finally decided that apart from certain factors arising from the uncontrollable working charecteristics of the LOS Machine (e.g. the automatic load maintainer devices can introduce a variation in final loading of $\pm$ 3%); the main source of these inconsistancies was the variation in strength of the control prisms and the fatigue specimens. Therefore, more precise methods of selection of fatigue specimens were developed and thereafter used throughout this part of the work.

9.4.2 Nondestructive method of quality control

The previous method and the new method developed may be summarised as follows.

Previous method: Out of 8 prisms in a batch, 3 control prisms were randomly selected and tested to determine the likely average static strength of the batch on which basis the stress levels were calculated and randomly assigned to 4 fatigue specimens. The last prism was tested statically at the completion of the fatigue tests to check the gain of strength during the period of the tests.

Note; This method was sometimes changed to the following pattern; 2 control prisms before, 1 during and 1 at the completion of the tests. This was adopted especially when the period of testing was longer than the normal 7-9 days/batch, in order that a slight gain in strength during the test period could be detected and the assigned load adjusted accordingly.

Present method

1. Prior to testing, pulse velocity measurements in both the lateral and the longitudinal direction were made to every prism in a batch to check the uniformity of the concrete. The prisms were then separated into several small groups, each consisting of prisms which had the same lateral and longitudinal pulse velocity values. It is interesting to note that the longitudinal pulse velocity values showed more variation between different prisms than the relatively consistent lateral values. This was probably due to the fact that the prisms were cast vertically at the same time in 3 layers, and also to the longer distance (203.2mm compared to 76.2mm) involved. Usually, there were 2-3 small groups in one batch, with sometimes 1 or 2 odd specimens which had pulse velocity values much lower or higher than those belonging to the groups, indicating that they were worse or better compacted than the others. Using the fact that the specimens with the higher pulse velocity values, were likely to be denser and consequently stronger, control prisms were randomly drawn from each group and tested to determine the likely static strength of the groups. The odd specimens were discarded but as a check were tested statically to failure. The results of these static tests together with the weighing of every prism as a supporting check verified the above assumption.

2. As another measure of quality control; strain measurements were performed on all four sides of all control specimens and a set of load-deformation curves was drawn for each specimen and set aside as reference curves. These curves were compared with the load-deformation curves obtained from an initial static loading cycle of the actual fatigue specimens which were randomly selected from the groups. In the event of the load-deformation curve of a fatigue specimen not approximating closely to the curve of the control specimen of the same group, that specimen was treated with caution as being likely to be stronger or weaker than the expected strength value. In the case of severe departure of the load-deflection curve from the control curve, in either direction the final assigned stress level would be changed to the value corresponding to the

nearest control curve even though it had come from a different group of specimens.

3. As a final measure, a continuous history of the change in pulse velocity in the lateral direction, of a fatigue specimen under the assigned cyclic stress level (viz 70% or 80%) was recorded. This was constantly monitored and any specimen which showed either little or excessive change in pulse velocity under repeated loading cycles, was judged as either too strong or too weak and rejected. This practice helped to screen out any specimen which showed signs that the assigned stress level was either too low or too high in relation to the TRUE strength. The fact that the specimens which were judged too strong or too weak for the assigned load, always failed at approximately 2-3 times more or less than the expected life at the particular stress levels proved that this practice was effective.

It should be emphasized that these non-destructive measures are not a substitute for destructive testing, at least as far as the determination of the variation in strength among the group of specimens in a batch is concerned. It is always necessary to test control specimens statically to failure to find out the most likely static strength of the small groups, classified with the help of the above nondestructive measures. Nondestructive tests by themselves are comparative rather than absolute, and they should be used with caution and their correlation with strength should not be relied upon. However, with experience, and enough background information (the concrete used in this present work was of the same proportions, contituent parts and under the strict control of laboratory conditions) these nondestructive measures could provide useful and effective supporting information. The methods developed were more flexible and sensitive than the previous method which was previously used by several investigators[27,29,46] and also by the writer in the tests described in the previous part of the work. They could be used to detect a slight variation in the strength among the specimens in a batch BEFORE the testing began so as to establish the correct stress levels immediately prior to the fatigue tests. Moreover, they were sufficiently flexible to discover in time those specimens which were

wrongly loaded at the commencement of the tests.

9.5 One-step test results

The results of the one-step tests are summarised in Table 9.3. It will be observed that four specimens were tested for each set of values of S_1, S_2 and n_1/N_1 and a total number of twelve specimens were tested in each programme of tests. The column marked S_1 and S_2 indicated the first and second stress amplitudes used in the test programmes. The value of $\Sigma(n/N)_{av}$ gives the average for all the specimens tested with a given set of values of S_1, S_2 and n_1/N_1. Also in the columns marked n_2/N_2 and $\Sigma n/N$, the results of each test are shown in increasing order of magnitude. The values of n_1/N_1, n_2/N_2 and $\Sigma n/N$ shown in the Table 9.3 were computed by using the mean (probability of failure = 0.5) value of N_1 and N_2 as determined from the S-N-P diagrams derived from the cumulative distribution function discussed in Chapter 5.

Curves showing the relationship between the percentage decrease of original pulse velocity (V) in maximum and minimum and the number of applied cycles (n) both in linear and logarithmic scale are shown in Fig. 9.4-9.5 for tests of $n_1/N_1 = 0.25$ ($S_1 > S_2$). It will be observed that the two types of graph showed different trends due to the different scales used. It was sometimes necessary to use the logarithmic scale in plotting n because of the large number of cycles involved, coupled with the rapid change of V in the early stages. However, this would be misleading in interpreting the results. Therefore, the plot of V against cumulative cycle ratio ($\Sigma n/N$) was investigated (Fig. 9.6) and it was found that there was a clearer relationship between V (which can be used as an indirect means to define fatigue damage) and fatigue life ($\Sigma n/N$). In subsequent tests, therefore, the relationships between V (damage) and fatigue life were represented in this way. (Fig. 9.7-9.11) The summary of all the results is shown in Fig. 9.12.

9.6 Analysis and interpretation of results

Fatigue damage is a difficult term to define or measure precisely or quantitatively. It may be defined qualitatively as a change in the properties of a material subjected to cyclic stressing which may reduce the number of cycles of stress the material will subsequently withstand before final failure. Fatigue damage in concrete may probably be expressed in terms of the following physical variables:-

1. The number of independent fatigue-initiating cracks which are progressively operative.
2. The length and width of these cracks.
3. The orientation of the cracks.

For the purpose of interpretation of the test results, fatigue damage is assumed to be representable by the parameter D which is zero at the commencement of the life of a specimen and unity or 100% the moment of failure. The fatigue damage in all of the one-step tests was continously monitored by the indirect method of measuring the decrease in ultrasonic pulse velocity through the stressed specimens in the lateral direction. It was suggested above that the rate at which fatigue damage accumulates in a specimen at any given time depends on the number of fatigue cracks present and the length and width of these cracks. It seems reasonable, therefore, to assume that the fatigue damage in concrete could be indirectly measured in terms of the decrease in ultrasonic pulse velocity since the latter is directly affected by the extent and location of cracks in the specimen under fatigue loading. It is assumed also that damage may be expressed quantitatively as a function of the cycle ratio n/N;

Thus, D or $V = f(n/N)$ ..... (9.4)

Some clue as to the form of this functional relationship may be deduced from the results of the constant-amplitude loading tests, from the results of the one-step tests shown in Fig. 9.4-9.11 and also from the observations which can be made of the physical appearance of fractured specimens and the phenomenon of progressive fracture itself.

Evidence from the curves of the relationship between V and n in log scale; V and cycle ratio (n/N) for specimens tested at different stress levels and V and Σ n/N in one-step tests together with Raju's plots of V against percentage of life $(n/N)^{29}$ seems to suggest that the functional form of D or V = f (n/N) may be represented by the exponential relationship.

$$D = a(n/N)^b \qquad \ldots\ldots\ldots \quad (9.5)$$

Where a and b are experimental constants

In view of the large scatter of the results obtained it seems that only statistical methods of analysis of the data could make possible any proper interpretation of the results. Therefore, the fit of the data points of V against n in log scale; V against n/N for results obtained from constant amplitude tests (chapter 7) and V against Σn/N in one-step tests was investigated using Non-linear regression to obtain the best fitting curve of the form $y = ax^b$ where n is the independant variable (n , n/N or Σ n/N) and y is the observed dependent variable (Damage or V)

The problem is reduced to one of linear regression by taking the log of both sides of the equation (9.5)

Thus, $\log D = \log (a) + b \log (n)$;

or $\log D = \log (a) + b \log (n/N)$;

or $\log D = \log (a) + b \log (\Sigma n/N)$;

and substituting $Y' = \log D$, $X' = \log(n)$; $\log (n/N)$ or $\log (\Sigma n/N)$,

and $A' = \log a$

Hence, $Y' = A' + BX'$

a linear regression analysis(by the method of least squares) was performed to determine A' and B', then A was determined by

$$A = e^{A'}$$

The formulea are as follows:[112]

$$B = \frac{n\sum_1^n(\text{LOG}_e X_i \text{LOG}_e Y_i) - (\sum_1^n \text{LOG}_e X_i)(\sum_1^n \text{LOG}_e Y_i)}{n\sum_1^n(\text{LOG}_e X_i)^2 - (\sum_1^n \text{LOG}_e X_i)^2}$$

$$A = \exp\left[\frac{1}{n}\left\{\sum_1^n(\text{LOG}_e Y_i) - (\sum_1^n \text{LOG}_e X_i)B\right\}\right]$$

$$r = \frac{n\sum_1^n(\text{LOG}_e X_i \text{LOG}_e Y_i) - (\sum_1^n \text{LOG}_e X_i)(\sum_1^n \text{LOG}_e Y_i)}{\sqrt{\left[n\sum_1^n(\text{LOG}_e X_i)^2 - (\sum_1^n \text{LOG}_e X_i)^2\right]\left[n\sum_1^n(\text{LOG}_e Y_i)^2 - (\sum_1^n \text{LOG}_e Y_i)^2\right]}}$$

The analysis of the experimental data was performed by using the WANG series 600 computer employing the standard programme in 2 stages. In the first stage, there were 3 trials in the fitting of curves to the data obtained from the constant amplitude tests. For convenience, they will be referred to as trials 1.1, 1.2(a) and 1.2(b) respectively.

Trial 1.1 Max. decrease in pulse velocity, $V = a(\log n/N)^b$;

also Total strain, $\varepsilon = c(\log n)^d$ and $\varepsilon = c \log (n/N)^d$.

The fit of $\varepsilon = c(\log n)^d$ and $\varepsilon = c \log (n/N)^d$ was done as an independent experimental check using data from chapter 6. It was observed that the expressions derived above did not represent the experimental data, therefore, the second trial was made.

Trial 1.2 (a) $V = a(n)^b$ and $V = a(n/N)^b$;

$\varepsilon = c(n)^d$ and $\varepsilon = c(n/N)^d$.

A summary of the results is given in Table 9.4-9.5. It will be observed that all of the correlation coefficients (r) were significant at less than 0.1% level and the correlation coefficients of the equations $V = a(n/N)^b$, and $\varepsilon = c(n/N)^d$ were generally better than those from $V = a(n)^b$ and $\varepsilon = c(n)^b$. Although the expressions in this trial seemed to represent the data fairly well, nevertheless, due to the problem that will be discussed later, a third trial 1.2(b) was considered to be necessary in which the first two expressions in the second trial were fitted to data which omitted values of specimens which, assessed by

the method described on p. 88 , were excessively weak or strong. The results are also summarised in Table 9.4-9.5. Again, the correlation coefficients (r) were all significant at less than 0.1% level indicating that there is a valid association between the two variables of the relationships established. It will be noticed that the r values have improved on account of the more consistent data. Curves showing the relationship derived from these equations and from the last two equations in trial 1.2(a) at different stress amplitudes are shown in Fig. 9.13-9.16.

After the data of the constant amplitude tests were analysed, the data from the one-step tests were analysed in the second stage which for convenience, they will be referred as 2.1, 2.2, and 2.3 as follows:

2.1 Curves of the equations $V = a(n)^b$ and $V = a(n/N)^b$ were fitted to all the data from specimens tested at stress levels of 80% and 70% respectively in the first stages of the one-step tests. This was done as an independent experimental check of the expressions derived from the constant amplitude test over the full life of the specimens. The results are shown in comparison with the results from stage 1 in Table 9.4-9.5, and graphically shown in Fig. 9.17-9.18. The values of r, in this stage of analysis show an improvement over those in the first stage probably on account of the more scrupulous control of the tested specimens.

2.2 For the purpose of detailed analysis and interpretation of the results of the one-step tests, the above equations were fitted to the data obtained from specimens tested at $S_1 = 80\%$ and $S_1 = 70\%$ for $n_1/N_1 = 0.25, 0.5$, and 0.75 separately. This enabled the course of damage in the first stage of the tests to be established from the same four specimens.that continued into the second stage. The summary of the results are shown in Table 9.6. The values of r which are significant at the 0.1% level provide an adequate assurance of the relationship established.

It will be observed that in the second stage of analysis (Table 9.6) all

the values of N, both at 80% and 70% stress levels, derived by extrapolation of the relationships established from all the data predicted lives of 1,689 cycles and 96,400 cycles. These are very close to those given by the S-N-P diagrams at P = 0.5 which are 1,632 cycles at S = 80% and 97,486 cycles at S = 70%. This observation is significant in two ways. Firstly, it implies that the results of the statistical analysis of the S-N-P diagram which was derived from all the data are still valid when applied to the more strictly controlled specimens. On the other hand, it also implies that the non-destructive method of quality control suggested in Section 9.4.2 of this chapter is an effective means for detecting variation in strength of the specimens prior to testing and providing a very sensitive means of predicting with accuracy the approximate number of cycles to failure of a specimen at a given stress level. Secondly, it improves the validity of the conclusions drawn from the results on one-step tests by increasing the accuracy with which the stress levels were applied in each test.

2.3 In order to determine the course of damage at the second stage of the one-step tests, the equations:

$$V_2 = a(n_2)^b \text{ and } V_2 = (n_2/N_2)^b$$

where V_2 = The maximum decrease in pulse velocity value due to n_2 at S_2

n_2 = number of cycles at S_2

n_2/N_2 = cycle ratio at S_2

were fitted to the group of data at S_2 = 70% and 80% after n_1/N_1 = 0.25; 0.5 ; 0.75 respectively. The summary of the results is shown in Table 9.7 and 9.8.

9.6.1 Stress Dependence

One of the problems in the investigation of fatigue damage in concrete is to determine whether or not the damage-cycle ratio relationship (D or V against

n/N) is stress-dependent. The method of analysis suggested in chapter 8 was employed to check the relationship using the expressions obtained from the regression analysis in trial 1.2(a) as follows:

a) The plot of $V_i = a_i(n/N)^{b_i}$ and $\varepsilon_i = c_i(n/N)^{d_i}$ at different stress amplitudes (indicated by the suffix i) were first investigated and the values of V_{ui} and ε_{ui} at the end of the fatigue life (n/N = 100%) were determined from the equations. (Fig. 9.19a)

b) The values of V_{ui} and ε_{ui} as above were substituted in the equations $V_i = a_i(n)^{b_i}$ and $\varepsilon_i = c_i(n)^{d_i}$ to arrive at the best estimate of the fatigue life at each stress amplitude. These values were used to establish the terminal points (N_i, V_{ui}) and (N_i, ε_{ui}) of the curves $V_i = a_i(n)^{b_i}$ and $\varepsilon_i = c_i(n)^{d_i}$ (Fig. 9.19.b)

c) The ultimate damage for a stress level of 80% was also assumed for the other stress levels, and normalised curves of V or ε against n/N were drawn.(Fig. 9.19.c)

The normalised curves (see Fig. 20) clearly indicate that the fatigue damage of concrete in compression is infact stress-dependent, that is to say the amount of damage at a given cycle ratio depends on the stress amplitude. It will be observed that the course of damage represented by plots of V against n/N was convex upward and with the exception of the damage curve at a stress amplitude of 75%, the trend was that during the early part of the life fatigue damage progressed more quickly at low than at high stress amplitudes while during the later stages of the life the opposite was the case. The seemingly identical damage-cycle ratio relationship at 65% and 70% stress amplitudes and the anomalous trend of damage at 75% were probably a reflection of the large scatter of the ecperimental data of the former and the limited data available for the latter. This was examined further in trial 1.2(b) where the data from obviously weak or strong specimens (assessed by the method described on p.88 were excluded from the analysis. Using the steps outlined above and the normalised damage (V) - cycle ratio curves (Fig. 9.21) at each stress amplitude

clearly indicate different damage curves at 80%, 70% and 65% stress amplitude. Apart from the exceptional curve at 75%, the general trend is the same as in trial 1.2(a) (Fig. 9.20). Plots of normalised ε against n/N from results of trial 1.2(a)(Fig.9.22) and normalised V against n/N from 1-step test results (Fig. 9.23) showed the sama trends of stress-dependence.

Evidence from the visual ovservations of the phenomena of progressive cracking of specimens under test at different stress amplitudes, together with a study of the physical appearance of the fractured specimens, confirms the relative values of V_{ui} and the trend of the normalised damage-cycle ratio relationships. The observation showed that there were no visible cracks up to a certain fraction of the life for specimens tested at high stress amplitudes (85-80%) (In fact, as indirectly indicated by the decrease in ultrasonic pulse velocity, some minute internal cracks must have existed.) As suggested earlier in this chapter, the rate at which the fatigue damage accumulates in a specimen at any given time depends on the number, length and width of the fatigue cracks. Therefore, this is a clear indication that fatigue damage in specimens which were stressed at high levels took place more slowly during the early part of its life than in specimens tested at low stress amplitudes (70-65%) but was higher during the later stages of the life of the specimens. It was observed that when the decrease in pulse velocity reached about 27-29% of the original velocity (at about 70-85% of its fatigue life) hairline cracks (about 0.1-0.2mm width) became visible to the naked eye on the surfaces in the middle portion of the specimens. From this moment until failure, cracking developed at a very rapid pace, mainly by lengthening and widening of the existing cracks rather than by the formation of new cracks. Thus the ends of the fractured specimens which were tested at high stress levels consistently showed less traces of visible damage (both visible cracks on the surfaces and bond failure at the aggregate-cement matrix interfaces) than specimens tested at low stress levels, as clearly illustrated by Plate 4. The curve of 80% in Fig. 9.21 represents the progress of fatigue damage in a highly stressed specimen.

On the contrary, visual observations indicated that during the early fraction of life of specimens tested at low stress amplitudes (70-65%), many cracks developed simultaneously. Hairline cracks developed at weak points, probably initiated by shrinkage, and progressively became a network of larger cracks. Thus, during the early stages, damage progressed more rapidly than in the corresponding period of the specimens tested at higher stress levels and hairline cracks (about 0.1-0.2mm width) became visible to the naked eye in a random pattern on all the surfaces of the specimens earlier, namely at about 49-64% of the life (in which the decrease in pulse velocity was about 27-29% of the original velocity) compared with at 70-85% of the life at high levels. However, from this moment until failure, cracking developed at a very slow pace, mainly by the formation of new cracks rather than by lengthening and widening of the existing cracks. It was observed that some cracks, especially those which were approximately perpendicular to the loading axis, exhibited the phenomena known as "breathing" i.e. closing and opening corresponding to the cyclic application and removal of load. This tends to delay the final disintegration of the specimen by absorbing some of the energy applied to the stressed specimen. This is substantiated by Fig. 9.24 which shows the state of damage of a specimen after 1,804,400 cycles at 65% (the dotted lines indicates the final fracture-patterns). This specimen even after suffering such a large amount of damage, was able to withstand another 309,307 cycles at stress level of 65% before failure, indicating that the rate of damage at later stages of the life of specimens tested at low levels was not so great as in highly stressed specimens. Thus the ends of the fractured specimens which were tested at low stress amplitudes (70-65%) consistently showed more visible cracks and a greater amount of bond failure at the aggregate-cement matrix interface (Plate 5) than could be seen in the specimens tested at high stress amplitudes. The damage curves of 70%,65% in Fig. 9.21 represent the rate of damage likely in a low stressed specimen.

It may be concluded from the analysed values of the coefficient of correlation, r, which were generally significant at less than 0.1%, that the relationships D (either measured in terms of the maximum decrease in pulse velocity in lateral direction, V, or total strain, ε,) = $a(n)^b$, $a(n/N)^b$ or = $c(n)^d$, $c(\frac{n}{N})^d$ were quite adequate to express the accumulation of the fatigue damage of concrete specimens subjected to cyclic stresses in compression. It also may be concluded that as the stress level increases, in the relationships: $V = a(n)^b$ and $\varepsilon = c(n)^d$; all of the constants (a,b,c and d) increase, a and b being greater than and c and d less than unity. On the other hand as the stress level increases, in the relationships: $V = a(n/N)^b$ and $\varepsilon = c(n/N)^d$; a and c are greater than unity and decrease, while b and d are less than unity.

An examination of Table 9.3 clearly establishes one significant fact. In every series of tests in which the stress amplitude was decreased from a high value to a low value, the value of $\Sigma(n/N)_{av}$ was less than unity, (i.e. less than the fatigue life predicted by the Palmgren-Miner hypothesis), that is the hypothesis is not safe when applied to this loading programme. On the other hand in every series of tests in which the stress amplitude was increased from a low to a high value, the value of $\Sigma(n/N)_{av}$ was greater than unity showing the fatigue life predicted by the hypothesis to be conservative. Thus the hypothesis did not accurately predict the fatigue life of the specimens tested in this investigation

It is of interest to mention that in the only other cumulative fatigue damage investigation of concrete, which was done in flexural tests,[36] the opposite trends appeared to apply. It was found that when cyclic loading at a high stress was followed by loading at a lower stress the fatigue life ($\Sigma n/N$) achieved was more than unity, but that it was less than unity when the first stress level was less than the second. The contradiction between the conclusions from these flexural tensile tests and those from the present investigation cannot easily be explained but suggests radically different modes of fatigue damage under the two different types of loading.

9.6.2 Stress interaction effects.

The other important factor to be taken into account in approaching the problems of cumulative fatigue damage is whether or not there are stress interaction effects. If the relationship between damage and cycle ratio at a certain stress amplitude (S_i) is affected by the magnitude and order of occurrance of other stress amplitudes, than there are said to be of stress interaction effects. It will be shown that these effects were in fact present in the two programmes of tests under consideration.

Having regard to the amount of scatter, the data from the one-step tests were analysed to find the best average of the damage courses in the first stage (S_1) and the second stage (S_2) of the loading programmes using the methods outlined in section 9.6.1 stage 2.1 and 2.3. The results are shown graphically in Fig. 9.25-9.30. From the graphs, the stress-interaction effects are clearly demonstrated by the fact that the damage courses due to S_2 (either less or more than S_1) have been altered due to the application of S_1 for n_1/N_1 when compared with the likely courses of damage over the full life of a specimen (n_1/N_1 = 100%) due to the application of S_1 and S_2 alone. A study of the curves of the relationships between V and $\Sigma(n/N)$ at different values of S_1, S_2 and n_1/N_1 clearly indicates that when a specimen which was subjected to a certain cycle ratio (n_1/N_1) at a high stress amplitude (n_1/N_1 = 0.25,0.5 and 0.75) was subsequently stressed at a lower stress amplitude a change of the course of damage took place i.e. the damage rate $\left[\frac{dD}{d(\frac{n}{N})}\right]$ seemed to increase markedly in the first part of n_2/N_2 (Fig 9.25-9.27). As $\Sigma(n/N)$ (in this instance, $n_1/N_1 + n_2/N_2$) increased, the damage increased and progressed to failure at a value of $\Sigma(n/N)$ less than unity. In contrast, in a specimen which was initially stressed at a lower value, and subsequently loaded at a higher stress level (Fig. 9.28-9.30) the damage due to the second stress amplitude progressed at a relatively slow and constant rate and failure occured when $\Sigma n/N$ was greater than unity. This strengthening effect which sometimes resulted in even the life (n_2/N_2) at the second stress level exceeding the predicted life (from S-N-P diagram) at that level for a virgin specimen, together

with the above behaviour, indicated that there was indeed a stress-interaction effect under compressive cyclic loading of varying amplitudes.

It is interesting to mention that the phenomenon known as 'understressing' which causes the strengthening of a concrete specimen as have been reported elsewhere[11,27,29](section 2.2.5,p.16) has been observed to occur when the specimen is subjected to about 10^6cycles of a constant amplitude loading of a magnitude less than the fatigue strength at 10^7cycles(about 55 %).

It is of importance to know the effect of the stage at which the stress amplitude was changed(i.e. the value of n_1/N_1). It was demonstrated earlier in this Chapter that the magnitude of the stress levels in the loading programme 1 and 2 (namely, $S_1 > S_2$ or $S_1 \leq S_2$) affected the damage to a specimen and the accuracy of the predicted life using the Palmgren-Miner hypothesis. It also could be seen from Figs. 9.25-9.30 that for loading programme 1 (Figs.9.25-9.27), the longer the specimen was subjected to S_1, the higher the rate of damage(dD/d(n/N))at S_2. The same conclusion can also be applied to loading programme 2 although,the magnitude of the rate of damage in the former is much more than the latter. (Figs. 9.28-9.30).

9.7 Conclusions

9.7.1 Cumulative fatigue damage of concrete under constant amplitude loading

1) A satisfactory relationship between the two variables namely, the damage (D), indirectly indicated by the maximum decrease in pulse velocity in the lateral direction (V) and the cycle ratio (n_i/N_i) can be achieved by a power function regression analysis, $Y = aX^b$.

2) Damage of a highly stressed specimen ($S_{max} \geq 80\%$) accumulates more slowly than that of a low-stressed specimen ($S_{max} \leq 70\%$) in the early fraction of life, but progresses more quickly than the latter in the later part of the life.

3) The amount of fatigue damage produced by a given cycle ratio is not the same for all stress levels but depends on the stress level to which the concrete is subjected (Stress dependence).

9.7.2 Cumulative fatigue damage of concrete under variable amplitude loading

1) The Palmgren-Miner hypothesis did not predict with accuracy the lives of specimens subjected to the loading programmes 1 and 2 used in this part of the study.

2) The specimens subjected to the loading programme 1 (high-low) had shorter lives than predicted by the hypothesis, which could not therefore be safely applied.

3) The hypothesis was too conservative when used to predict the life of a specimen subjected to the loading programme 2 (low-high sequence).

4) From the curves showing the relationship between V and $\sum n/N$ of one-step tests indicated that stress interaction effects existed and the magnitude and the order of application of the stress levels in a loading programme affected the fatigue behaviour.

5) The application of a high stress level(i.e. 80 %) to a specimen for a certain cycle ratio was found to cause a marked increase of the damage rate (dD/d(n/N)) at a second and lower stress level so that $\frac{\text{Actual life } (\Sigma n/N)}{\text{Life predicted by Palmgren-Miner hypothesis}} < 1.$

6) The application of a low stress level(i.e. 70 %) to a specimen before it was subsequently loaded at a higher stress level was found to have a beneficial effect so much so that the actual life at the second stress level (n_2/N_2) sometimes exceeded the life predicted by the S-N-P diagram.

7) The longer the specimen was subjected to the first stress level, the higher the rate of damage dD/d(n/N) at the second stress level. This is particularly true in the loading programme 1.

CHAPTER TEN

MULTIPLE STAGE CUMULATIVE DAMAGE TESTS

10.1 Introduction

In Chapter 9, the results of one step tests in which the maximum stress level was changed only once (loading programme 1 and 2 in Figs. 9.3a and 9.3b), have been discussed and compared with the predictions derived from the Palmgren-Miner hypothesis. Such tests are not truely representative of the actual conditions to which a structural member may be exposed. Furthermore, there is a possibility that one-step tests may engender strong emphasis on interaction effects that could be less significant in randomly variable loading conditions. It has also been seen that this type of test, especially the low-high one-step test, appears to accentuate the amount of scatter normally encountered in fatigue experiments. In order to test under conditions closer to the varying load spectrums encountered in service, a number of multiple stage (i.e. 2-step and 4-step) cumulative damage tests were performed by the writer and will be discussed in this chapter. The test programmes were also designed with the objective of studying whether the number and order of application of the steps in a loading programme would affect the value of the cumulative cycle ratio ($\Sigma n_i/N_i$), that is the total fatigue life.

10.2 Test procedure

There are 2 main types of multi-step test reported in this Chapter. They are as follows:

10.2.1 Two-step tests (D-series, part A and B) Five specimens were tested for each loading programme (Programme 3 and 4 in Tables 10.7 and 10.8) which consists of a sequence of two changes of the maximum load between the two stress levels S_1 = 80% and S_2 = 70% of the ultimate. In programme 3 (D-series, part A), n_1 cycles of repeated loads were applied

at a stress level S_1. After n_1 cycles the stress level was decreased to S_2 for a further n_2 cycles. Finally, the stress level was increased to S_3 (which is equal to S_1) and the test continued until the specimen failed after an additional n_3 cycles. Program 4 (D-series part B) is an inversion of Program 3 insofar as the lower stress level (70%) was applied first, and after n_1 cycles the load was increased from 70% to 80% for another n_2 cycles. Finally, the load was decreased from 80% to 70% and test continued until failure occurred after an additional n_3 cycles.

10.2.2 Four-step tests (E-series, part A and B) Five specimens were also tested for each loading programme (Programme 5 and 6 in Tables 10.9 and 10.10) which consists of a sequence of four changes of the maximum load between the two stress levels S_1 = 80% and S_2 = 70% of the ultimate. In programme 5 (E-series part A), n_1, n_2, n_3, n_4 of repeated loads were applied at stress levels 80, 70, 80, and 70% respectively. The number of cycles n_1 to n_4 were assigned so that they corresponded to about one-fifth of the fatigue life at 80% and 70% stress levels. After n_4 cycles at 70% the stress level was increased to 80% and the test continued until the specimen failed after an additional n_5 cycles. Program 6 is the inversion of Programme 6 insofar as the lower stress level was applied first and continued until failure occurred in the fifth and final stage.

The method of selecting the fatigue specimens was the same as in section 9.4.2. The ultimate static strength of cubes and prisms of test series D and E are summarised in Tables 10.1 - 10.2 and 10.3 - 10.4 respectively.

10.3 Two-step test results

The results of both loading programme 3 and 4 are summarised in Table 10.5. The columns S_1, S_2 and S_3 indicate the first, second and third stress levels used in the sequence and the columns n_1/N_1, n_2/N_2 and

n_3/N_3 the corresponding cycle ratios. $\sum_1^3 (n/N)$ is the cumulative cycle ratio and $\sum_1^3 (n/N)_{av}$ is the average cumulative cycle ratio for all five specimens tested in a programme. All values of $\Sigma (n/N)$ shown in Table 10.5 were computed by using the value of N_i as determined from the S-N-P diagram derived from the cumulative distribution function at P (probability of failure) = 0.5. It will be observed that all but one specimen in each loading programme have a cumulative cycle ratio greater than unity, with $\sum_1^3 (n/N)_{av}$ = 1.408 and 1.734 for programmes 3 and 4 respectively. These values are both greater than the prediction of the Palmgren-Miner hypothesis ($\Sigma (n/N) = 1$). [94,96] This implies that the hypothesis is generally conservative and cannot be applied accurately to loading programmes 3 and 4. It is also observed that, just as when programme 2 (one-step low-high tests), was compared with programme 1 (high-low tests) the results of programme 4 (low-high-low) exhibit greater scatter than those of the programme 3 (high-low-high). According to the results, the number of steps and the order of the application of the steps in a programme both have a considerable influence on the fatigue behaviour. For a number of steps greater than one, the fatigue life under variable amplitude loading at stress levels 70% and 80% is generally greater than predicted by the Palmgren-Miner hypothesis and $\sum_1^3 (n/N)_{av}$ is larger if the low preceded the high stress level in a varying programme. It will be interesting to see whether the above observation applies to the loading programme 5 and 6 in which the number of steps was increased from two to four.

10.3.1 Analysis of two step test results

In order to study the mechanism by which fatigue damage accumulates under the programme 3 and 4, the internal changes of the specimens were continuously monitored throughout the cyclic load tests by the pulse velocity technique, the results of which are shown in Figs. 10.1 - 10.6. To give a complete picture, both the maximum and minimum decrease of pulse

velocity is shown, and the number of cycles is shown both in linear and logarithmic scales for a specimen tested under the programme 3 in Figs. 10.1 - 10.2. The relationship between both the maximum and minimum decrease of pulse velocity and the cycle ratio of the same specimen is also shown in Fig. 10.3. It is obvious that Fig. 10.3 gives the best and clearest representation of the variation of pulse velocity throughout the life of the specimen. In Fig. 10.4 the same relationship is shown for a specimen tested under the programme 4. Fig. 10.3 indicates that after a ratio n_1/N_1 at S_1, the rate of damage ($d\,V/d(\frac{n}{N})$) was increased when the stress level was changed from S_1 to a lower stress level S_2 confirming the results observed in a high-low sequence in programme 1 (Chapter 9). However, after a further ratio n_2/N_2 at S_2, the stress was increased again to S_1, and the rate of damage was observed to reduce and later to increase gradually when approaching failure. In Fig. 10.4, the contrary was observed in that after the usual early rapid increase in the damage at the stress level S_1, the rate of damage fell to zero in the latter part of the period n_2/N_2 when the load was increased to a higher stress level S_2. After a cycle ratio n_2/N_2 at S_2, the stress was decreased to the original level S_1 and the rate of damage was again observed to increase gradually as the cumulative cycle ratio increased to failure. The behaviour is summarised in Figs. 10.5 - 10.6 in which for clarity only the maximum decrease of the pulse velocity is shown, for specimens tested in the programmes 3 and 4. The results were analysed using the equations established in Chapters 7 and 9 and the best average curves were plotted to show the curves of damage against cumulative cycle ratio. The summary of the analysis is shown in Tables 10.7 and 10.8 and the correlation coefficients which were generally significant at less than the 0.1% level provide an adequate assurance of the relationships established. In Figs. 10.5 - 10.6, it also will be seen that one out of five specimens tested in

each programmed failed before the completion of the test with the resulting $\sum_{1}^{3} n/N$ less than unity. It is observed that the failure was preceded by an increase in the rate of damage, in each case, as a result of the application of a high stress level followed by a lower stress level in the sequence. For example, in Fig. 10.5, the specimen (D2 - F4) failed during the second stage of the programme in which the stress level was changed to 70% after n_1 at S_1 = 80%. In Fig. 10.6, the specimen (D4 - F2) failed during the third stage of the programme during which the stress level was changed to 70% after n_1 at S_1 = 70% and n_2 at S_2 = 80%.

10.4 Four-step test results

The results of programmes 5 and 6 are summarised in Table 10.6. The columns S_1, S_2, S_3, S_4 and S_5 indicate the stress levels for the first, second, third, fourth and fifth stages in the programme; n_1/N_1, ... n_4/N_4, n_5/N_5 indicate the respective cycle ratios at each stress level. $\sum_{1}^{5} (n/N)$ is the cumulative cycle ratio of a specimen and $\sum_{1}^{5} (n/N)_{av}$ the average for all five specimens tested in a programme. All values of $\Sigma (n/N)$ were computed using the same value of N_i as in Table 10.5. Again, it will be seen that one out of five specimens tested in the programme 5 failed before the completion of the programme with $\sum_{1}^{3} (n/N) = 0.512$, and one specimen in the loading programme 6 failed during the fifth stage with $\sum_{1}^{5} (n/N) = 0967$. However, the rest of the specimens tested in both programmes failed when the cumulative cycle ratios reached a value greater than that of unity predicted by the Palmgren-Miner hypothesis. The average values of $\sum_{1}^{5} (n/N)$ in the programmes 5 and 6 are 1.738 and 1.685 respectively. The scatter of the results in programme 6 is observed to be larger than programme 5. In all the multi-stage cumulative damage tests conducted, an increase in the number of steps did not seem to reduce the scatter of the results, rather the contrary. An observation that can clearly be made is that the scatter was greater, when the low preceded the

high stress level in any alternating single or multiple step cycle loading test, than in the opposite loading arrangement. With the exception of the average value of $\sum_{1}^{5} (n/N)$ in the programme 5, the observation made in section 10.5 applies to the four-step tests, that is to say an increase in the number of the steps in a sequence leads to a slight increase in the average value of the cumulative cycle ratio at failure which is generally greater than the prediction of the Palmgren-Miner hypothesis.

10.4.1 Analysis of four-step test results

The internal changes in each of the specimen tested in the programme 5 and 6 as indicated by the decrease of the original pulse velocity are shown against the cumulative cycle ratio in Figs. 10.7 and 10.8 respectively. The cumulative damage behaviour in the two programmes is also summarised by the maximum decrease of pulse velocity in Figs. 10.9 - 10.10. The data were analysed using the method outlined in Chapters 7 and 9 and the best average curves derived from the analysis were fitted to the data as shown in the figures. The summary of the results of the analysis is also presented in Tables 10.9 and 10.10.

From Figs. 10.7 and 10.9, it will be observed that when S_1 was 80%, the rate of damage increased markedly when the stress level was changed to S_2 = 70%. However, this sharp increase was reduced to a uniform rate when the stress level was changed to S_3 = 80%. During the fourth stage of the test, the load was decreased from S_3 to S_4 = 70%, and it was observed that the rate of damage was again increased markedly due to the influence of the previous loading history of the cycle ratio n_3/N_3 at stress S_3, but the rate was not as great as during n_2/N_2 at S_2. Finally, the load was increased to S_5 = 80% and the test continued to failure. During this final stage the damage increased uniformly to failure. In Figs. 10.8 and 10.10, it was observed that when the stress was increased from S_1 = 70% to S_2 = 80% after n_1/N_1 = 0.2, the rate of damage fell from

the usual early rapid increase of damage at the stress level S_1 to a uniform rate. The rate was, however, again increased when the stress was decreased to $S_3 = 70\%$. During the following fourth and fifth stages of the sequence in which the stress level changed to $S_4 = 80\%$ for n_4/N_4 and $S_5 = 70\%$ to failure, the rate of damage was observed to be continuously uniform during n_4/N_4 at S_4 and n_5/N_5 at S_5 to failure. In the specimen which failed at the third stage of programme 5 (Fig. 10.9) failure was observed to be preceded by a great increase in the rate of damage during the second stage, in which the stress level was changed to a lower stress, and in which the application of the high stress at the third stage failed to arrest this sharp increase.

10.5 Discussion and conclusions

The study of the cumulative fatigue damage under multiple stage variable amplitude tests investigated in this chapter has demonstrated that the interaction effect or load history has a significant rôle in the general behaviour. The results shown confirmed that in a loading programme, if a low stress level was preceded by the application of a higher stress level for a fraction of the fatigue life, the damage (initiation and propagation of microcracks) rate accelerated to a rate somewhat beyond the value to be expected from the application of the low stress in the constant amplitude test alone. An opposite though smaller effect was found when the stress changed from a low to a high level, i.e. after the change the damage rate was retarded for some time and gradually accelerated when failure approached. In alternating multi-step tests such as the loading programmes 3 - 6, the overall effect of the above acceleration and retardation of the damage rate was to give values of $\Sigma \frac{n}{N}$ at failure greater than the value derived from the Palmgren-Miner hypothesis, that is $\Sigma \frac{n}{N} = 1$. It is likely that $\Sigma \frac{n}{N}$ will be greater than unity under two possible conditions; firstly, in a loading sequence which consists of a number of

long periods at low stress level interrupted by occasional short periods at high stress level ($S \not> 80\%$), and secondly, when there are alternating short periods of low and high stress levels. $\Sigma \frac{n}{N}$ can also be improved by the initial application of a low cyclic stress for a short period of about 20 - 30 per cent of the fatigue life at that stress level followed by mixed cyclic stresses. These assumptions are, however, confined to the speed of loading, maximum stress level and constant environmental conditions observed in this investigation and their applicability to concrete of other mix proportions, age, etc. and environmental conditions requires caution and has to be justified experimentally.

To explain the above behaviour, i.e. retardation and acceleration in the damage rate in stepped tests requires more detailed fundamental studies of the behaviour and interaction of the constituent component of concrete - aggregate, water, and cement gel. However, a probable phenomenological explanation of the above characteristics will be attempted here:

Under cyclic load tests, assuming the specimen to have some fatigue life, the applied maximum stress level may not be sufficient to favour the propagation of the existing microcracks induced during setting and subsequently on drying due to local breakdown in the adhesion between the aggregates and the matrix. However, concrete as a heterogeneous material is not perfectly elastic; some energy is therefore stored in the material with cyclic loading and this build-up of energy as manifested by an increase in the internal temperature, when it reaches a sufficient magnitude, favours the growth of cracks. Because of the lower constant stress amplitude and hence limited store of energy, it is more likely that a larger number of new cracks forms, favoured by local discontinuities, under a low cyclic stress compared to a fewer, well defined cracks in the

case of high stress (Chapter 9). The greater decrease of pulse velocity at low than high cyclic stress also confirms the formation of such cracks. If the applied stress is decreased from high to low after a fraction of life, the excess energy after losses will mainly help towards the growth of the existing cracks hence there is a rapid decrease in the pulse velocity. On the other hand, if the high stress is preceded by a low stress in a cyclic load test, most of the energy will be absorped by the closing of a large number of microcracks and the energy demand required for the formation and propagation of the existing microcracks will not be met within a reasonable period of time unless the test is continued to failure at the second and higher cyclic stress. This may probably explain the retardation in the decrease of the pulse velocity (damage rate). It should be emphasized that the above explanation is empirical and has yet to be proved fundamentally.

The following conclusions can be drawn from the research investigation:

1. The Palmgren-Miner hypothesis does not accurately predict the fatigue life and generally gives too conservative a value of $\Sigma \frac{n}{N}$ for multiple step loading programmes.

2. Stress interaction effects are significant in the cumulative fatigue study of multiple stages and generally give $\Sigma \frac{n}{N} > 1$ at failure.

3. The fatigue life of concrete subjected to cyclic loads of varying amplitude is influenced by the number of steps and the order in which they are applied. Generally, a larger number of short steps gives a higher value of $\Sigma \frac{n}{N}$. Also, a low followed by a high cyclic stress in step-tests gives a higher value of $\Sigma \frac{n}{N}$.

CHAPTER ELEVEN

DESIGN CONSIDERATIONS; SUMMARY OF CONCLUSIONS AND SUGGESTIONS FOR FURTHER RESEARCH

11.1 Design considerations

The Palmgren-Miner hypothesis is a common method for the design of concrete structure subjected to varying repeated loads. It is very simple and, therefore, can be applied even to complex load programmes. Nevertheless, the discussion in Chapter 9-10 has shown that the hypothesis does not represent the actual behaviour of concrete and it may, in some cases give unconservative results. More particularly, it has been shown that the hypothesis is affected by the factors summarised below.

11.1.1 Factors affecting the accuracy of $\Sigma \frac{n}{N}$ derived from the Palmgren-Miner hypothesis

a. Effects of stress dependence and interaction:

The fatigue damage of concrete in compression has been seen to be stress dependent (Chapter 9) that is, under constant amplitude loading, the shape of the curve of damage against percentage life (cycle ratio) differs according to the stress level. It has also been proved[95, 97] that:

a) Under constant amplitude loading, the relative rate of damage accumulation ($dD/d(n/N)$) varies with the stress at a given cycle ratio (n/N), (i.e. there are different curves of damage against percentage life for different stresses) and;

b) The damage rate under spectrum loading is a simple average of $(dD/d(n/N))_{CA}$ of constant amplitude loading weighted according to the probability of occurrence, $P_m(S)$ of stress cycles at stress S so that the damage rate under spectrum loading is equal to

$$\left[\frac{dD}{d(\frac{n}{N})}\right]_{spectrum} = \int_0^{\infty} \left[\frac{dD}{d(\frac{n}{N})}\right]_{CA} P_m(S)dS \qquad \ldots 11.1$$

Then failure is predicted at $\Sigma \frac{n}{N} < 1$, i.e. due to the above effect alone the Palmgren-Miner hypothesis will overestimate the life.

However, the results shown in Chapters 9 and 10 have also demonstrated that stress-interaction effects exist alongside stress-dependence in the fatigue process, showing that equation (11.1) is not strictly true. Stress interaction effects have been shown to increase $\Sigma \frac{n}{N}$ so that at failure it is greater than unity (Chapter 10). The effects, for example 'strengthening effect' etc., are summarised below.

b. Effect of low-level stress cycles

It has been shown that low-level stress cycles may be beneficial or damaging depending on the order of their application in a loading sequence (i.e. before or after high stress cycles). The circumstances under which the strengthening effect ensures that low-level stress cycles do no damage, or are beneficial, are as follows:

The strengthening effect occurs in a loading sequence consisting of a limited period of low cyclic stress level followed by a period at a higher stress level (low-high one-step tests) to failure. Under these conditions the value of $\Sigma \frac{n}{N}$ may be from 1.1 to 2.6 times the life of specimens tested only at the higher stress level. When under a multiple step loading programme (programme 3 - 6 in Chapter 10) there is a large number of short periods of low stress cycles and/or high preceded by a low stress cycle $\Sigma \frac{n}{N}$ is generally greater than unity.

On the other hand, when a low cyclic stress level was preceded by a high stress, the initiation and propagation of cracks was found to progress rapidly and unless the stress level was increased within a reasonable time $\Sigma \frac{n}{N}$ was less than unity. Nevertheless, in a multiple-step variable amplitude test, the overall effect of interaction will generally give values of $\Sigma \frac{n}{N}$ greater than unity.

11.2 A conceptual damage-cycle ratio relationship

A mathematical formulation of the more sophisticated hypothesis which allows for both stress-dependence and interaction, such as a modification of Coten-Dolan[104] hypothesis, will result in expressions far too complicated to be used as a design tool. A simpler empirical damage concept to express the cumulative fatigue behaviour of concrete under variable cyclic compression is presented in the following:

Fatigue damage, D, can be defined as a variable, beginning at zero at the start of the fatigue life of a specimen and reaching unity at failure. The curve of damage against percentage life (or cycle ratio) at one selected constant amplitude cyclic stress can be given an arbitrary form. For example, in Fig. 11.1 which is derived from the present series of one-step tests the curve for the 70% stress level is represented by a straight line. This line, together with the curve marked 80% (1) are the two curves to be used in the evaluation of the fatigue life in high-low one-step tests. The 70% line is used with the curve marked 80% (2) to determine the fatigue life in low-high one step tests. The two curves 80% (1) and (2) are derived from the average of the results of one-step tests (Chapter 9), and the fact that there are two and not one 80% curve is a clear proof of interaction. The procedures for the determination of the fatigue life are as follows:

a. For a programme consisting of two main levels in high-low sequence, draw a vertical line from the value of n_1/N_1 (the fraction of the life at the first stress level) to intercept the 80% (1) line. From this point draw a line parallel to the horizontal axis to the right to intercept the 70% line and read the value of n_2/N_2 (the fraction of the life at constant amplitude loading at the second stress level) from the scale below. $\Sigma\, n/N$ is equal to $n_1/N_1 + n_2/N_2$ and will always be less than unity.

b. For a one step low-high sequence, draw a vertical line at the given value of n_1/N_1 to intercept the 70% line, then draw a horizontal line to the left to intercept the 80% (2) line and read the value of n_2/N_2 from the scale. Σ n/N is equal to $n_1/N_1 + n_2/N_2$ and is always greater than unity.

To determine the probable fatigue life in two-step and four-step sequences, it is necessary to define the area beneath the 70% line as negative and the area enclosed by the 80% (2) as a positive (or strengthening area). This is because we are now dealing with the combined results of positive (low-high sequence) and negative (high-low sequence) interaction effects, each of which has influence over the subsequent sequences. As an example the fatigue life will be determined for a low-high-low loading programme consisting of 30% of the life at a stress level of 70% followed by 30% of the life at 80% and a further period of unknown length at 70%. The use of the diagram is represented in Fig. 11.1 by the points: B, C, D, E, F, G. The cycle ratio at the third stage is equal to

EF = HX - GX = (from n_2/N_2 scale), = 1.55 - 0.46 = 1.09

$\therefore$ The net cycle ratio = 0.3 + 0.3 + 1.09 = 1.69

Compared with the experimental average result = 1.734

For a high-low-high programme (Programme 3), the points in Fig. 11.1 are B, I, F, J, K and

n_3/N_3 = 0.67 - 0.16 = 0.51 (KJ = KL - JL)

$\therefore$ Σ n/N = 0.3 + 0.3 + 0.51 = 1.11

Compared to the experimental result = 1.408

The same procedure can also be applied to four step tests. For example, a loading programme consists of alternate stress levels of 70%, 80%, 70%, 80% for a fixed 20% of the life in each period and a further period of unknown length at 70% stress level. The use of the diagram in this case

is represented in Fig. 11.1 by the points a', b', c', d', e', f', g' and h', i'. The cycle ratio at the fifth stage, n_5/N_5, is equal to $\acute{h}j' - ij$ =

$= h'i' = .995 - 0.255 = 0.74$

therefore $\Sigma \frac{n}{N} = 0.2 + 0.2 + 0.2 + 0.2 + 0.74 = 1.54$

Compared to the experimental average result = 1.685

For a loading programme similar to the programme 6 ;

$n_5/N_5 = 0.52 - 0.12 = 0.4$

$\therefore \quad \Sigma n/N = 0.8 + 0.4 = 1.2$ (1.738 average)

It will be seen that the predicted life derived from the conceptual damage-cycle ratio relationships approximates to the average experimental values, and generally predicts slightly lower values of $\Sigma \frac{n}{N}$ than the actual $\Sigma \frac{n}{N}$ thus providing some safety margin. Therefore, the interaction effects between a high and low stress level forming a complex loading sequence could be determined from relatively simple one-step tests.

To improve the accuracy, it is proposed that the conceptual damage-cycle ratio should be derived from a large number of experimental results, this could be done by varying the cycle ratio n_1/N_1 at the first stage of the tests from 0.05 to 0.95 with an increment of 0.5 after which the tests continue to failure under the second stress level. It should also be emphasized that the derived concept is purely empirical and is only one of the possible approaches to the problem of cumulative damage. Its applicability to concrete of other mix proportions, age, etc., requires caution and must be justified by further experiments.

11.3 Summary of conclusions and suggestions for further research

Most of the conclusions resulting from the analysis and discussion of the test data are presented at the end of each Chapter. However, the conclusions which are considered as a significant outcome from the present work will be summarised here.

Analysis of several models of S-N-P diagrams in the light of experimental data reveals that the conventional diagram of stress against number of loading cycles (S-N) diagram, extended to include the probability of failure, P, derived from the cumulative normal distribution function, is generally applicable for stress levels between 65 and 85% of the static ultimate strength.

Cyclic stresses of constant amplitude have a progressive effect on the properties of concrete each of which is affected to a varying degree depending on the level of stress. Generally, the changes consist of 3 stages, firstly a rapid decrease in the area of the hysteresis loop and modulus of elasticity and an increase in the total strain, elastic strain, inelastic strain, volumetric strain and Poisson's ratio up to 0 - 10% of the total life. This is followed by a uniform decrease of the first two and a uniform increase of the other characteristics mentioned. Finally when fatigue failure occurs, there is a slight increase in the hysteresis area, the total strain, elastic and inelastic strain, volumetric strain and Poisson's ratio while the modulus of elasticity shows a slight decrease.

The progressive internal changes of concrete under constant amplitude cyclic stress can be indirectly indicated by the decrease of the original pulse velocity. Empirical relations are proposed relating the decrease of pulse velocity with the cycle ratio or the fatigue life and the number of loading cycles.

Fatigue damage of concrete is stress-dependent, that is, the damage at a certain cycle ratio is not the same for all stress levels and depends on the stress level to which the concrete is subjected. Damage of a highly stressed specimen accumulates more slowly than that of a low-stressed specimen in the early fraction of life, but progresses more quickly than the

latter in the later part of the life. The magnitude of the stress levels and the order in which they are applied also affects the general fatigue behaviour (stress-interaction) when the concrete is subjected to variable amplitude cyclic loading.

The Palmgren-Miner hypothesis is a stress-dependent, interaction-free hypothesis, and therefore, does not accurately predict the fatigue life of concrete subjected to multiple step variable amplitude loading programmes as conducted in the present work. Generally, it gives too conservative a value of $\Sigma \frac{n}{N}$, but sometimes it gives an unsafe prediction by over-estimating of the actual value of $\Sigma \frac{n}{N}$.

A conceptual damage-cycle ratio relationship is proposed in which the stress-interaction effects is introduced and generally fair agreement is obtained from its use with multi-step sequence at two stress levels. There are, however, some difficulties that must be resolved by further experimental justification.

11.3.1 Suggestions for further research

1. This investigation was restricted to one mix and one set of environmental conditions. It would be advantageous to establish whether the same findings occur independent of these parameters.

2. Pulse velocity measuring instruments are now available with facilities for connection to a chart recorder and it is hence possible to record the decrease in pulse velocity continuously throughout failure. It would be useful to establish whether there is a limiting value of the decrease of pulse velocity at failure for specimens tested at constant and variable amplitude tests. If there is, the decrease of pulse velocity and the fatigue life relationships established could be used to determine the true amount of damage at any given value of the fatigue life.

3. The acceleration and suppression of the decrease of pulse

velocity observed when a low cyclic stress was preceded by a high level and vice versa in stepped tests was attributed to the growth of the existing well-defined cracks and the absorption of energy by a large number of microcracks. Supporting evidence from crack studies, i.e. studies with inclusions of different shape and orientation, cracking in partially fatigued specimens, etc., will be needed to prove the assumption.

4. A more extensive investigation of the cumulative fatigue damage behaviour under variable amplitude cyclic stresses other than the two maximum stress levels used in the present work is required to establish whether the interaction effects vary with the range of stress.

5. It will be advantageous to check the validity of the proposed empirical damage concept when applied to other types of variable amplitude loading, i.e. random, and/or block loading programmes.

REFERENCES

1. Freudenthal, A.M., "The inelastic behaviour of engineering materials and structures", John Wiley and Sons, New York, London, 1964, p.11.

2. Neal, J.A., and Kesler, C.E., "The fatigue of plain concrete", International Conference on the Structure of Concrete, London, 1965, Paper E2, pp.1-12.

3. A.C.I. Committee 215: "Consideration for design of concrete structures subjected to fatigue loading", Jour. A.C.J., Vol.11, No.10, March 1974, pp.97-121.

4. Mills, R.E., and Dawson, R.F., "Fatigue of concrete", Proceedings, 7th Annual Meeting, Highway Research Board, Dec. 1927, pp.160-172.

5. Cassie, W.F., "The fatigue of concrete", Jour. Inst. Civil Engrs. (London), Vol.11, 1939.

6. Nordby, G.M., "Fatigue of concrete - a review of research", Jour. A.C.I., Vol.30, No.2, August 1958, pp.191-215.

7. Bate, S.C.C., "The strength of concrete members under dynamic loading", Proc. of Symposium on Strength of Concrete Structures, London, C. & C.A., 1958, pp.487-556.

8. A.C.I. Bibliography No.3, "Fatigue of concrete", A.C.I., Detroit, Michigan, 1960, 38pp.

9. Murdock, J.W., "A critical review of research on fatigue of plain concrete", Bulletin No.475, V.62, No.62, University of Illinois Engineering Experiment Station, Feb. 1965, p.25.

10. Neal, J.A., and Kesler, C.E., "Some aspects of fatigue of concrete", T. & A.M. Report No.657, University of Illinois, July 1965, 22pp.

11. Raithby, K.D., and Whiffin, A.C., "Failure of plain concrete under fatigue loading - a review of current knowledge, R.R.L. Report LR.231, T.R.R.L., Ministry of Transport, 1968, 23pp.

12. A.C.I. Special Publication 41, "Fatigue of Concrete", Proceedings Abeles Symposium on Fatigue of Concrete, A.C.I. - SP.41, Detroit, Michigan, 1974, 360pp.

13. Bennett, E.W., "Fatigue in Concrete", Concrete, Current Paper Sheets No.14, C. & C.A., London, May 1974, pp.43-45.

14. Van Ornum, J.L., "Fatigue of cement products", Trans. A.S.C.E., Vol.51, 1903, p.443.

15. Van Ornum, J.L., "Fatigue of Concrete", Trans. A.S.C.E. Vol.58, 1907, pp.294-320.

16. Williams, G.M., "Some determinations of the stress deformation relations for concrete under repeated and continuous loadings", Proc. A.S.T.M., Vol.20, part II, p.238.

17. Mehmel, A., "Untersuchungen über den Einfluss häufig wiederholter Druckbeanspruchungen auf Druckelastizitat und Druckfestigkeit von Beton" (Investigations on the effect of frequently repeated stress on the elasticity under compression and the compressive strength of concrete), Miteilungen des Institut fur Beton und Eisenbeton an der Technishchen Hochschule, Karlsruhe, 74pp. (in German), 1926.

18. Probst, E., "The influence of rapidly alternating loading on concrete and reinforced concrete", Jour. Inst. of Struct. Engrs. (London), Vol.9, No.12, Dec. 1931, pp.326-340.

19. Ban, Shizuo, "Der Erumedungsvorgang von Beton", (The fatigue phenomenon in concrete), Bauingenieur (Berlin), Vol.14, No.13-14, pp.188-192 (in German).

20. Graf, O., and Brenner,E.,"Versuchezur Ermithung der Widerstandsfahigkeit von Beton gegen oftmals wiederholte Druckbelastung", (Experiments for investigating the resistance of concrete under often repeated compression loads) Buleetin No.76. Deutscher Ausschuss fur Eisenbeton pp.1-13, 1934.

21. Graf, O., and Brenner, E., "Experiments for investigating the resistance of concrete under often repeated loads", Part 2, Bulletin No.83, pp.1-12. Deutscher Ausschuss fur Eisenbeton, 1936.

22. Berry, H.C. "Some tests of concrete beams under often repeated loading", Proc. A.S.T.M. Vol.8, 1908, pp.454.

23. Antrim, J.D., and McLaughlin, J.F., "Fatigue study of Air-entrained concrete", Jour. A.C.I., Vol.30, No.11, May 1959, pp.1173-1183.

24. Gray, W.H., McLaughlin, J.F., and Antrim, J.D., "Fatigue properties of light weight aggregate concrete", Jour. A.C.I., Vol.58, No.2, August 1961, pp.149-162.

25. Linger, D.A. and Gillespie, H.A., "A Study of the mechanism of concrete fatigue and fracture", Paper presented to the 44th Highway Research Board, Jan. 1965, H.R.B. Research News No.22, Feb. 1966, pp.40-51.

26. Muir, S.E., "Some aspects of the fatigue of plain concrete prisms in compression", M.Sc. Thesis, Dept. of Civil Engrg., University of Leeds, 1964, pp.65.

27. Bennett, E.W., and Muir, S.E., "Some fatigue tests of high strength concrete in axial compression", M.C.R., Vol.19, No.59, June 1967, pp.113-117.

28. Raju, N.K., "Fatigue of high strength concrete in compression", Ph.D. Thesis, Dept. of Civil Engrg., University of Leeds, 1968, 160 pp.

29. Bennett, E.W., and Raju, N.K., "Cumulative fatigue damage in concrete in compression", International Conference on Structure, Solid Mechanics and Engineering Design in Civil Engineering Materials, University of Southampton, (1969).

30. McCall, John, T., "Probability of fatigue failure of plain concrete", Jour. A.C.I. Vol.55, Aug. 1958, pp.233-244.

31. Ople, F.S. and Hulsbos, C.L., "Probable fatigue life of plain concrete with stress gradient", Jour. A.C.I. Vol.63, No.1, Jan. 1966, pp.51-81.

32. Awad, M.E. and Hilsdorf, H.K., "Strength and deformation characteristics of plain concrete subjected to high repeated and sustained loads", Abeles Symposium on Fatigue of Concrete, A.C.I. Special publication -41, A.C.I., Detroit, Michigan, 1974, pp.1-9.

33. Raithby, K.D. and Galloway, J.W., "Effects of moisture condition, age, and rate of loading on fatigue of plain concrete", Abeles Symposium on Fatigue of Concrete, A.C.I. S.P.-41, A.C.I., Detroit, Michigan, 1974, pp.15-25.

34. Assimacopoulos, M., Warner, R.F., and Ekberg, Jr., C.E., "High speed fatigue tests on small specimens of plain concrete", Jour. P.C.I. Vol.4, No.2, Sept. 1959, pp.53-70.

35. Sparks, P.R. and Menzies, J.B., "The effect of rate of loading on plain concrete", Building Research Establishment Current Paper, CP. 23/73, 1973, also M.C.R. Vol.25, No.83, June 1973, pp.73-80.

36. Hilsdorf, H. and Kesler, E., "Fatigue strength of concrete under varying flexural stresses. Proc. A.C.I. Vol.63, No.10, Oct. 1966, pp.1059-1075.

37. McIntosh, J.D. and Erntroy, H.C., "The workability of concrete with $\frac{3}{8}$ inch aggregates", C. & C.A. Research Report No.2, London, June 1955.

38. Gonnerman, H.F., "Effect of size and shape of test specimen on compressive strength of concrete", Proc. A.S.T.M. Vol.25, Part II, 1925, pp.237-250.

39. Johnson, J.W. "Effect of height of test specimens on compressive strength of concrete", Bulletin, A.S.T.M., No.120, Jan. 1943, pp.19-21.

40. Kesler, C.E., "Effect of length to diameter ratio on compressive strength", Proc. A.S.T.M. Vol.59, 1959, pp.1216-1228.

41. Kuezynski, W., "Strength of concrete studied on specimens of various shapes and dimensions", International Union of testing and Research Laboratories for Materials and Structures, (RILEM), Bulletin No.8, New series, Sept. 1960, pp.77-92.

42. Rilem Commission for Concrete, "Correlation factors between the strength of different specimen types", Rilem Bulletin No.39, 1957, pp.81-105, No.12, New series, Sept. 1961, pp.155-156.

43. Hansen, H.K., Nielson, A. and Thavlow, S., "Compressive strength of concrete cube or cylinder", Rilem Bulletin No.17, New series, Dec. 1962, pp.32-30.

44. Gyengo, T., "Effect of type of test specimen and gradation of aggregate on compressive strength of concrete", Proc. A.C.I. Vol.34, 1938, pp.269-282.

45. Newman, K. and Lachance, L., "The testing of brittle materials under uniform uniaxial compressive stress", Proc. A.S.T.M., Vol.64, pp.1044-1067.

46. Whaley, C.P., "The creep of concrete under cyclic uniaxial compression", Ph.D. Thesis, Dept. of Civil Engrg., University of Leeds, 1971, 118pp.

47. Teychenne, D.C., "Recommendations for the treatment of the variations of concrete strength in code of practice", RILEM's Materials and Structures, Vol.6, No.34, July-Aug. 1973, pp.259-267.

48. Gonnerman, H.F., "Effect of end condition of cylinder on compressive strength of concrete", Proc. A.S.T.M. 24, Part II, p.1036, 1924.

49. Ahmed, S., "Effect of capping on the compressive strength of concrete cubes", M.C.R., Vol.7, No.19, March 1955, pp.21-24.

50. Werner, G., "The effect of type of capping material on the compressive strength of concrete cylinders", Proc. A.S.T.M., Vol.58, 1958, pp.1166-1181.

51. Thaulow, S., "Apparent compressive strength of concrete as affected by height of test specimen and friction between the load surfaces", RILEM Bulletin No.17, New series, Dec. 1962, pp.31-33.

52. Neville, A.M., "Properties of Concrete", Sir Isaac Pitman and Sons Ltd., London, 1973, 689pp.

53. Kupfer, H., Hilsdorf, H.K., and Rüsch, H., "Behaviour of concrete under biaxial stresses", Jour. A.C.I., Vol.66, No.52, August 1969, pp.656-665.

54. Nelissen, L.J.M., "Biaxial testing of normal concrete", HERON, Stevin Laboratory Technological University, Delft, Vol.18, No.1, 1972, 90pp.

55. Butcher, W.S., "The effect of air drying before test: 28 days strength of concrete", Constructional Review, Sydney, Dec.1958, pp.31-32.

56. Losenhausenwerk Fatigue Testing Machine Manual.

57. Morice, P.B. and Base, G.D., "The design and use of a demountable mechanical strain gauge for concrete structures", M.C.R., No.13, August 1953, pp.37-42.

58. Jones, R., "The non-destructive testing of concrete", M.C.R., No.2, June 1949, pp.67-78.

59. Jones, R., and Gatfield, E.N., "Testing concrete by an ultrasonic pulse technique", R.R.L., Technical Paper No.34, H.M.S.O., London, 1955.

60. Leslie, J.R., and Chessman, W.J., "An ultrasonic method of studying deterioration and cracking in concrete structures", Proc. A.C.I., Vol.46, No.1, Sept. 1949, pp.17-36.

61. Elvery, R.H., "Non-destructive testing of concrete and its relationship to specifications", Concrete, Vol.5, No.5., May 1971, pp.137-141.

62. Shar, S.P., and Chandra, S., "Mechanical behaviour of concrete examined by ultrasonic measurements", Journal of Material, Vol.5, 1970, pp.550-563.

63. "Manual on Fatigue Testing", A.S.T.M. Publication STP.91, 1949.

64. "Method of Fatigue Testings", British Standard 3518: Part I, General Principles: 1962, Part 5, Guide to the application of statistics: 1966.

65. Weibull, W., "Fatigue testing and analysis of results", Pergamon Press, London, 1961, 305p.

65a. Weibull, W., "Planning and interpretation of fatigue tests", Symposium on statistical aspects of fatigue, A.S.T.M., Special Technical Publication No.121, 1951, p.3-22.

66. Weibull, W., "A statistical representation of fatigue failure in solids", Transactions, Royal Institute of Technology (Stockholm), No.27, 1949.

67. Gumbel, E.J., "Statistical control-curves for flood-discharges", Transactions, American Geophysical Union, V.23, 1942, p.489.

68. Sinclair, G.M., and Dolan, T.J., "Effect of stress amplitude on statistical variability in fatigue life of 75 S - T6 Aluminium Alloy", Transactions, A.S.M.E. Vol.75, July 1953, pp.867-872.

69. Dixon, W.J., and Massey, F.J., "Introduction to statistical analysis", McGraw-Hill Book Co., New York (1957).

70. Hald, A., "Statistical Tables and Formulas", John Wiley & Sons, New York (1952).

71. Venuti, W.J., "A statistical approach to the analysis of fatigue of prestressed concrete beams", Jour. A.C.I. Vol.62 No.11, Nov. 1965, pp.1375-1393.

72. Raju, N.K., "Prediction of the fatigue life of plain concrete in compression", Build. Sci., Vol.4, pp.99-102. Pergamon Press 1969.

73. Hsu, T.C.C., "Inelastic behaviour of concrete under short time loading", Colloquium on the nature of inelasticity of concrete and its structural effects. Report No.322, Cornell University, Ithaca, New York, Nov. 1965, pp.6.

74. Lloyd, J.P., Lott, J.L., and Kesler, C.E., Final summary report: fatigue of concrete, T. & A.M. Report No.675, Department of Theoretical and Applied Mechanics, University of Illinois, Sept. 1967, pp.33.

75. Kaplan, M.F., "Strains and Stresses of concrete at initiation of cracking and near failure", Proc. Journal of A.C.I., Vol.60, No.7, July 1963, pp.853-880.

76. Reinius, Earling, "A theory of the deformation and the failure of concrete", Magazine of Concrete Research, Vol.8, No.24, Nov. 1956, pp.157-160.

77. Long, B.G., Kurtz, H.J., and Sandenaw, T.A., "An instrument and technique for field determination of the modulus of elasticity and flexural strength of concrete pavements", Proc. A.C.I., Vol.41, 1945, pp.217-231.

78. Thomson, W.T., "Measuring changes in physical properties of concrete by the dynamic method", Proc. A.S.T.M., Vol40, 1940, pp.1113-1121.

79. Jones, R., "A method of studying the formation of cracks in a material subjected to stress", British Journal of Applied Physics, Vol.3, July 1952, pp.229-232.

80. Rüsch, H., Physikaalische Fragen der Betonprüfung (Physical problems in the testing of concrete), Zement-Kalk-Gips. Vol.12, No.1., Jan. 1959, London, C. & C.A., March 1960, pp.21. Library Translation Cj.86.

81. Kaplan, M.F., "The relationship between ultrasonic pulse velocity and the compressive strength of concretes having the same workability but different mix proportions. M.C.R., Vol.12, No.34, March 1960, pp.3-8.

82. Shankar, K.N., "Non-destructive testing of concrete by ultrasonic methods", Indian Concrete Journal, July 1964, pp.261-263.

83. Highway Research Board Bulletin 206, "Effects of concrete characteristics on the pulse velocity", A SYMPOSIUM. Jan. 6-10, 1958, Washington D.C., Highway Research Board, 1959, pp.74.

84. Jones, R., "Non-destructive testing of concrete", Cambridge University Press, 1962.

85. Whitehurst, E.A., "Evaluation of concrete properties from sonic tests", Detroit, A.C.I., 1966, pp.ix, 94. A.C.I. Monograph No.2.

86. Jones, Ronald, "A review of the non-destructive testing of concrete," symposium on non-destructive testing of concrete and timber, London, June 1969. London Institution of Civil Engineers, 1970, pp.1-7.

87. Newmark, K., "Criteria for the behaviour of plain concrete under complex states of stress." The structure of concrete and its behaviour under load. Proceedings of an International Conference, London, Sept. 1965, London, C. & C.A., 1968, pp.225-274.

88. Robinson, S.G., "Methods of detecting the formation and propagation of microcracks in concrete". The structure of concrete and its behaviour under load. Proc. of an International Conference, London, Sept. 1965, London, C. & C.A., 1968, pp.225-274.

89. Nwokoye, N.D., "Prediction and assessment of concrete properties from pulse-velocity tests", M.R.C., Vol.25, No.82, March 1973, pp.39-46.

90. British Standard Institution: B.S.4408: 1971. Recommendations for Non-destructive Methods of Test for Concrete.

91. Jones, R., and Kaplan, M.F., "The effect of coarse aggregate on the mode of failure of concrete in compression and flexure." M.C.R., Vol.9, No.26, 1957, pp.89-94.

92. Evans, R.H., "Extensibility and modulus of rupture of concrete", The Structural Engineer, Vol24, 1946, pp.639-657.

93. Hsu, T.T.C., Slate, F.O., Sturman, G.M., and Winter, G., "Microcracking of plain concrete and the shape of the stress-strain curves. Proc. Jour. A.C.I., Vol60, No.2, Feb. 1963, pp.209-224.

94. Miner, M.A., "Cumulative damage in Fatigue", Journal of Applied Mechanics, Vol.12, No.3, Sept. 1945, pp.A-159/A-164.

95. Kaechele, L., "Review and analysis of cumulative fatigue damage hypotheses", Rand Corporation. Memorandum RM-3650-PR, August 1963.

96. Palmgren, A., "Die Lebensdauer von Kugellagern", Zeitschrift des Vereines Deutscher Ingenieure, Vol.68, No.14, 1924, pp.339-341.

97. Edwards, P.R., "Cumulative damage in fatigue with particular reference to the effects of residual stresses", Aeronautical Research Council, Current Paper No.1185 (London, H.M.S.O., 1971).

98. Langer, B.F., "Fatigue failures from stress cycles of varying amplitude", Trans. A.S.M.E., Vol.59, 1937, p.A160; also J. Appl. Mech. Vol.4, No.4, Dec. 1937.

99. Doland, T.J., Richard, F.E., and Work, C.E., "The influence of fluctuations in stress amplitude on the fatigue of metals", Proc. A.S.T.M., Vol.49, p.646, 1949.

100. Valluri, S.A., "A unified engineering theory of high stress level fatigue", Aerospace Engineer, vol.20, No.10, Oct. 1961.

101. Newmark, N.M., "A review of cumulative damage in fatigue", Fatigue and Metal, 1952, p.197. Edited by W.M. Murray (John Wiley and Sons, Inc., N.Y.).

102. Marco, S.M., and Starkey, W.L., "A concept of fatigue damage", Trans. A.S.M.E., May 1954, pp.627-632.

103. Grover, H.J., "An observation concerning the cycle ratio in cumulative damage", Symposium on fatigue of aircraft structures", A.S.T.M. Special Technical Publication, No.274, 1960.

104. Corten, H.T. and Dolan, T.J., "Cumulative fatigue damage", International conference on fatigue of metals, I.M.E. and A.S.M.E., 1956, pp.235-240.

105. Liu, H.W. and Dolan, T.J., "Fatigue damage during complex stress histories", NASA TN D-256, Nov. 1959.

106. Liu, H.W. and Corten, H.T., "Fatigue damage under varying stress amplitudes", NASA TN D-647, Nov. 1960.

107. Freudenthal, A.M., and Heller, R.A., "On stress interaction in fatigue and cumulative damage rule," Journal of Aerospace, Vol.26, No.7, July 1959.

108. Shanley, F.R., "A theory of fatigue based on unbonding during reversed slip", The RAND Corporation, p.350, Nov. 11, 1952.

109. Henry, D.L., "A theory of fatigue-damage accumulation in steel." Trans. A.S.M.E. Vol.77, August 1955, pp.913-918.

110. Mann, J.Y., "Fatigue of Materials", Melbourne University Press, 1967, 155pp.

111. Kibbey, D.R., "Cumulative Damage in fatigue in steel", Thesis in Mechanical Engineering, The Ohio State University, 1949.

112. Roscoe, John, T., "Fundamental Research Statistics", Holt Rinehart and Winston, Inc., 1969, p.273.

Table 3.1 is on the same page as Fig. 3.1

TABLE 4.1 SUMMARY OF TEST PROGRAMME

SERIES DESIGNATION	SIZE OF SPECIMENS	NUMBER OF SPECIMENS			OBJECT OF TESTS
		CONTROL TESTS		FATIGUE TESTS	
		4"CUBE	PRISMS		
A	76.2X76.2 X203.2mm. (3X3X8in)	12 X 11	4 X 11	4 X 11	S.N.P. Relation-Stress Strain Characteristics-Hysteresis Changes-Modulus of Elasticity-Pulse Velocity Changes in Concrete, under constant amplitude loading.
B		12	4	4	Effect of constant amplitude loading on Longitudinal and Lateral Strain, Volumetric Strain and Poisson's Ratio.
C		12 X 13	4 X 13	4 X 13	Verification of the Palmgren-Miner Cumulative Fatigue Damage Hypothesis for concrete under variable amplitude cyclic loadings.
D		12 X 4	4 X 4	4 X 4	
E		12 X 4	4 X 4	4 X 4	

TABLE 5.1 ULTIMATE STATIC STRENGTH OF CONTROL CUBES

SERIES-A

BATCH No.	28th DAYS*			COMMENCEMENT OF TEST*			COMPLETION OF TEST*		
	lbf/in^2	N/mm^2	s.d. N/mm^2	Age, days / lbf/in^2	N/mm^2	s.d. N/mm^2	Age, days / lbf/in^2	N/mm^2	s.d. N/mm^2
A-1	6240	43.00	0.44	(36) 7250	50.00	1.82	(38) 7150	49.28	1.87
A-2	6490	44.75	0.22	(37) 7360	50.76	1.21	(40) 7445	51.34	1.42
A-3	6365	43.88	1.47	(36) 7315	50.42	0.82	(40) 7810	53.86	1.27
A-4	6345	43.74	1.16	(35) 6970	48.07	2.66	(37)** 7480	51.58	1.87
A-5	6310	43.49	1.43	(38) 7200	49.64	1.70	(44) 7760	53.52	0.62
A-6	6210	42.81	0.78	(37) 7200	49.64	0.92	(49) 7940	54.73	0.39
A-7	6500	44.80	0.84	(44) 7870	54.25	1.89	(48) 7640	52.68	1.21
A-8	6250	43.10	0.96	(47) 7590	52.31	1.76	(55) 7905	54.49	1.65
A-9	5955	41.05	1.38	(44) 7325	50.49	0.61	(51) 7410	51.10	1.65
A-10	6110	42.14	0.39	(45) 7325	50.49	1.20	(63) 7760	53.52	1.51
A-11	6060	41.78	1.44	(36) 7095	48.92	0.88	(61) 7850	54.12	1.27
AVERAGE	6260	43.14	1.05	7320	50.45	1.52	7650	52.74	1.41
Coeff. of variation:			2.44%			3.02%			2.68%

* - Average of 4 cubes.

**- Test stopped due to the break-down of fatigue testing machine.

s.d. = Standard deviation.

TABLE 5.2 ULTIMATE STATIC STRENGTH OF CONTROL PRISMS

SERIES-A

BATCH No.	COMMENCEMENT OF TEST*				COMPLETION OF TEST+			
	Age days	lbf/in^2	N/mm^2	s.d. N/mm^2	Age days	lbf/in^2	N/mm^2	s.d. N/mm^2
A-1	36	4810	33.17	1.04	38	4790	33.03	
A-2	37	5095	35.13	0.60	40	5675	39.12	
A-3	37	4870	33.56	0.44	40	5090	35.10	
A-4	35	5225	36.02	0.63	37**	5080**	35.02**	1.29**
					** NOTE: TEST STOPPED DUE TO M/C BRAKE DOWN.			
A-5	38	5285	36.44	0.52	44	5040	34.75	
A-6	37	5295	36.51	0.50	49	5170	35.64	
A-7	44	5680	39.14	0.24	48	6415	44.22	
A-8	47	5450	37.59	0.18	55	5730	39.52	
A-9	44	5345	36.85	2.53	51	5370	37.01	
A-10	45	5435	37.46	0.03	63	5600	38.62	
A-11	36	4940	34.07	1.27	47'	5145'	35.46'	0.17'
					61	5110	35.24	
AVERAGE		5220	35.99	0.98		5350	36.89	
Coefficient of variation:				2.73%				

* Average of 3 prisms.

\+ Test result of 1 prism.

' Average of 2 prisms.

TABLE 5.3 SUMMARY OF STATIC TESTS

DESIGNATION	CONTROL CUBES			PRISMS
	28 days	COMMENCEMENT	COMPLETION	COMMENCEMENT
SERIES-A	43.14 N/mm^2	50.45 N/mm^2	52.74 N/mm^2	35.99 N/mm^2
-B	43.83 "	51.01 "	52.43 "	35.24 "
-C	42.78 "	49.28 "	50.47 "	35.02 "
-D	42.51 "	47.95 "	51.12 "	36.32 "
-E	43.86 "	51.77 "	52.98 "	38.37 "
AVERAGE	43.22 N/mm^2	50.09 N/mm^2	51.94 N/mm^2	36.18 N/mm^2
av. $\hat{S}_M$	1.26 N/mm^2	1.62 N/mm^2	1.35 N/mm^2	1.31 N/mm^2
Coeff. of variation	2.93 %	3.24 %	2.60 %	3.63 %

s.d. = Standard deviation, ($\hat{S}$).

TABLE 5.4 SUMMARY OF FATIGUE TEST RESULTS

SERIES-A

BATCH No.	SPECIMEN No.	AVERAGE STATIC STRENGTH OF PRISMS N/mm^2	MAXIMUM STRESS LEVEL, %	No. OF CYCLES TO FAILURE, N
A-1	F-1	33.17	80	1 512
	F-2	33.17	80	1 951
	F-3	33.17	75	4 481
	F-4	33.17	75	17 541
A-2	F-1	35.00	80	931
	F-2	35.00	75	17 861
	F-3	35.00	75	6 691
	F-4	35.00	70	18 731
A-3	F-1	33.56	80	201
	F-2	33.56	75	1 111
	F-3	33.56	70	37 771
	F-4	33.56	70	109 031
A-4	F-1	36.02	80	1 241
	F-2	36.02	85	331
	F-3	36.02	--	M.B*
	F-4	36.02	--	M.B*
A-5	F-1	36.44	70	70 251
	F-2	36.44	70	17 783
	F-3	36.44	75	34 421
	F-4	36.44	75	15 351
A-6	F-1	36.51	65	F.L**
	F-2	36.51	80	5 351
	F-3	36.51	65	1 850 885
	F-4	36.51	80	17 511
A-7	F-1	39.14	85	361
	F-2	39.14	85	651
	F-3	39.14	70	86 364
	F-4	39.14	70	54 283
A-8	F-1	37.59	85	51
	F-2	37.59	85	491
	F-3	37.59	85	151
	F-4	37.59	65	1 500 577
A-9	F-1	36.85	85	261
	F-2	36.85	85	F.L.**
	F-3	36.85	85	621
	F-4	36.85	65	1 452 399
A-10	F-1	37.46	80	1 533
	F-2	37.46	65	551 234
	F-3	37.46	65	2 113 707
	F-4	37.46	--	M.B.*
A-11	F-1	34.07	65	2 265 054
	F-2	34.07	65	2 962 823
	F-3	34.07	60	R.O.++
	F-4	34.07	60	R.O.++

NOTE: M.B.* -Test abandoned due to fatigue testing machine broke down.

F.L.**-Failure during loading. R.O.++-Run out specimens, ($N > 3X10^6$ cycles)

Table 5.5 is on page 40

TABLE 5.6

FREQUENCY DISTRIBUTION OF FATIGUE LIFE

SERIES A

m	N			P	m	N		P
	S=85	S=80	S=75			S=70	S=65	
1	0.051	0.201	1.111	0.1111	1	17.783	551.234	0.125
2	0.151	0.931	4.003	0.2222	2	18.731	1452.399	0.250
3	0.261	1.241	4.481	0.3333	3	37.771	1500.577	0.375
4	0.331	1.512	6.691	0.4444	4	54.283	1850.885	0.500
5	0.361	1.531	15.351	0.5555	5	70.251	2113.707	0.625
6	0.491	1.951	17.541	0.6666	6	86.364	2265.054	0.750
7	0.621	5.351	17.861	0.7777	7	109.031	2962.823	0.875
8	0.651	17.511	34.421	0.8888	n=7			
n=8								

S = Stress level - Percentage of static strength.

n = Number of specimens tested at any stress level.

N = Number of cycles to failure in thousands.

m = Ranking of a specimen of a group based on the magnitude of N.

P = Probability of failure-cumulative frequency= $\frac{m}{n+1}$

TABLE 5.7 STATISTICS OF FATIGUE DATA AT EACH STRESS LEVEL

STRESS LEVEL, S	No OF SPECIMENS, n	FATIGUE LIFE, N		LOG FATIGUE LIFE, Log N				Log N = (a+bP)**		
		$\bar{N}$	$\hat{S}_N$	$\overline{\text{Log N}}$	VARIANCE	$\hat{S}_{\text{Log N}}$	C_v	a	b	r
85	8	0.36475	0.21367	2.459784	0.135635	0.368287	0.14972	1.83478	0.01250	0.9242
80	8	3.77862	5.74843	3.249056	0.318026	0.563938	0.17357	2.28661	0.01925	0.9293
75	8	12.68250	10.97074	3.917986	0.230396	0.479996	0.12251	3.07049	0.01695	0.9612
70	7	56.31628	34.45144	4.664988	0.097366	0.312036	0.06688	4.09948	0.01131	0.9788
65	7	1813.81128	756.96716	6.214126	0.054837	0.234173	0.03768	5.82512	0.00778	0.8975
60	2*	-	-	-	-	-	-	-	-	-

* - Run out, not included in computations.

$\bar{N}$ - Mean fatigue life x 10^3 cycles.

$\overline{\text{Log N}}$ - Mean of Log fatigue life.

$\hat{S}$ - Standard deviation = $\sqrt{\frac{n\Sigma(x)^2 - (\Sigma x)^2}{n(n-1)}}$; where, x = variate value, n = the number of values.

C_v - Coefficient of variation = $\frac{\hat{S}}{\text{Mean}}$

** - St. Line Equation, Log N = (a + bP); where, P = Probability of failure (Table5.6).

a,b = Coefficient of St. Line Equation.

r = Coefficient of Correlation.

TABLE 5.8

STATISTICS OF LINEAR REGRESSION ANALYSIS

S-N DIAGRAM

Regression Coefficients:

$a = 17.422118$

$b = -0.177616$

Mean of 'S' $= 75.000000$

Mean of 'LogN' $= 4.101188$

SOURCE	SUM OF SQ.	DEGREE OF FREEDOM	MEAN SQ.
Regression	58.965158	1	58.965158
Residual	7.655837	36	0.212662
Total	66.620995	37	

F-Test for r, $F_r = \frac{r^2(n-2)}{1-r^2} = 277.271525$

Coefficient of Determination $= r^2 = 0.885084$

Coefficient of Correlation $= r = -0.940788$

Standard Error of Estimate $= 0.461153$

Regression Equation:

$$\text{LogN} = 17.422118 - 0.177616\ S$$

This equation is statistically reliable for $65 \leq S \leq 85$.

Table 5.9 is on page 43

TABLE 5.10

STATISTICS OF MULTIPLE LINEAR REGRESSION ANALYSIS

S-N-P DIAGRAM(Mc'Call's MODEL)

Multiple Regression Coefficients :

A = 6.933756

B = -3.350850

C = 0.119501

Mean of 'Log(LogN)' = 0.581152

Mean of 'LogS' = 1.873116

Mean of 'Log(-LogL)' = -0.571172

SOURCE	SUM OF SQ	DEGREE OF FREEDOM	MEAN SQ
Regression	0.793381	2	0.396690
Residual	3.024375×10^{-2}	35	8.641071×10^{-4}
Total	0.823625	37	

F-Test = 459.075745

Coefficient of Determination = 0.963279

Coefficient of Multiple Correlation= 0.981468

Standard Error of Estimate = 2.939570×10^{-2}

Multiple Regression Equation:

$$\text{Log(LogN)} = 6.933756 - 3.350850\,\text{LogS} + 0.119501\,\text{Log(-LogL)}$$

where $L = 1-P$; P = Probability of failure.

TABLE 5.11

STATISTICS OF MULTIPLE LINEAR REGRESSION ANALYSIS

S-N-P DIAGRAM (MODIFIED Mc'Call's MODEL)

Multiple Regression Coefficients :

A = 5.637252

B = -2.659922

C = -2.151478

D = 1.210185

Mean of 'Log(LogN)' = 0.581152

Mean of 'Log S' = 1.873116

Mean of 'Log(-LogL)' = -0.571172

Mean of 'LogS[Log(-LogL)]' = -1.071818

SOURCE	SUM OF SQ	DEGREE OF FREEDOM	MEAN SQ
Regression	0.807166	3	0.269056
Residual	1.645809×10^{-2}	34	4.840615×10^{-4}
Total	0.823625	37	

F -Test = 555.829413

Coefficient of Determination = 0.980017

Coefficient of Multiple Correlation = 0.989958

Standard Error of Estimate = 2.200140×10^{-2}

Multiple Regression Equation:

$$\text{Log(LogN)} = 5.637252 - 2.659922\,\text{LogS} - 2.151478\,\text{Log(-LogL)} + 1.210185\,\text{LogS[Log(-LogL)]}$$

where L = 1-P ; P = Probability of failure.

TABLE 6.1 ULTIMATE STATIC STRENGTH OF CONTROL CUBES AND PRISMS OF CONCRETE IN B-SERIES

CONTROL CUBES								
28th DAYS*			COMMENCEMENT OF TEST*			COMPLETION OF TEST*		
lbf/in^2	N/mm^2	s.d. (N/mm^2)	(Age-days) lbf/in^2	N/mm^2	s.d. (N/mm^2)	(Age-days) lbf/in^2	N/mm^2	s.d. (N/mm^2)
			(40)			(54)		
6360	43.83	1.21	7400	51.01	2.43	7605	52.43	0.61
Coeff. of variation		2.76%			4.76%			1.16%
CONTROL PRISMS+								
			(40)					NOTE: Result of one prism
			5110	35.24	0.34	5570	38.42	
			Coefficient of variation		0.96%			

NOTE: * - Average of 4 cubes

\+ - Average of 3 prisms

s.d. - Standard deviation

TABLE 9.1 ULTIMATE STATIC STRENGTH OF CONTROL CUBES

SERIES-C

BATCH No.	28th DAYS*			COMMENCEMENT OF TEST*			COMPLETION OF TEST*		
	lbf/in^2	N/mm^2	s.d. N/mm^2	Age, days lbf/in^2	N/mm^2	s.d. N/mm^2	Age, days lbf/in^2	N/mm^2	s.d. N/mm^2
C-1	6830	47.10	1.74	(37) 7905	54.49	2.25	(42) 7830	54.00	1.22
C-2	6250	43.10	1.18	(36) 6990	48.19	0.48	(42) 7340	50.62	0.92
C-3	6095	42.02	1.07	(35) 6885	47.46	0.79	(40) 7025	48.44	0.48
C-4	6250	43.11	1.67	(36) 7025	48.44	0.88	(39) 7095	48.92	1.63
C-5	5970	41.17	1.18	(35) 6970	48.07	0.72	(38) 6970	48.07	0.46
C-6	6145	42.38	1.65	(35) 6655	45.89	1.07	(42) 7270	50.13	2.15
C-7	6235	42.98	0.72	(39) 7905	54.49	1.65	(41) 7830	53.98	1.04
C-8	6305	43.47	0.72	(38) 7305	50.38	2.37	(49) 7760	53.52	1.51
C-9	6235	42.98	0.46	(39) 7235	49.89	1.97	(43) 7410	51.10	1.65
C-10	5815	40.08	1.33	(38) 6865	47.34	2.10	(43) 6605	45.53	1.37
C-11	6090	41.98	1.83	(37) 6780	46.74	3.09	(44) 7375	50.86	1.85
C-12	5955	41.05	1.82	(37) 6960	47.98	0.39	(46) 7130	49.16	1.45
C-13	6480	44.68	1.60	(37) 7445	51.34	1.37	(44) 7515	51.82	1.67
AVERAGE	6205	42.78	1.37	7150	49.28	1.67	7320	50.47	1.42
Coefficient of variation			3.20%			3.40%			2.80%

* -Average of 4 cubes.

s.d. = Standard deviation.

TABLE 9.2 ULTIMATE STATIC STRENGTH OF CONTROL PRISMS

SERIES-C

BATCH	COMMENCEMENT OF TEST*				COMPLETION OF TEST+			
No.	Age days	lbf/in^2	N/mm^2	s.d. N/mm^2	Age days	lbf/in^2	N/mm^2	Remark
C-1	37-39'	4910	33.84	1.26	42	5410	37.34	>av.
C-2	36-39"	4935	34.01**	0.57	42	--	-	
C-3	35	4600	31.70	2.14	40	4700	32.38	
C-4	36-38"	4510	31.09**	2.09	39	--	-	
C-5	36	4725	32,58	0.49	38	4580	31.59	
C-6	36	5350	36.89	0.40	42	5930	40.90	>av.
C-7	39	5920	40.80**	0.28	41	--	-	
C-8	39	5530	38.12	1.04	49	5475	37.74	
C-9	39	4780	32.96	2.19	43	4210	29.02	>av.
C-10	38	5130	35.38	0.81	43	4525	31.19	>av.
C-11	37	5615	38.72	0.68	43	5135	35.40	>av.
C-12	37	5135	35.40	1.36	46	5360	36.94	
C-13	37	4910	33.86**	3.39	44	--	-	
AVERAGE		5080	35.02	1.56		5036	34.72	
Coefficient of variation				4.45%				

* - Average of 3 prisms.

** - Average of 4 prisms.

+ - Test result of 1 prism.

' - 2 prisms at the beginning, 1 prism in the middle of the test.

" - 3 prisms at the beginning, 1 prism in the middle of the test.

s.d. = Standard deviation.

TABLE 9.3 SUMMARY OF ONE STEP TEST RESULTS
C-SERIES

SPECIMEN NUMBER	S_1 %	S_2 %	n_1/N_1	n_2/N_2	$\sum(n/N)=\frac{n}{N_1}1+\frac{n}{N_2}2$	$\sum(n/N)_{av.}$	$\hat{S}$	PALMGREN-MINER'S $\sum n/N$
C1 -F1	80	70	0.251	0.383	0.633			
C6 -F4	80	70	0.251	0.408	0.659	0.764	0.152	1.000
C13-F2	80	70	0.251	0.550	0.801			
C11-F3	80	70	0.251	0.715	0.965			
C8 -F2	80	70	0.502	0.146	0.648			
C13-F1	80	70	0.502	0.189	0.692			
C11-F4	80	70	0.502	0.218	0.720	0.748	0.125	1.000
C1 -F3	80	70	0.502	0.428	0.931			
C10-F2	80	70	0.753	0.037	0.791			
C2 -F1	80	70	0.753	0.039	0.792			
C3 -F3	80	70	0.753	0.074	0.827	0.816	0.032	1.000
C5 -F3	80	70	0.753	0.103	0.856			
C10-F4	70	80	0.250	1.010	1.260			
C8 -F3	70	80	0.250	1.880	2.130			
C1 -F2	70	80	0.250	1.990	2.240	2.120	0.655	1.000
C2 -F3	70	80	0.250	2.600	2.850			
C12-F4	70	80	0.500	0.851	1.351			
C13-F4	70	80	0.500	1.127	1.628			
C4 -F3	70	80	0.500	2.105	2.605	2.104	0.725	1.000
C1 -F4	70	80	0.500	2.385	2.835			
C13-F5	70	80	0.750	0.349	1.099			
C2 -F2	70	80	0.750	0.453	1.203			
C6 -F2	70	80	0.750	1.120	1.870	1.716	0.734	1.000
C9 -F2	70	80	0.750	1.942	2.692			

S_1 = Stress level for the first stage -%of prism static strength
S_2 = Stress level for the second stage-%of prism static strength
N_1 = Fatigue life at constant stress level S_1
N_2 = Fatigue life at constant stress level S_2,

n_1 = $N\bar{o}$ of cycles for the first stage
n_2 = $N\bar{o}$ of cycles for the second stage (continue to failure)
$\hat{S}$ = Standard deviation

TABLE 9.4 SUMMARY OF CONSTANT AMPLITUDE AND 1 STEP TEST ANALYSIS

STRESS LEVEL	$\varepsilon = c(n/N)^d$	$V = a(n/N)^b$		
	Trial 1.2(a)	Trial 1.2(a)	Trial 1.2(b)	Trial 2.1
80%	c = 1840.1371 d = 0.0955 r = 0.8822 Degree of Freedom = 6	a = 6.1682 b = 0.3495 r = 0.8050 At $\frac{n}{N}$ = 100% V = 30.846% Degree of Freedom = 231	a = 6.3574 b = 0.3220 r = 0.8408 At $\frac{n}{N}$ = 100% V = 28.008% Degree of Freedom = 138	a = 7.3798 b = 0.3024 r = 0.9064 At $\frac{n}{N}$ = 100% V = 29.707% Degree of Freedom = 127
75%	c = 1855.5041 d = 0.0974 r = 0.8722 Degree of Freedom = 7	a = 5.5906 b = 0.3884 r = 0.8774 At $\frac{n}{N}$ = 100% V = 33.450% Degree of Freedom = 20	The same as Trial 1.2(a)	
70%	c = 1873.5170 d = 0.0716 r = 0.8315 Degree of Freedom = 23	a = 10.2738 b = 0.2426 r = 0.9036 At $\frac{n}{N}$ = 100% V = 31.410% Degree of Freedom = 101	a = 9.4372 b = 0.2572 r = 0.9094 At $\frac{n}{N}$ = 100% V = 30.842% Degree of Freedom = 74	a = 10.1407 b = 0.2535 r = 0.9195 At $\frac{n}{N}$ = 100% V = 32.591% Degree of Freedom = 250
65%	c = 2335.3697 d = 0.0877 r = 0.8692 Degree of Freedom = 61	a = 11.5660 b = 0.2162 r = 0.8973 At $\frac{n}{N}$ = 100% V = 31.306 Degree of Freedom = 81	a = 10.4483 b = 0.2206 r = 0.9177 At $\frac{n}{N}$ = 100% V = 28.865% Degree of Freedom = 32	

V = Percentage decrease of original pulse velocity
ε = Total strain in micron
n/N = Cycle ratio

a,b,c and d = Experimental constants
r = Coefficient of correlation

TABLE 9.5 SUMMARY OF CONSTANT AMPLITUDE AND 1 STEP TEST ANALYSIS

STRESS LEVEL	$\varepsilon = c(n)^d$	$V = a(n)^b$		
	Trial 1.2(a)	Trial 1.2(a)	Trial 1.2(b)	Trial 2.1
80%	c = 1406.6909 d = 0.0970 r = 0.8822 Degree of Freedom = 8-2 = 6	a = 2.7790 b = 0.3043 r = 0.7639 At V = 30.846% N = 2722 Degree of Freedom = 233-2 = 231	a = 3.2019 b = 0.2833 r = 0.7577 At V = 28.008% N = 2113 Degree of Freedom = 140-2 = 138	a = 3.0961 b = 0.3042 r = 0.8752 At V = 29.707% N = 1689 Degree of Freedom = 129-2 = 127
75%	c = 1107.4238 d = 0.0980 r = 0.8729 Degree of Freedom = 7	a = 0.4915 b = 0.4402 r = 0.9627 At V = 33.450% N = 14559 Degree of Freedom = 20	The same as Trial 1.2(a)	
70%	c = 1104.9795 d = 0.0749 r = 0.8684 Degree of Freedom = 23	a = 2.8832 b = 0.2080 r = 0.8114 At V = 31.410% N = 97,000 Degree of Freedom = 101	a = 1.8043 b = 0.2475 r = 0.8868 At V = 30.842% N = 95703 Degree of Freedom = 74	a = 1.7556 b = 0.2545 r = 0.9204 At V = 32.591 N = 96399 Degree of Freedom = 250
65%	c = 955.2368 d = 0.0897 r = 0.8725 Degree of Freedom = 61	a = 1.4047 b = 0.2146 r = 0.8942 At V = 31.306% N = 1915463 Degree of Freedom = 81	a = 1.3746 b = 0.2153 r = 0.9037 At V = 28.865% N = 1380815 Degree of Freedom = 32	

V = Percentage decrease of original pulse velocity
ε = Total strain in micron
n = Number of applied cycles
a,b,c and d = Experimental constants
r = Coefficient of correlation

TABLE 9.6 SUMMARY OF 1 STEP TEST ANALYSIS

STRESS LEVEL S_1 80 %	$V = a(n/N)^b$		
	n_1/N_1 = 25 %	n_1/N_1 = 50 %	n_1/N_1 = 75 %
	a = 9.1956 b = 0.2194 r = 0.7776 At n/N = 100 % V_u = 25.266 Degree of Freedom = 25 - 2 = 23	a = 7.2147 b = 0.3022 r = 0.9192 At n/N = 100 % V_u = 29.011 Degree of Freedom = 47 - 2 = 45	a = 6.0249 b = 0.3647 r = 0.9642 At n/N = 100 % V_u = 32.313 Degree of Freedom = 57 - 2 = 55
	$V = a(n)^b$		
	n_1/N_1 = 25 %	n_1/N_1 = 50 %	n_1/N_1 = 75 %
	a = 4.9604 b = 0.2203 r = 0.7778 At V_u = 25.266 N = 1 620 Degree of Freedom = 15 - 2 = 13	a = 3.0858 b = 0.3030 r = 0.9196 At V_u = 29.011 N = 1 627 Degree of Freedom = 48 - 2 = 46	a = 2.1641 b = 0.3656 r = 0.9644 At V_u = 32.313 N = 1 628 Degree of Freedom = 57 - 2 = 55
STRESS LEVEL S_1 70 %	$V = a(n/N)^b$		
	n_1/N_1 = 25 %	n_1/N_1 = 50 %	n_1/N_1 = 75 %
	a = 9.1688 b = 0.2166 r = 0.9102 At n/N = 100 % V_u = 24.870 Degree of Freedom = 117 - 2 = 115	a = 10.9894 b = 0.2507 r = 0.9126 At n/N = 100 % V_u = 34.864 Degree of Freedom = 98 - 2 = 96	a = 9.4489 b = 0.2858 r = 0.9013 At n/N = 100 % V_u = 35.235 Degree of Freedom = 150 - 2 =148
	$V = a(n)^b$		
	n_1/N_1 = 25 %	n_1/N_1 = 50 %	n_1/N_1 = 75 %
	a = 2.1741 b = 0.2106 r = 0.9220 At V_u = 24.870 N = 106 137 Degree of Freedom = 65 - 2 = 63	a = 1.9380 b = 0.2517 r = 0.9140 At V_u = 34.864 N = 96 786 Degree of Freedom = 95 - 2 = 93	a = 1.2544 b = 0.2898 r = 0.9365 At V_u = 35.235 N = 99 462 Degree of Freedom = 150 - 2 =148

TABLE 9.7 SUMMARY OF 1 STEP TEST ANALYSIS

STRESS LEVEL S_1	S_2	% n_1/N_1	% n_2/N_2	$V_2 = a(n_2)^b$ a	b	r
80 %	70 %	25.1	TO FAILURE (51.30)	0.1968	0.4436	0.9007
				DEGREE OF FREEDOM = 70-2 = 68		
		50.2	TO FAILURE (24.60)	0.0888	0.5386	0.9532
				DEGREE OF FREEDOM = 63-2 = 61		
		75.3	TO FAILURE (6.23)	0.6543	0.3559	0.7100
				DEGREE OF FREEDOM = 50-2 = 48		
70 %	80 %	25	TO FAILURE (187.00)	0.01867	0.8308	0.9401
				DEGREE OF FREEDOM = 62-2 = 60		
		50	TO FAILURE (160.40)	0.0266	0.8434	0.9252
				DEGREE OF FREEDOM = 83-2 = 81		
		75	TO FAILURE (196.60)	0.1275	0.5737	0.8006
				DEGREE OF FREEDOM = 42-2 = 40		

V_2 = Maximum decrease in ultrasonic pulse velocity in percent due to n_2 at S_2 .

n_2 = Actual loading cycles at S_2 after n_1/N_1 at S_1.

a,b = Experimental constants.

r = Coefficient of correlation.

TABLE 9.8 SUMMARY OF 1 STEP TEST ANALYSIS

STRESS LEVEL S_1	S_2	% n_1/N_1	% n_2/N_2	$V_2 = a(n_2/N_2)^b$ a	b	r
80 %	70 %	25.1	TO FAILURE (51.30)	4.1748	0.4430	0.9008
			DEGREE OF FREEDOM = 70-2 = 68			
		50.2	TO FAILURE (24.60)	3.6308	0.5372	0.9528
			DEGREE OF FREEDOM = 63-2 = 61			
		75.3	TO FAILURE (6.23)	6.9582	0.4918	0.8608
			DEGREE OF FREEDOM = 50-2 = 48			
70 %	80 %	25	TO FAILURE (187.00)	0.1903	0.8306	0.9401
			DEGREE OF FREEDOM = 62-6 = 60			
		50	TO FAILURE (160.40)	0.2764	0.8482	0.9256
			DEGREE OF FREEDOM = 83-2 = 81			
		75	TO FAILURE (96.60)	0.6334	0.5736	0.8006
			DEGREE OF FREEDOM = 42-2 = 40			

V_2 = Maximum decrease in ultrasonic pulse velocity in percent due to n_2/N_2 at S_2.

n_2/N_2 = Actual cycle ratio at S_2 after n_1/N_1 at S_1.

a,b = Experimental constants

r = Coefficient of correlation.

TABLE 10.1 ULTIMATE STATIC STRENGTH OF CONTROL CUBES

SERIES-D

BATCH No.	28th DAYS*			COMMENCEMENT OF TEST*			COMPLETION OF TEST*		
	lbf/in^2	N/mm^2	s.d. N/mm^2	Age,days / lbf/in^2	N/mm^2	s.d. N/mm^2	Age,days / lbf/in^2	N/mm^2	s.d. N/mm^2
D-1	6155	42.43	0.82	(37) 6605	45.53	1.93	(43) 6990	48.19	0.92
D-2	6535	45.04	0.96	(37) 7290	50.25	1.27	(43) 8150	56.18	1.79
D-3	5850	40.32	0.72	(37) 6920	47.71	2.25	(45) 7290	50.25	1.27
D-4	6130	42.26	1.07	(38) 7010	48.31	1.39	(44) 7235	49.89	1.04
AVERAGE	6165	42.51	0.90	6955	47.95	1.75	7415	51.12	1.29
Coeff. of variation:	2.12%				3.66%			2.54%	

* - Average of 4 cubes.

s.d. = Standard deviation.

TABLE 10.2 ULTIMATE STATIC STRENGTH OF CONTROL PRISMS

SERIES-D

BATCH No.	COMMENCEMENT OF TEST**				COMPLETION OF TEST+			
	Age days	lbf/in^2	N/mm^2	s.d. N/mm^2	Age days	lbf/in^2	N/mm^2	Remark
D-1	37	5285	36.44	1.24	43	4970	34.26	
D-2	37	5375	37.06	0.60	43	5930	40.89	>av.
D-3	37	5055	34.85	2.35	45	5415	37.34	
D-4	38	5360	36.94	0.90	44	5845	40.30	>av.
AVERAGE		5270	36.32	1.43		5540	38.19	
Coeff. of variation:				3.94%				

** - Average of 3 prisms.

\+ - Test result of 1 prism.

TABLE 10.3 ULTIMATE STATIC STRENGTH OF CONTROL CUBES

SERIES-E

BATCH No.	28th DAYS*			COMMENCEMENT OF TEST*			COMPLETION OF TEST*		
	lbf/in^2	N/mm^2	s.d. N/mm^2	Age, days / lbf/in^2	N/mm^2	s.d. N/mm^2	Age, days / lbf/in^2	N/mm^2	s.d. N/mm^2
E-1	6375	43.95	1.07	(37) 7375	50.86	0.88	(44) 7620	52.55	0.48
E-2	6165	42.52	2.00	(38) 7410	51.10	1.21	(45) 7620	51.10	1.65
E-3	6585	45.41	2.47	(39) 7750	53.42	0.57	(46) 8050	55.50	0.34
E-4	6325	43.59	0.42	(42) 7500	51.70	2.10	(44) 7655	52.79	1.38
AVERAGE	6365	43.86	1.68	7510	51.77	1.32	7685	52.98	1.11
Coeff.of variation:			3.85%			2.55%			2.10%

* -Average of 4 cubes.

TABLE 10.4 ULTIMATE STATIC STRENGTH OF CONTROL PRISMS

SERIES-E

BATCH No.	COMMENCEMENT OF TEST**				COMPLETION OF TEST+			
	Age days	lbf/in^2	N/mm^2	s.d. N/mm^2	Age days	lbf/in^2	N/mm^2	Remark
E-1	37	5845	40.30	1.09	44	-	--	
E-2	38	5190	35.78	0.69	45	-	--	
E-3	39	5940	40.96	1.60	46	7215	49.72'	> av.
E-4	42	5285	36.44"	1.47	44	-	--	
AVERAGE		5565	38.37	1.26				
Coefficient of variation				3.29%				

** - Average of 3 prisms.

\+ - Test result of 1 prism.

' - Average of 2 prisms.

" - Average of 5 prisms.

s.d. = Standard deviation.

TABLE 10.5 SUMMARY OF TWO STEP TEST RESULTS

D-SERIES

SPECIMEN NUMBER	S_1 %	S_2 %	S_3 %	$\frac{n_1}{N_1}$	$\frac{n_2}{N_2}$	$\frac{n_3}{N_3}$	$\sum_1^3 \frac{n}{N} = \frac{n_1}{N_1} + \frac{n_2}{N_2} + \frac{n_3}{N_3}$	$\sum_1^3 (n/N)_{av}$	s.d.	PALMGREN-MINER HYPOTHESIS $\sum \frac{n}{N}$
D2-F4	80	70	80	0.300	0.233	-	0.533			
D1-F1	80	70	80	0.300	0.300	0.858	1.458			
D2-F1	80	70	80	0.300	0.300	0.913	1.513	1.408	0.519	1.000
D3-F3	80	70	80	0.300	0.300	1.030	1.630			
D1-F4	80	70	80	0.300	0.300	1.310	1.910			
D4-F2	70	80	70	0.300	0.300	0.205	0.805			
D4-F4	70	80	70	0.300	0.300	0.829	1.429			
D2-F2	70	80	70	0.300	0.300	0.995	1.595	1.734	0.792	1.000
D4-F3	70	80	70	0.300	0.300	1.275	1.875			
D1-F3	70	80	70	0.300	0.300	2.365	2.965			

S_1, S_2, S_3 = Stress levels for the first, second and third stage (Percentage of prism ultimate static strength)

N_1, N_2, N_3 = Fatigue life at constant stress levels S_1, S_2, and S_3

n_1, n_2 = Number of cycles for the first and second stage

n_3 = Number of cycles for the third stage (continue to failure)

s.d. = Standard de viation.

TABLE 10.6 SUMMARY OF FOUR TEST RESULTS
E-SERIES

SPECIMEN NUMBER	S_1 %	S_2 %	S_3 %	S_4 %	S_5 %	$\frac{n_1}{N_1}$	$\frac{n_2}{N_2}$	$\frac{n_3}{N_3}$	$\frac{n_4}{N_4}$	$\frac{n_5}{N_5}$	$\sum_1^5 \frac{n}{N}$	$\sum_1^5 (\frac{n}{N})_{av.}$	s.d.	PALMGREN-MINER $\sum \frac{n}{N}$
E1-F1	80	70	80	70	80	0.202	0.200	0.110	-	-	0.512			
E1-F3	80	70	80	70	80	0.202	0.200	0.202	0.227	0.747	1.578			
E1-F4	80	70	80	70	80	0.202	0.200	0.202	0.200	1.030	1.834	1.738	0.798	1.000
E2-F1	80	70	80	70	80	0.202	0.200	0.202	0.200	1.287	2.091			
E2-F3	80	70	80	70	80	0.202	0.200	0.202	0.200	1.875	2.679			
E4-F2	70	80	70	80	70	0.200	0.202	0.200	0.202	0.163	0.967			
E2-F2	70	80	70	80	70	0.200	0.202	0.200	0.202	0.420	1.224			
E2-F4	70	80	70	80	70	0.200	0.202	0.200	0.202	0.575	1.379	1.685	0.819	1.000
E2-F5	70	80	70	80	70	0.200	0.202	0.213	0.202	0.995	1.812			
E1-F5	70	80	70	80	70	0.200	0.202	0.200	0.202	2.240	3.044			

S_1, S_2, S_3, S_4, S_5 = Stress levels for the first, second, third, fourth, fifth stage (% of prism static strength)
N_1, N_2, N_3, N_4, N_5 = Fatigue life at constant stress levels S_1, S_2, S_3, S_4 and S_5
n_1, n_2, n_3, n_4 = Number of cycles for the first, second, third and fourth stage
n_5 = Number of cycles for the fifth stage (continue to failure)
s.d. = Standard deviation

TABLE 10.7 SUMMARY OF TWO STEP TEST ANALYSIS

D - SERIES/PART A

S_1 = 80%	S_2 = 70%	S_3 = 80%
n_1/N_1 = 0 - 30.02%	$\Sigma n/N$ = 30.02-60.02%	$\Sigma \frac{n}{N}$ = 60.02%-To FAILURE
$V_1 = a\,(n_1/N_1)^b$	$V_2 = a\,(\Sigma n/N)^b$	$V_3 = a\,(\Sigma n/N)^b$
a = 6.1119 b = 0.2785 r = 0.9910 DEGREE OF FREEDOM = 30-2 = 28 AT n/N = 100% V_u = 22.039%	a = 0.9462 b = 0.8598 r = 0.9674 DEGREE OF FREEDOM = 60	a = 10.3642 b = 0.2774 r = 0.7266 DEGREE OF FREEDOM = 79
$V_1 = a\,(n_1)^b$		
a = 2.7934 b = 0.2794 r = 0.9909 DEGREE OF FREEDOM = 30-2 = 28 AT V_u = 22.039% N = 1622		

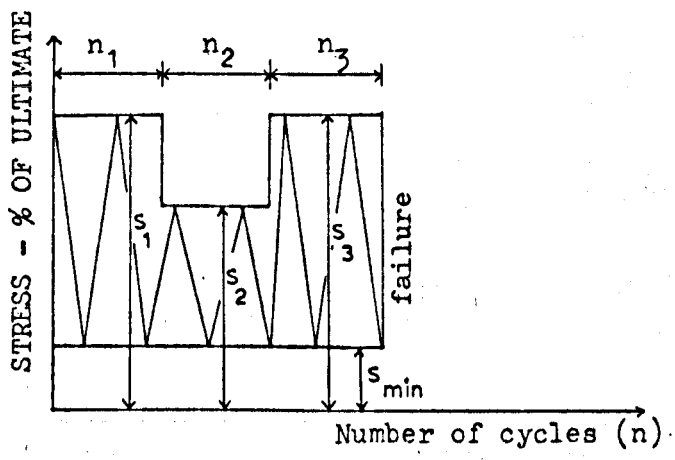

LOADING PROGRAMME 3

S_1, S_2, S_3 = Stress levels for the first, second and third stage

V_1, V_2, V_3 = Max. decrease of original pulse velocity in percent dut to n_1/N_1 at S_1; n_2/N_2 at S_2 and n_3/N_3 at S_3

$\Sigma \frac{n}{N}$ = Cumulative cycle ratio

a, b = Experimental constants

r = Coefficient of correlation

TABLE 10.8 SUMMARY OF TWO STEP TEST ANALYSIS

D - SERIES/PART B

S_1 = 70%	S_2 = 80 %	S_3 = 70%
n_1/N_1 = 0-30.00%	$\Sigma n/N$ = 30.00-60.02%	$\Sigma \frac{n}{N}$ =60.02-TO FAILURE
$V_1 = a(n_1/N_1)^b$	$V_2 = a(\Sigma n/N)^b$	$V_3 = a(\Sigma n/N)^b$
a = 8.7233 b = 0.2184 r = 0.9469 DEGREE OF FREEDOM = 50-2=48 AT n/N = 100% V_u = 23.844%	a = 9.41 39 b = 0.2237 r = 0.3787 DEGREE OF FREEDOM = 27	a = 2.7968 b = 0.5349 r = 0.8344 DEGREE OF FREEDOM = 40
$V_1 = a(n_1)^b$	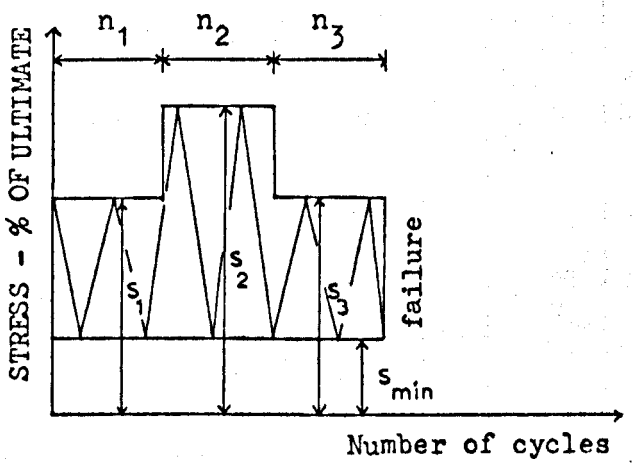	
a = 2.0233 b = 0.2115 r = 0.9369 DEGREE OF FREEDOM = 50-2 = 48 AT V_u = 23.844% N = 116,253	LOADING PROGRAMME 4	

NOTE all expressions are of the same meanings as in Table 10.8

TABLE 10.9 SUMMARY OF FOUR STEP TEST ANALYSIS
E - SERIES/PART A

S_1 = 80%	S_2 = 70%	S_3 = 80%	S_4 = 70%	S_5 = 80%
n_1/N_1 = 20.20%	$\Sigma n/N$ = 20.02 - 40.02%	$\Sigma n/N$ = 40.02 - 60.04%	$\Sigma n/N$ = 60.04 - 80.04%	$\Sigma \frac{n}{N}$ = 80.04 - TO FAILURE
$V_1 = a(n_1/N_1)^b$	$V_2 = a(\Sigma n/N)^b$	$V_3 = a(\Sigma n/N)^b$	$V_4 = a(\Sigma n/N)^b$	$V_5 = a(\Sigma n/N)^b$
a = 5.3547	a = 0.6809	a = 8.0246	a = 0.8922	a = 5.5072
b = 0.2270	b = 0.9123	b = 0.2338	b = 0.7735	b = 0.3684
r = 0.9591	r = 0.8974	r = 0.4400	r = 0.7436	r = 0.7543
DEGREE OF FREEDOM	DEGREE OF FREEDOM	DEGREE OF FREEDOM	DEGREE OF FREEDOM	DEGREE OF FREEDOM
= 18-2=16	= 38	= 19	= 50	= 59
AT n/N = 100%				
V_u = 15.231%				

$V_1 = a(n_1)^b$	
a = 2.8284	
b = 0.2278	
r = 0.9589	
DEGREE OF FREEDOM	
= 16	
AT V_u; N = 1620	

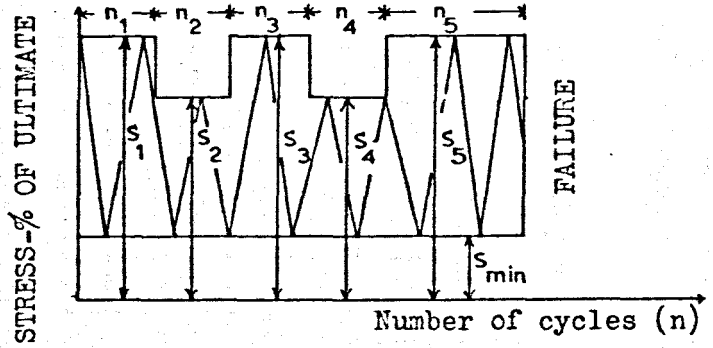

LOADING PROGRAM 5

NOTE: All expressions are of the same meanings as in Table 10.6

EXCEPT: V_1, V_2, V_3, V_4, V_5 = Max decrease of original pulse velocity in percent due to S_1, S_2, S_3, S_4 and S_5.

$\Sigma \frac{n}{N}$ = Cumulative cycle ratio

a, b = Experimental constants

r = Coefficient of correlation

TABLE 10.10 SUMMARY OF FOUR STEP TEST ANALYSIS
E - SERIES/PART B

S_1 = 70%	S_2 = 80%	S_3 = 70%	S_4 = 80%	S_5 = 70%
n_1/N_1 = 20.20%	$\Sigma n/N$ = 20 - 40.20%	$\Sigma n/N$ = 40.20 - 60.20%	$\Sigma n/N$ = 60.20 - 80.40%	$\Sigma \frac{n}{N}$ = 80.4 - TO FAILURE
$V_1 = a(n_1/N_1)^b$	$V_2 = a(\Sigma n/N)^b$	$V_3 = a(\Sigma n/N)^b$	$V_4 = a(\Sigma n/N)^6$	$V_5 = a(\Sigma n/N)^b$
a = 7.8228 b = 0.2152 r = 0.9246 DEGREE OF FREEDOM = 52-2=50 AT n/N = 100% V_u = 21.075%	a = 8.6932 b = 0.2157 r = 0.4000 DEGREE OF FREEDOM = 24	a = 1.8639 b = 0.6406 r = 0.5480 DEGREE OF FREEDOM = 31	a = 2.9273 b = 0.5252 r = 0.3400 DEGREE OF FREEDOM = 22	a = 3.4402 b = 0.4935 r = 0.4218 DEGREE OF FREEDOM = 37
$V_1 = a(n_1)^b$ a = 1.7677 b = 0.2159 r = 0.9250 DEGREE OF FREEDOM = 50 AT V_u; N = 96,589	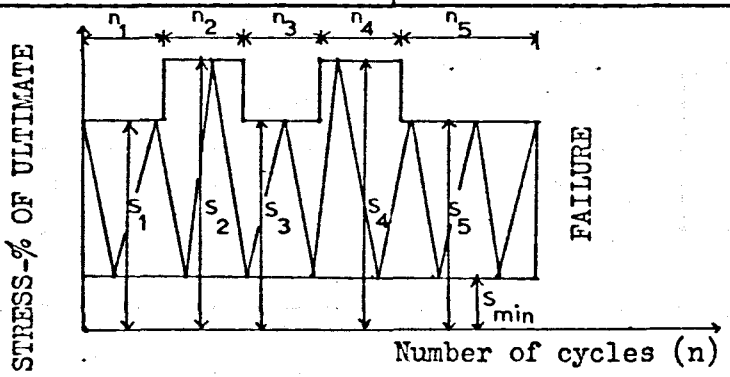 LOADING PROGRAMME 6		NOTE: All expressions are of the same meanings as in Table 10.9	

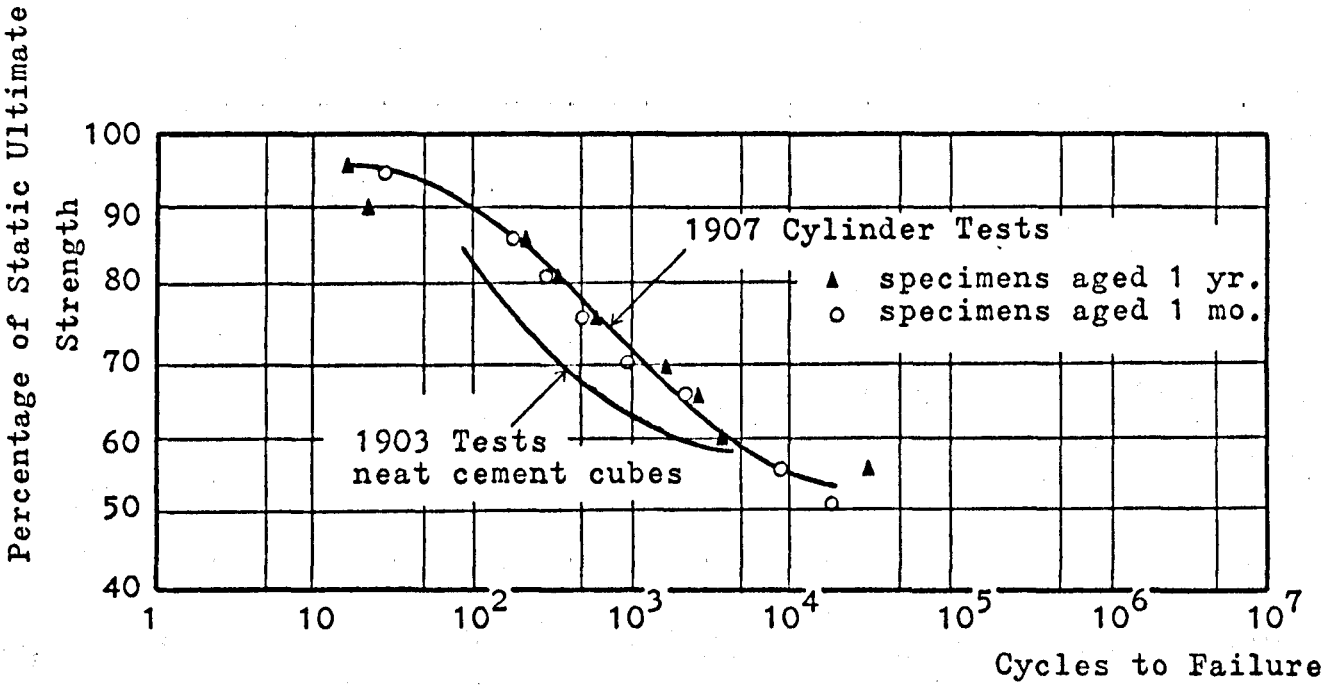

FIG..2.1 S-N RELATIONSHIPS FOR CONCRETE SUBJECTED TO REPEATED AXIAL COMPRESSIVE LOADING. BASED ON VAN ORNUM[8]. [MEAN STATIC STRENGTH 8.27 N/mm^2]

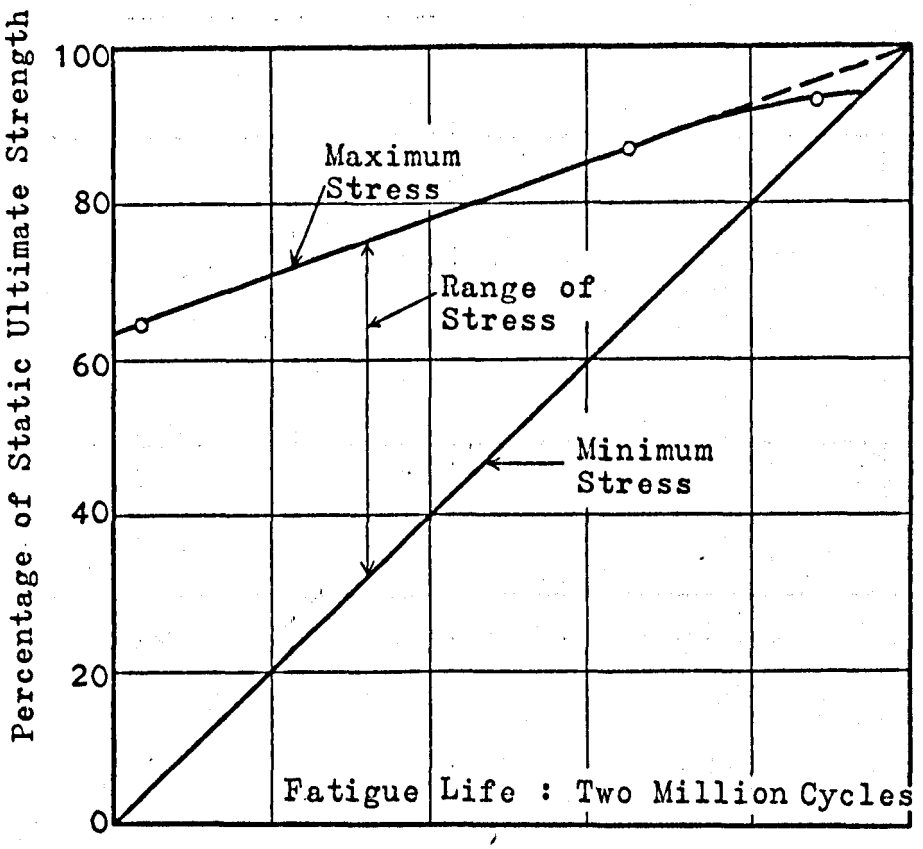

FIG. 2.2 MODIFIED GOODMAN DIAGRAM FOR CONCRETE SUBJECTED TO REPEATED AXIAL LOADING. BASED ON GRAF AND BRENNER[8]. [MEAN STATIC STRENGTH 17.58 N/mm^2]

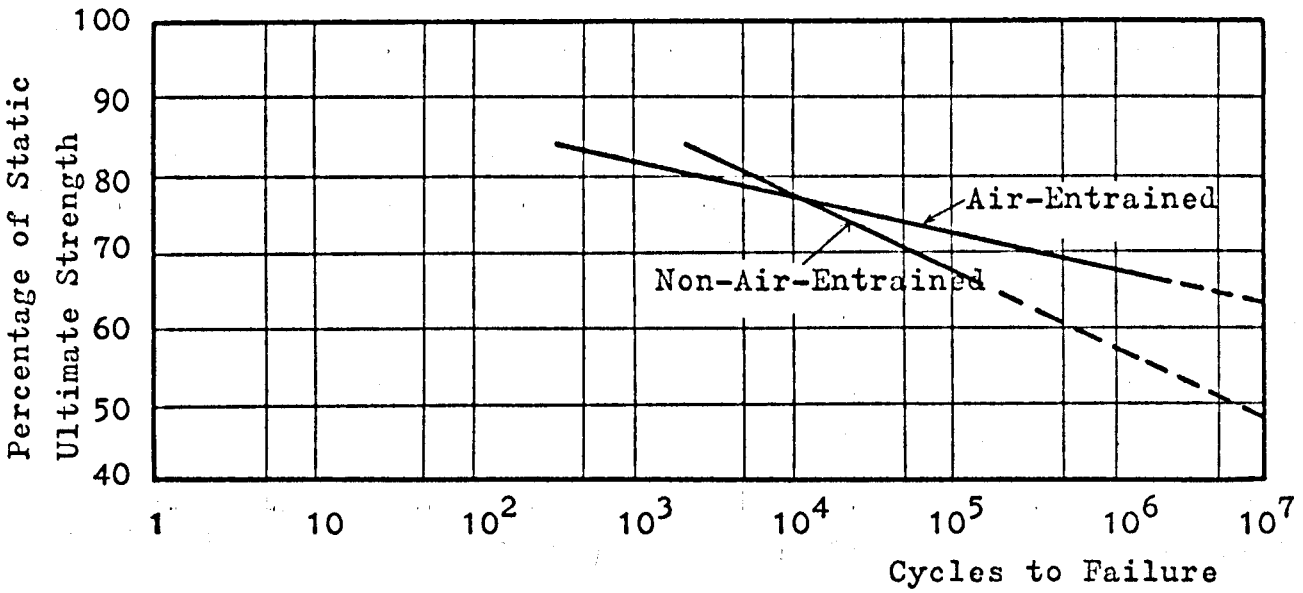

FIG. 2.3 S-N DIAGRAM FOR AIR-ENTRAINED CONCRETES SUBJECTED TO REPEATED AXIAL COMPRESSIVE LOADING. BASED ON ANTRIM AND McLAUGHLIN.[23]

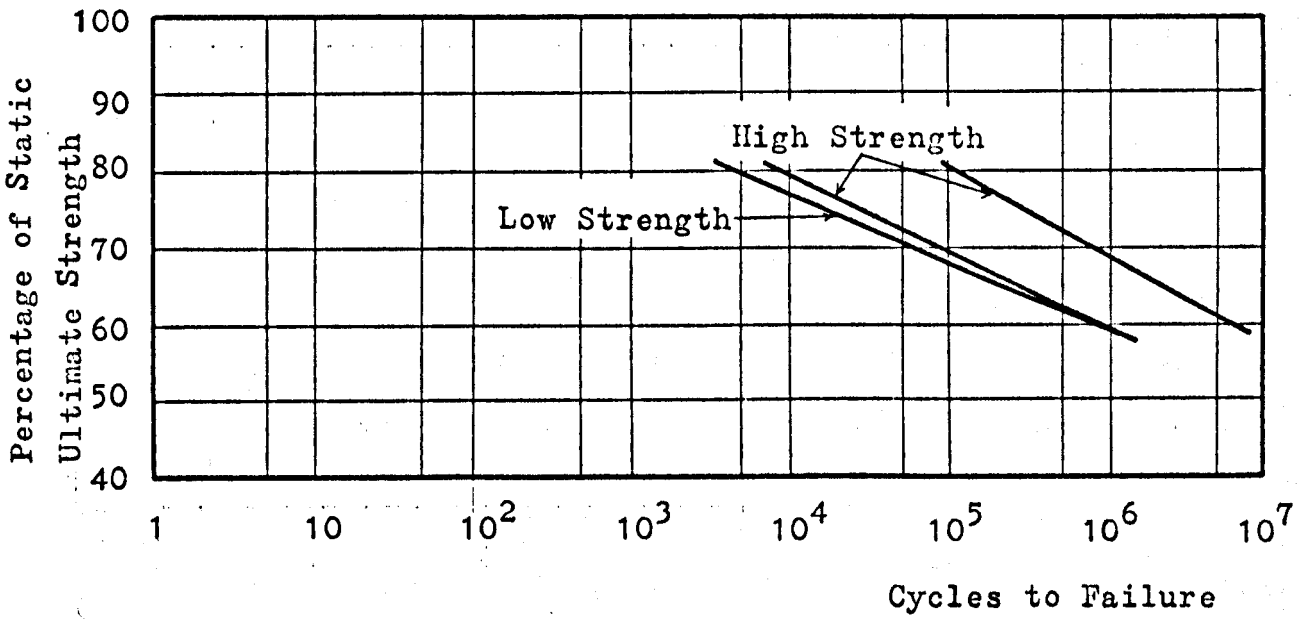

FIG. 2.4 S-N DIAGRAMS FOR HIGH AND LOW STRENGTH LIGHTWEIGHT AGGREGATE CONCRETE SUBJECTED TO REPEATED AXIAL COMPRESSIVE LOADING. BASED ON GRAY, McLAUGHLIN, AND ANTRIM.[24]

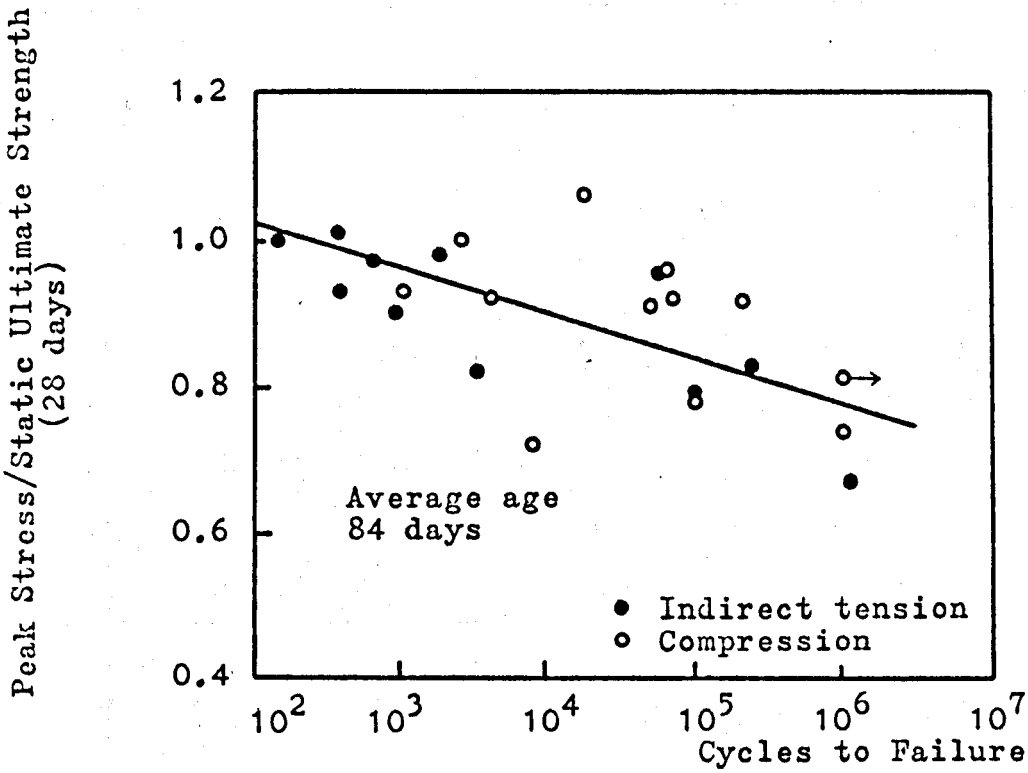

FIG. 2.5 FATIGUE LIFE OF CONCRETE IN TENSION AND COMPRESSION BASED ON LINGER AND GILLESPIE.[25] [MEAN STATIC STRENGTH = 23.16 N/mm^2]

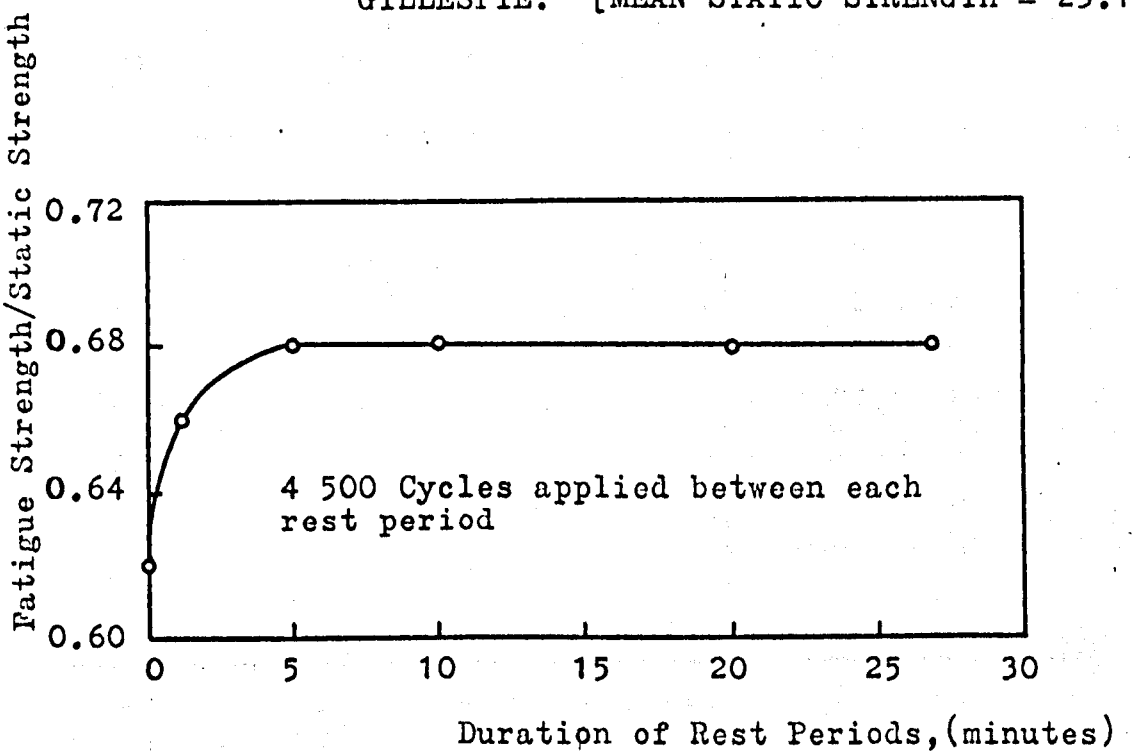

FIG. 2.6 EFFECT OF REST PERIODS ON FATIGUE STRENGTH AT 10^7 CYCLES BASED ON HILSDORF AND KESLER[36].

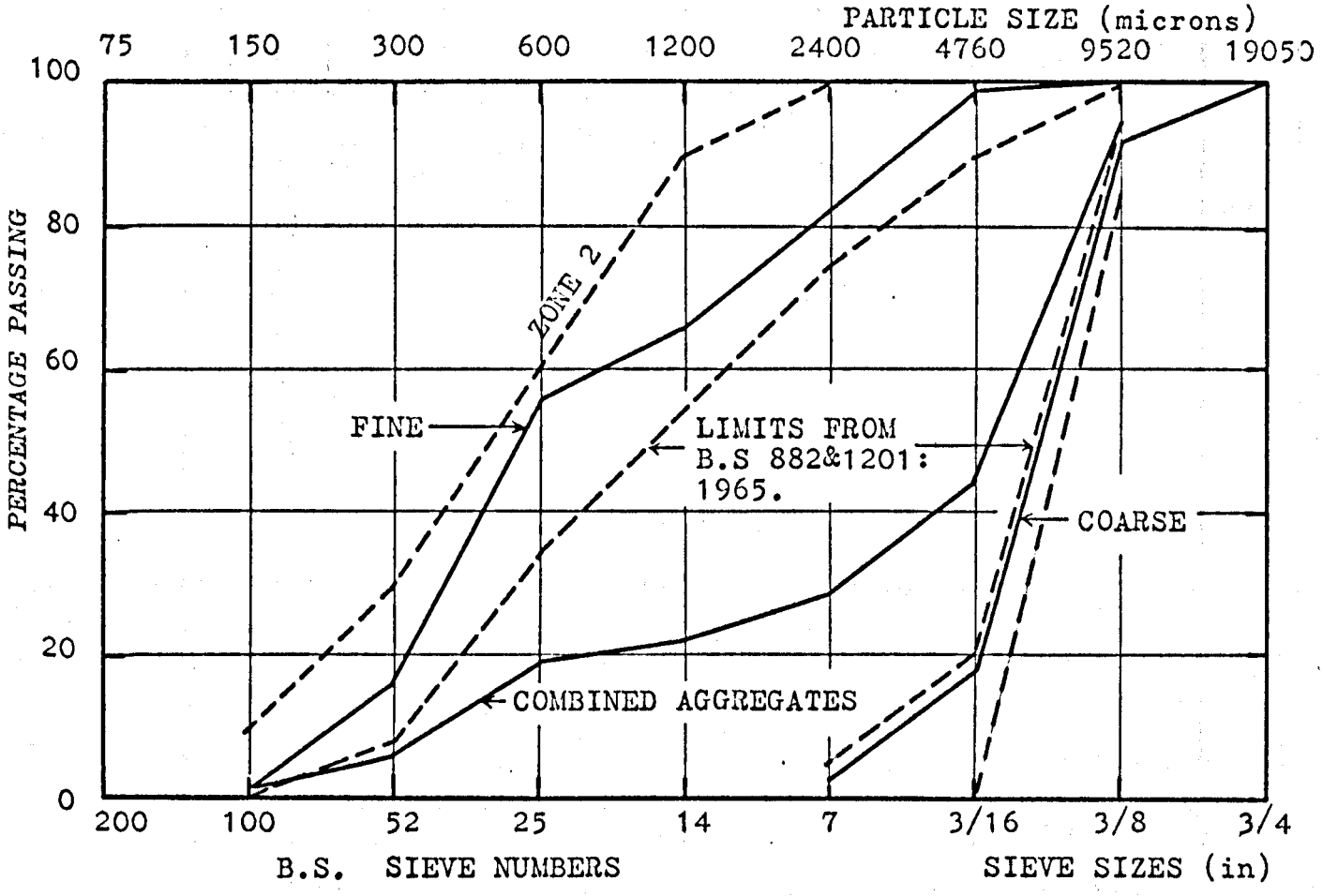

FIG. 3.1 TYPICAL AGGREGATE GRADING CURVES

CHEMICAL	SiO_2	21.11 %	LSF	91.6	%
	Al_2O_3	6.50 %	LCF	90.0	%
	Fe_2O_3	2.61 %	SR	2.32	%
	CaO	64.53 %	AR	2.49	%
	MgO	1.00 %	C_3S	43.6	%
	SO_3	2.41 %	C_2S	27.6	%
	Na_2O	0.28 %	C_3A	12.8	%
	K_2O	0.62 %	C_4AF	7.9	%
	Loss on Ignition	0.81 %			
	Insoluble Residue	1.29 %			
	Free Lime	1.1 %			
PHYSICAL	Water for Standard Consistency			27.7	%
	Setting Times: Initial			135	minutes
	Final			185	minutes
	Expansion 1 mm.		Surface Area	428	m^2/kg

TABLE 3.1 TEST RESULTS OF R.H.P.C. IN ACCORDANCE WITH B.S 12:PHYSICAL AND CHEMICAL TESTS.

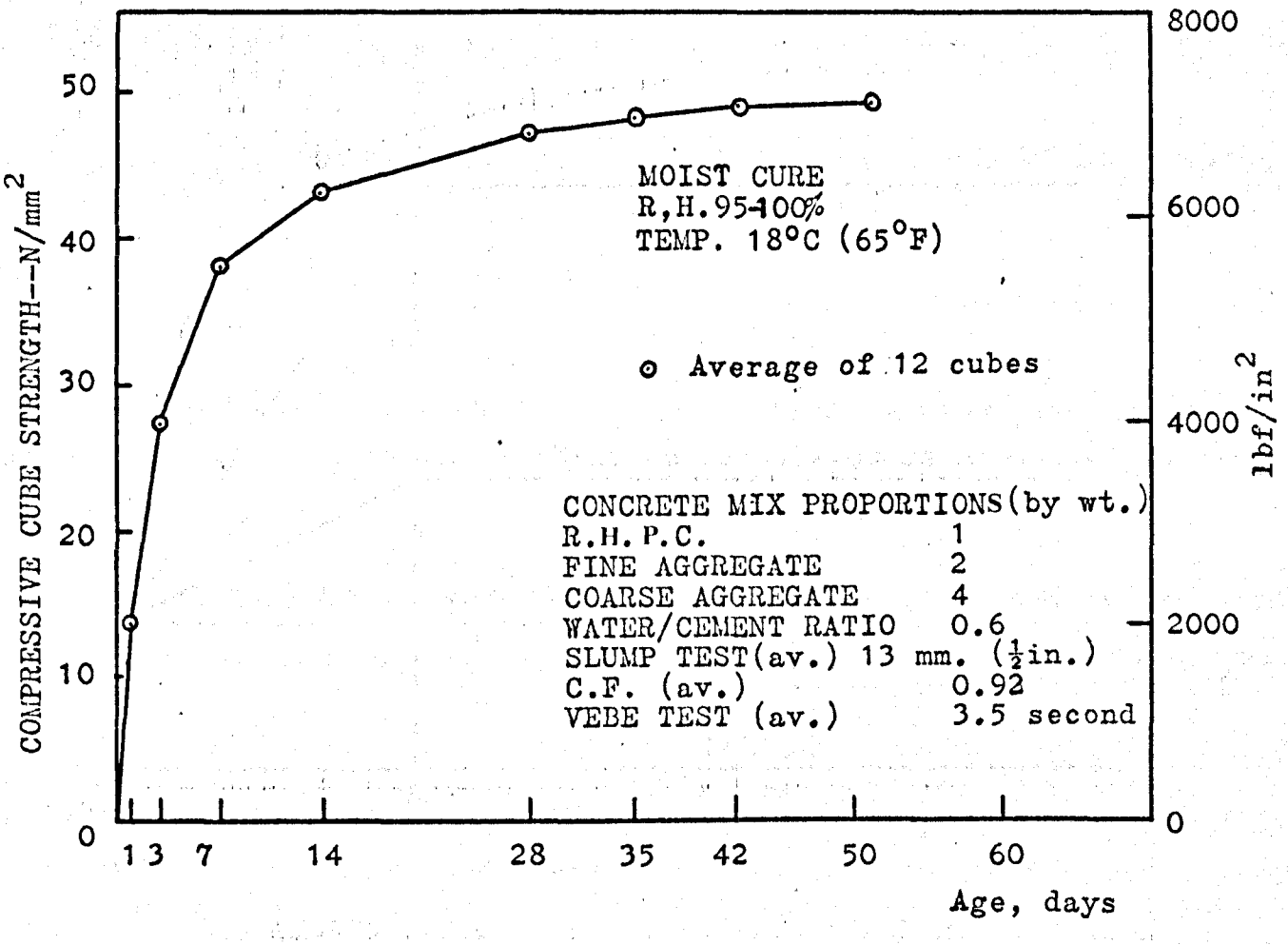

FIG. 3.2 TYPICAL GAIN OF STRENGTH OF CONCRETE WITH TIME.

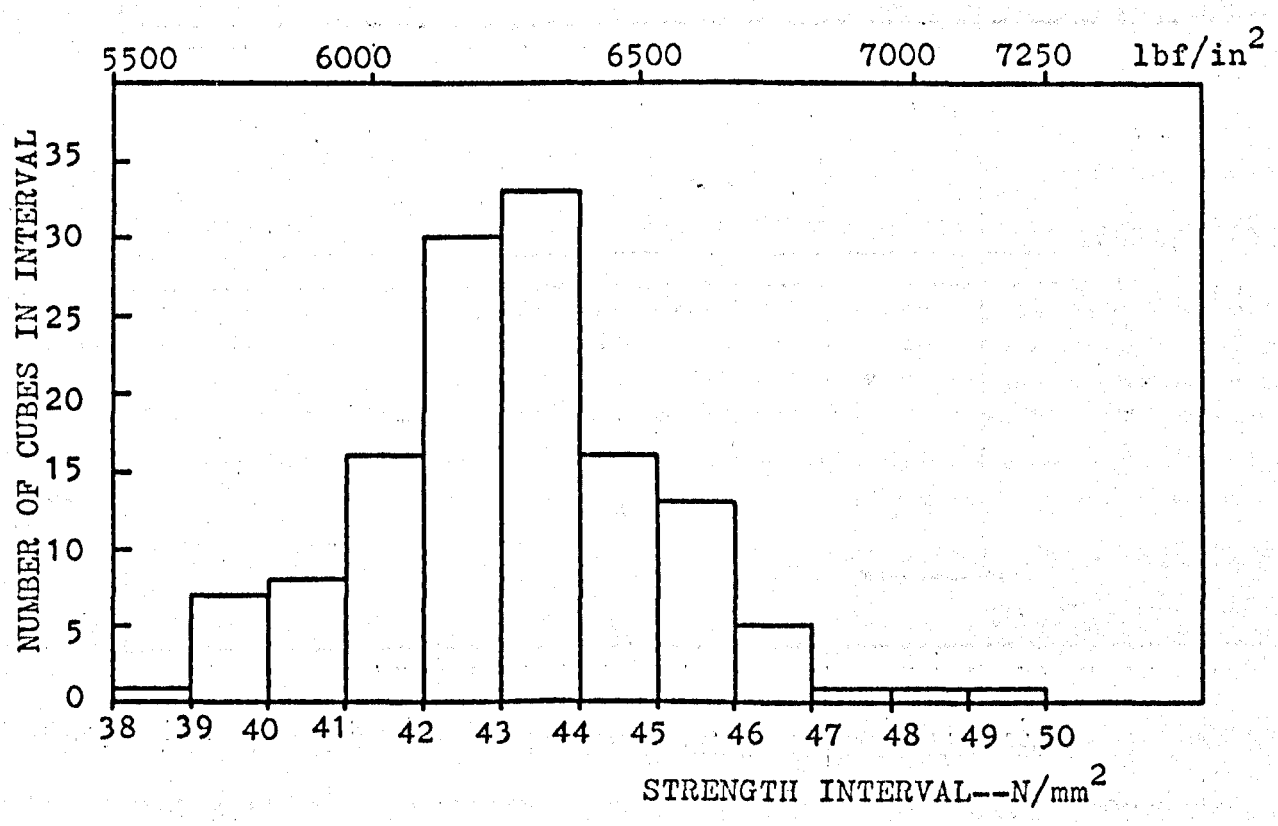

FIG. 3.3 HISTOGRAM OF ULTIMATE CUBE STRENGTH (Age 28 days)

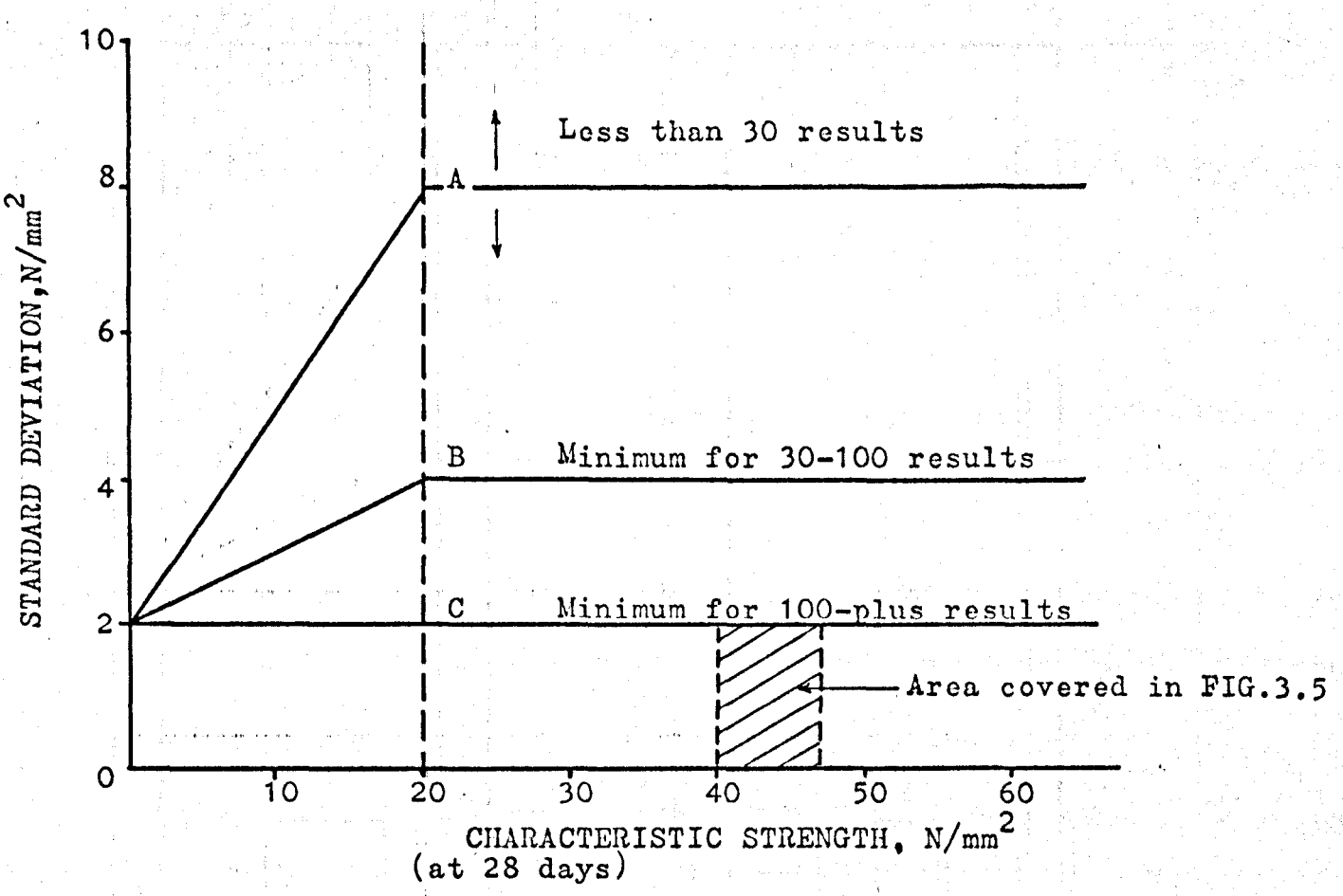

FIG.3.4 PROPOSED RELATIONSHIP BETWEEN STANDARD DEVIATION AND THE CHARACTERISTIC STRENGTH (47)

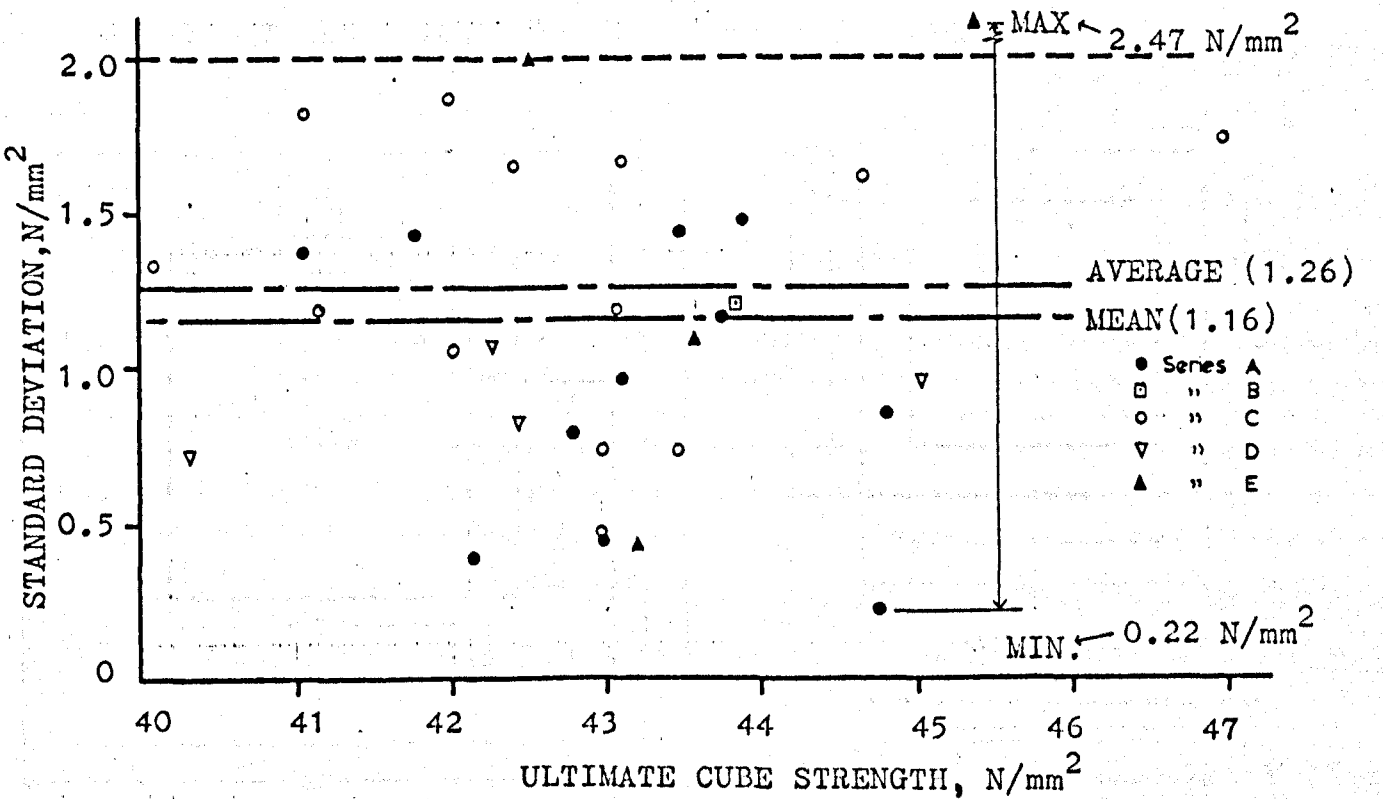

FIG.3.5 RELATIONSHIP BETWEEN THE STANDARD DEVIATION AND THE ULTIMATE CUBE STRENGTH AT 28 DAYS IN THIS STUDY.
[Each point is the average of 4 cubes.
33 @ 4 = 132 cubes)]

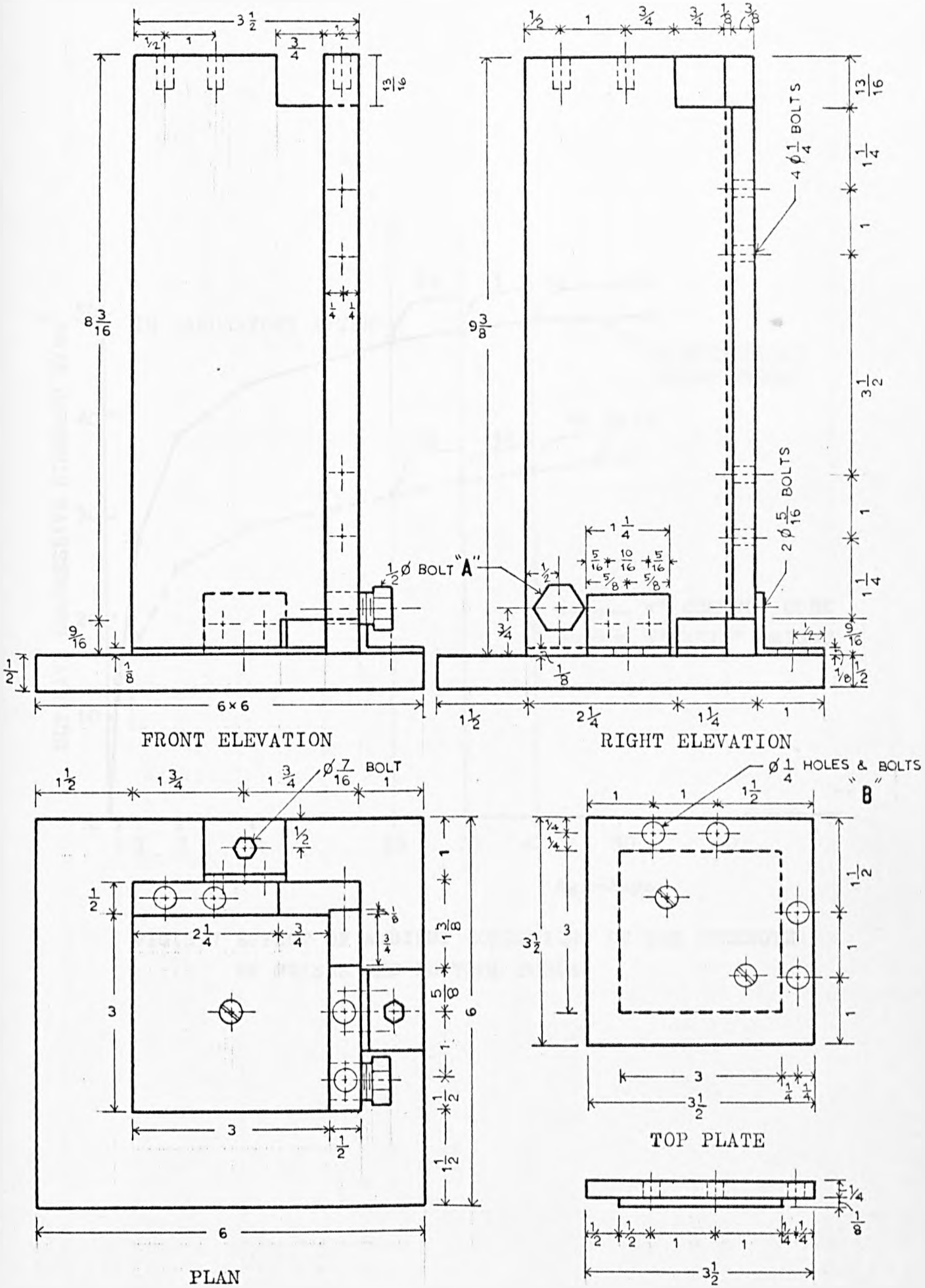

FIG. 3.6 NEW CAPPING JIG [Scale 1:2]
All dimensions are in inches
(1 inch = 25.4 mm.)

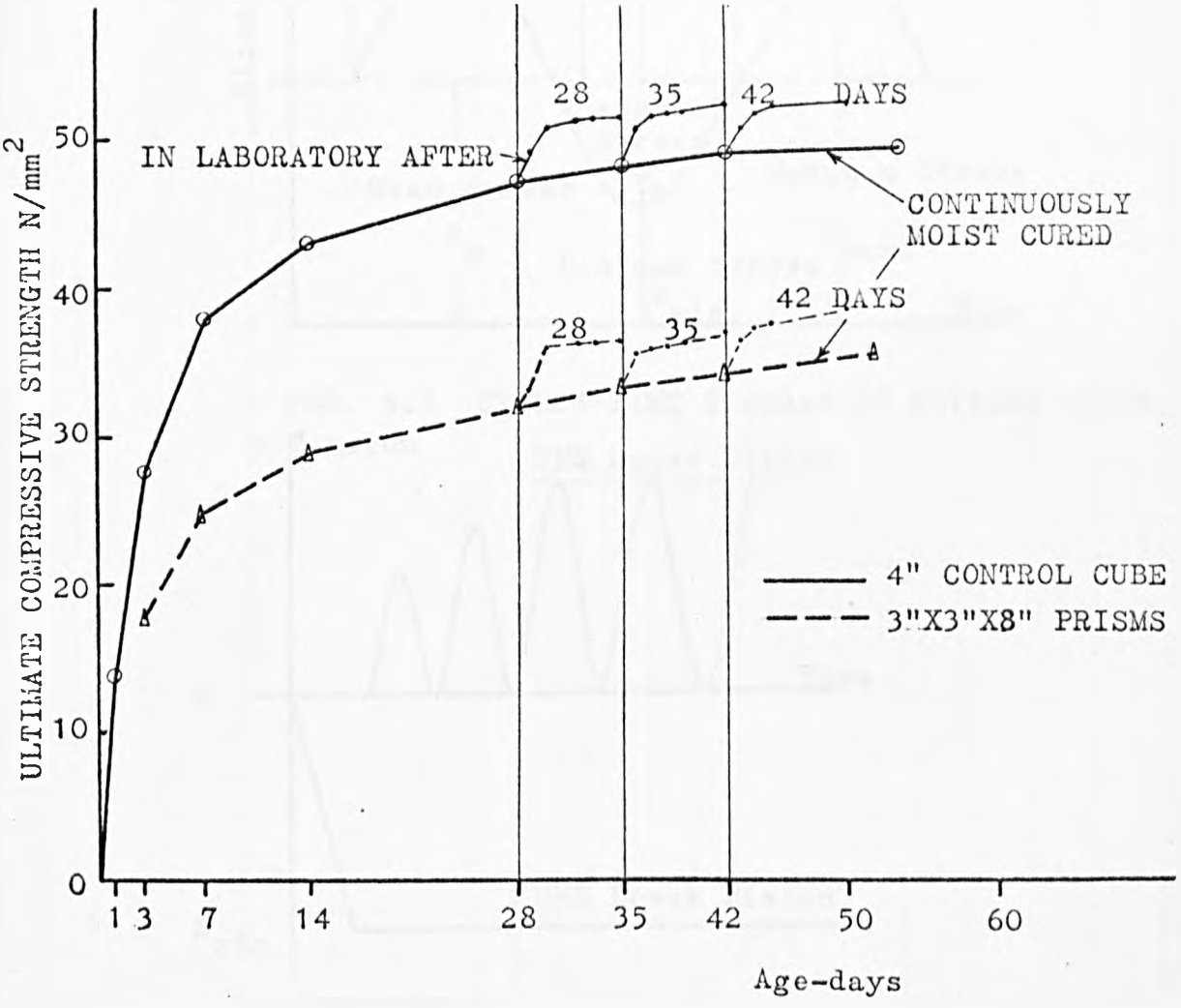

FIG.3.7 EFFECT OF AMBIENT CONDITIONS ON THE STRENGTH OF PRISMS AND CONTROL CUBES.

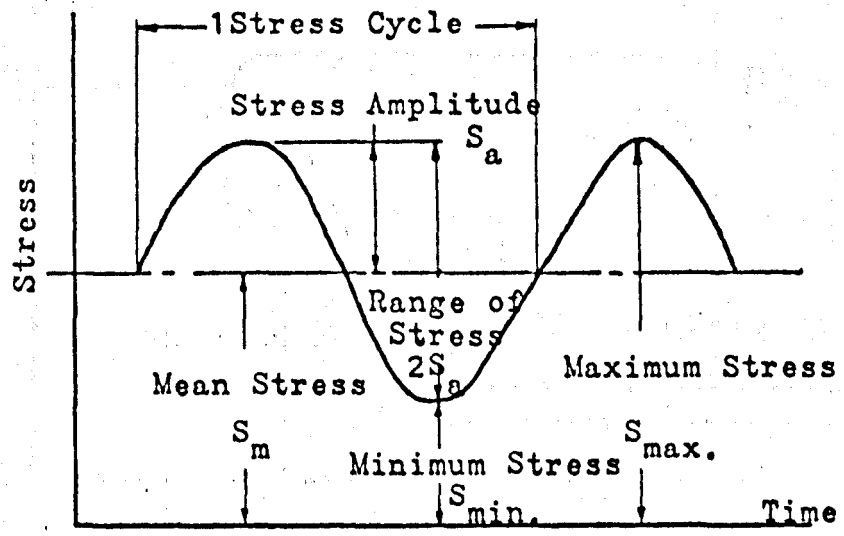

FIG. 4.1 STRESS-TIME DIAGRAM IN FATIGUE TESTS

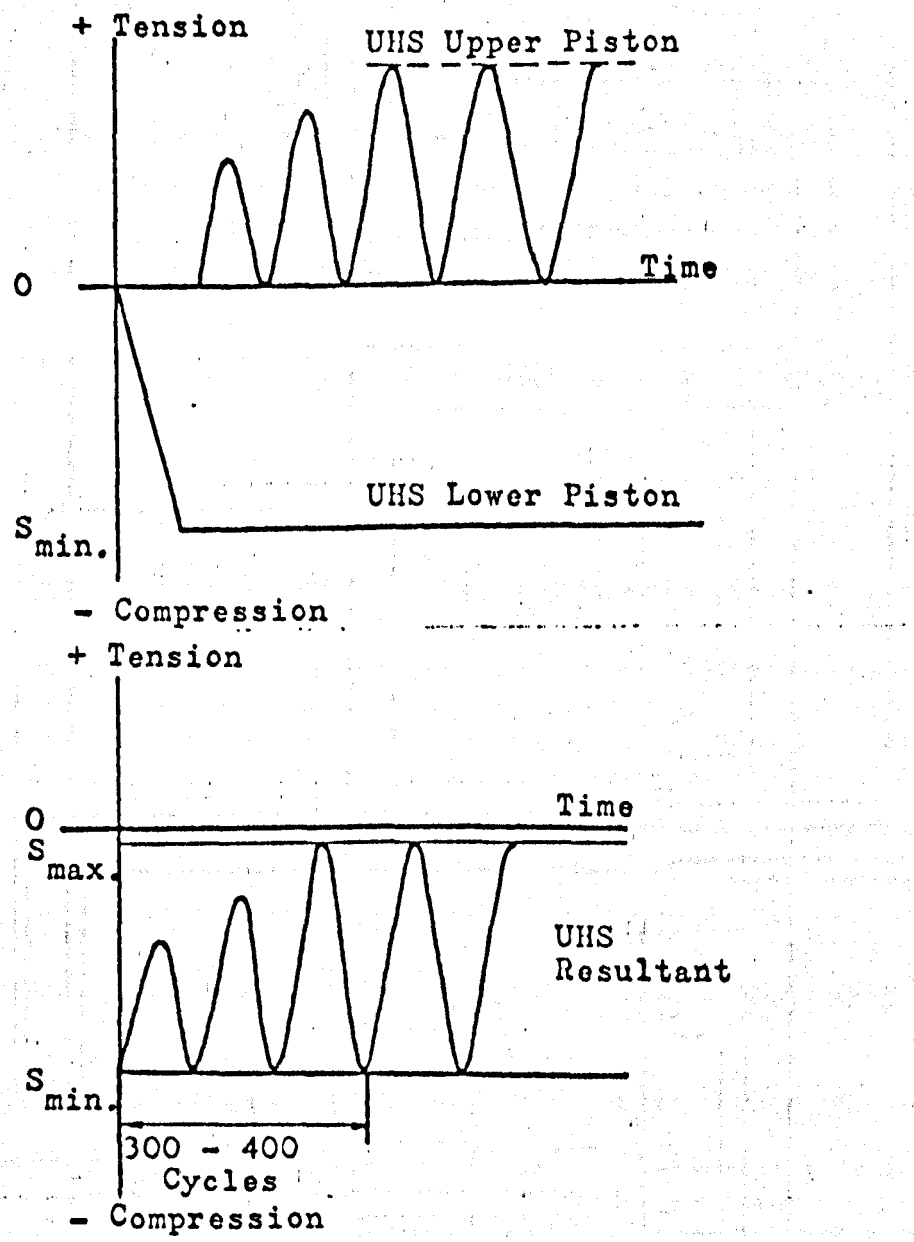

FIG. 4.2 UHS LOADING DIAGRAM

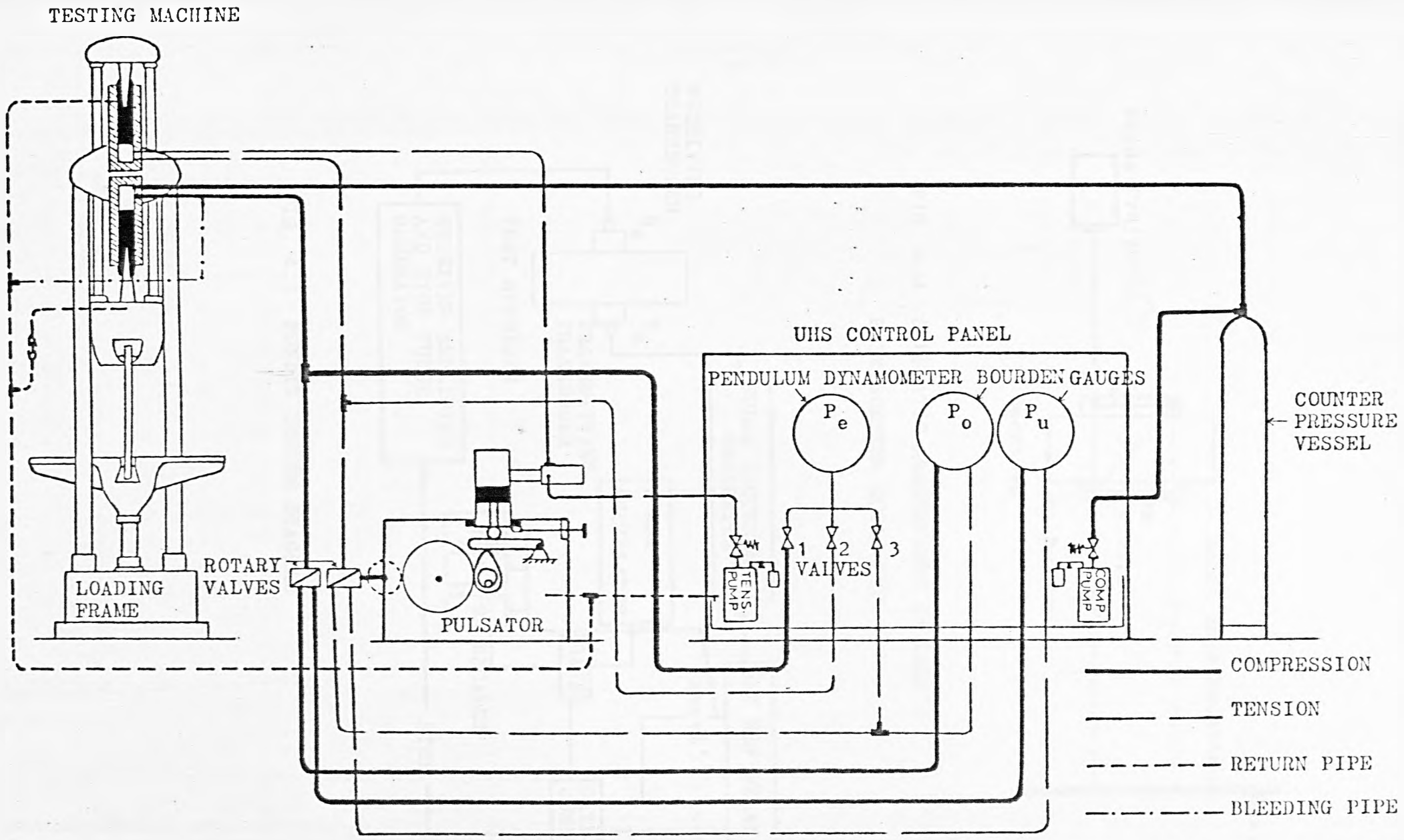

FIG. 4.3 SCHEMATIC LAYOUT OF LÖSENHAUSEN UHS 60 FATIGUE TESTING MACHINE.

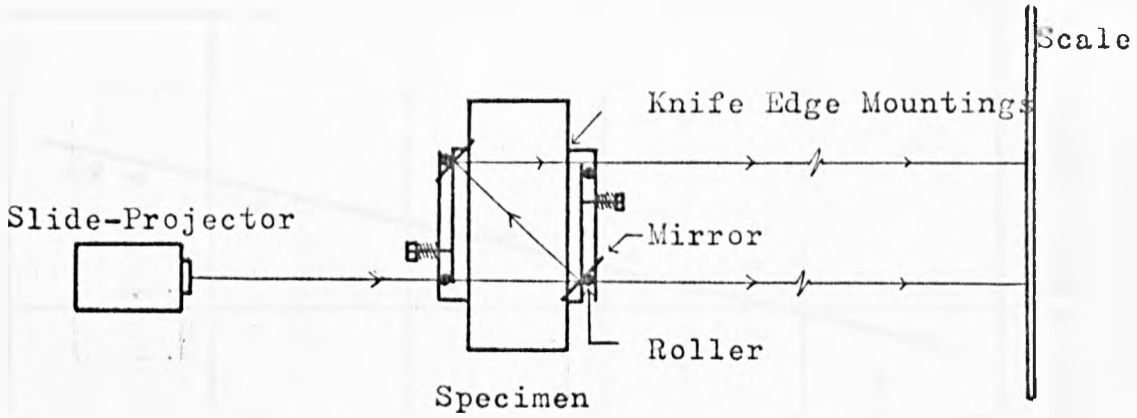

FIG. 4.4 SCHEMATIC ARRANGEMENT OF LAMB'S EXTENSOMETER EQUIPMENT.

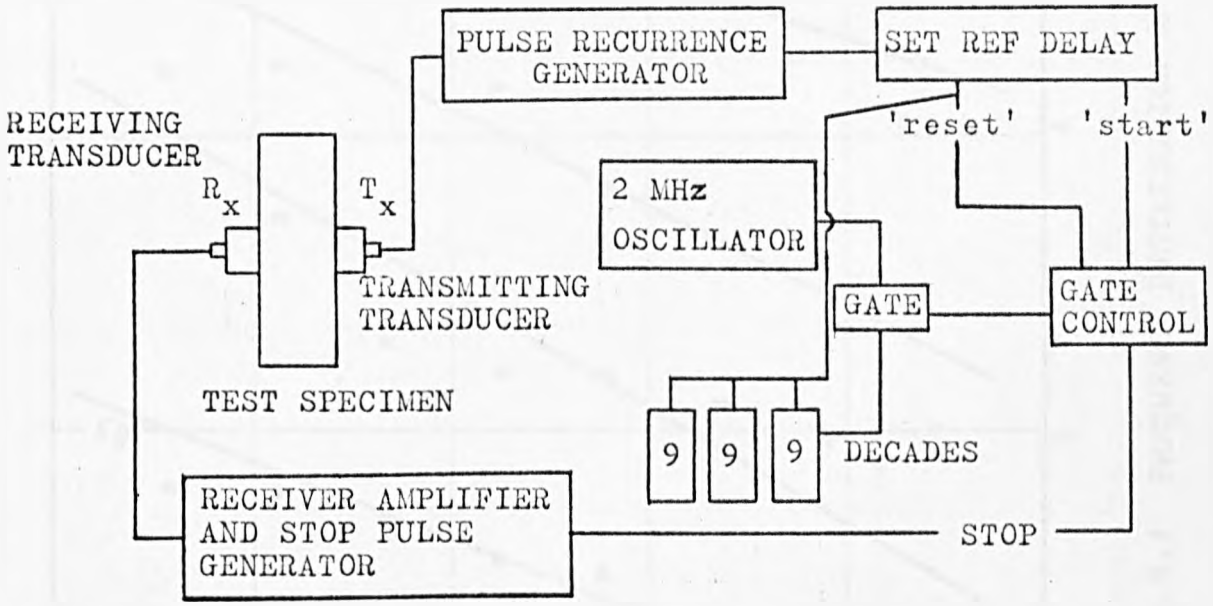

FIG. 4.5 PUNDIT SYSTEM DIAGRAM

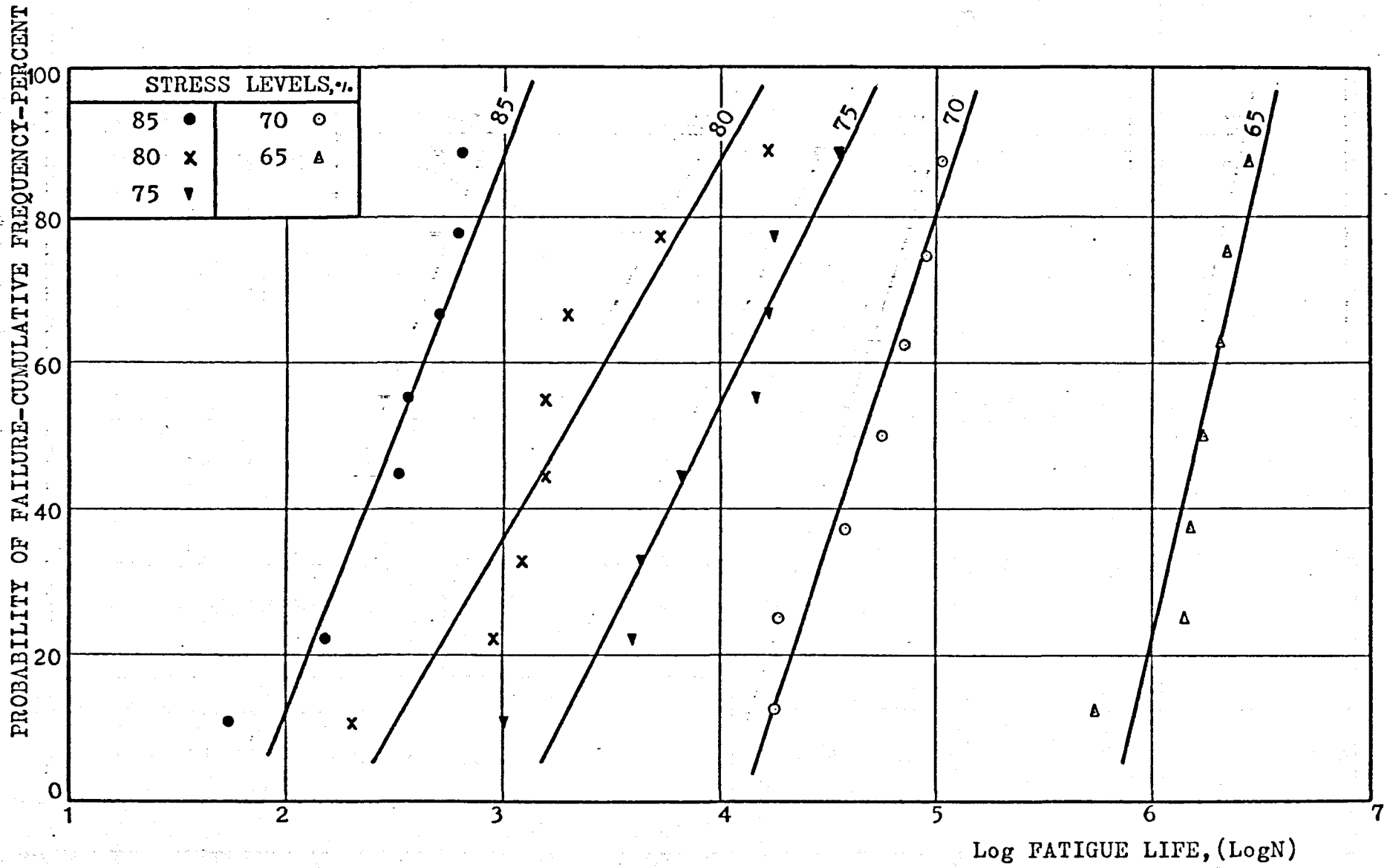

FIG. 5.1 FREQUENCY DISTRIBUTION OF FATIGUE LIFE

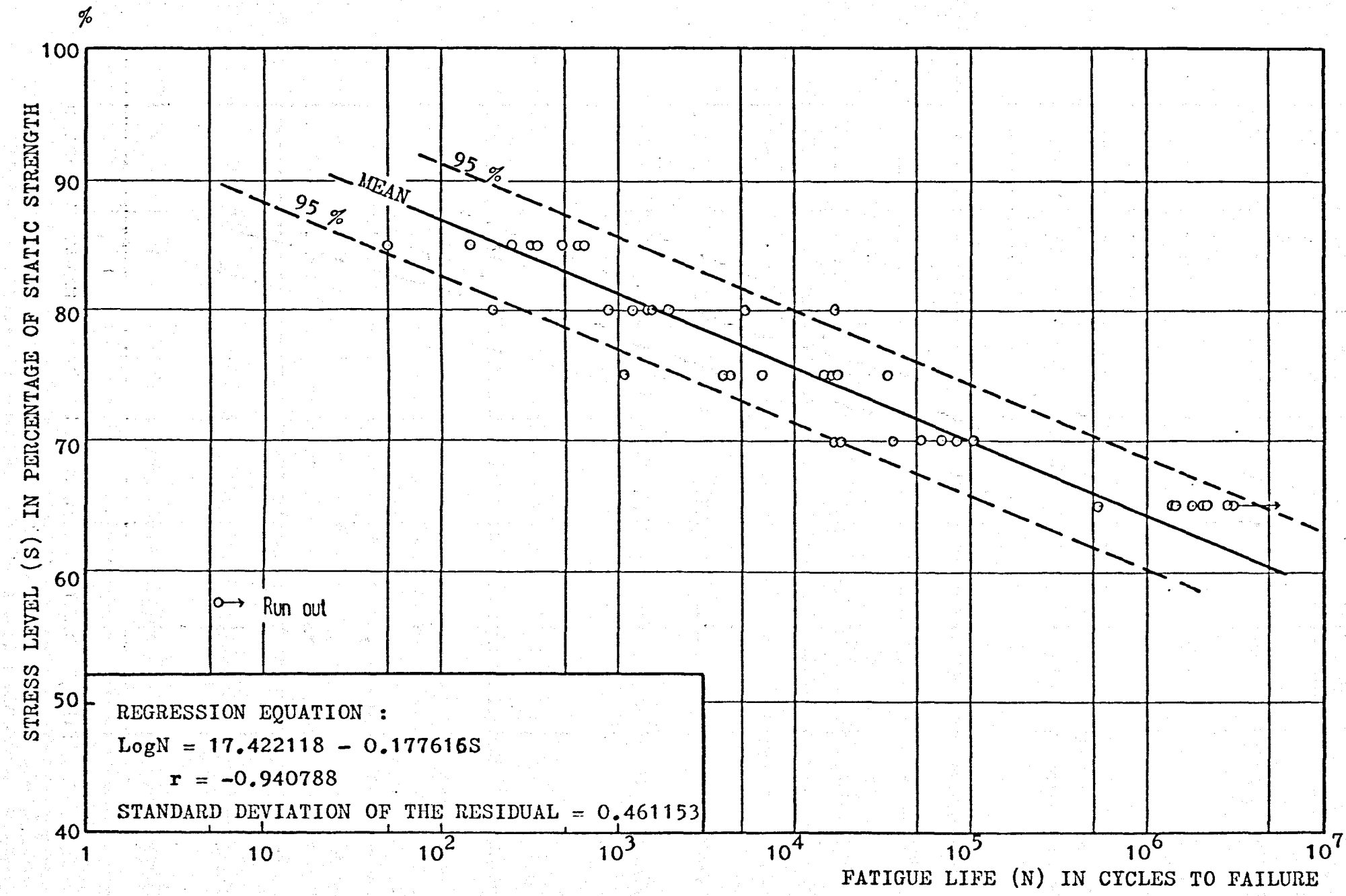

FIG. 5.2 S-N DIAGRAM FOR CONCRETE IN COMPRESSION

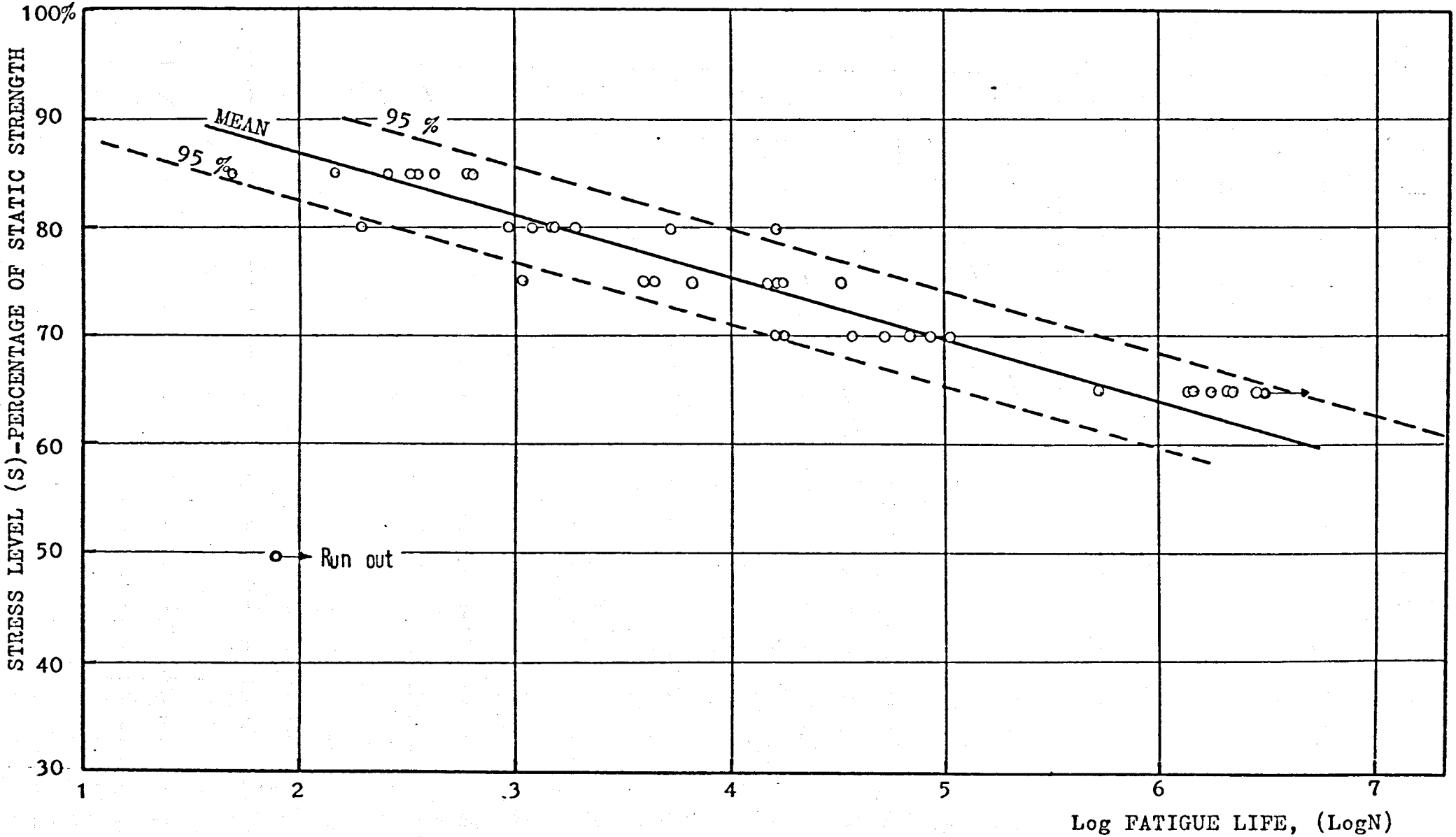

FIG. 5.2a FATIGUE CHARACTERISTIC OF CONCRETE IN COMPRESSION

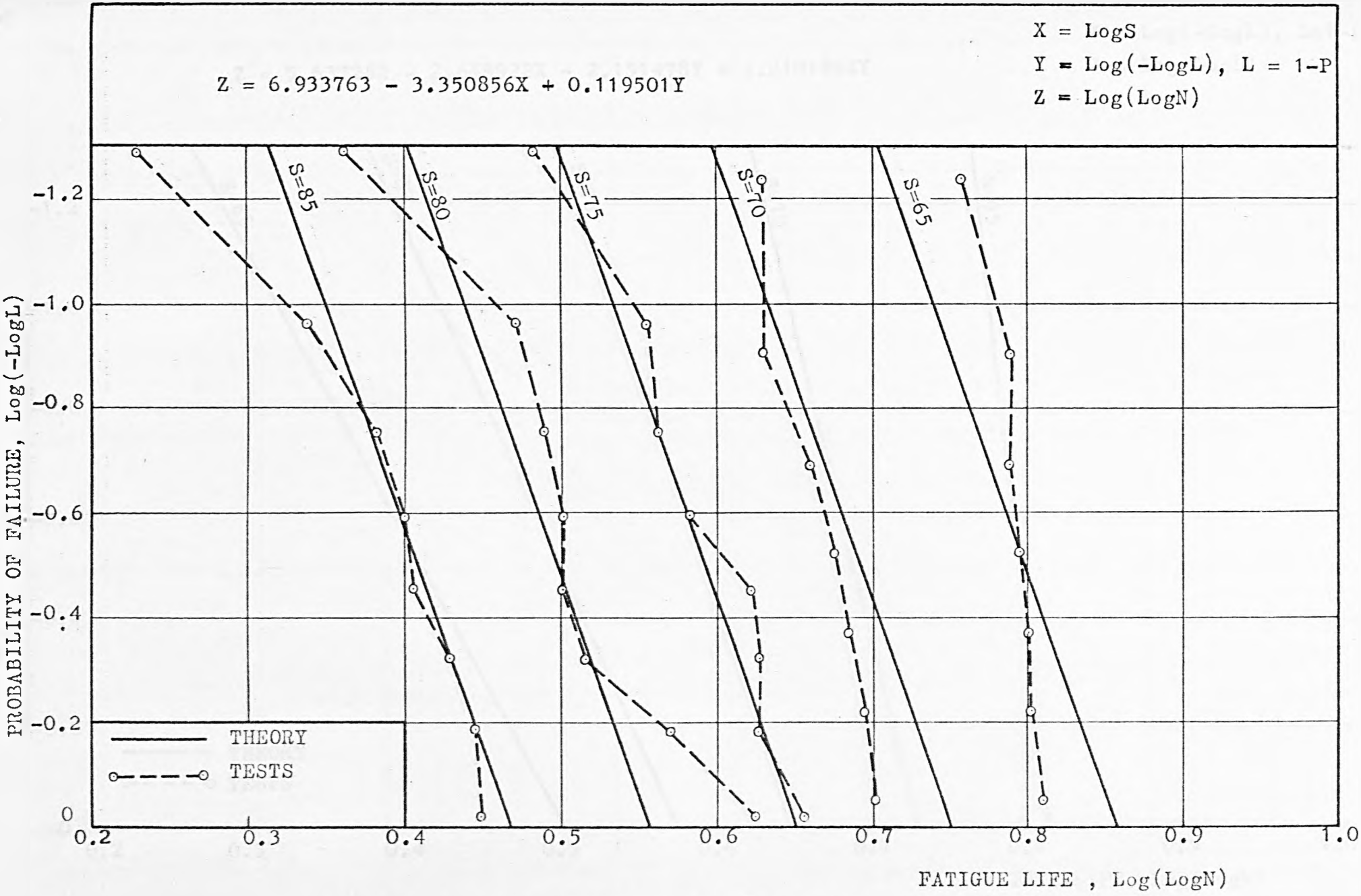

FIG. 5.3 S-N-P RELATIONS (FROM McCALL'S MODEL)

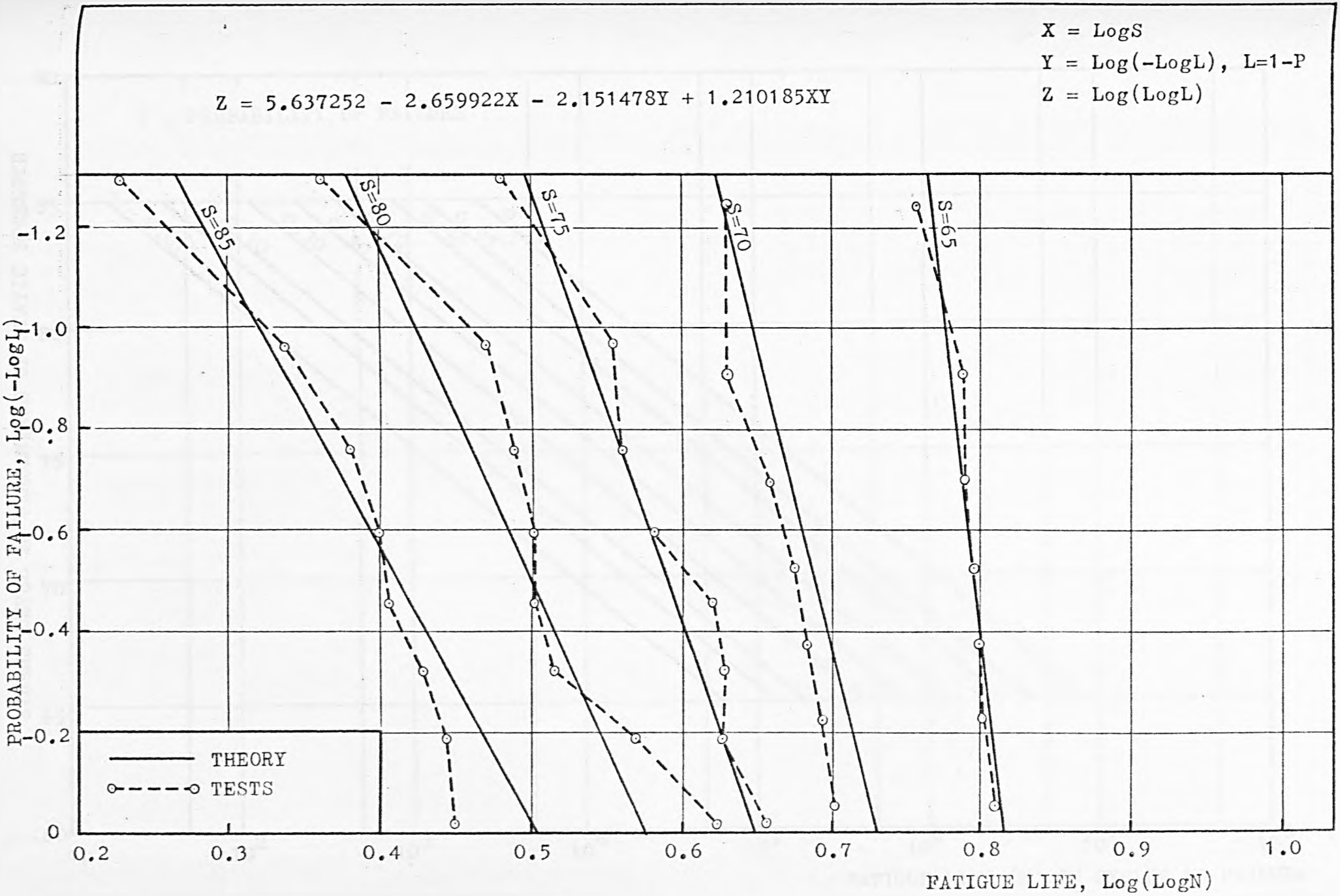

FIG. 5.4 S-N-P RELATIONS (FROM MODIFIED McCALL'S MODEL)*
* RAJU'S PROPOSAL.

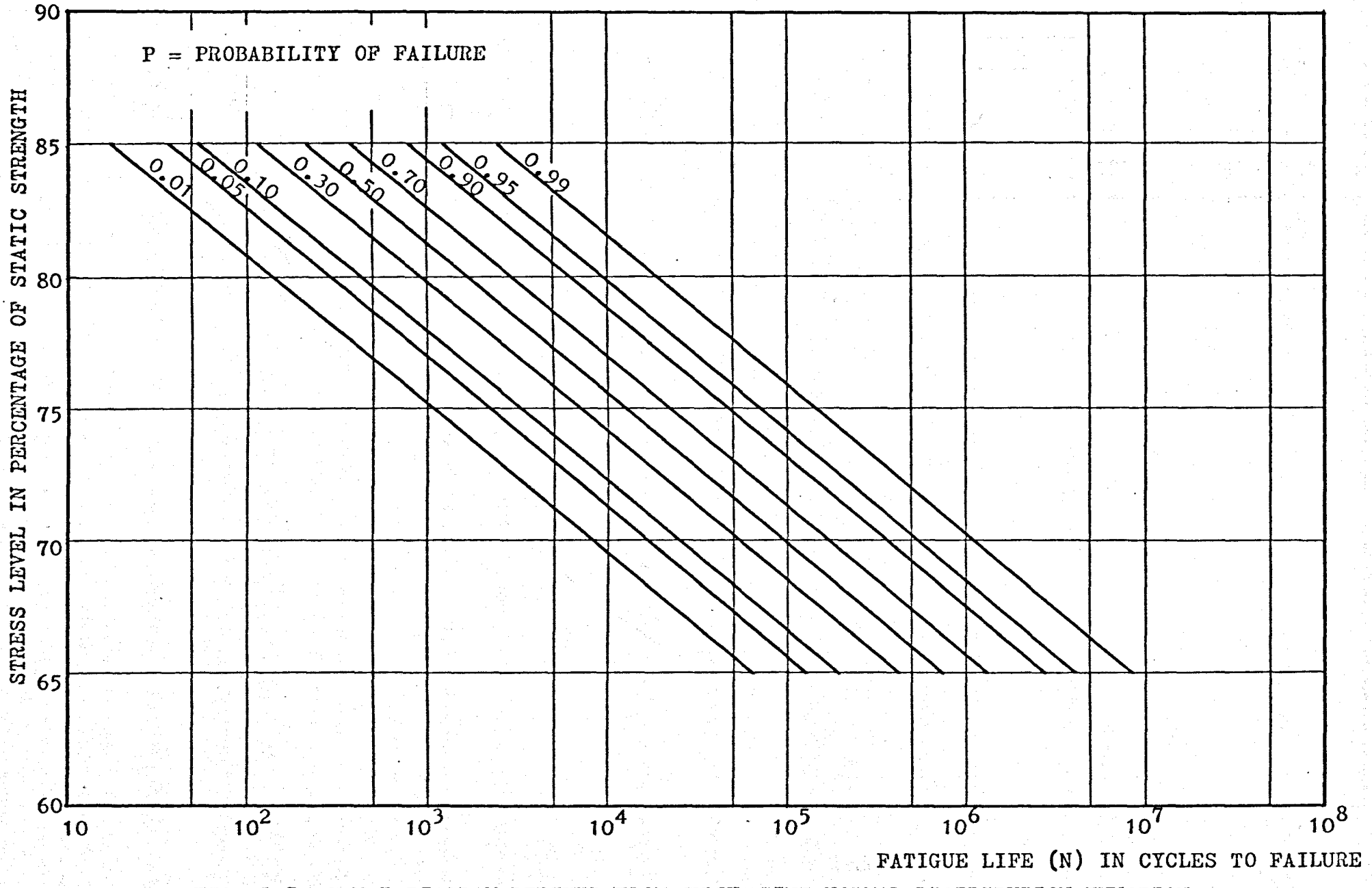

FIG, 5.5 S-N-P DIAGRAM DERIVED FROM CUMULATIVE NORMAL DISTRIBUTION FUNCTION

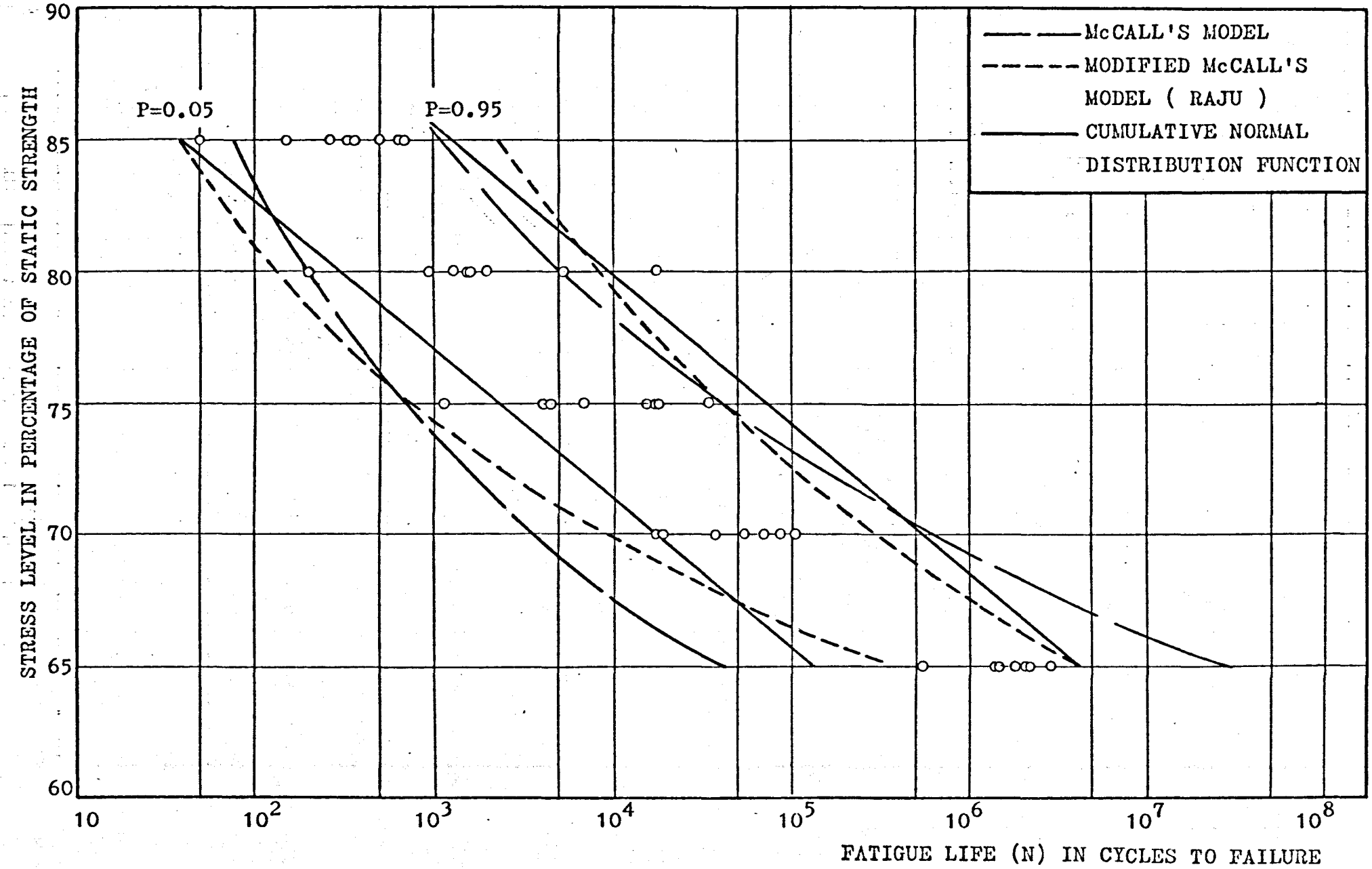

FIG. 5.6 S-N-P DIAGRAMS DERIVED FROM 3 MODELS

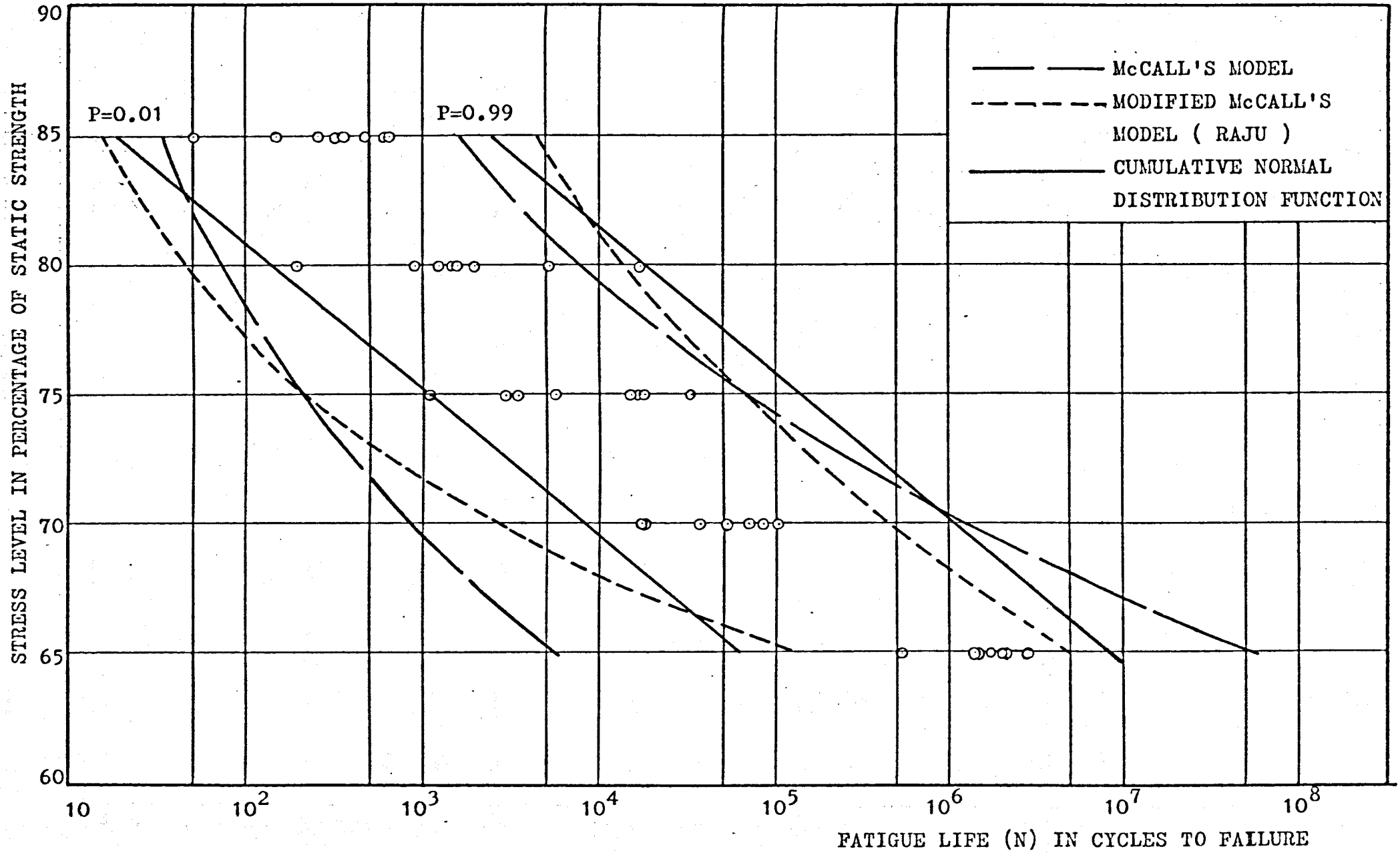

FIG. 5.7 S-N-P DIAGRAMS DERIVED FROM 3 MODELS

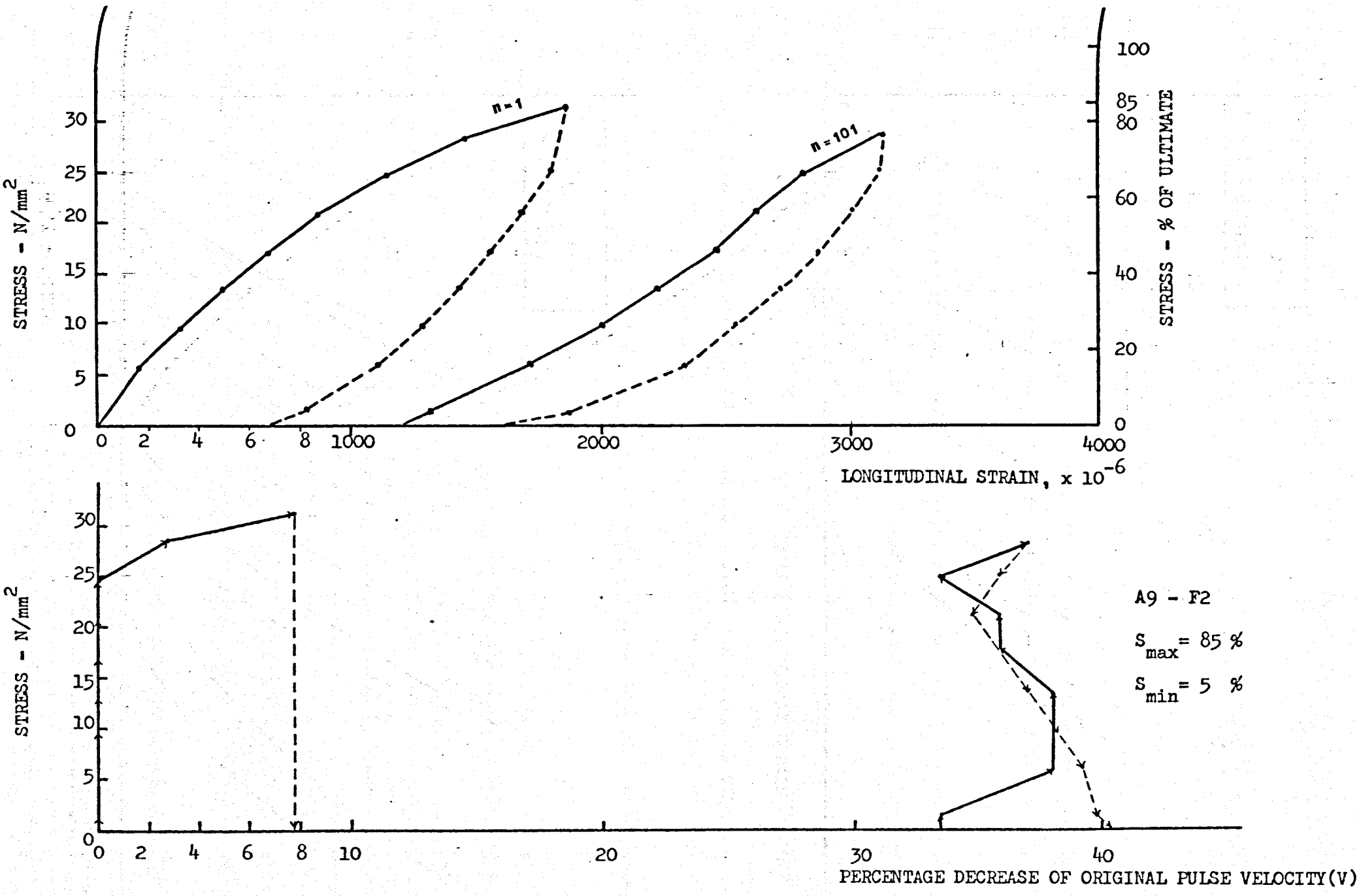

FIG. 6.1 STRESS-STRAIN AND STRESS-(V)CURVES OF A SPECIMEN UNDER STATIC COMPRESSION

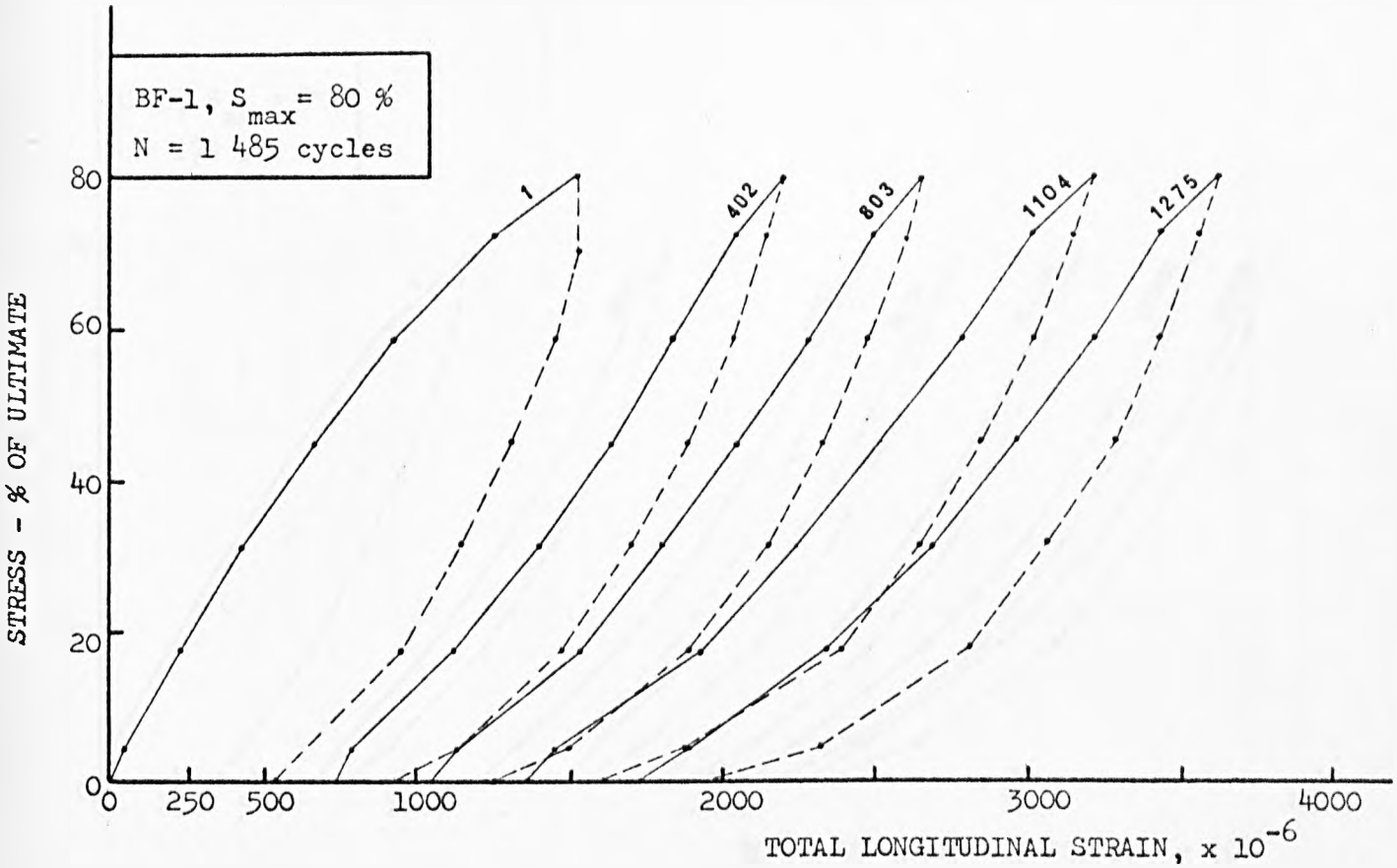

FIG. 6.2 VARIATION OF STRESS-STRAIN CURVES WITH NUMBER OF CYCLES

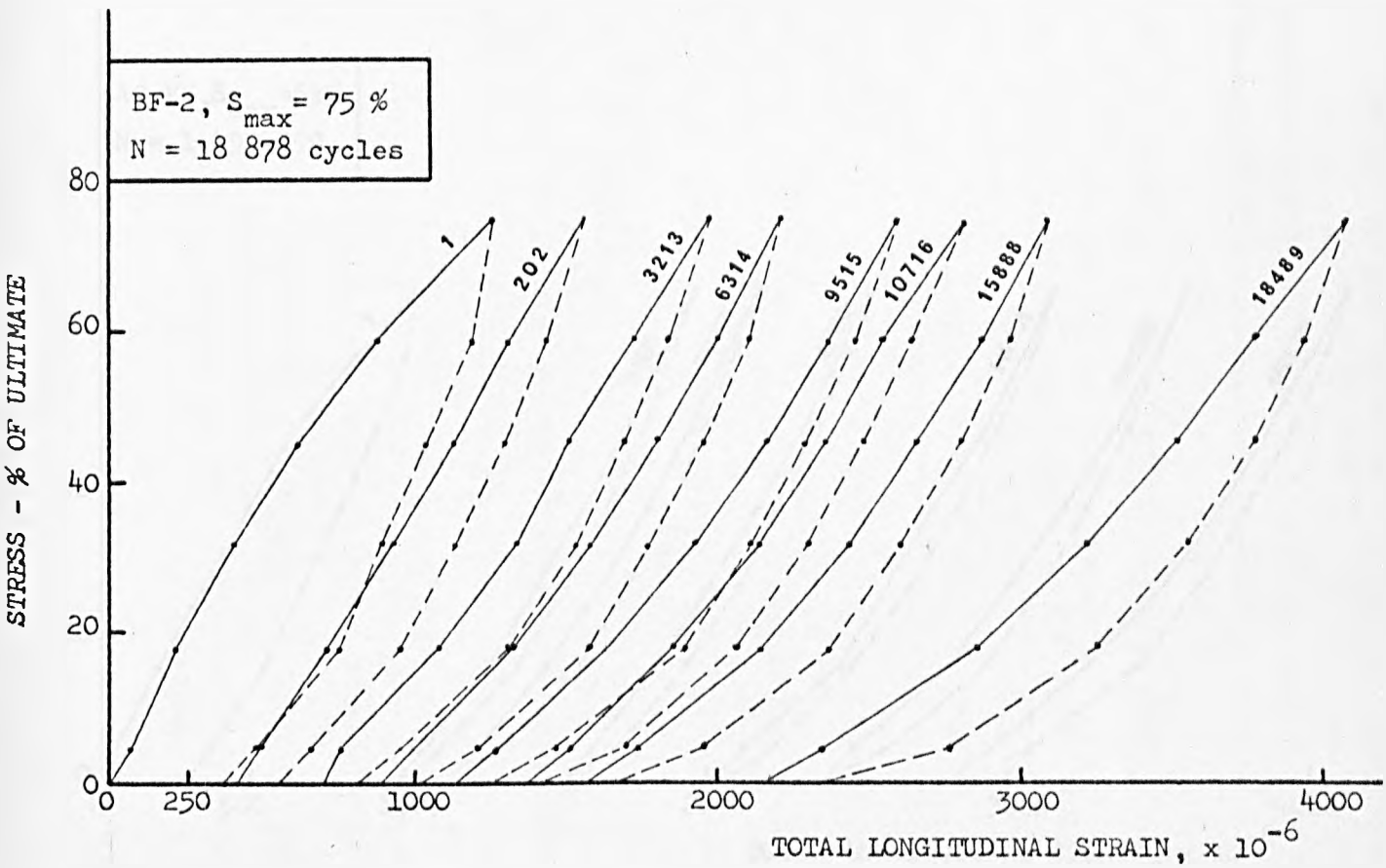

FIG. 6.3 VARIATION OF STRESS-STRAIN CURVES WITH NUMBER OF CYCLES

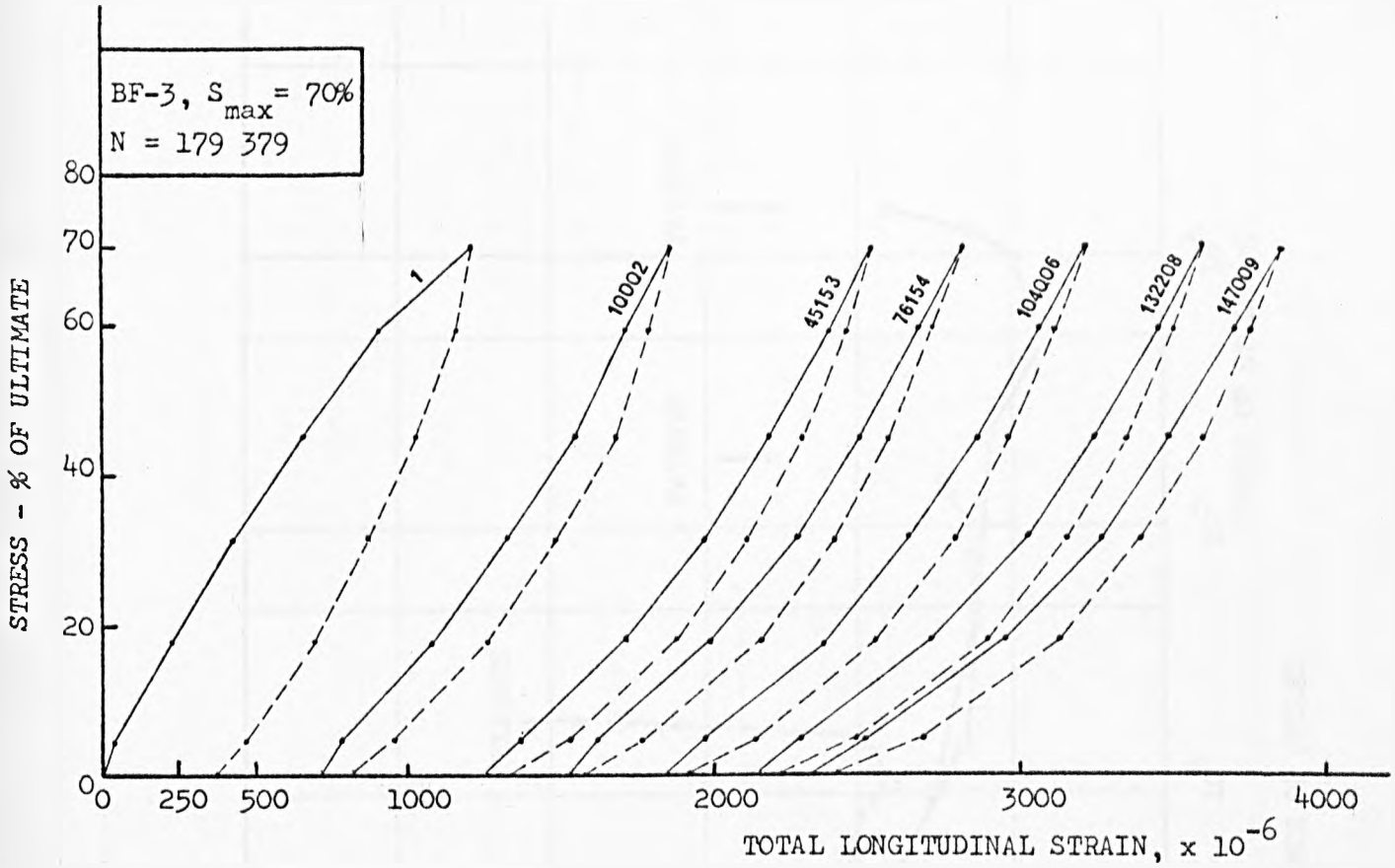

FIG. 6.4 VARIATION OF STRESS-STRAIN CURVES WITH NUMBER OF CYCLES

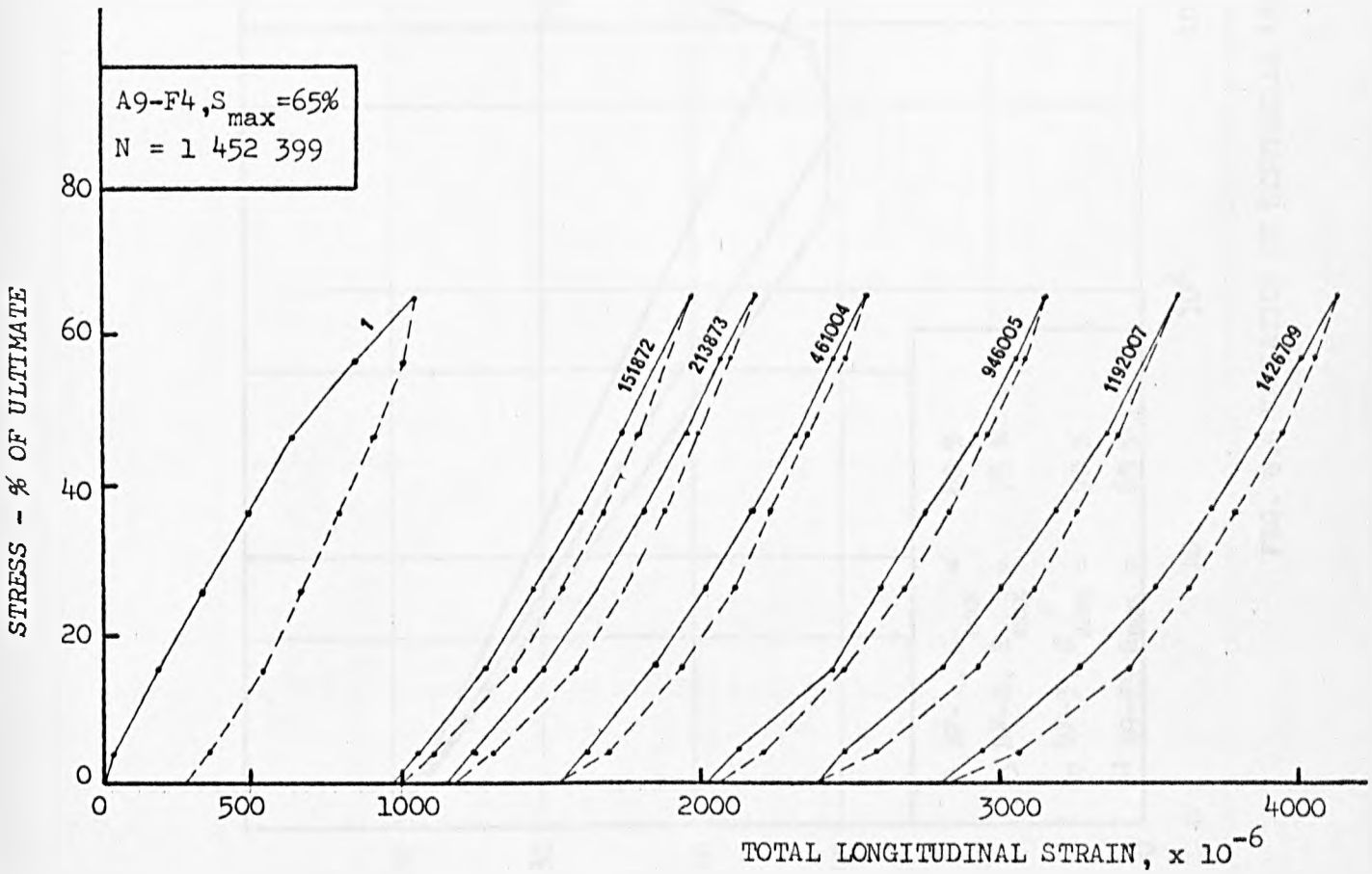

FIG. 6.5 VARIATION OF STRESS-STRAIN CURVES WITH NUMBER OF CYCLES

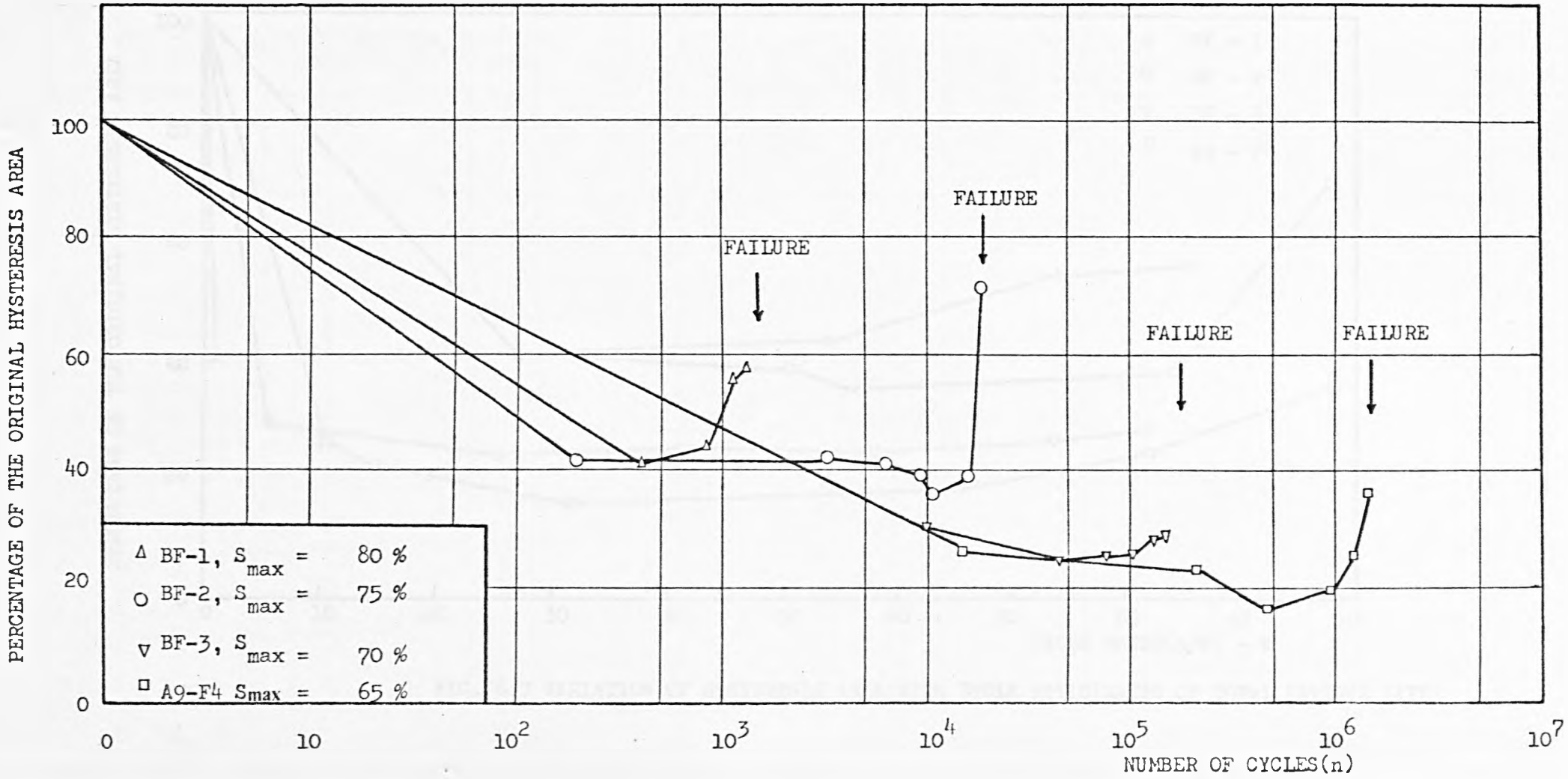

FIG. 6.6 VARIATION OF HYSTERESIS AREA WITH NUMBER OF CYCLES

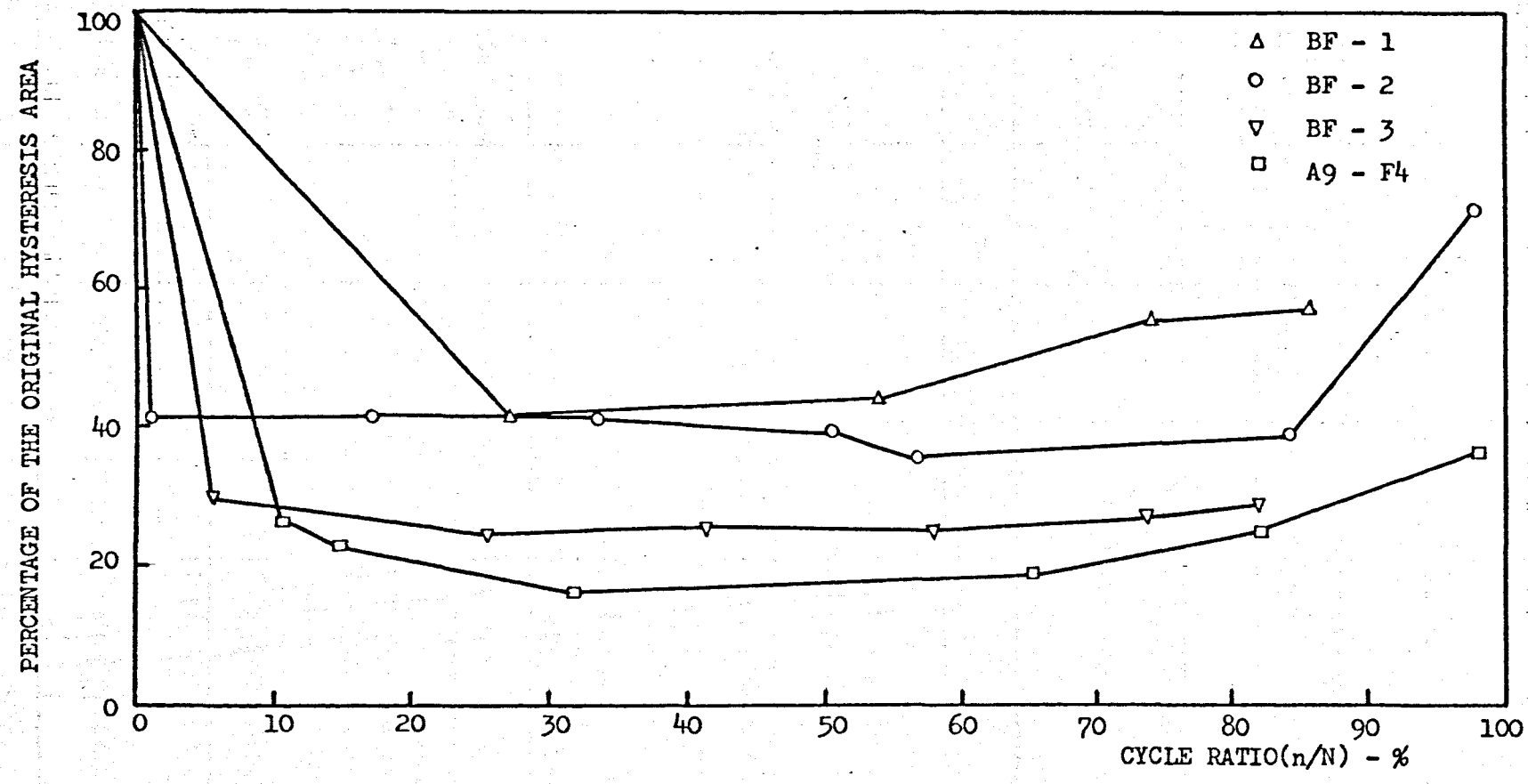

FIG. 6.7 VARIATION OF HYSTERESIS AREA WITH CYCLE RATIO(RATIO OF TOTAL FATIGUE LIFE)

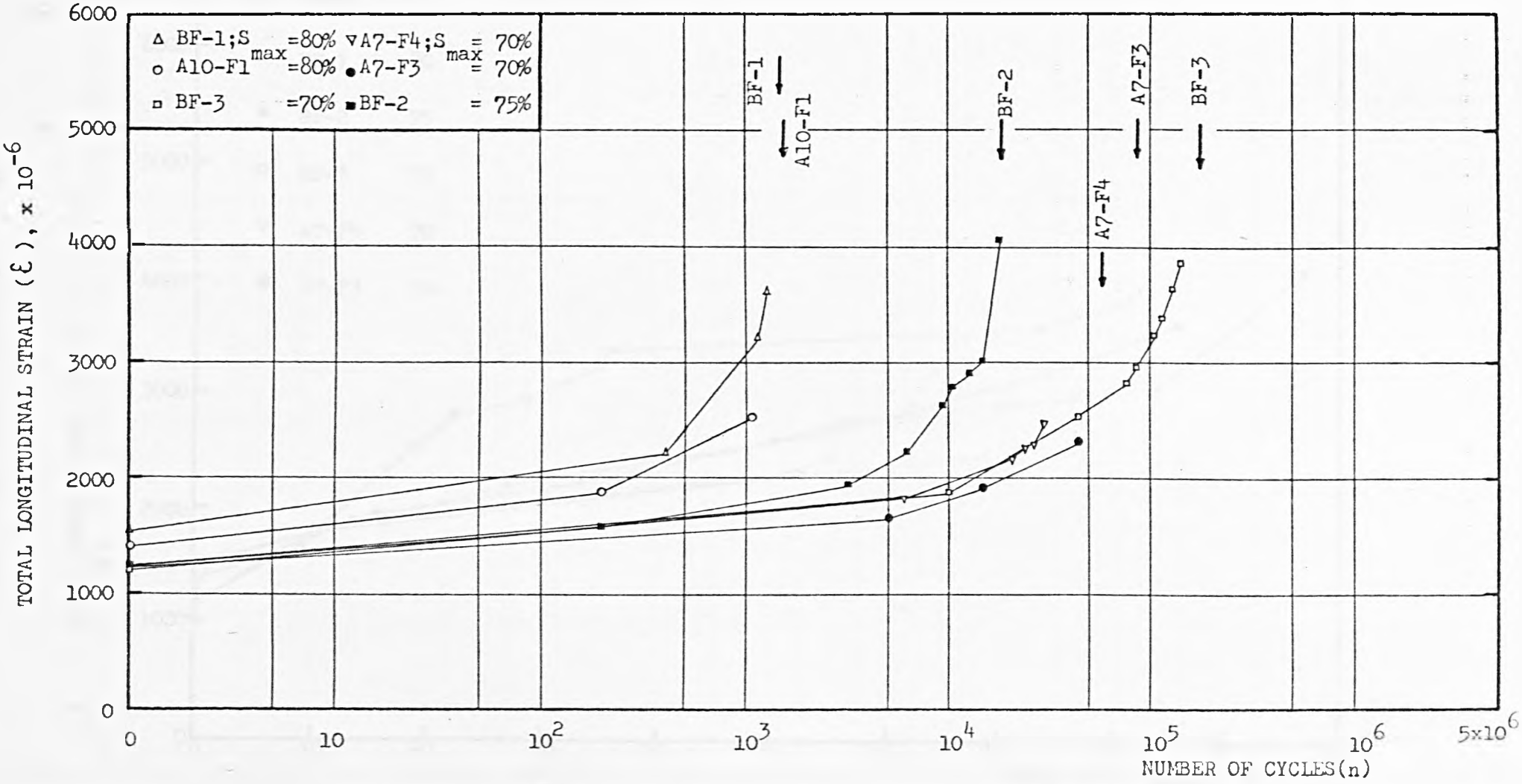

FIG. 6.8 VARIATION OF TOTAL LONGITUDINAL STRAIN WITH NUMBER OF CYCLES

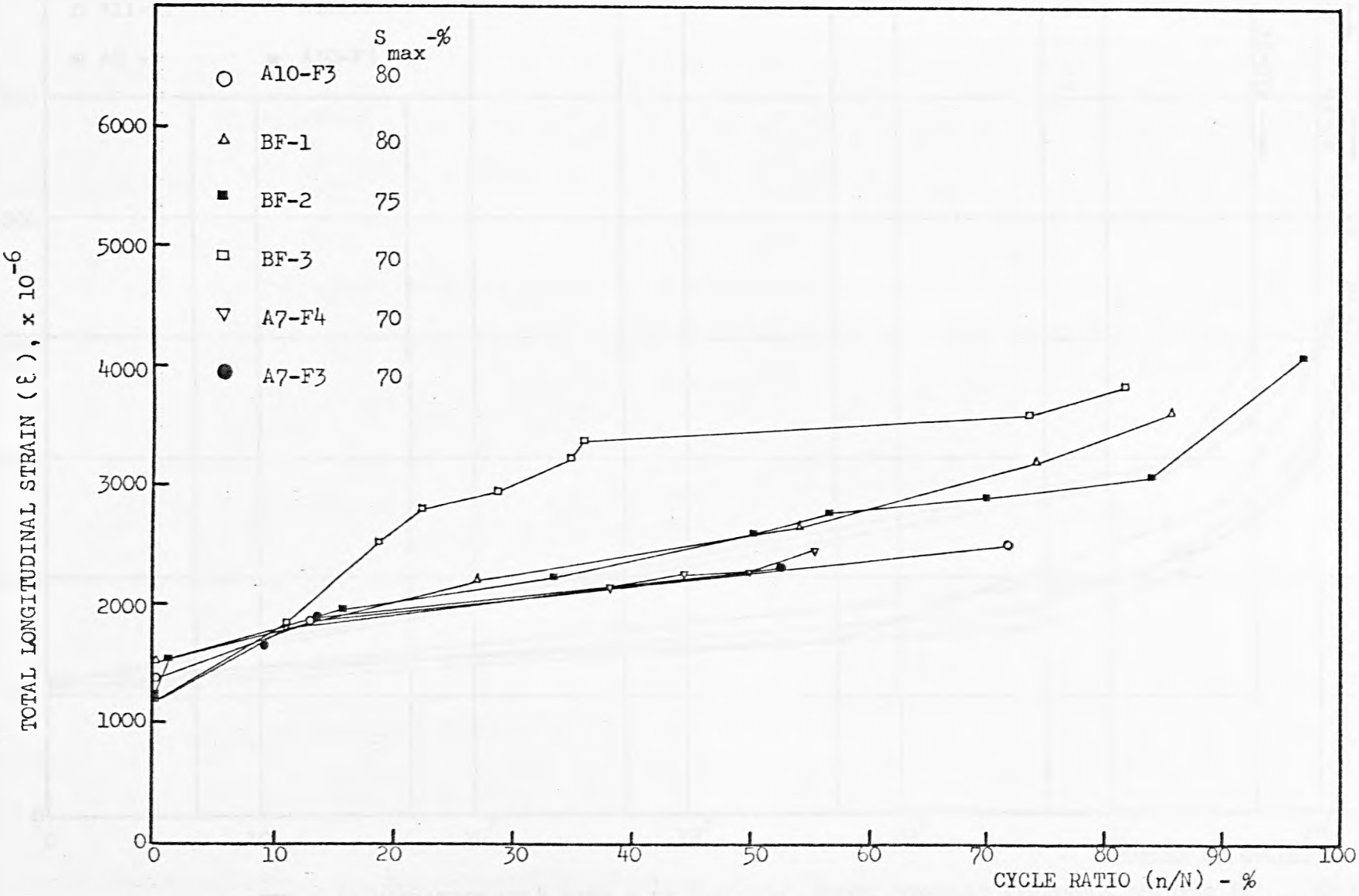

FIG. 6.9 VARIATION OF ε WITH n/N OF SPECIMENS UNDER CONSTANT AMPLITUDE LOADING

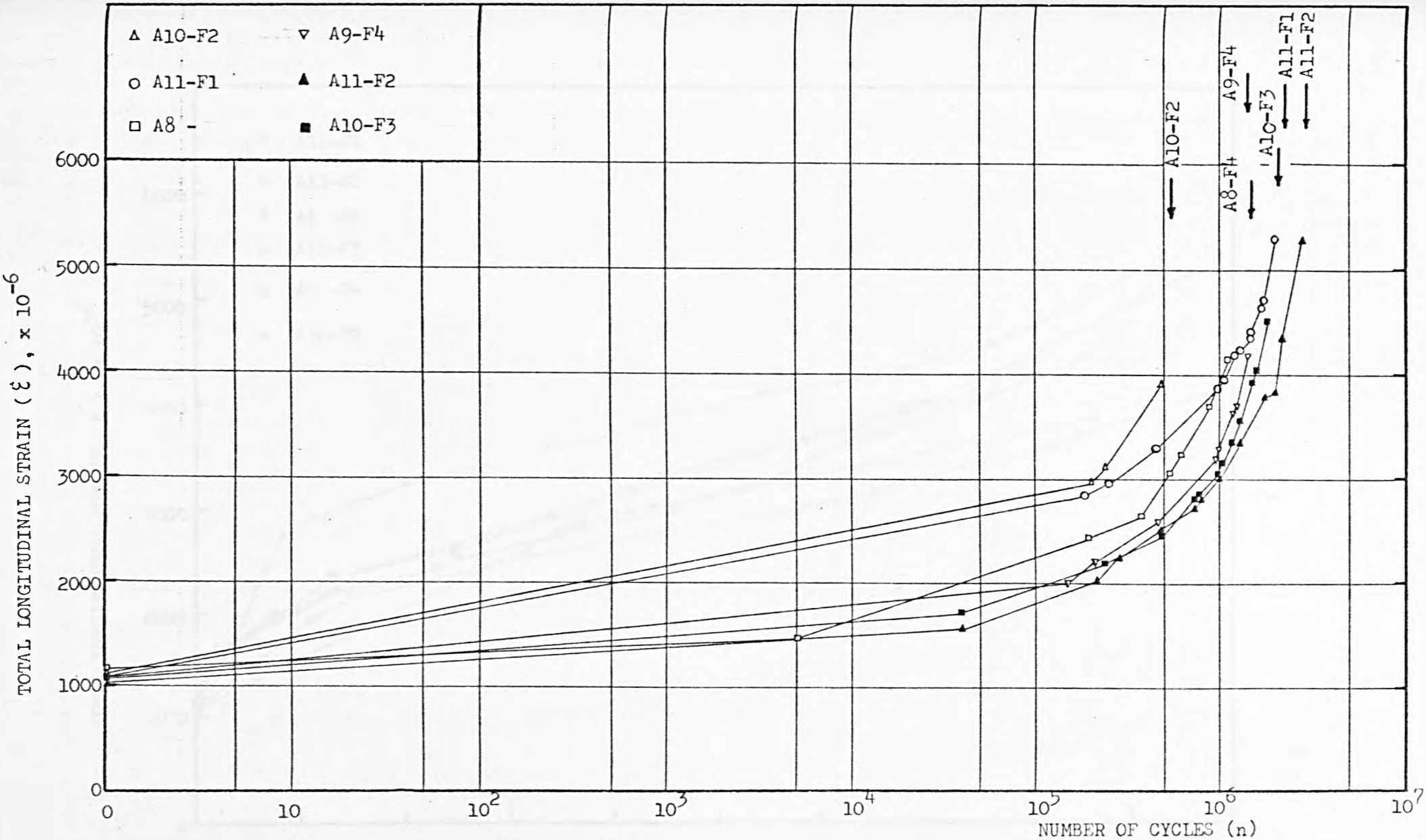

FIG.6.10 VARIATION OF ε WITH n OF SPECIMENS UNDER CONSTANT AMPLITUDE LOADING (S_{max} = 65 %)

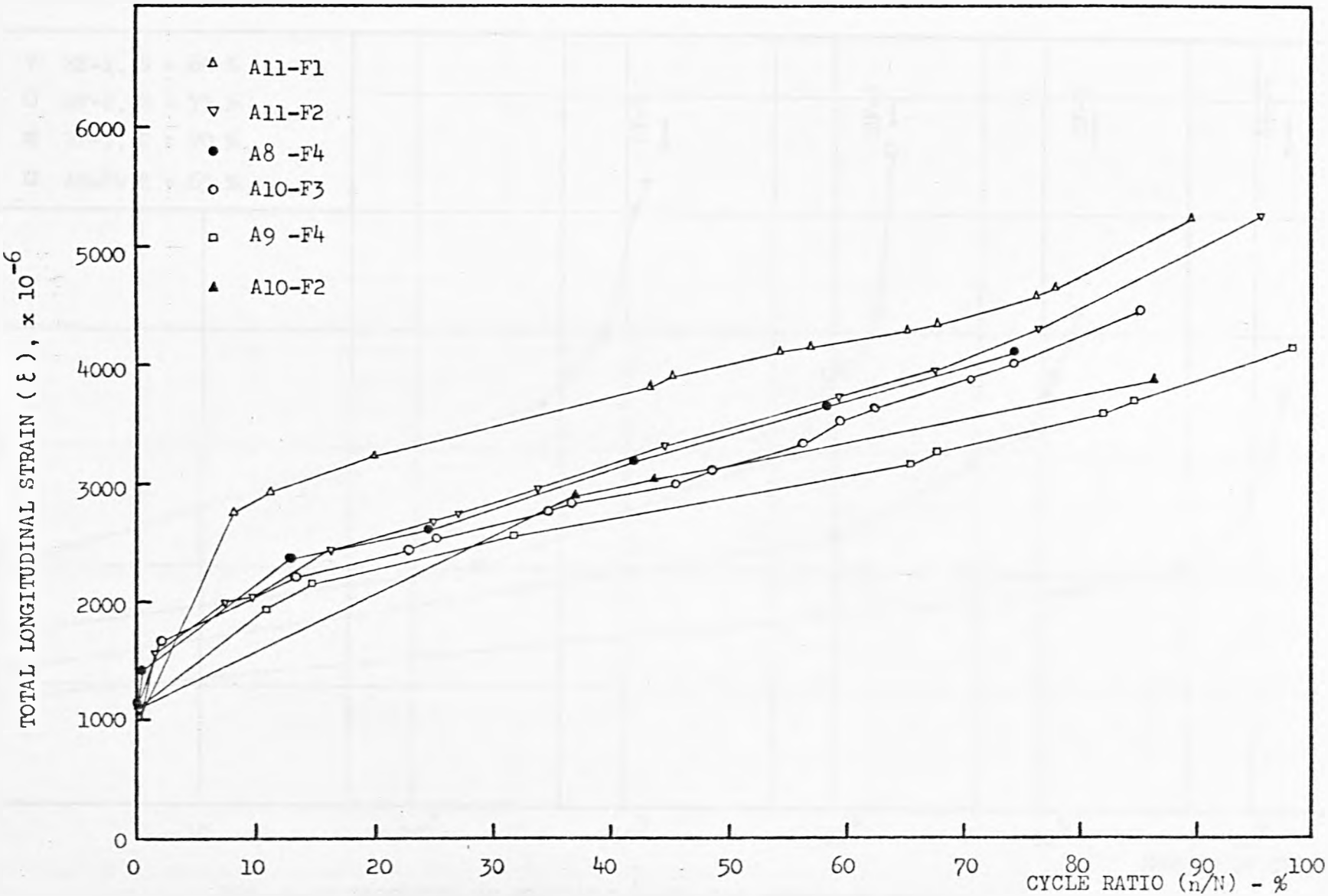

FIG. 6.11 VARIATION OF ε WITH n/N OF SPECIMENS UNDER CONSTANT AMPLITUDE LOADING (S_{max} = 65%)

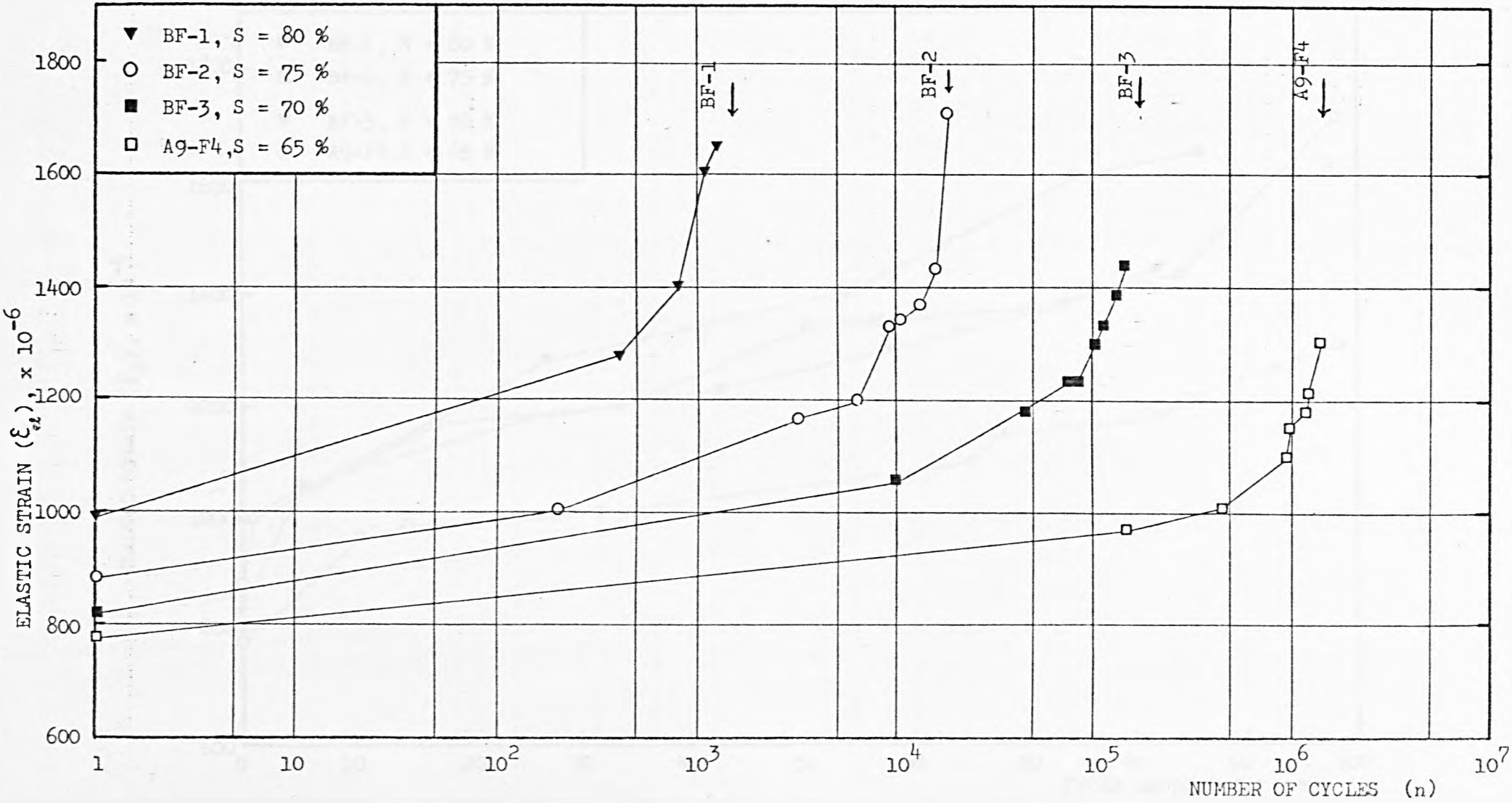

FIG. 6.12 VARIATION OF ELASTIC STRAIN WITH NUMBER OF CYCLES

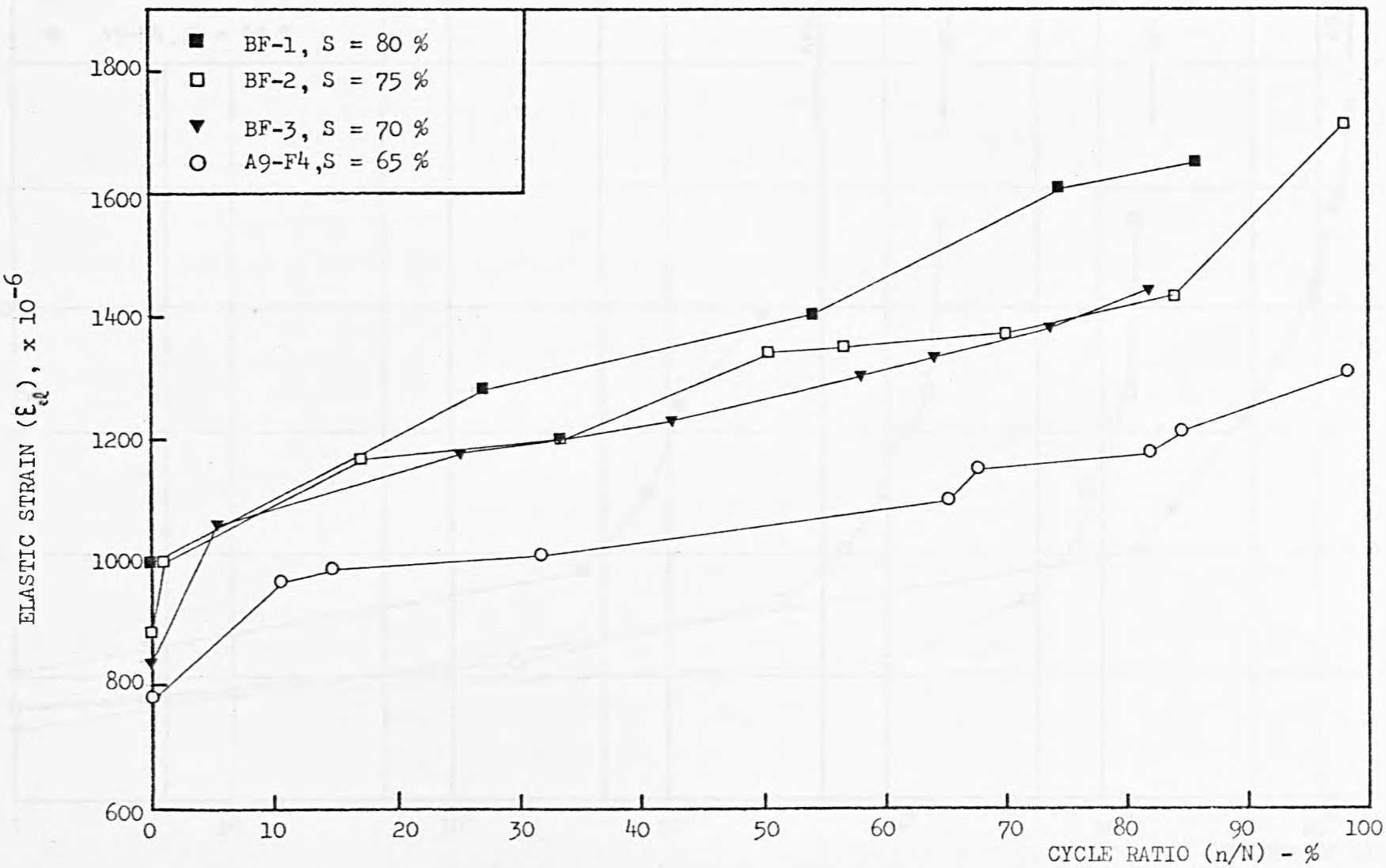

FIG. 6.13 VARIATION OF ELASTIC STRAIN WITH CYCLE RATIO

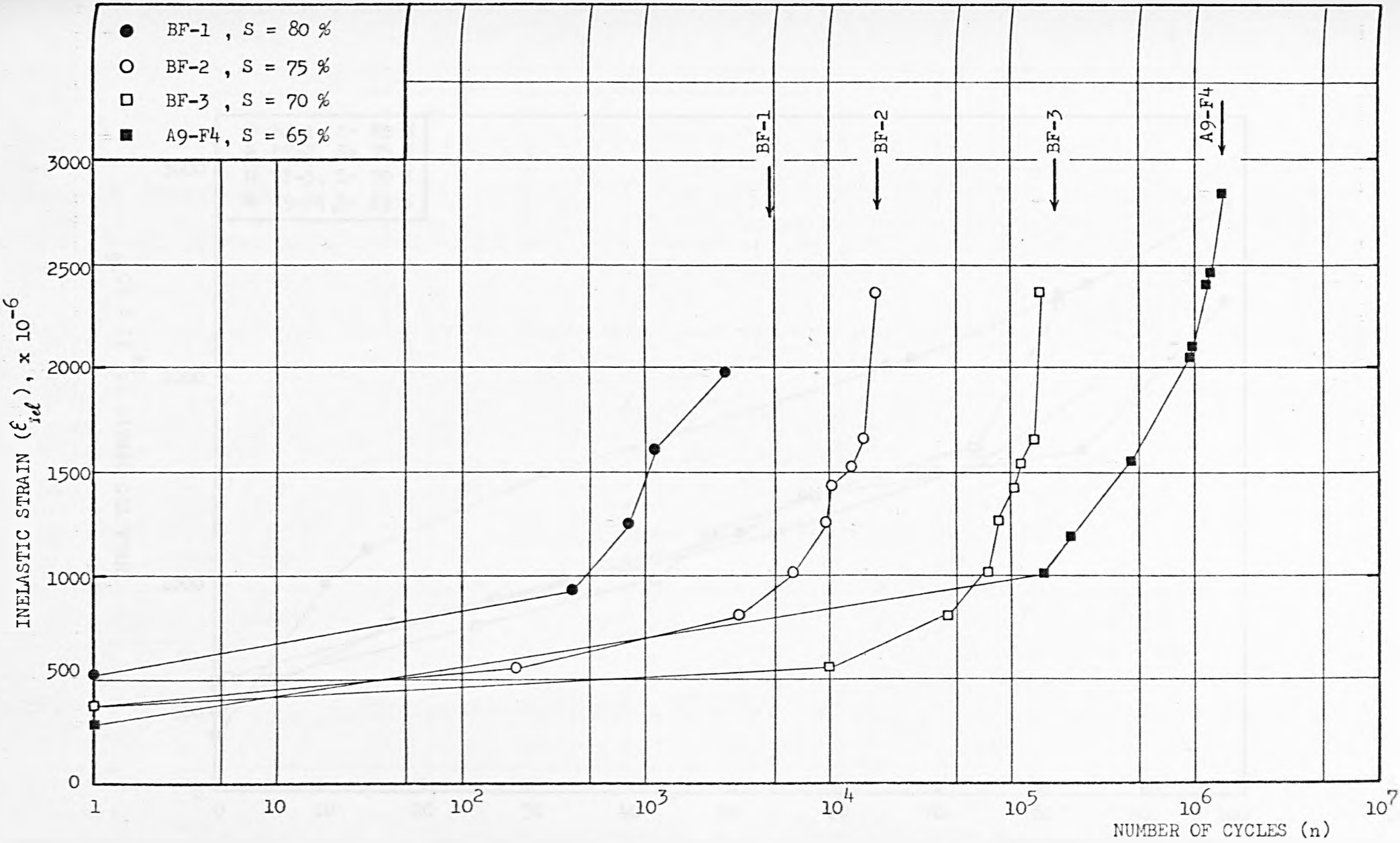

FIG. 6. 14 VARIATION OF INELASTIC STRAIN WITH NUMBER OF CYCLES

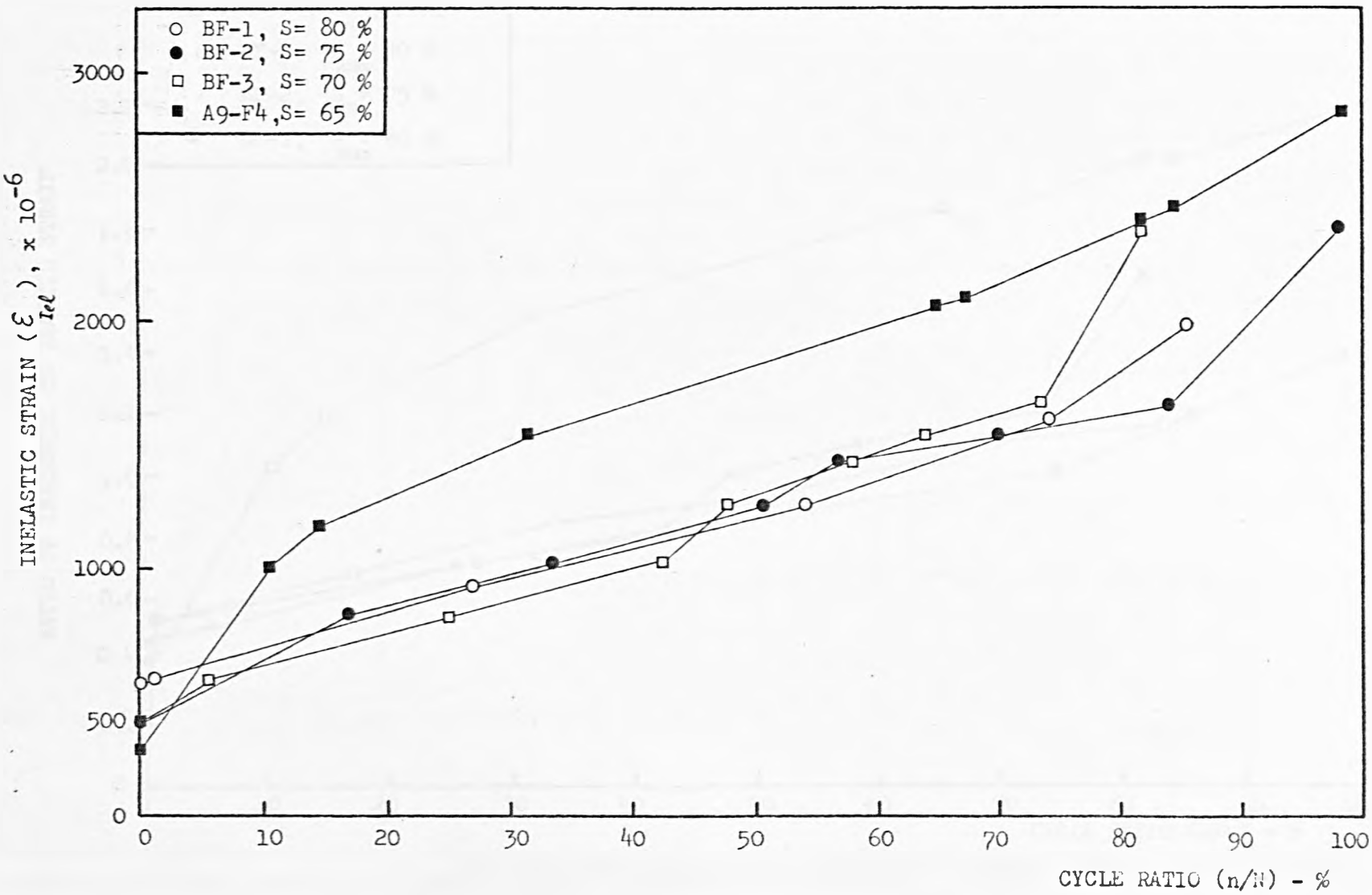

FIG. 6.15 VARIATION OF INELASTIC STRAIN WITH CYCLE RATIO

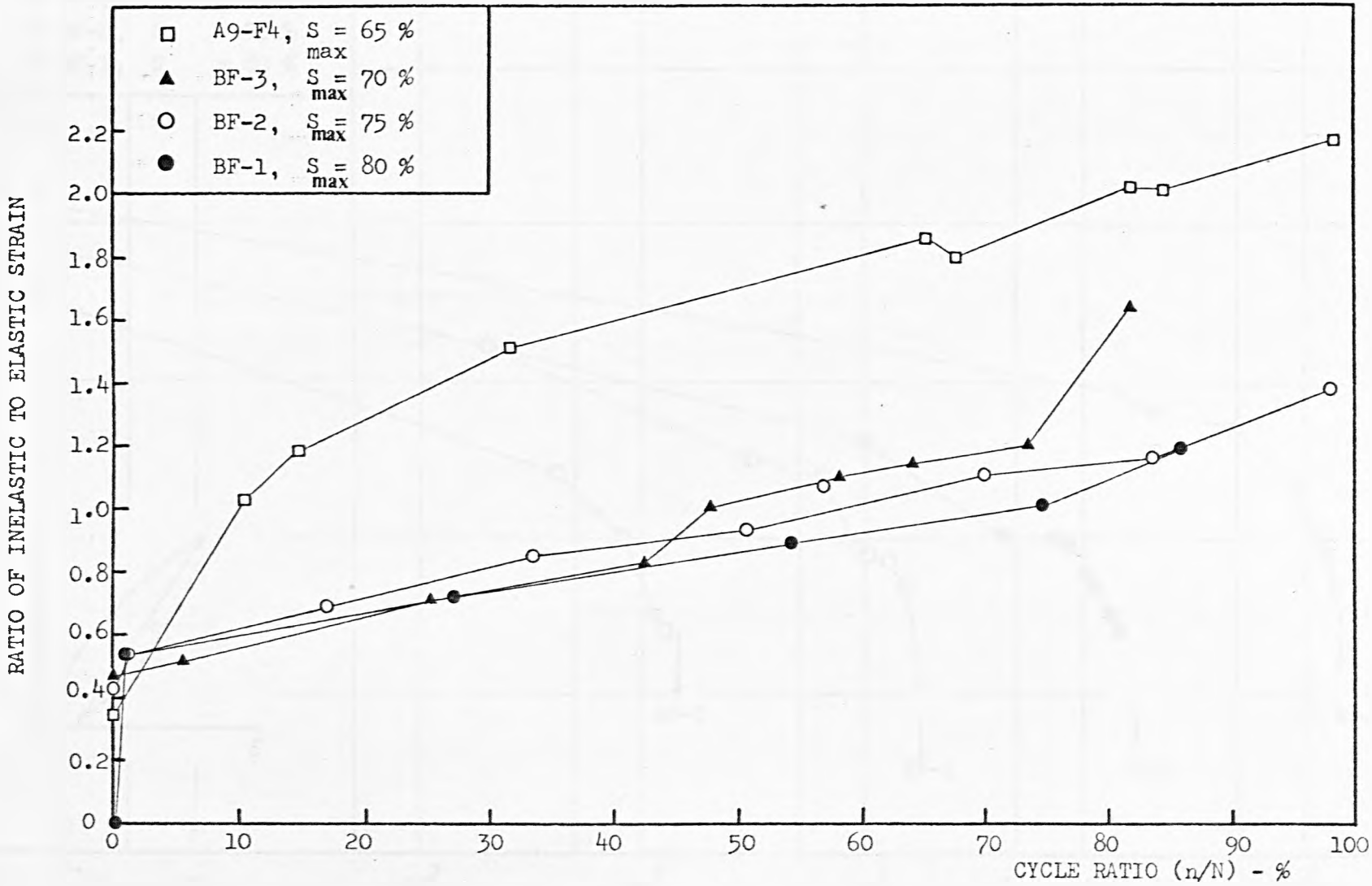

FIG. 6.16 VARIATION OF RATIO OF INELASTIC TO ELASTIC STRAIN WITH CYCLE RATIO

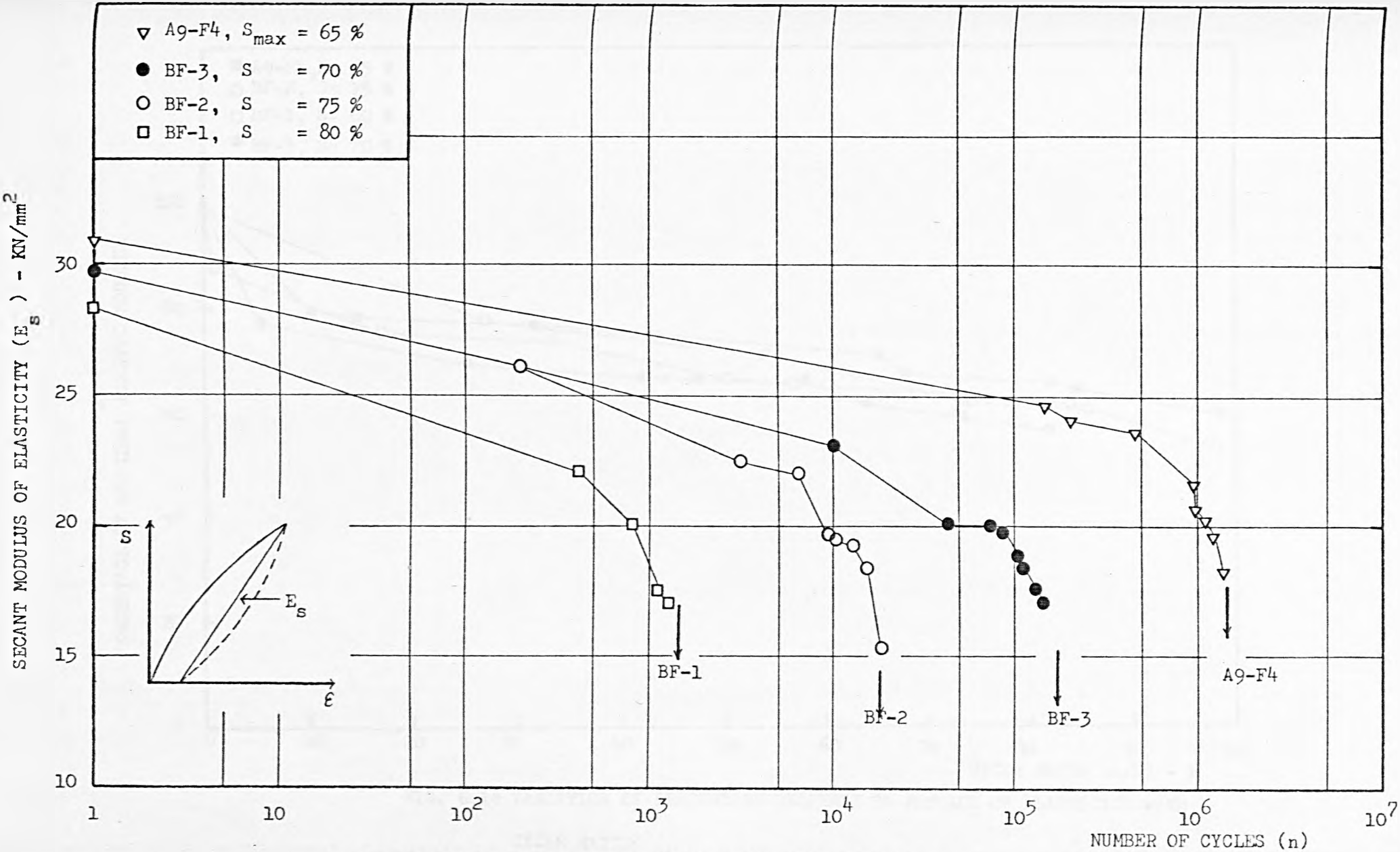

FIG. 6.17 VARIATION OF SECANT MODULUS OF ELASTICITY WITH NUMBER OF CYCLES

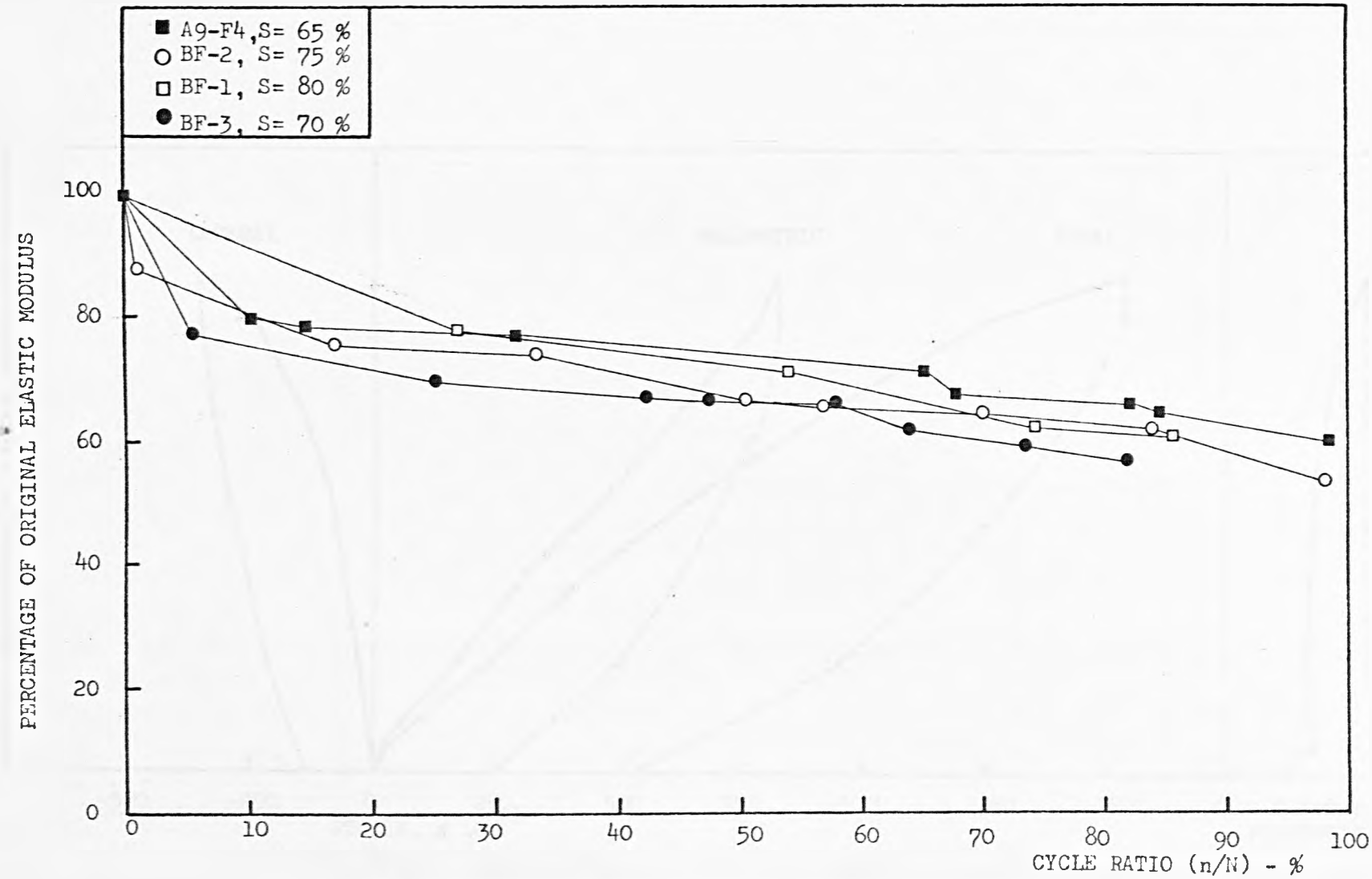

FIG. 6.18 VARIATION OF PERCENTAGE DECREASE IN MODULUS OF ELASTICITY WITH CYCLE RATIO

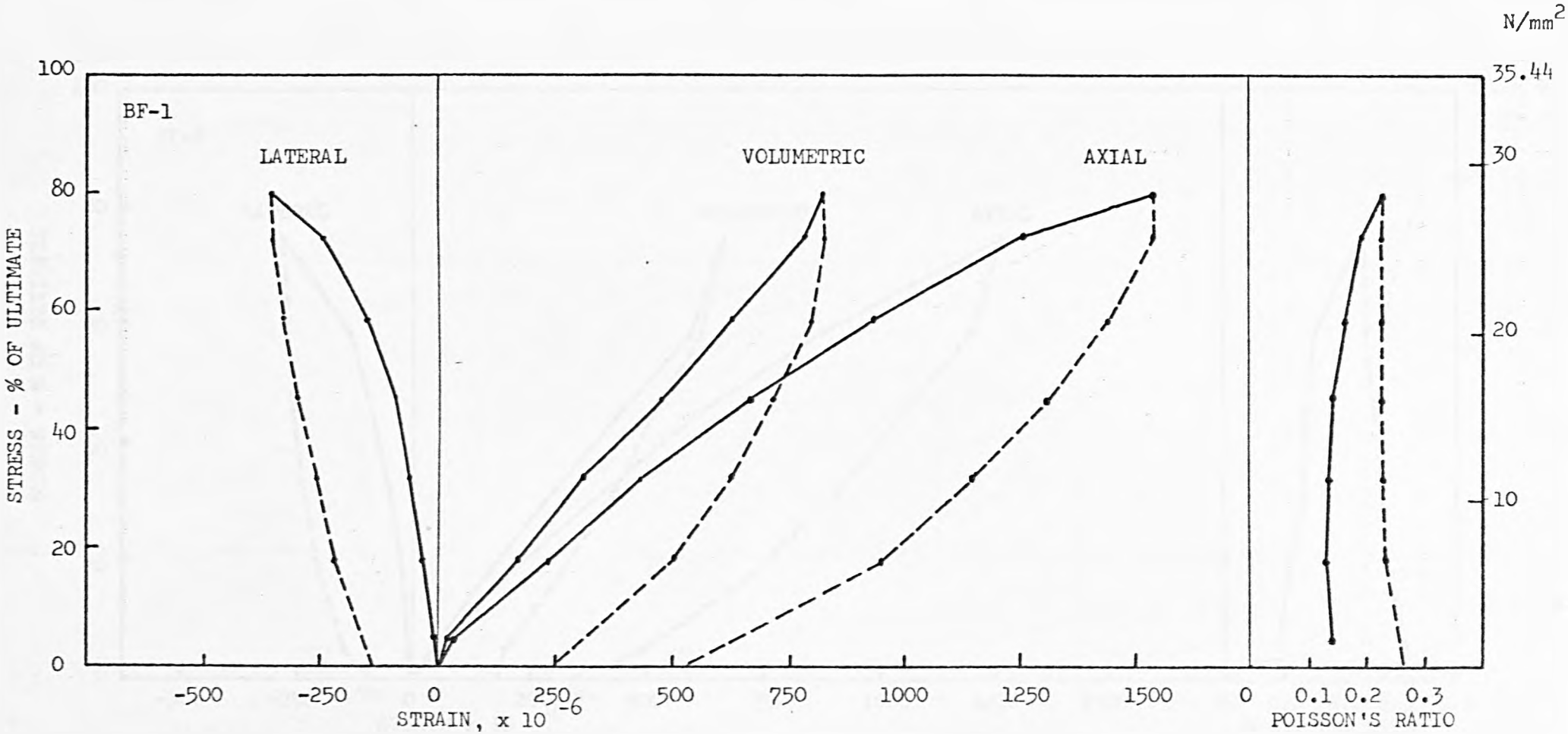

FIG. 6.19 STRESS - AXIAL, LATERAL & VOLUMETRIC STRAIN CURVES OF A SPECIMEN IN STATIC COMPRESSION

(S_{max} = 80 %)

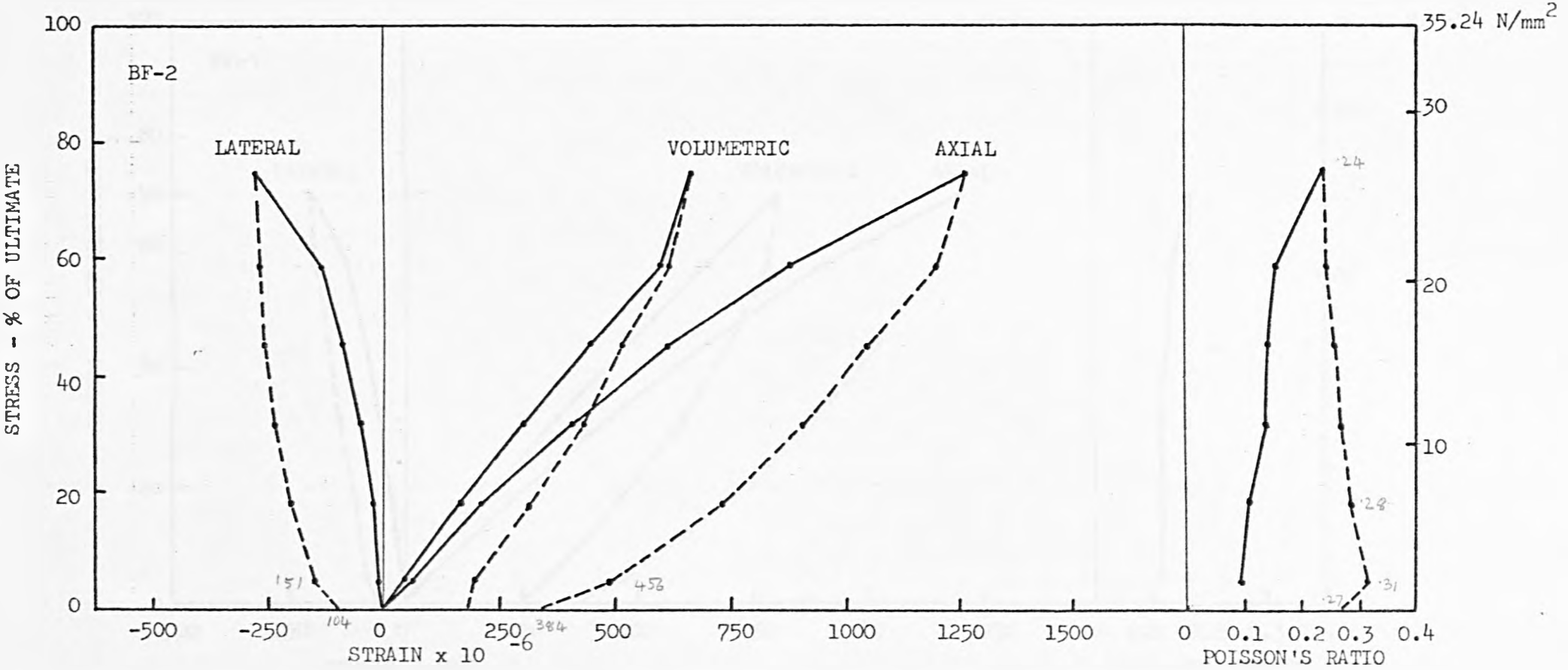

FIG. 6.20 STRESS - AXIAL, LATERAL & VOLUMETRIC STRAIN CURVES OF A SPECIMEN IN STATIC COMPRESSION

(S_{max} = 75 %)

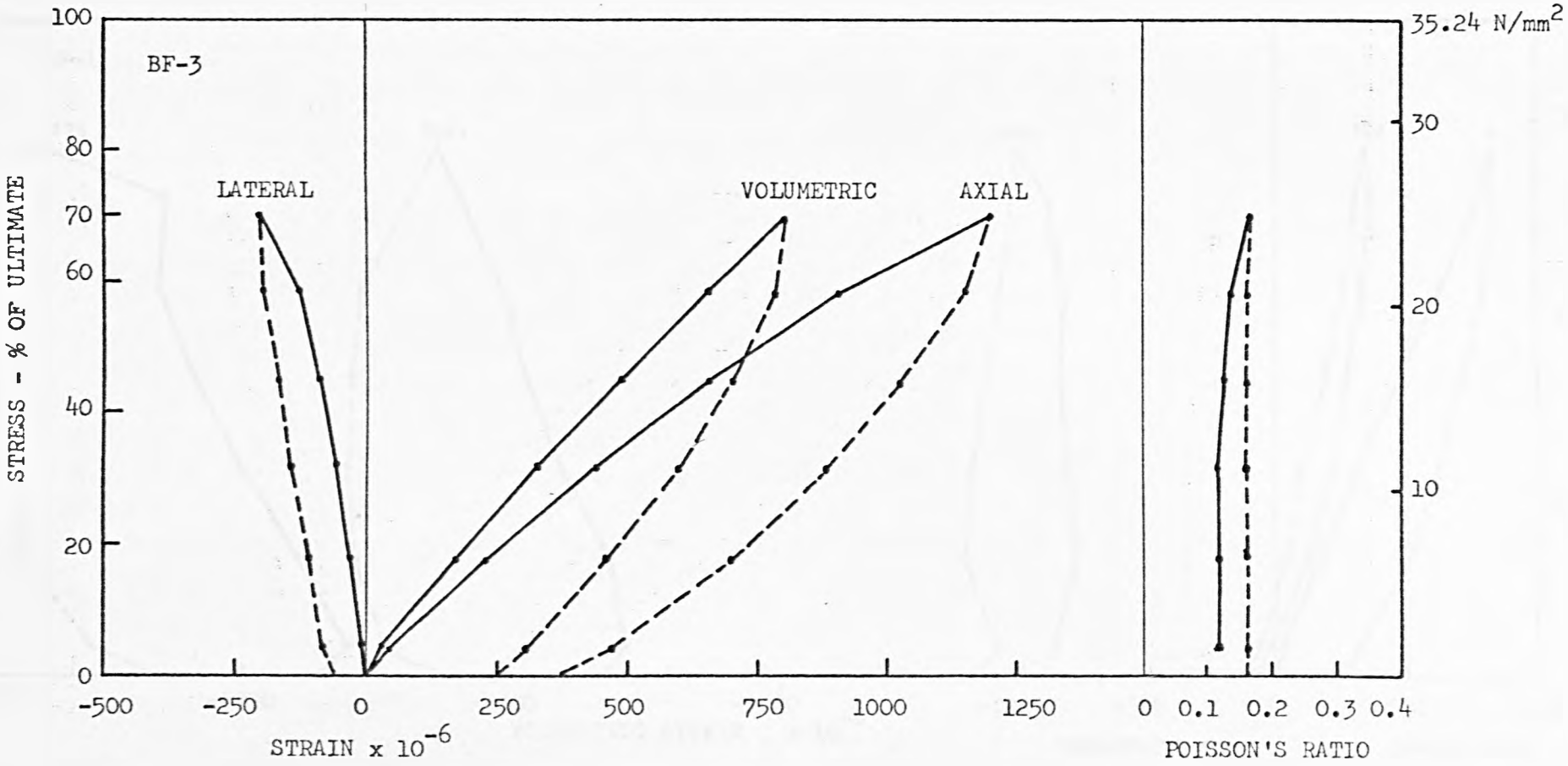

FIG. 6. 21 STRESS - AXIAL, LATERAL & VOLUMETRIC STRAIN CURVES OF A SPECIMEN IN STATIC COMPRESSION (S_{max} = 70 %)

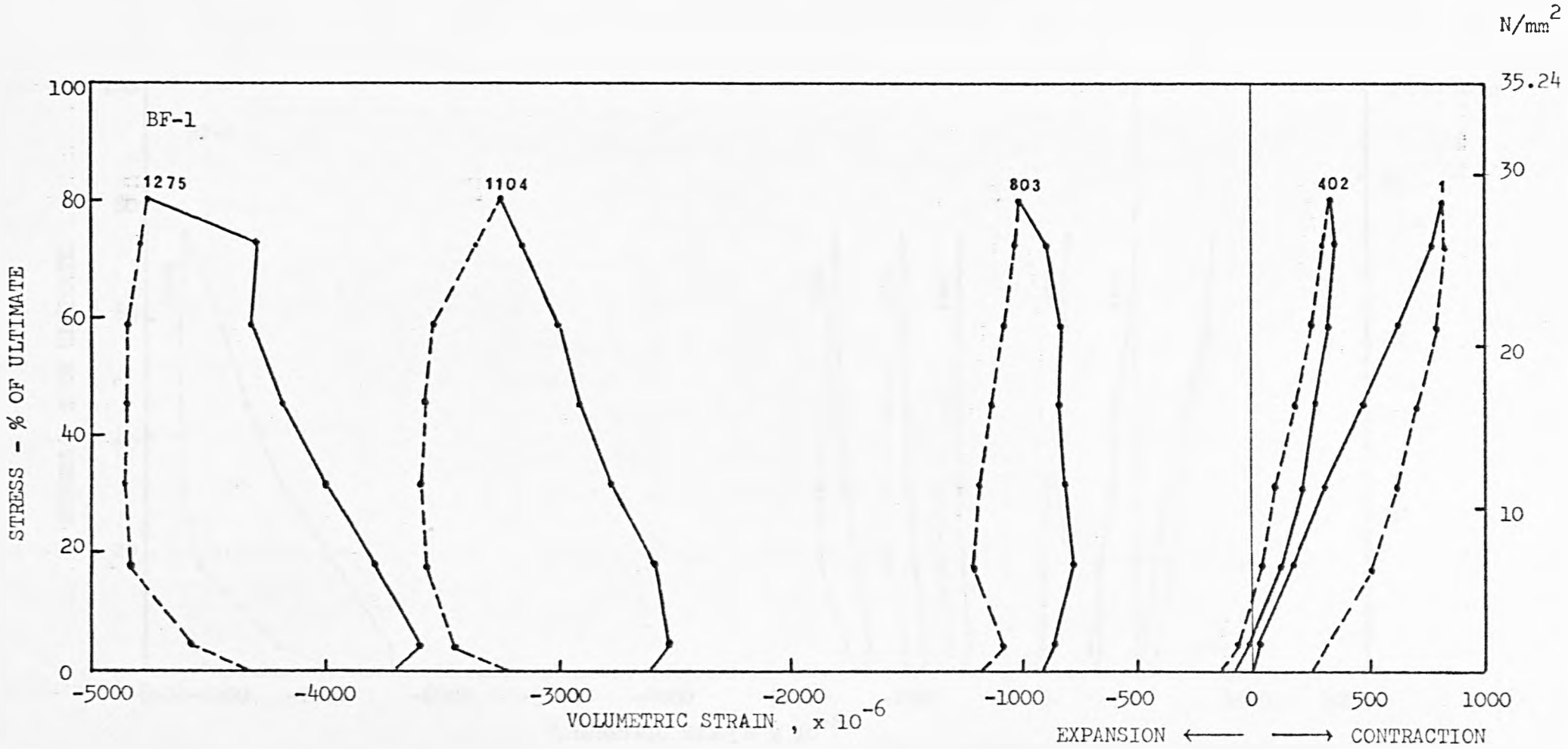

FIG. 6.22 STRESS - VOLUMETRIC STRAIN CURVES OF A SPECIMEN IN CYCLIC COMPRESSION (S_{max} = 80 %)

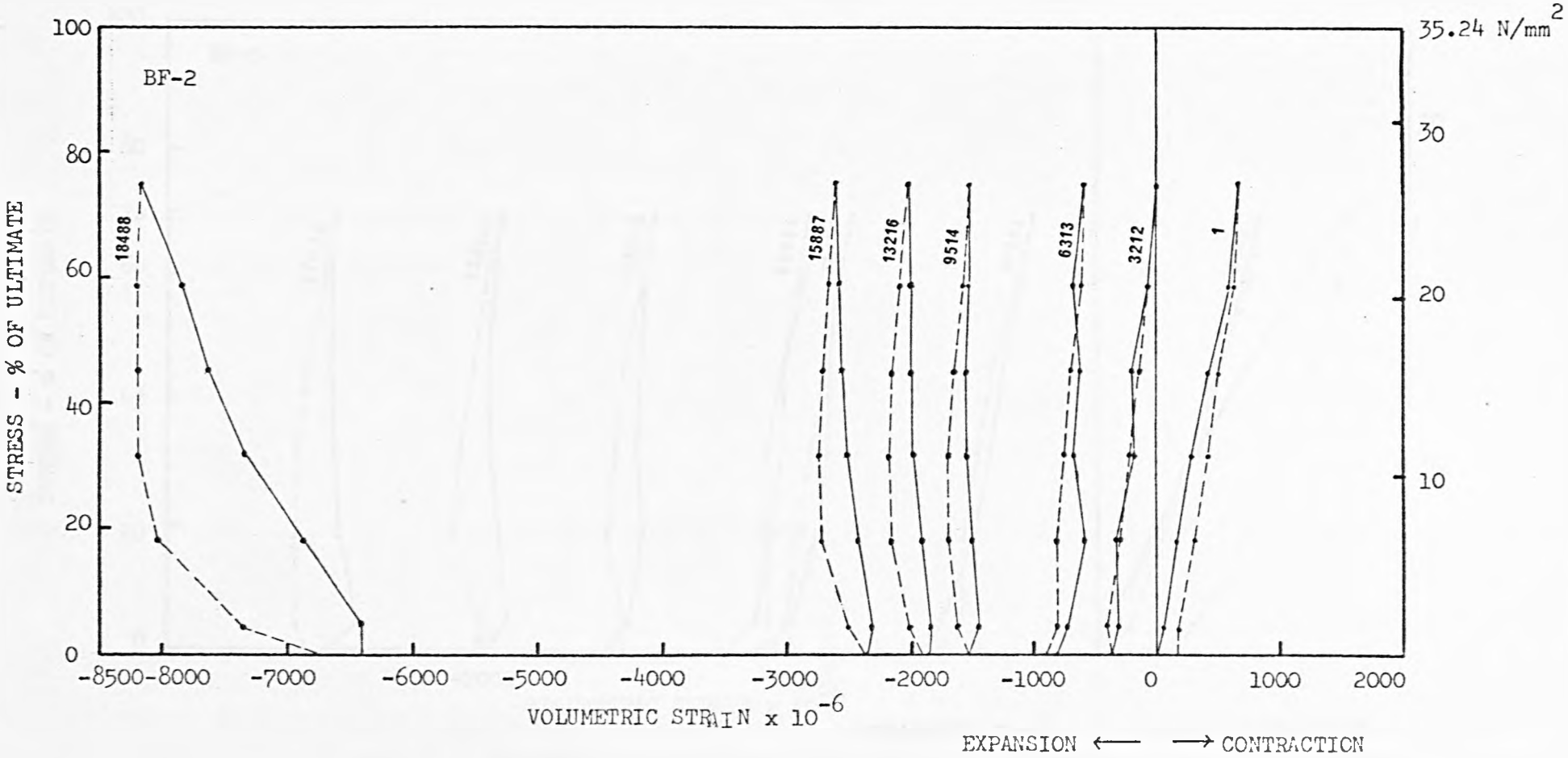

FIG. 6.23 STRESS - VOLUMETRIC STRAIN CURVES OF A SPECIMEN IN CYCLIC COMPRESSION (S_{max} = 75 %)

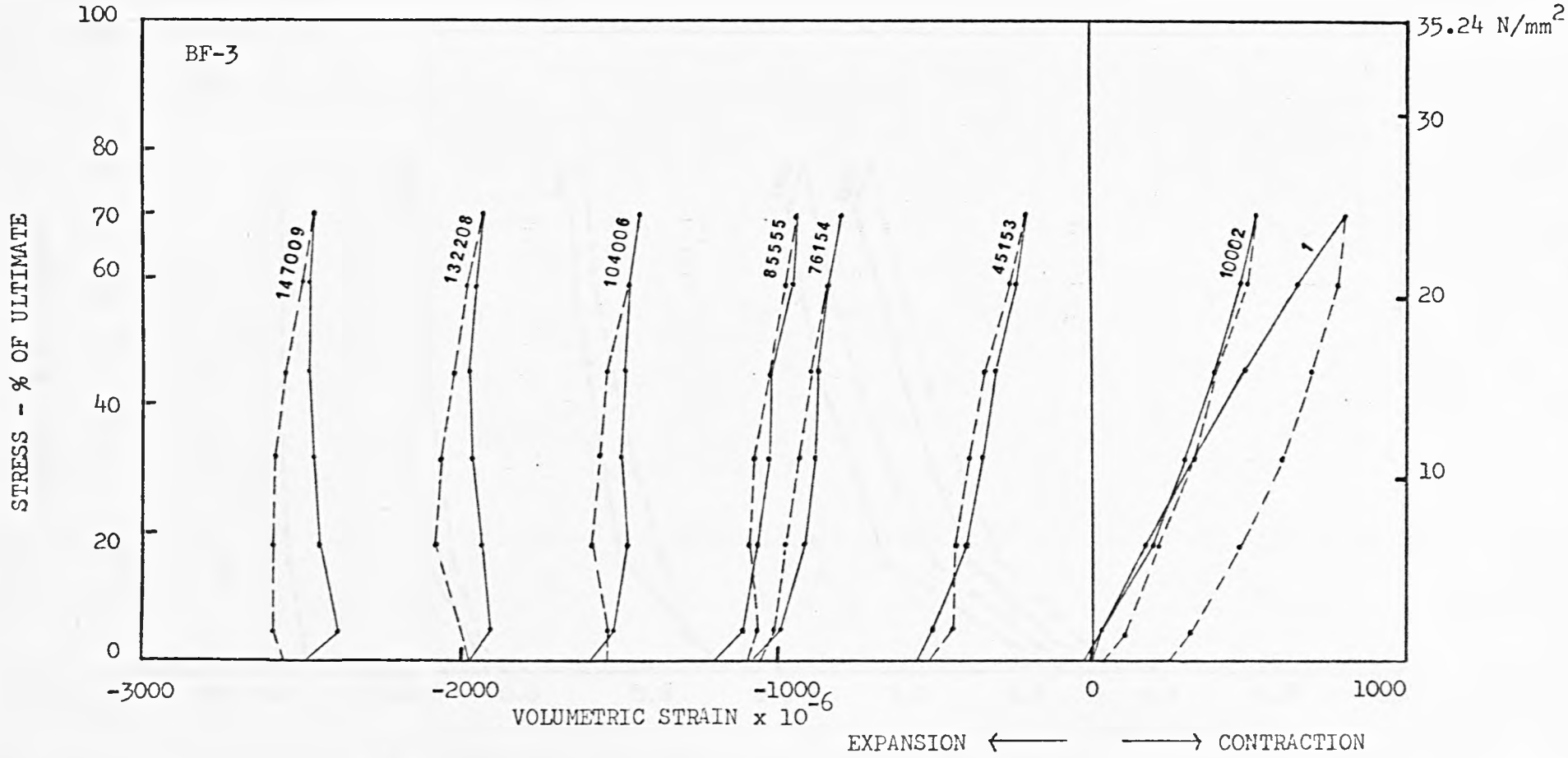

FIG. 6.24 STRESS - VOLUMETRIC STRAIN CURVES OF A SPECIMEN IN CYCLIC COMPRESSION(S_{max} = 70 %)

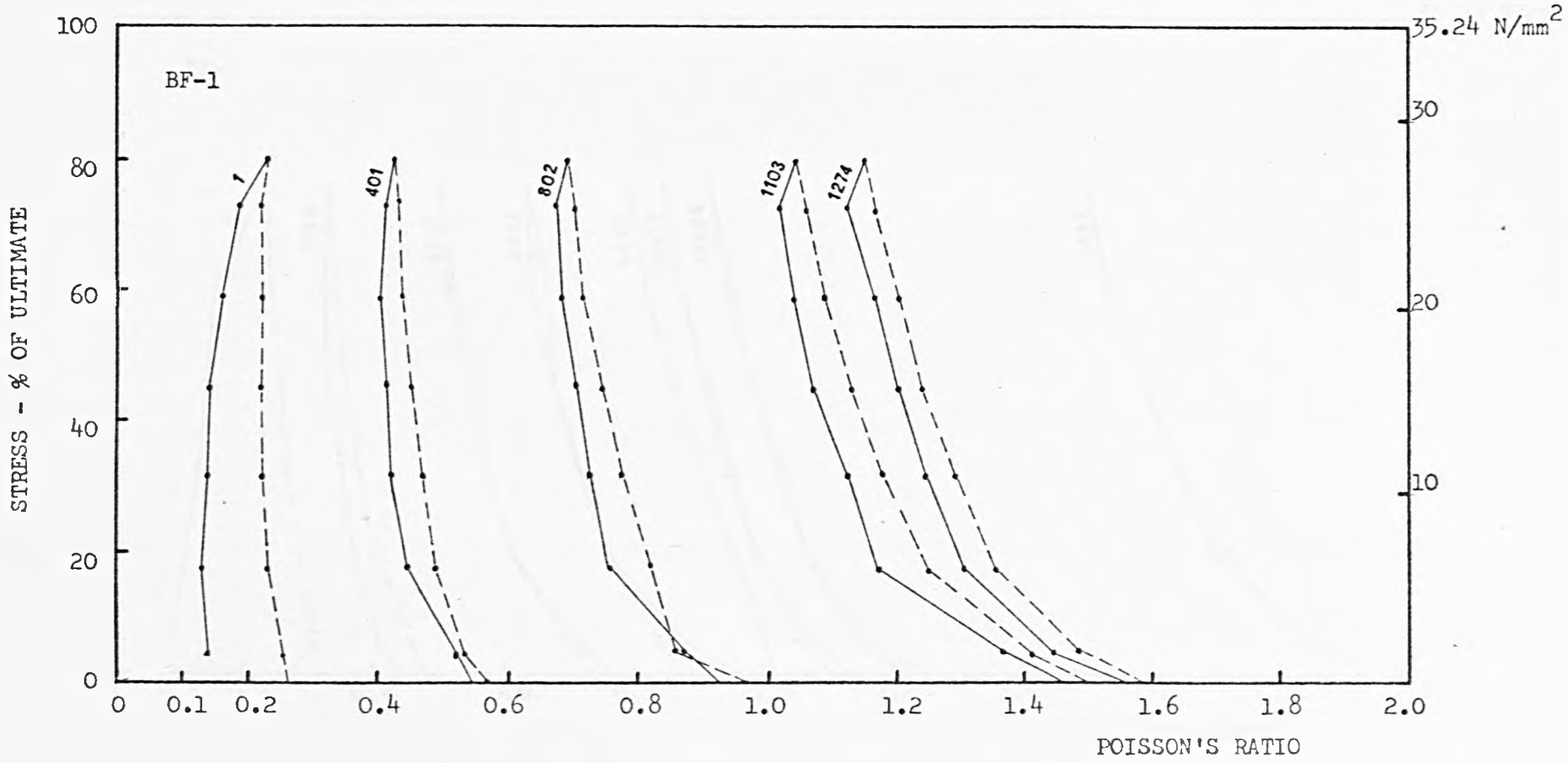

FIG. 6. 25 STRESS - POISSON'S RATIO CURVES OF A SPECIMEN IN CYCLIC COMPRESSION

(S_{max} = 80 %)

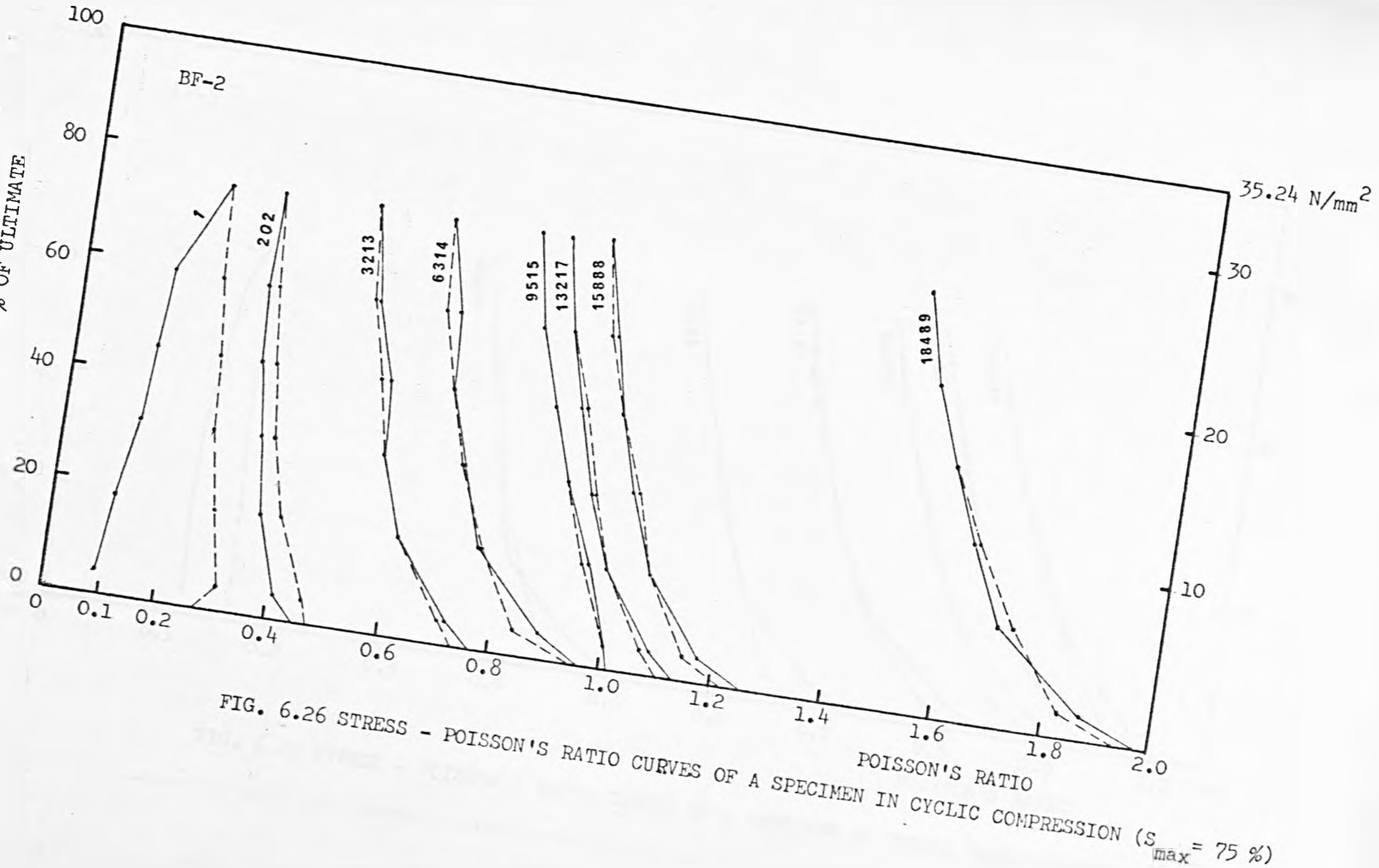

FIG. 6.26 STRESS - POISSON'S RATIO CURVES OF A SPECIMEN IN CYCLIC COMPRESSION (S_{max} = 75 %)

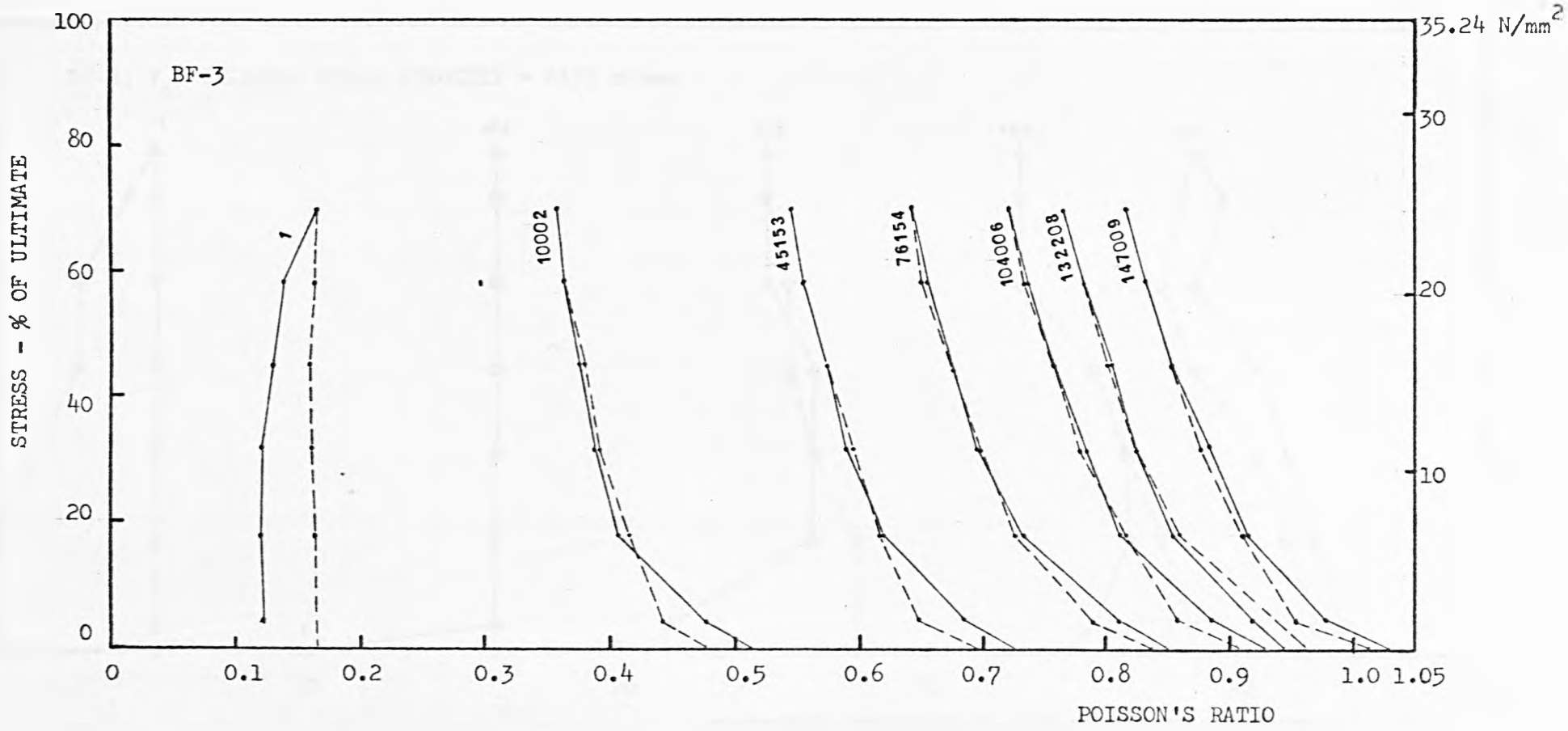

FIG. 6.27 STRESS - POISSON'S RATIO CURVES OF A SPECIMEN IN CYCLIC COMPRESSION(S_{max} = 70 %)

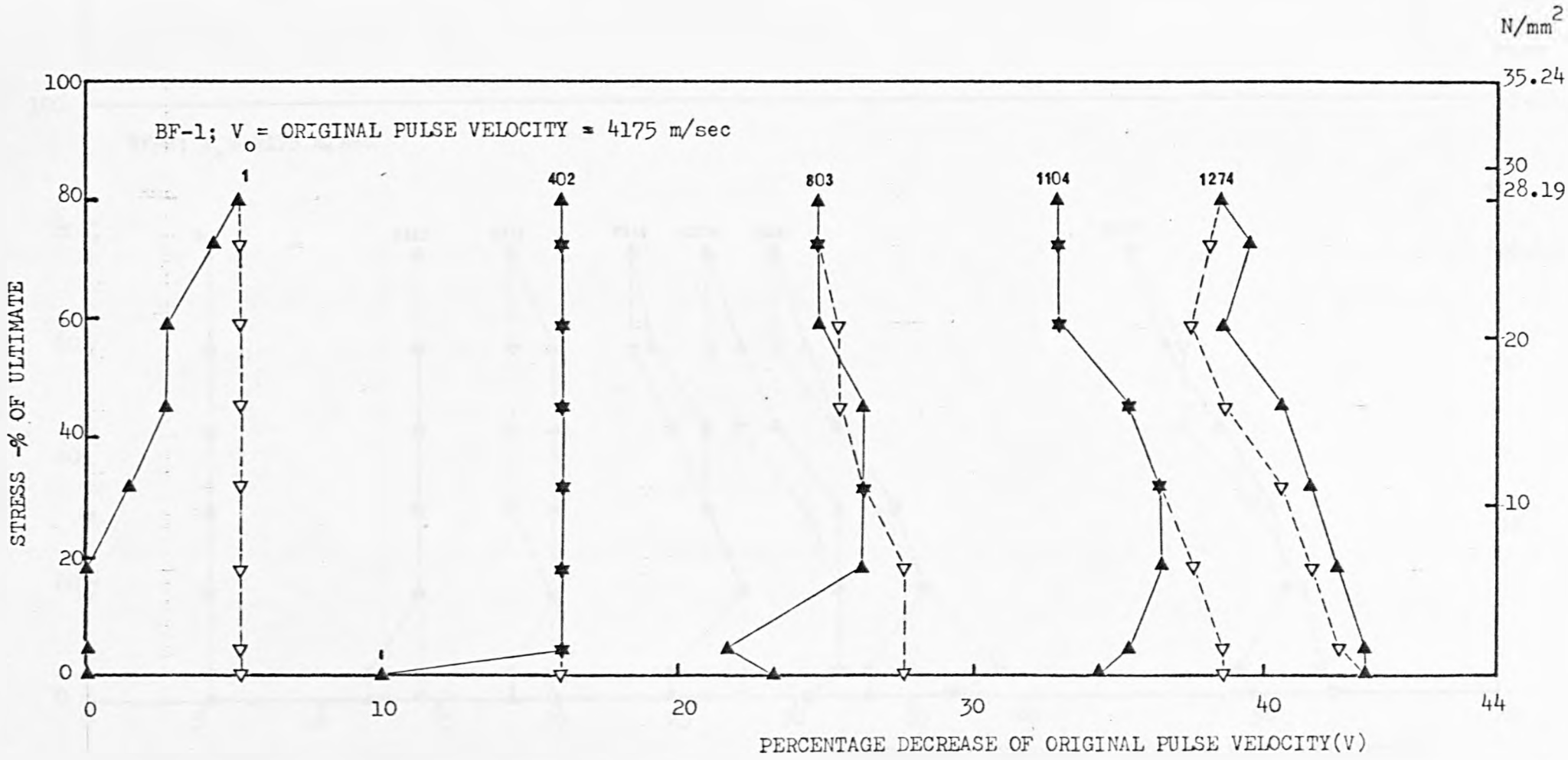

FIG. 7.1 VARIATION OF STRESS - PERCENTAGE DECREASE OF THE ORIGINAL PULSE VELOCITY CURVES WITH NUMBER OF CYCLES

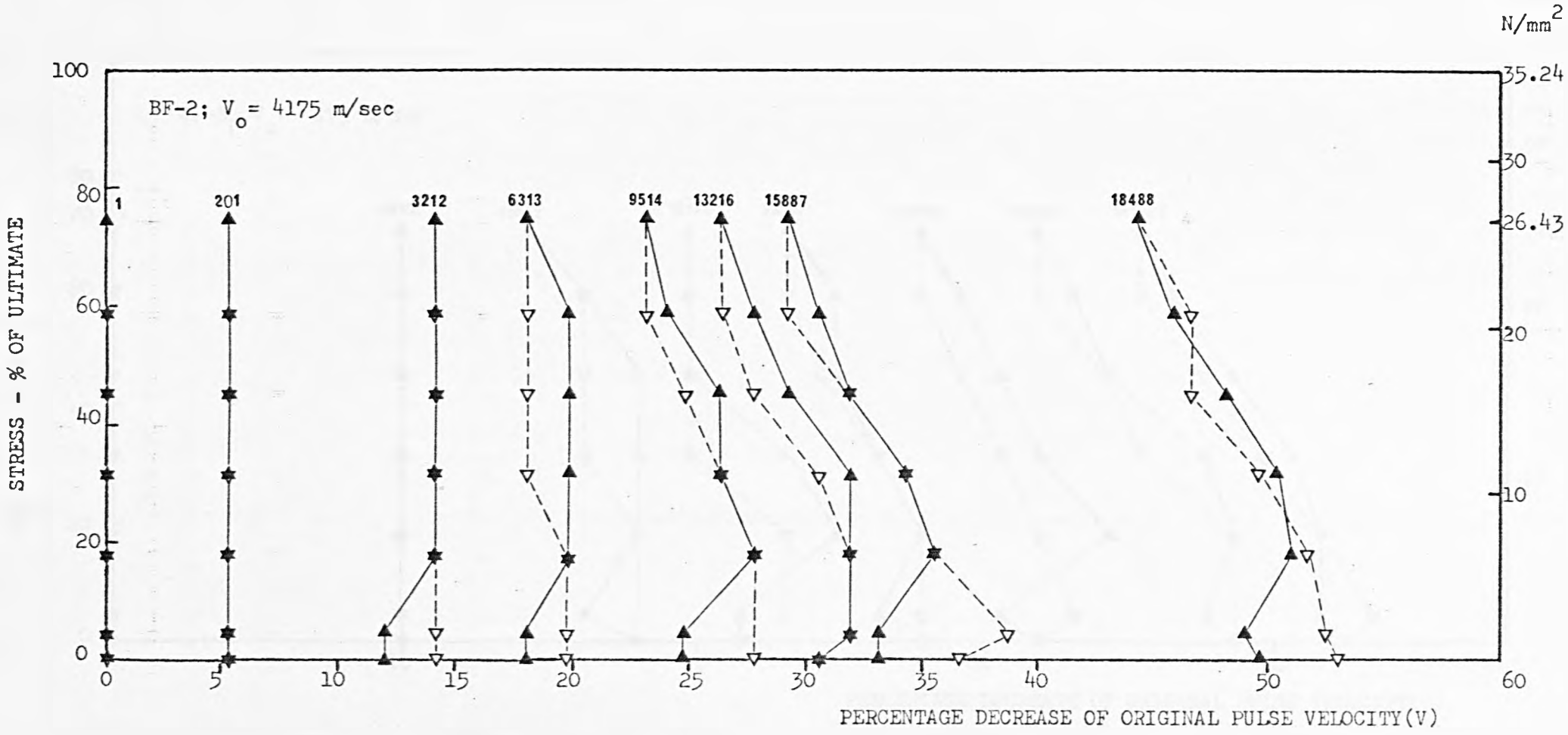

FIG. 7.2 VARIATION OF STRESS - DECREASE OF PULSE VELOCITY CURVES WITH NUMBER OF CYCLES

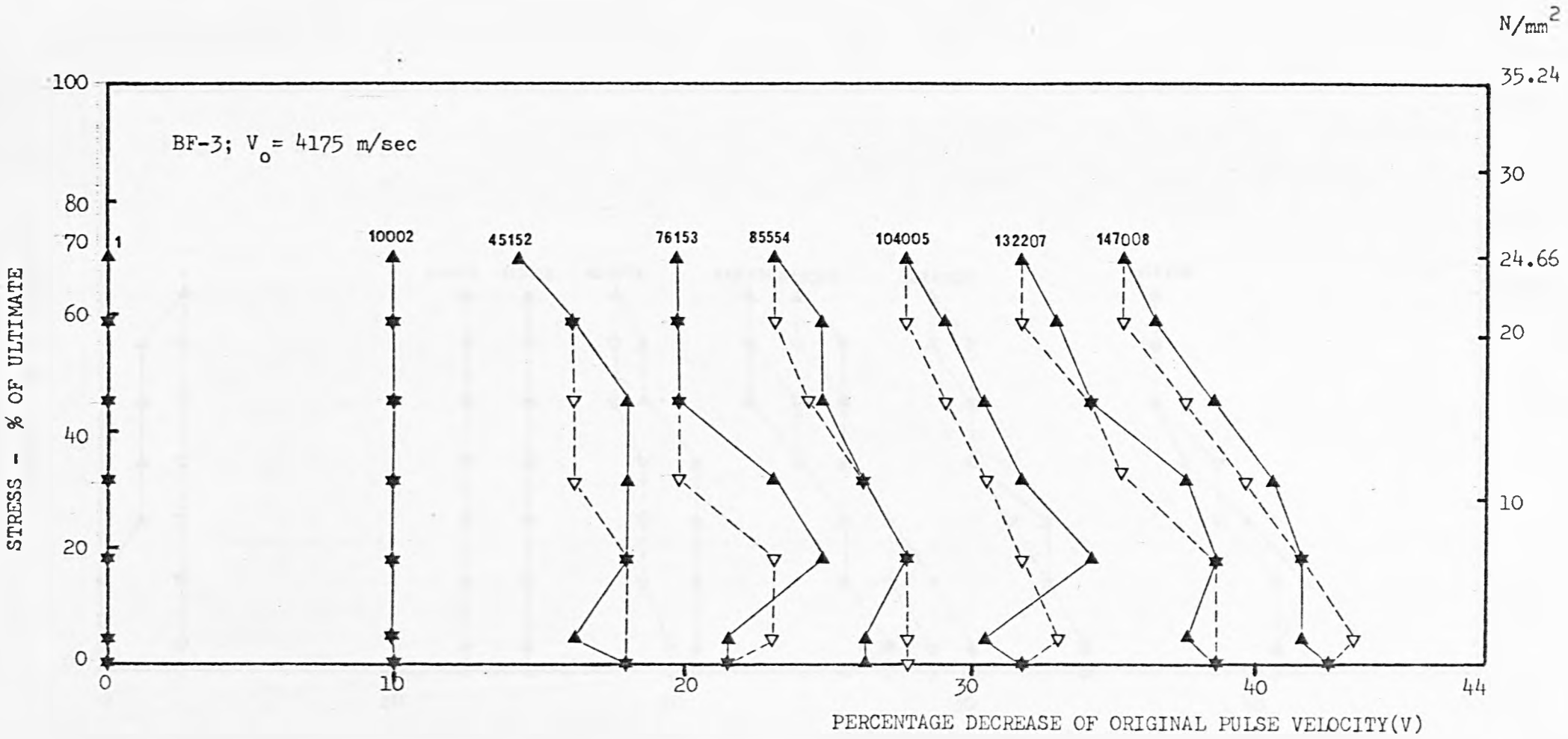

FIG. 7.3 VARIATION OF STRESS - DECREASE OF PULSE VELOCITY CURVES WITH NUMBER OF CYCLES

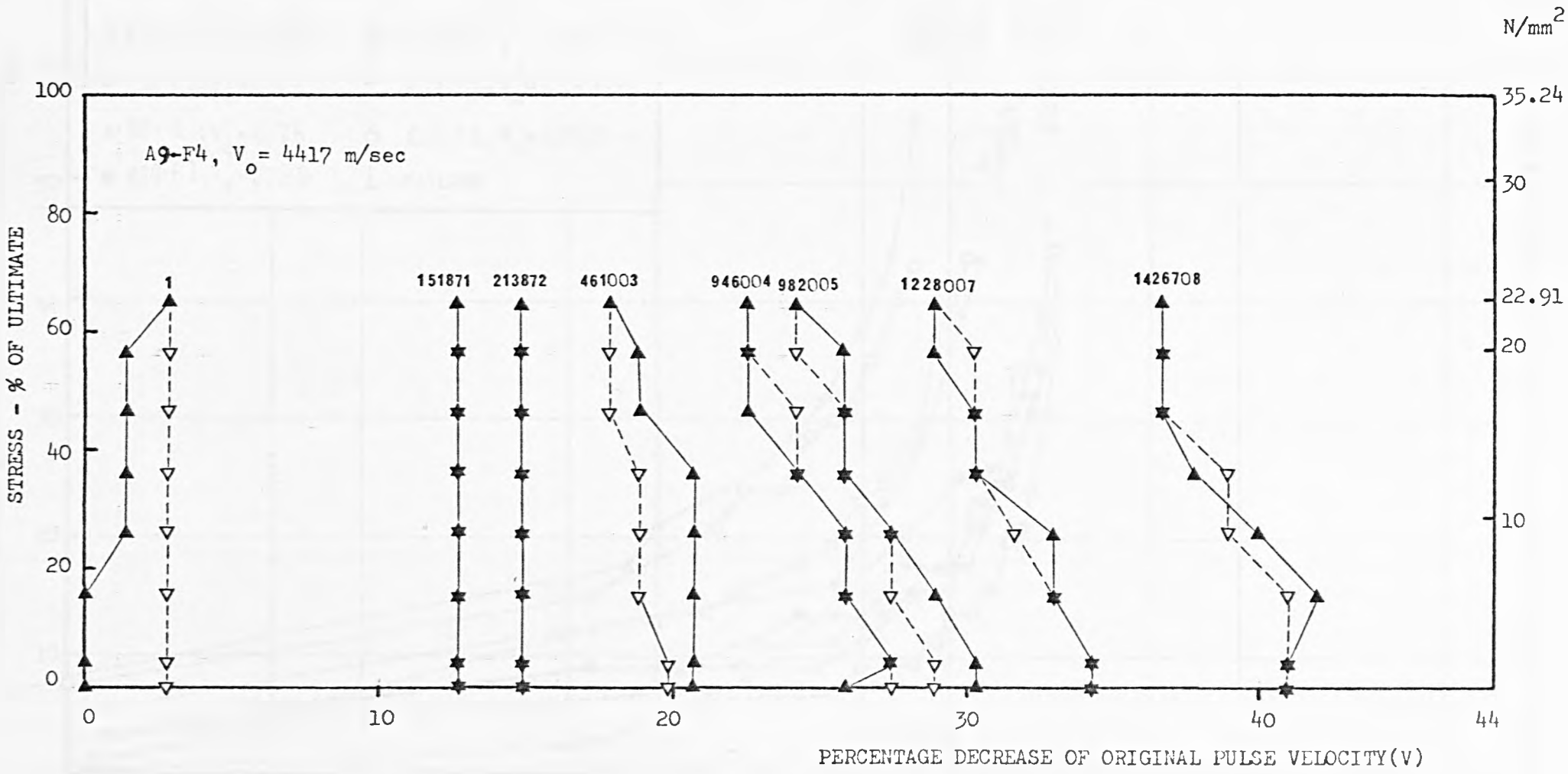

FIG. 7.4 VARIATION OF STRESS - DECREASE OF PULSE VELOCITY CURVES WITH NUMBER OF CYCLES

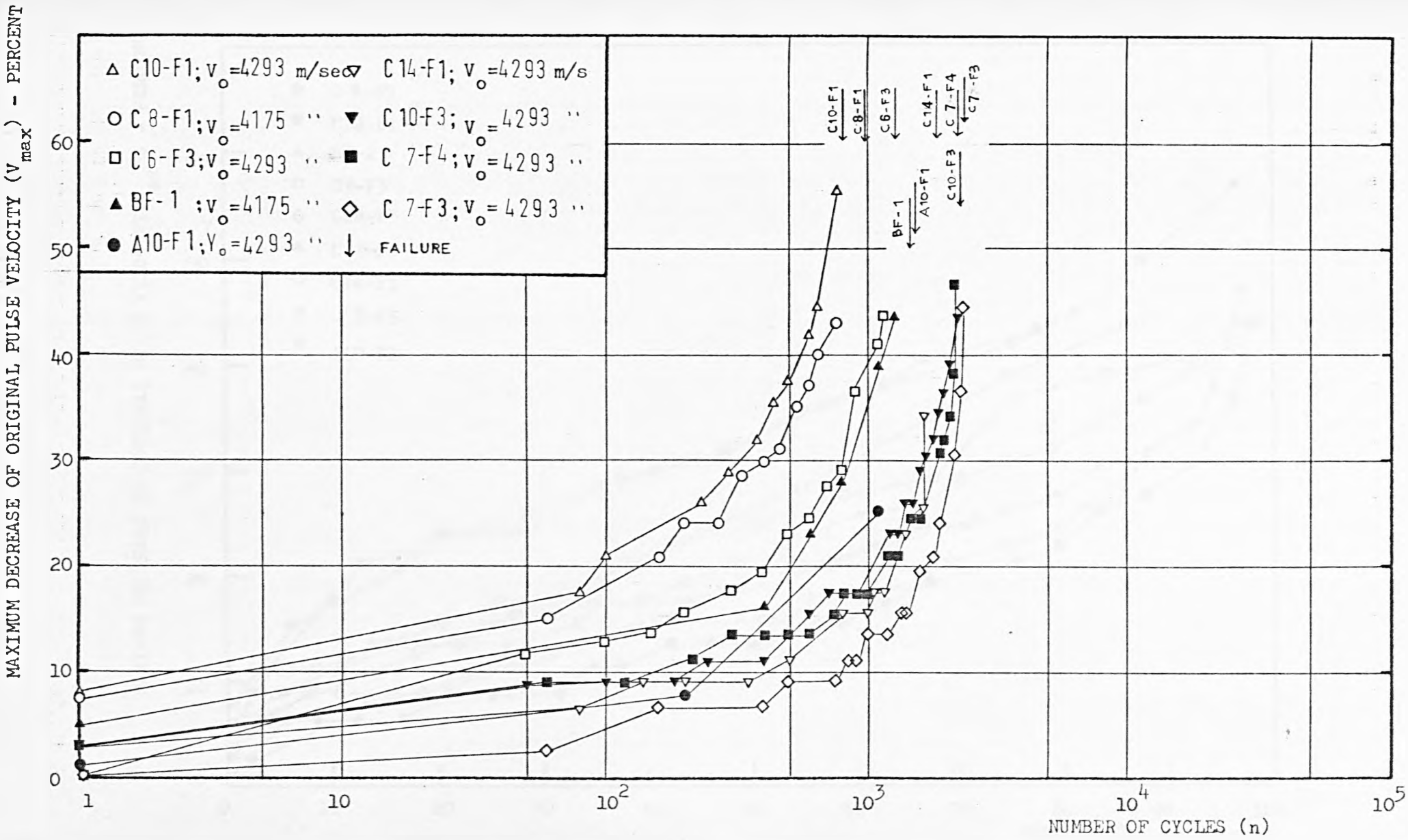

FIG. 7.5 VARIATION OF V_{max} WITH n OF SPECIMENS TESTED UNDER CONSTANT AMPLITUDE STRESS

(S_{max} = 80 %)

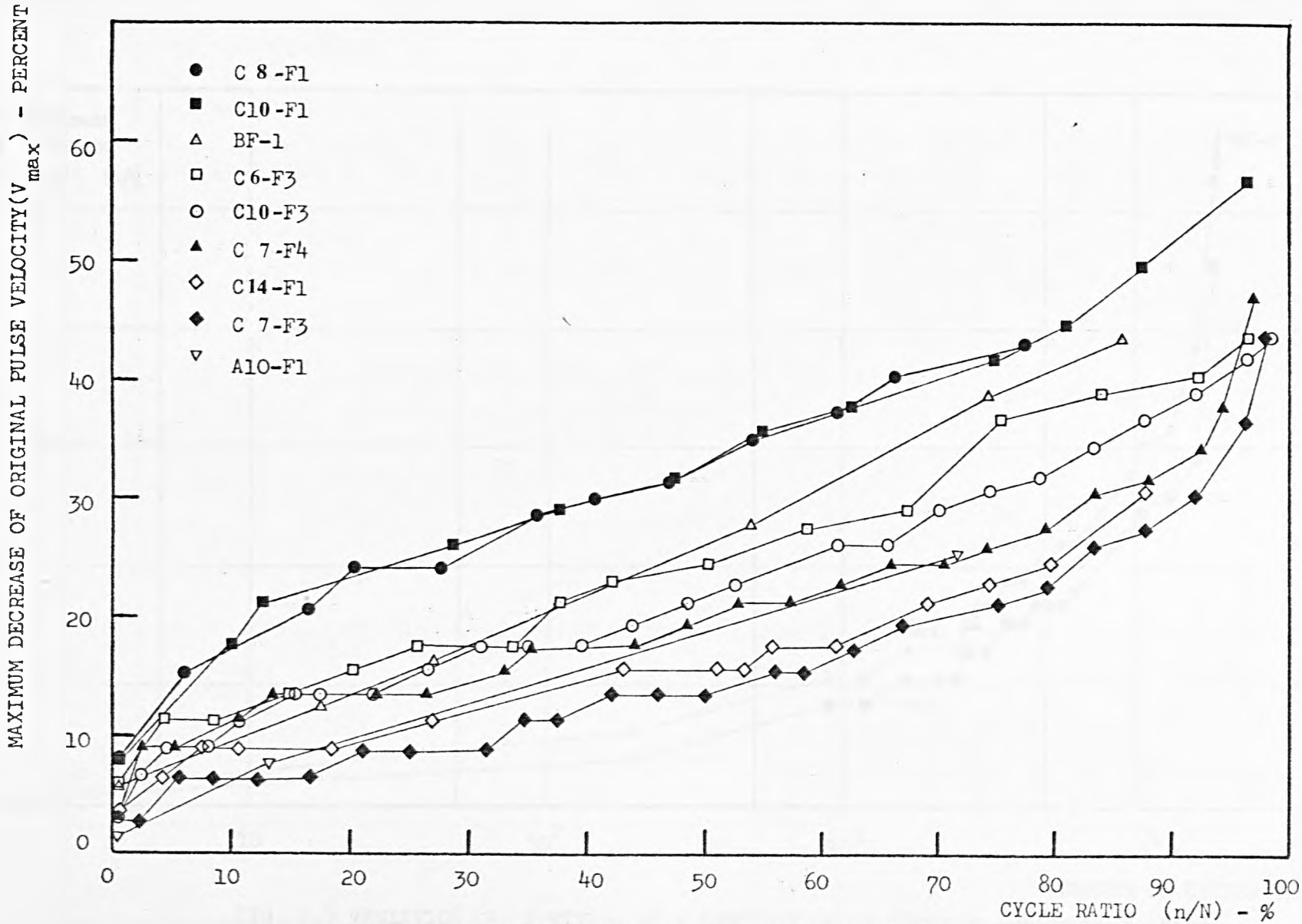

FIG. 7.6 VARIATION OF V_{max} WITH n/N OF SPECIMENS TESTED UNDER CONST NT STRESS (S_{max} = 80 %)

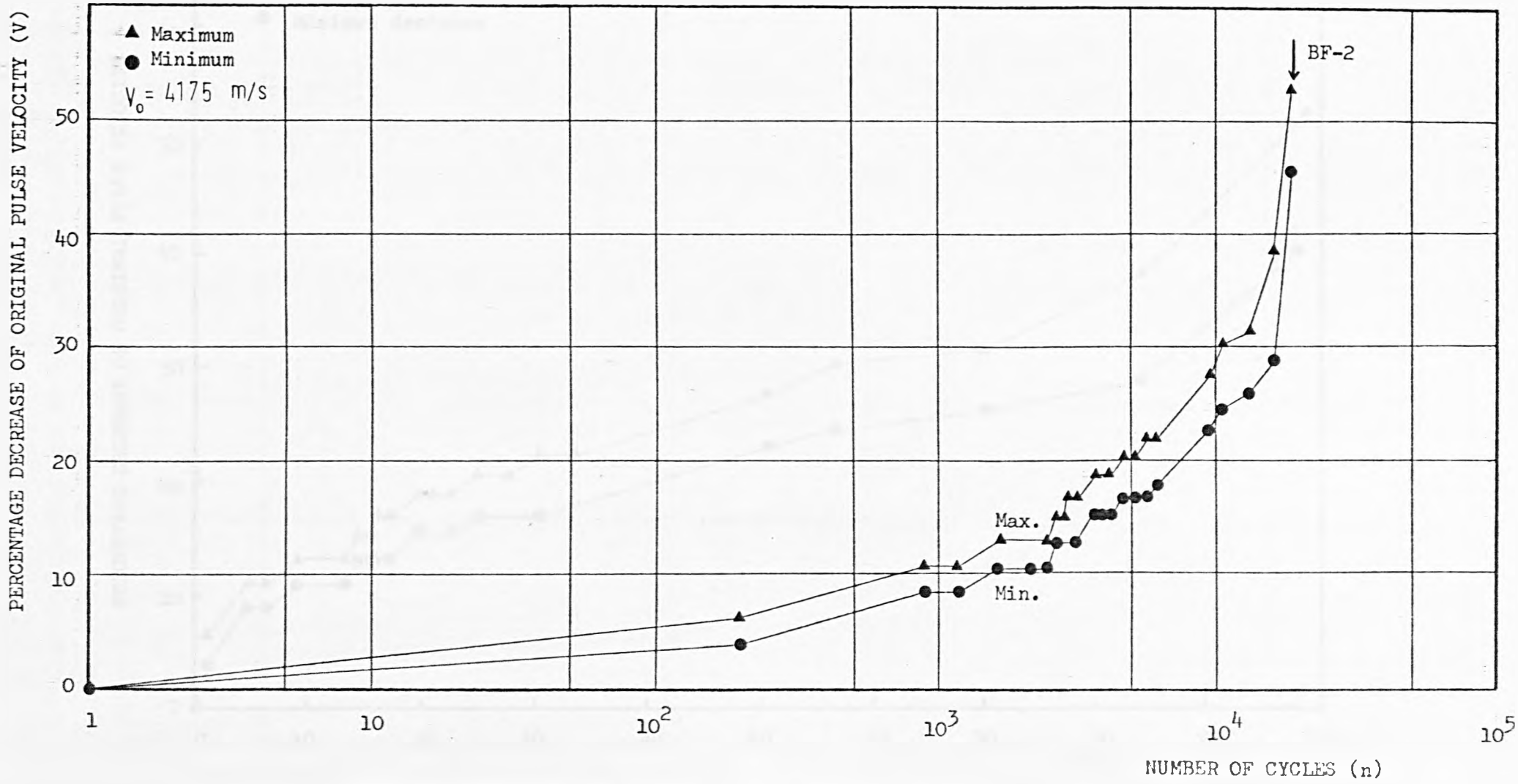

FIG. 7.7 VARIATION OF V WITH n OF A SPECIMEN UNDER CONSTANT AMPLITUDE LOADING (S_{max} = 75 %)

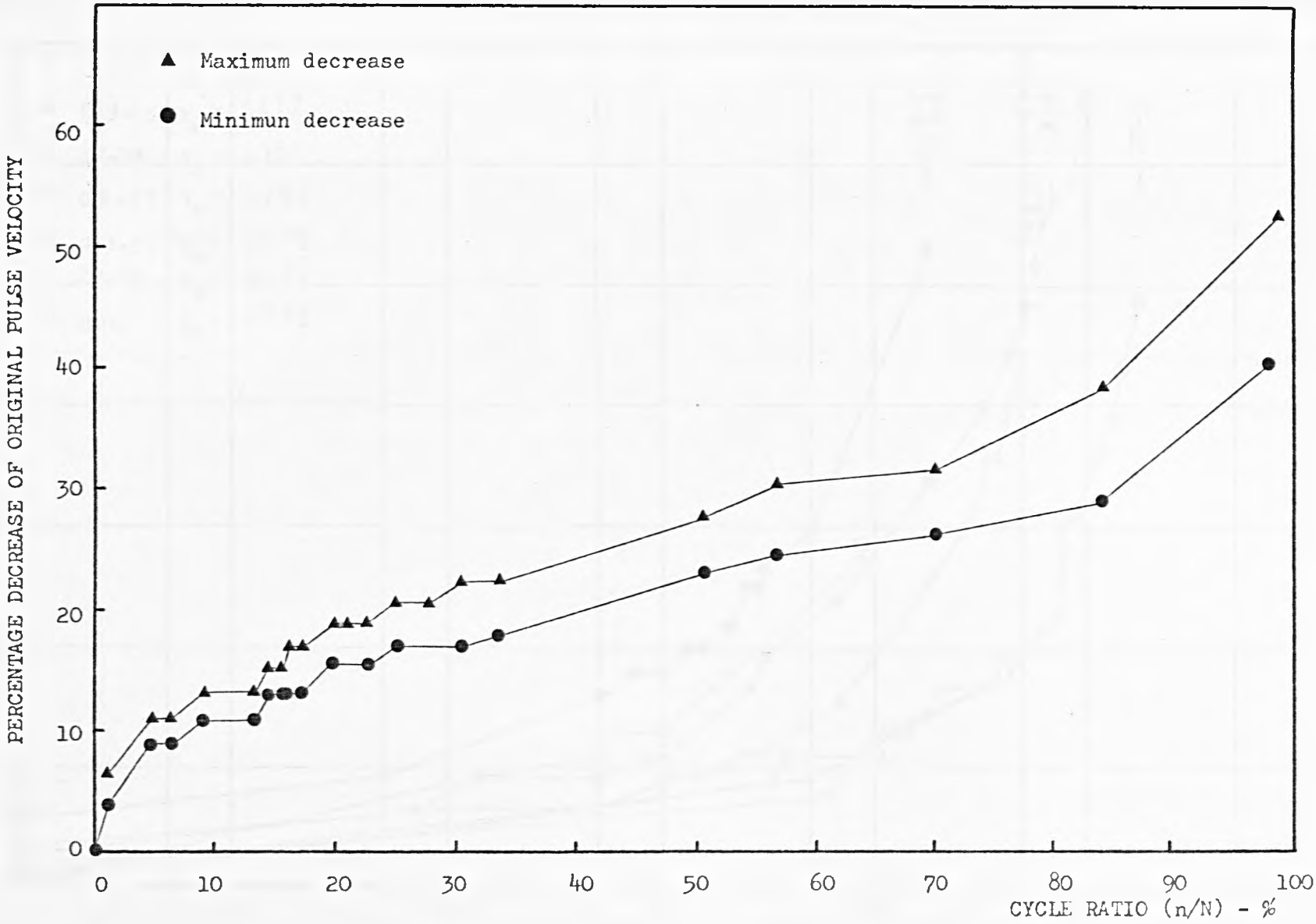

FIG. 7.8 VARIATION OF V WITH n/N OF A SPECIMEN UNDER CONSTANT AMPLITUDE (S_{max} = 75 %)

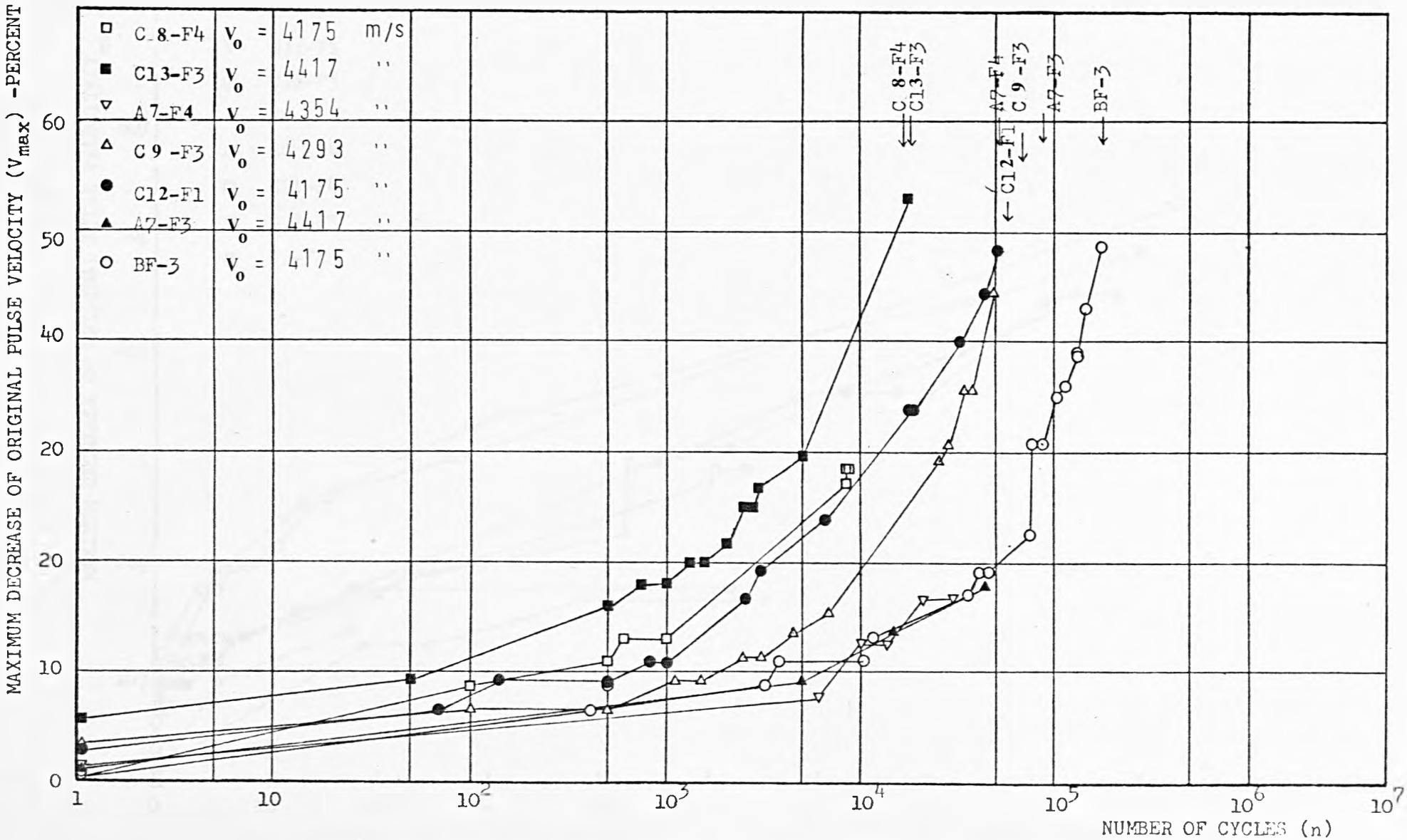

FIG. 7.9 VARIATION OF V_{max} WITH n OF SPECIMENS UNDER CONSTANT AMPLITUDE LOADING (S_{MAX} = 70 %)

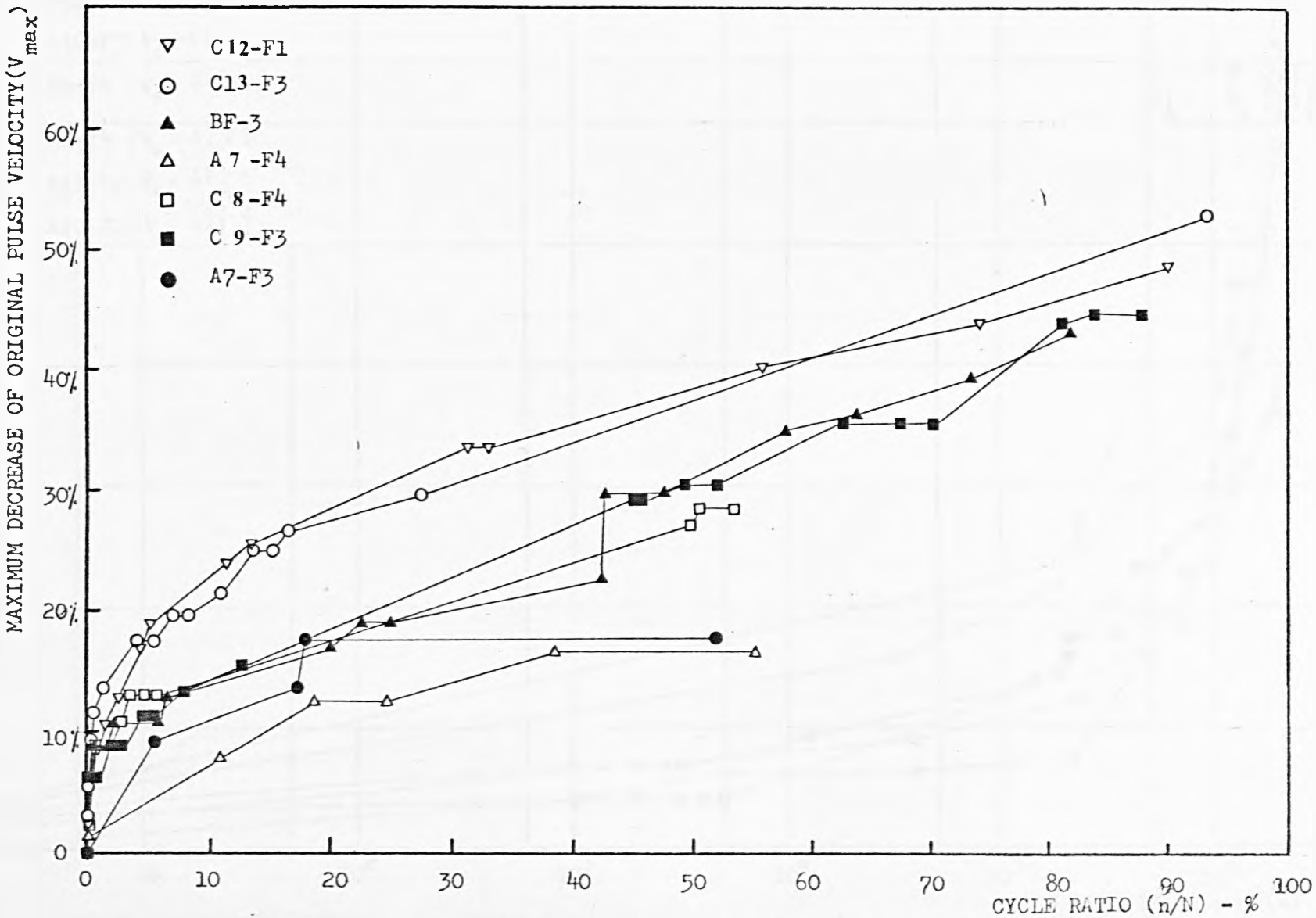

FIG. 7.10 VARIATION OF V_{max} WITH n/N OF SPECIMENS UNDER CONSTANT AMPLITUDE LOADING: (S_{max} = 70%)

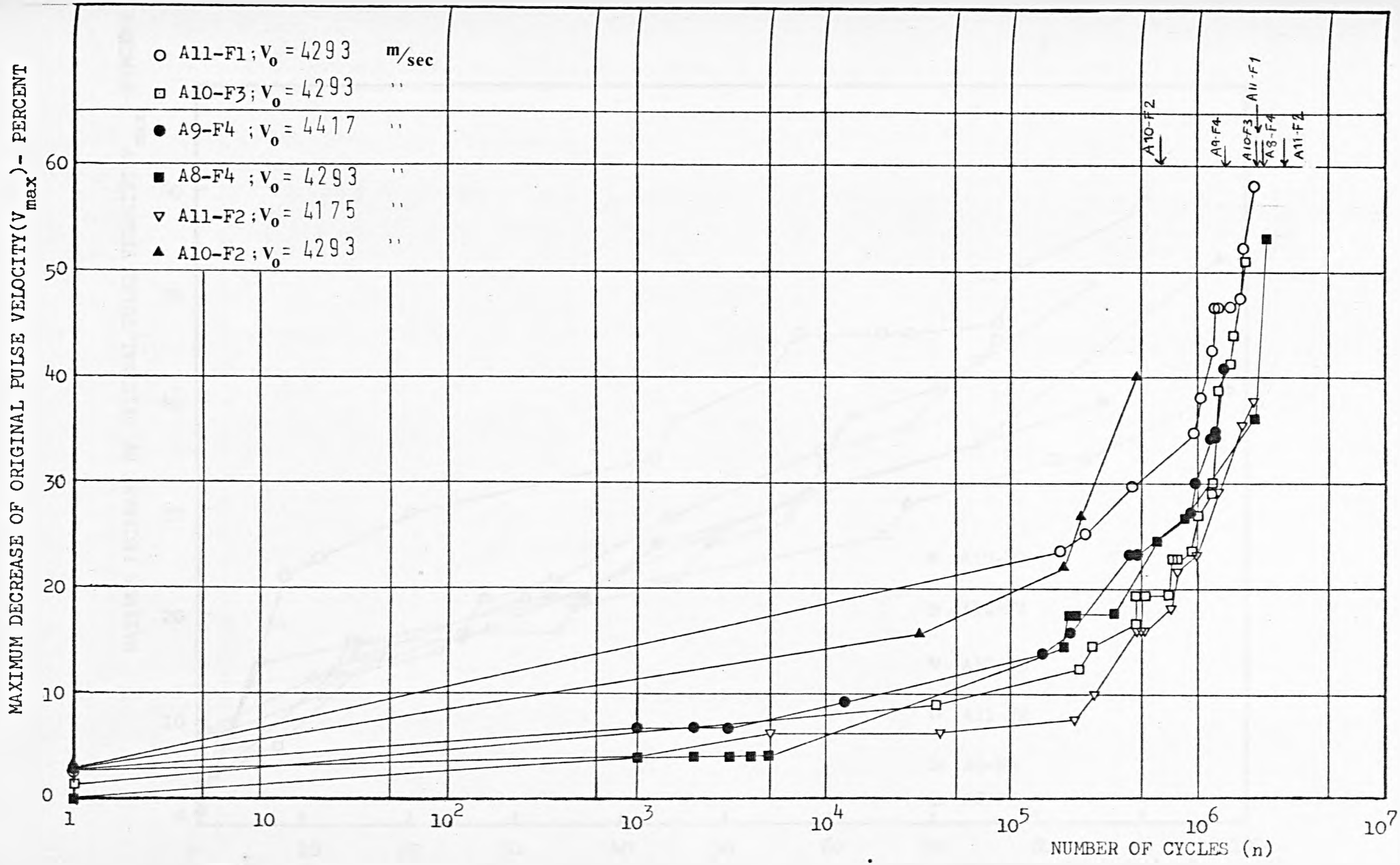

FIG. 7.11 VARIATION OF V_{max} WITH n OF SPECIMENS UNDER CONSTANT AMPLITUDE LOADING (S_{max} = 65 %)

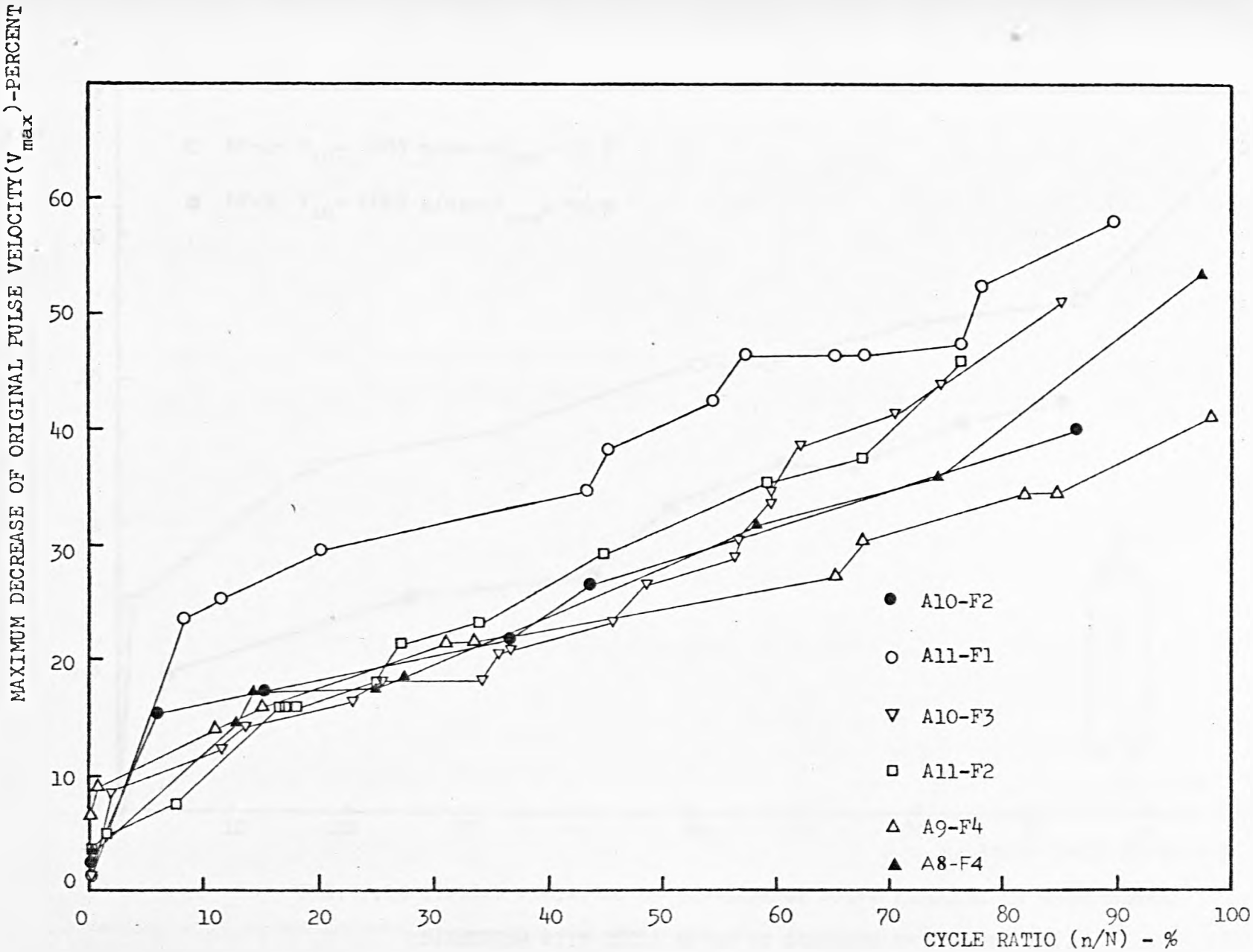

FIG. 7.12 VARIATION OF V_{max} WITH n/N OF SPECIMENS UNDER CONSTANT AMPLITUDE LOADING (S_{max} = 65 %)

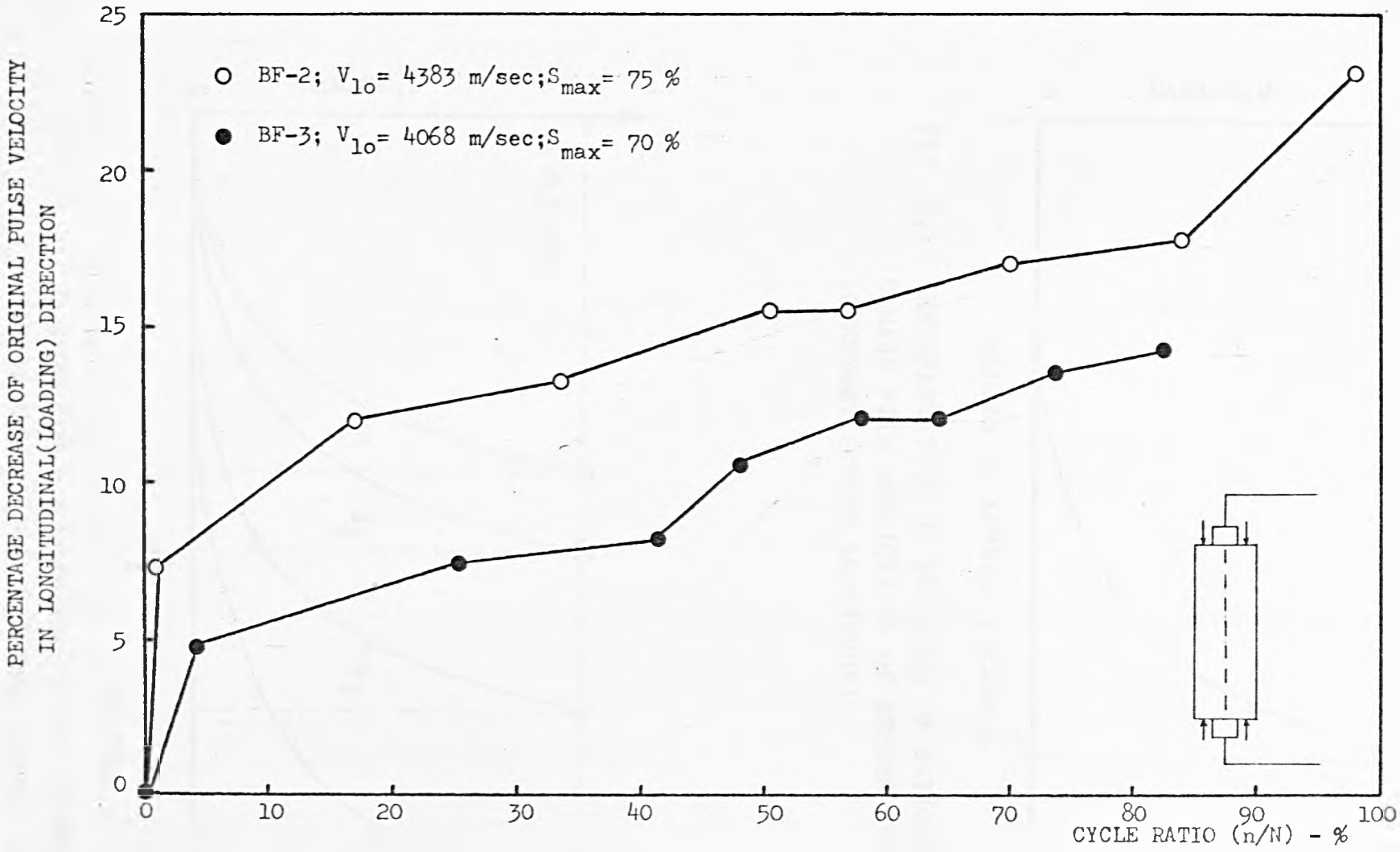

FIG. 7.13 TYPICAL VARIATION OF DECREASE OF PULSE VELOCITY IN LONGITUDINAL DIRECTION WITH CYCLE RATIO OF CONCRETE IN COMPRESSION.

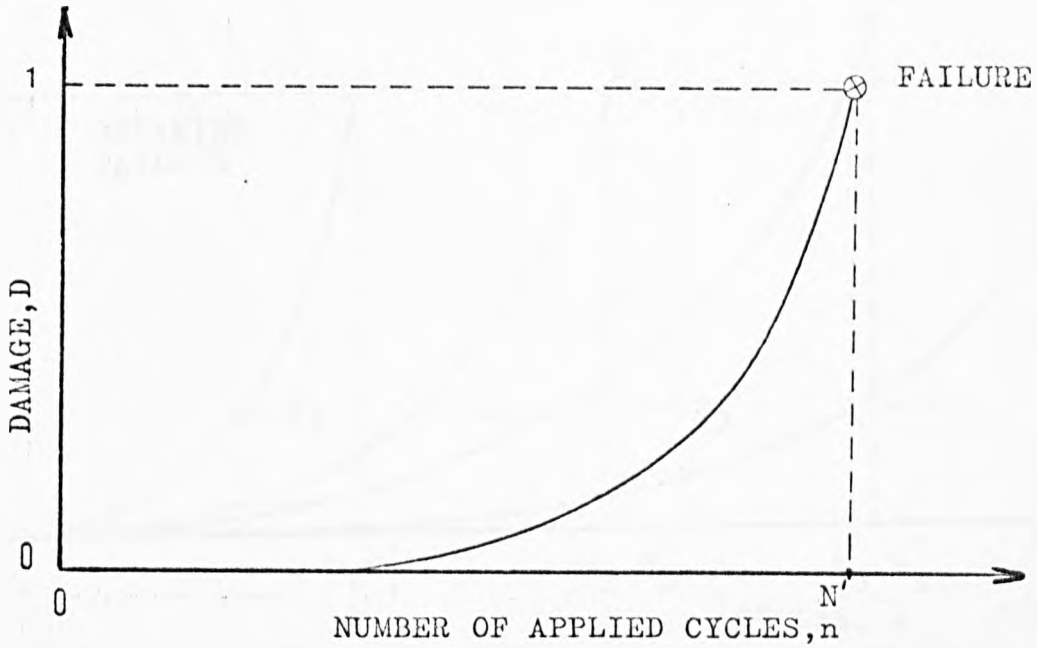

FIG. 8.1 REPRESENTATION OF PROGRESS OF FATIGUE DAMAGE WITH APPLICATION OF STRESS CYCLES (CONSTANT STRESS AMPLITUDE)

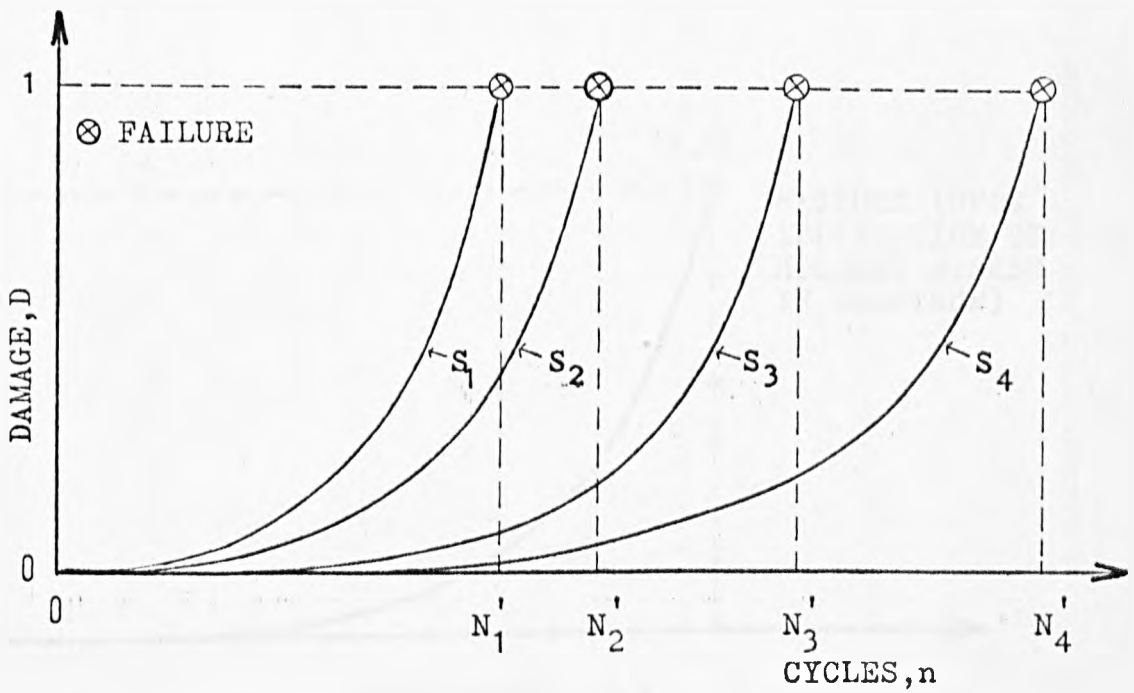

FIG. 8.2 DAMAGE-CYCLE RELATIONSHIPS FOR SEVERAL STRESS AMPLITUDES, CONSTANT STRESS AMPLITUDE TESTS ($S_1 > S_2 > S_3 > S_4$)

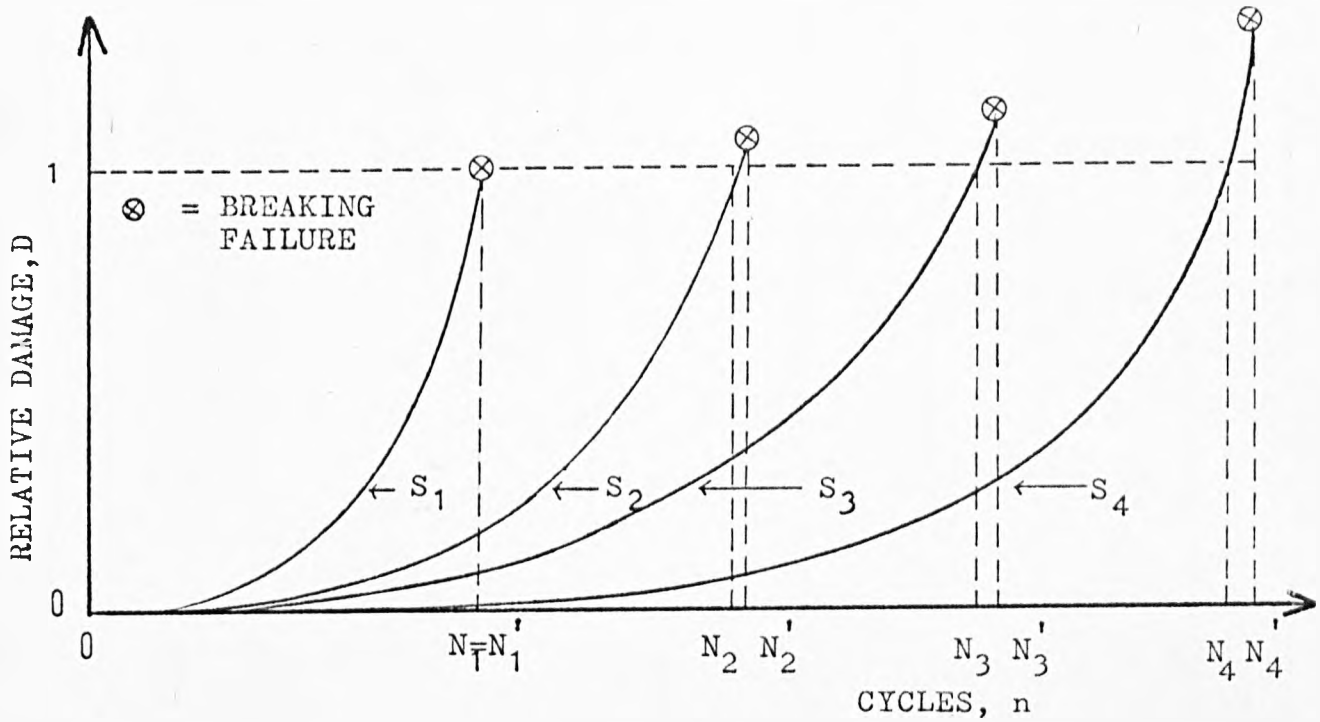

FIG. 8.3 DAMAGE-CYCLE RELATIONSHIPS FROM FIG. 8.2 NORMALIZED TO FAILURE DAMAGE AT HIGHEST STRESS AMPLITUDE IN SPECTRUM, S_1 .

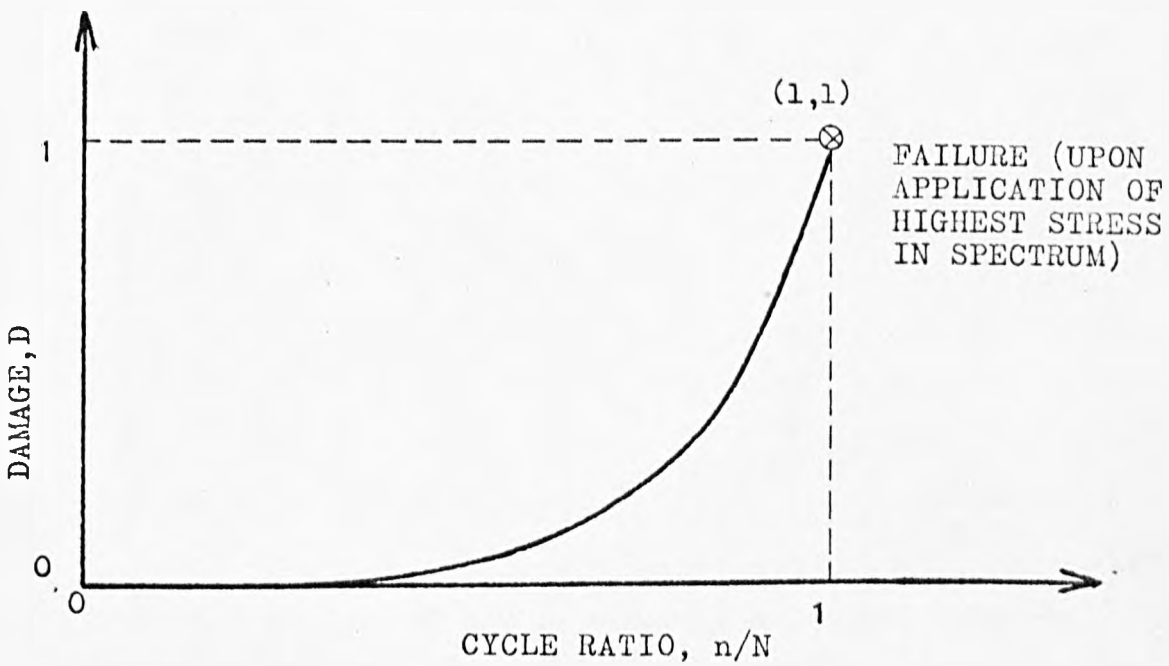

FIG. 8.4 TYPICAL STRESS INDEPENDENT DAMAGE-CYCLE RATIO RELATIONSHIP (FIG. 8.3 WITH CYCLES NORMALIZED; CURVES ARE IDENTICAL FOR ALL STRESS AMPLITUDES)

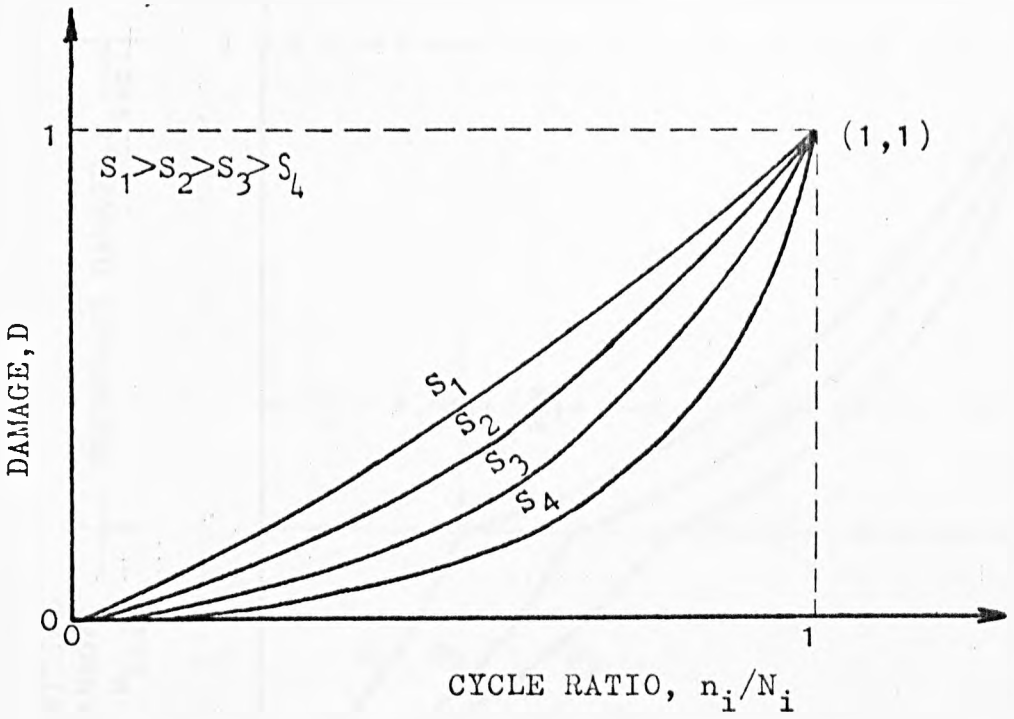

FIG. 8.5 TYPICAL STRESS-DEPENDENT DAMAGE-CYCLE RATIO RELATIONSHIPS.

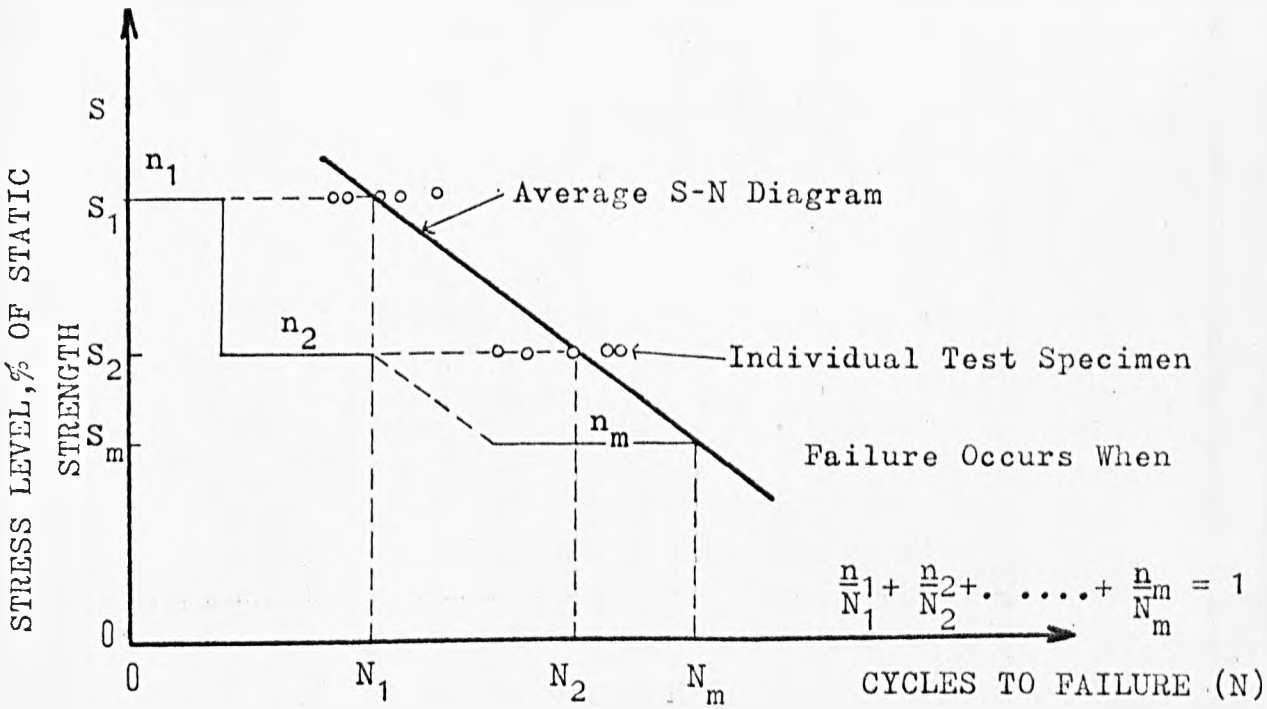

FIG. 8.6 PALMGREN-MINER HYPOTHESIS.

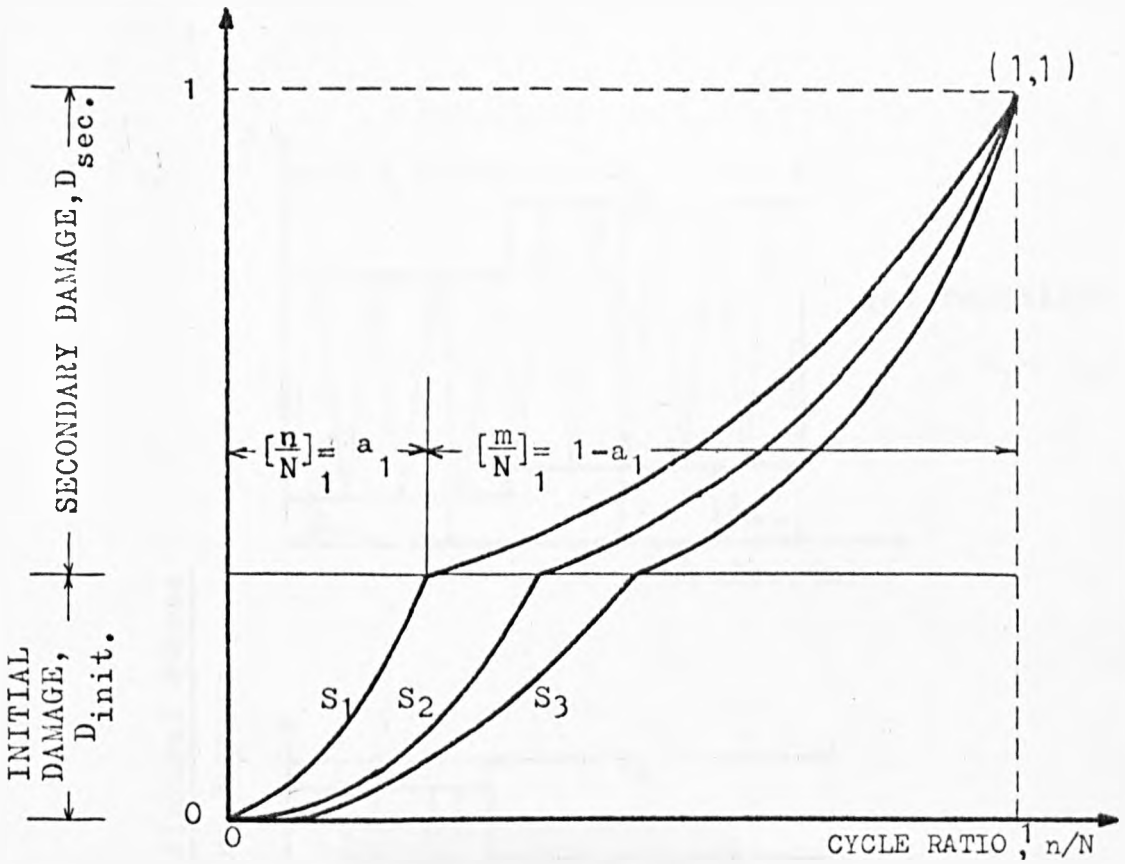

FIG. 8.7 — FORM OF DAMAGE-CYCLE RATIO RELATIONSHIP

(Grover)

Fig. 9.1 is on page 83

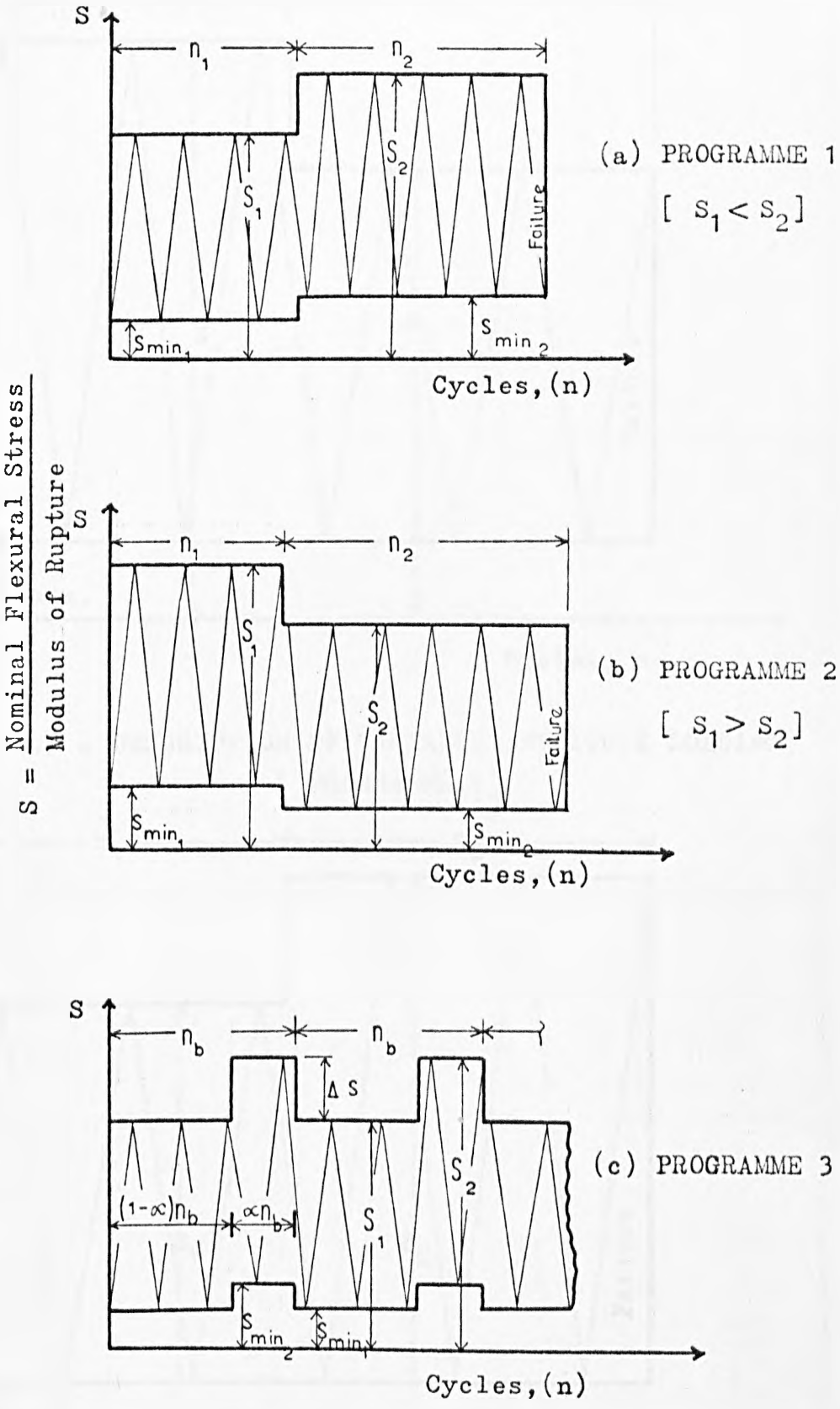

FIG. 9.2 LOADING SEQUENCES FOR VARIABLE LOAD STUDIES (HILSDORF AND KESLER)[36]

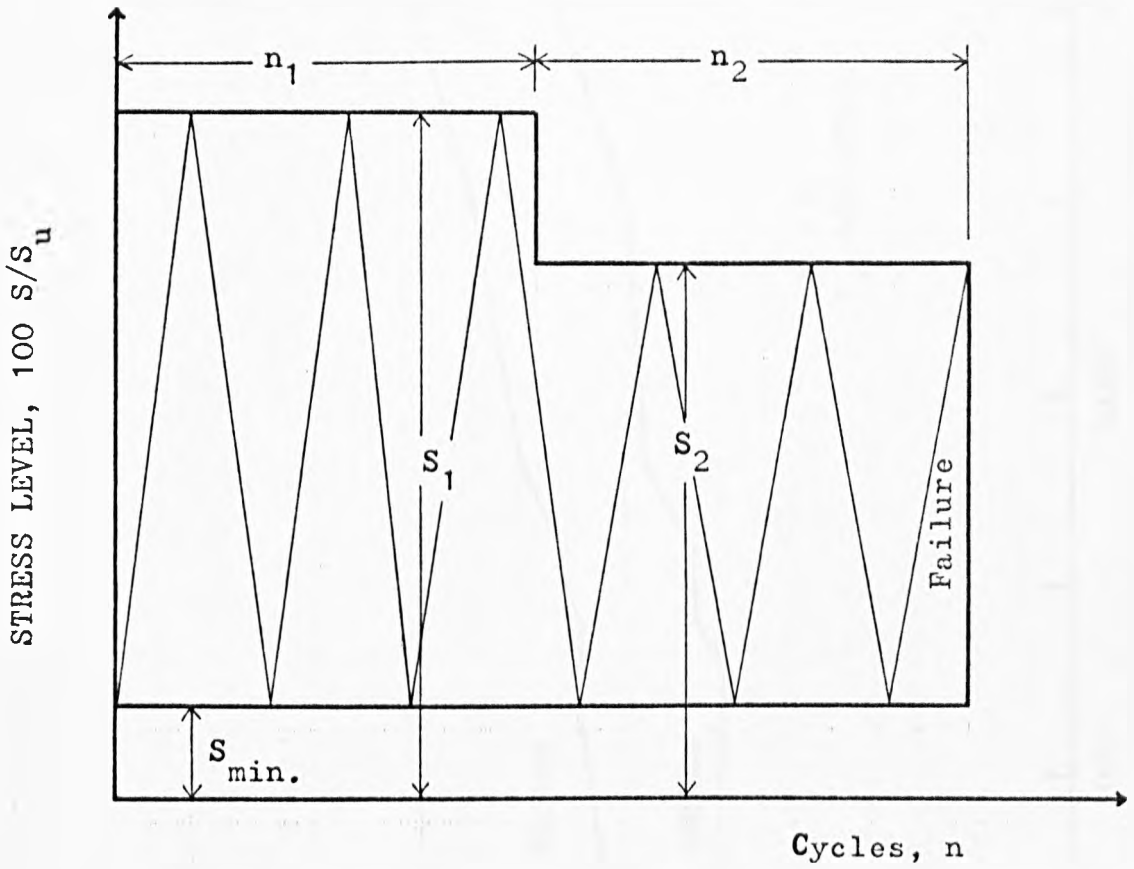

FIG. 9.3 a DESCRIPTION OF VARIABLE AMPLITUDE LOADING
[PROGRAMME 1]

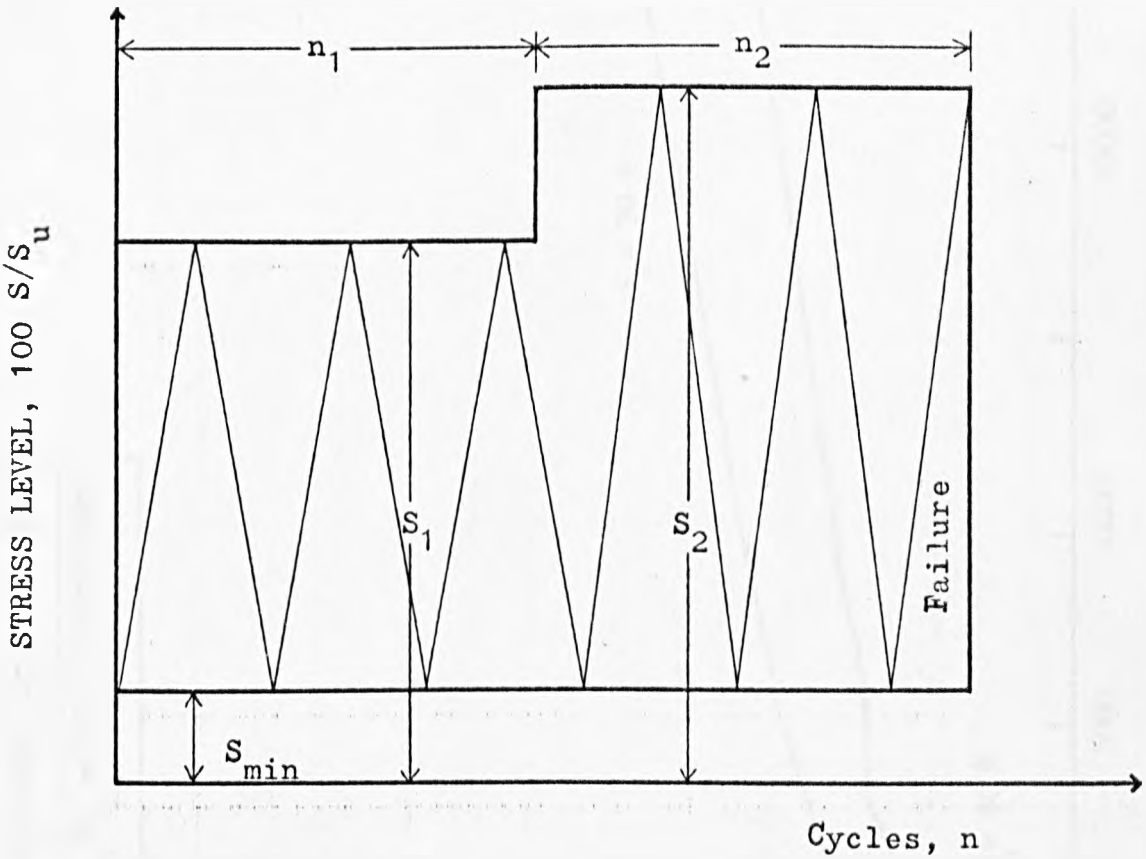

FIG.9.3 b DESCRIPTION OF VARIABLE AMPLITUDE LOADING
[PROGRAMME 2]

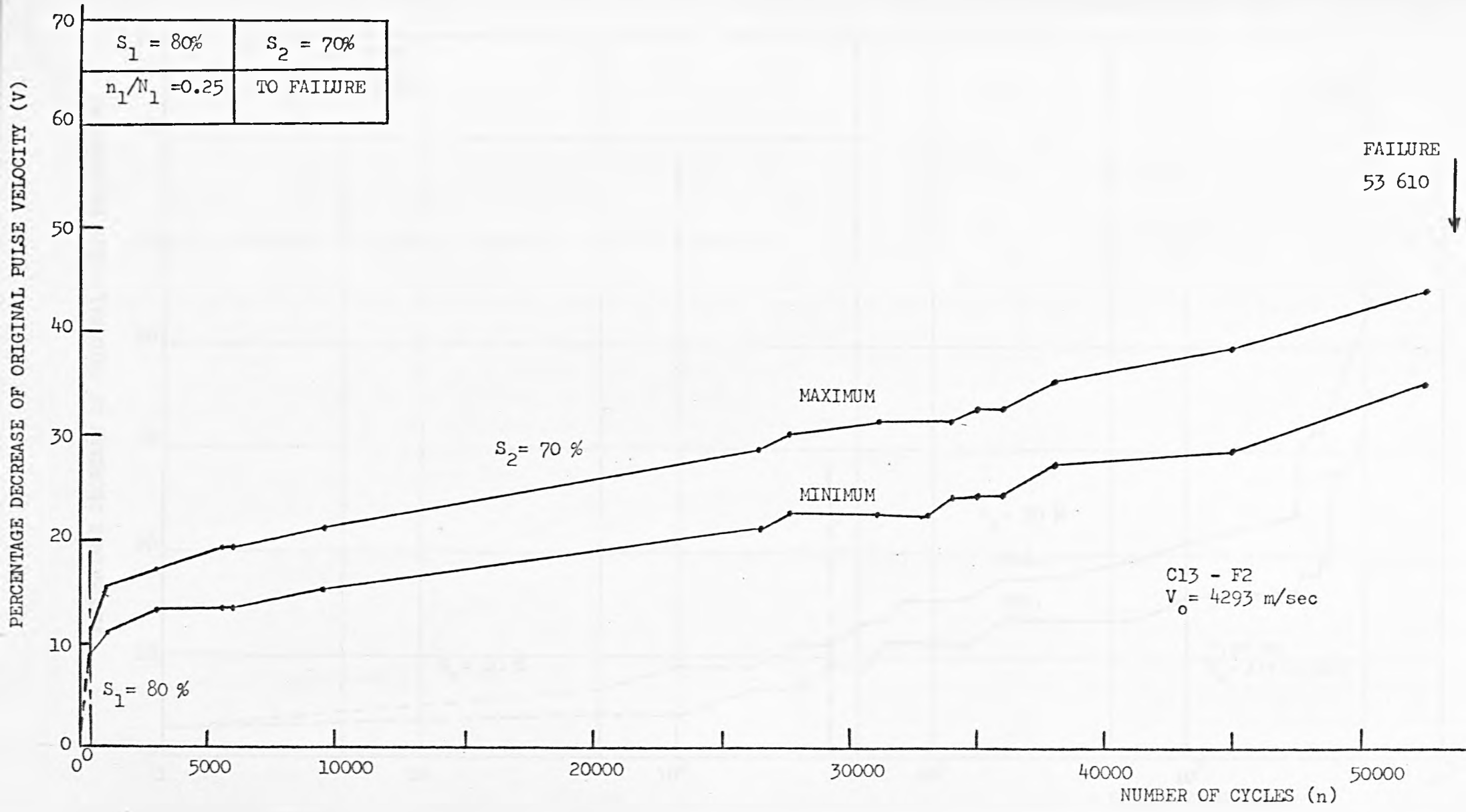

FIG. 9.4 VARIATION OF V WITH n OF A SPECIMEN UNDER LOADING PROGRAMME 1

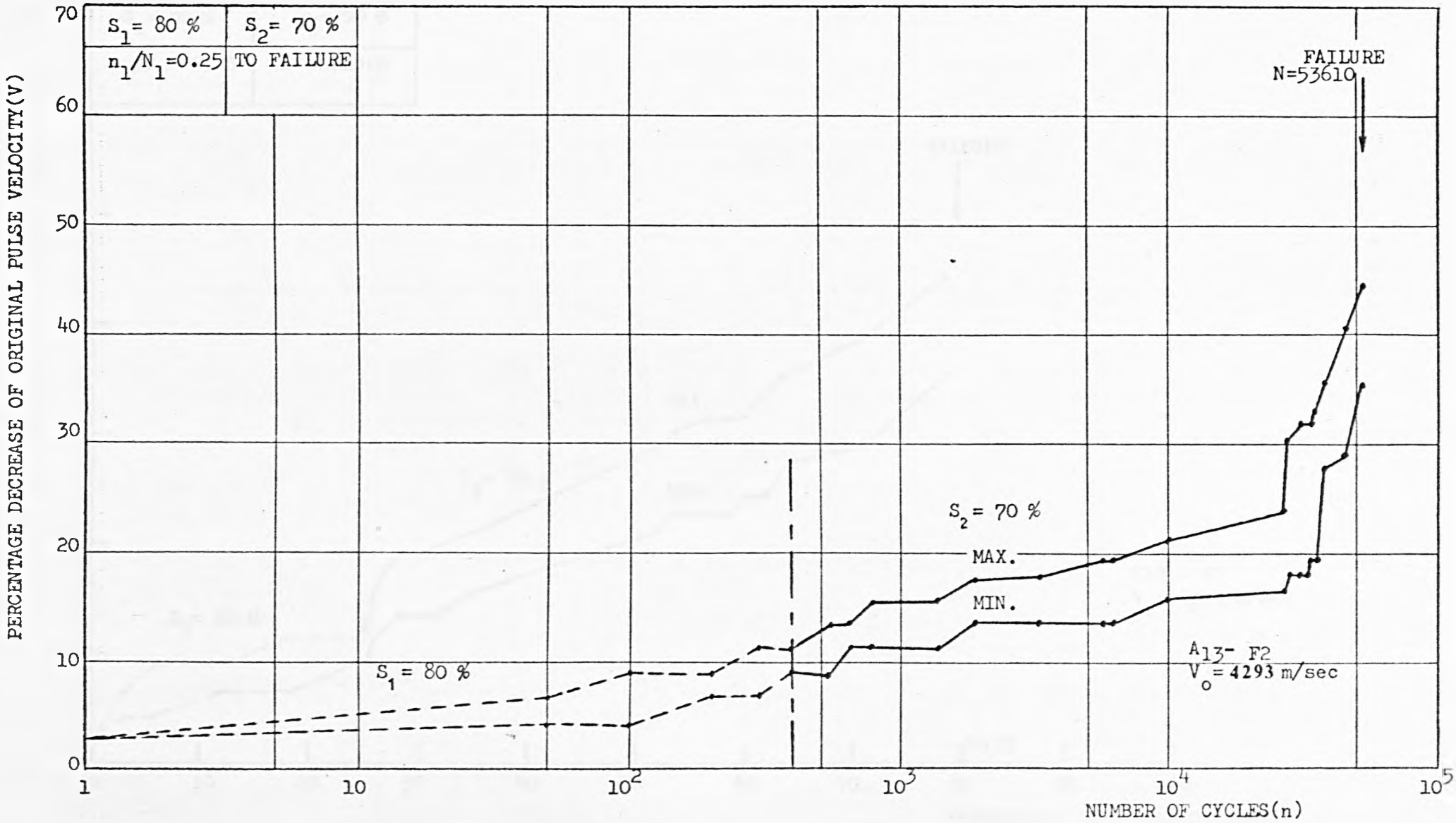

FIG. 9.5 VARIATION OF V WITH n OF A SPECIMEN UNDER LOADING PROGRAMME 1

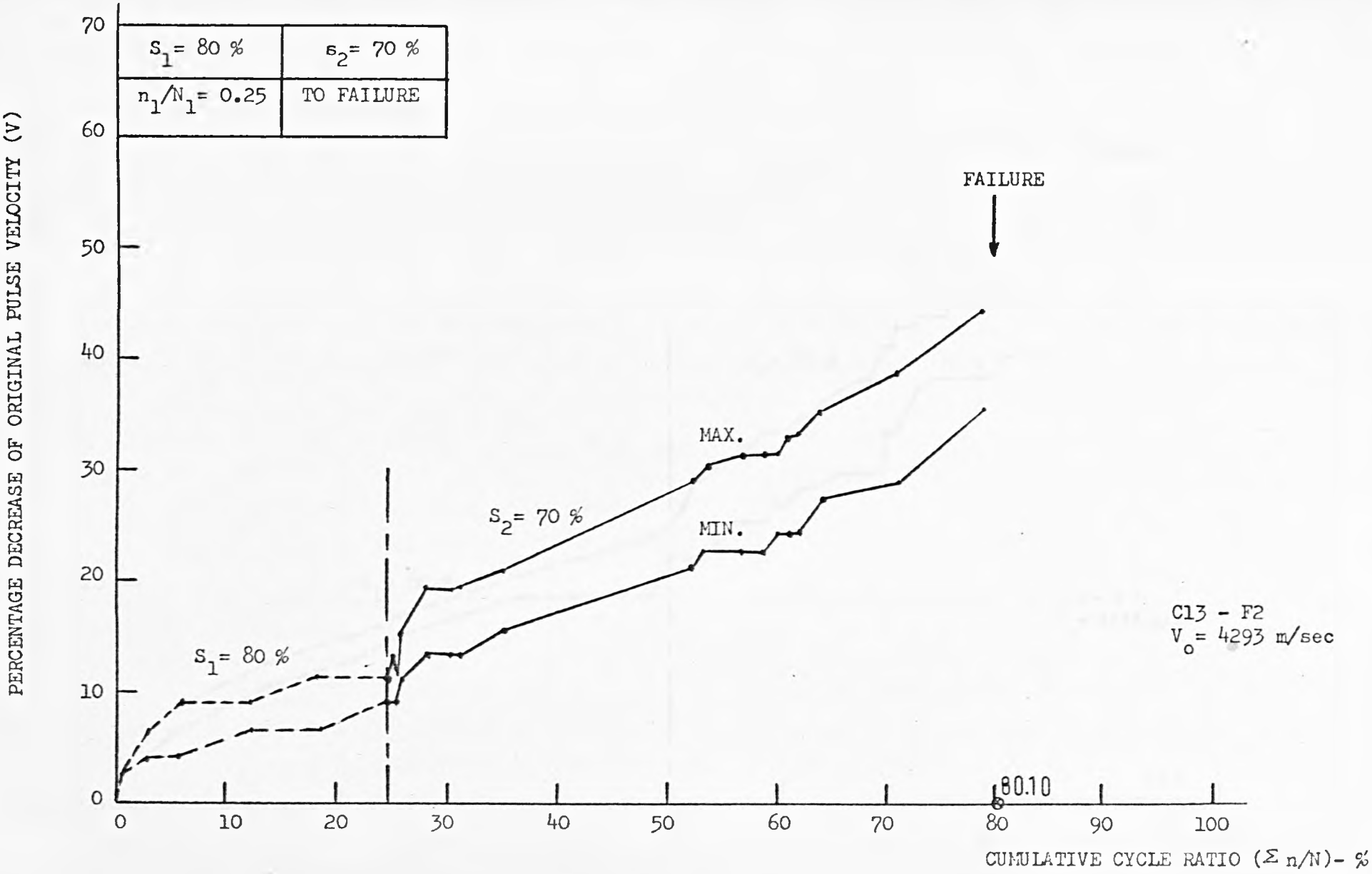

FIG. 9.6 VARIATION OF V WITH Σ n/N OF A SPECIMEN UNDER LOADING PROGRAMME 1

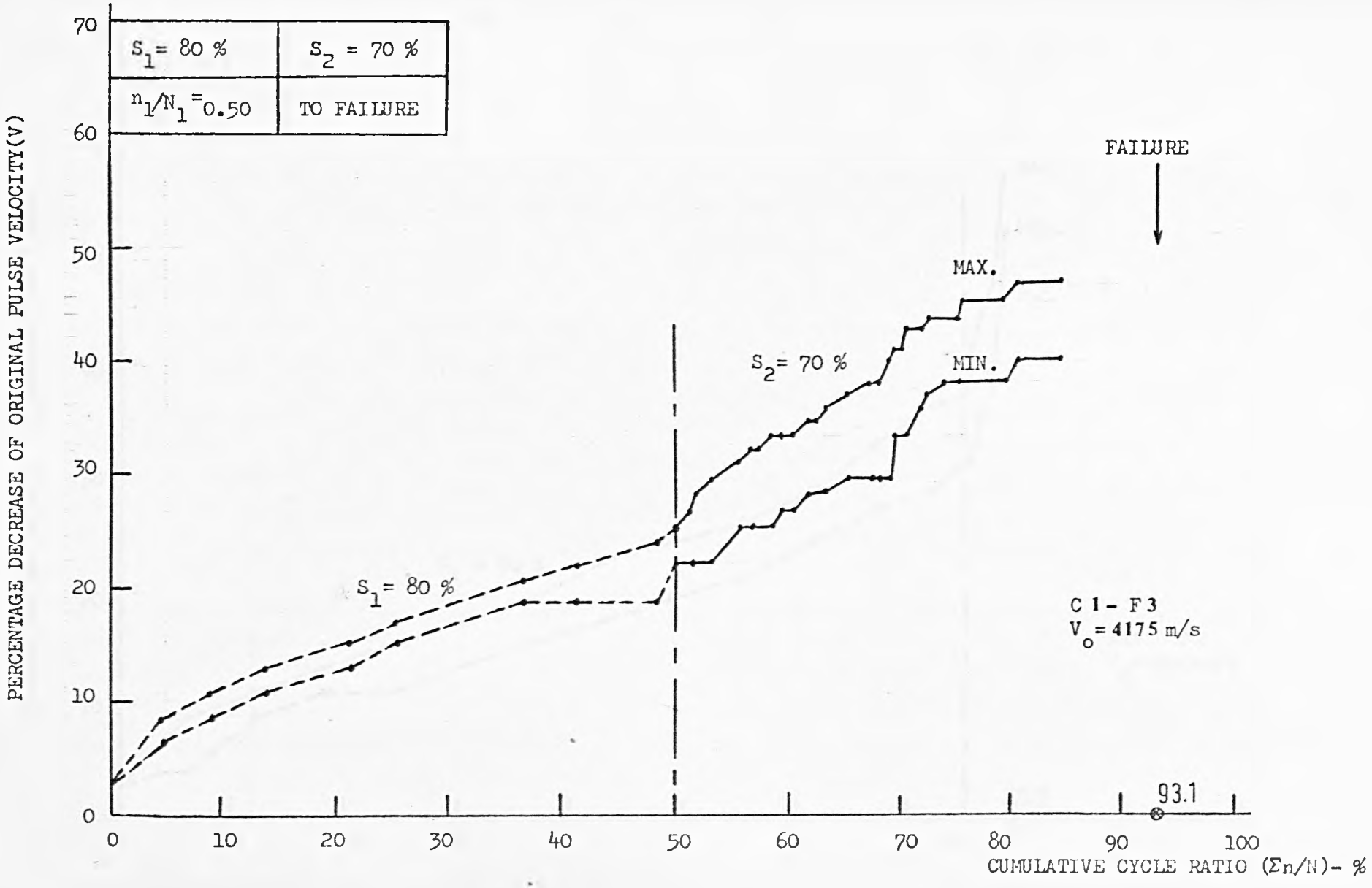

FIG. 9.7 VARIATION OF V WITH $\Sigma n/N$ OF A SPECIMEN UNDER LOADING PROGRAMME 1

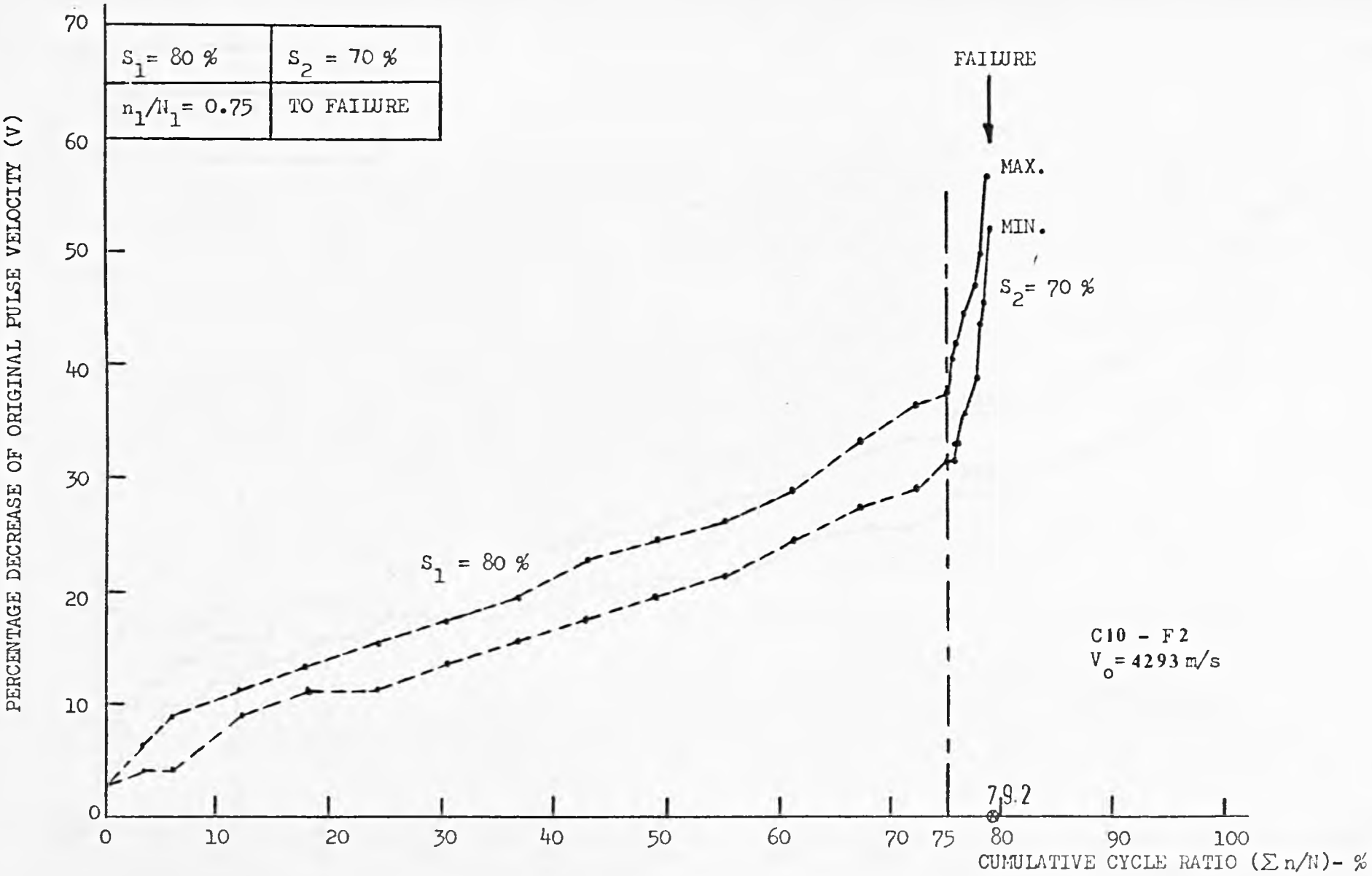

FIG. 9.8 VARIATION OF V WITH Σ n/N OF A SPECIMEN UNDER LOADING PROGRAMME 1

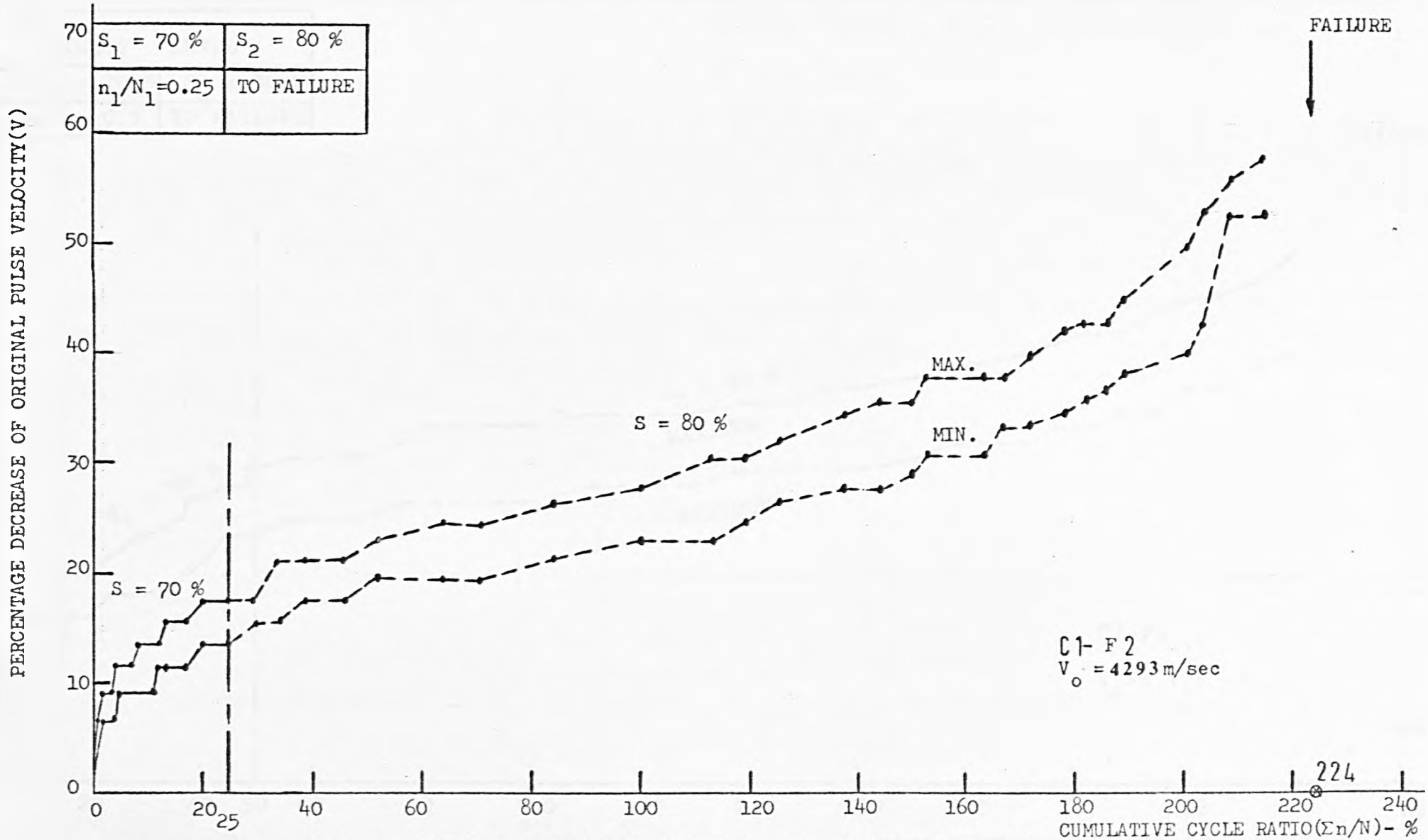

FIG. 9.9 VARIATION OF V WITH $\Sigma n/N$ OF A SPECIMEN UNDER LOADING PROGRAMME 2

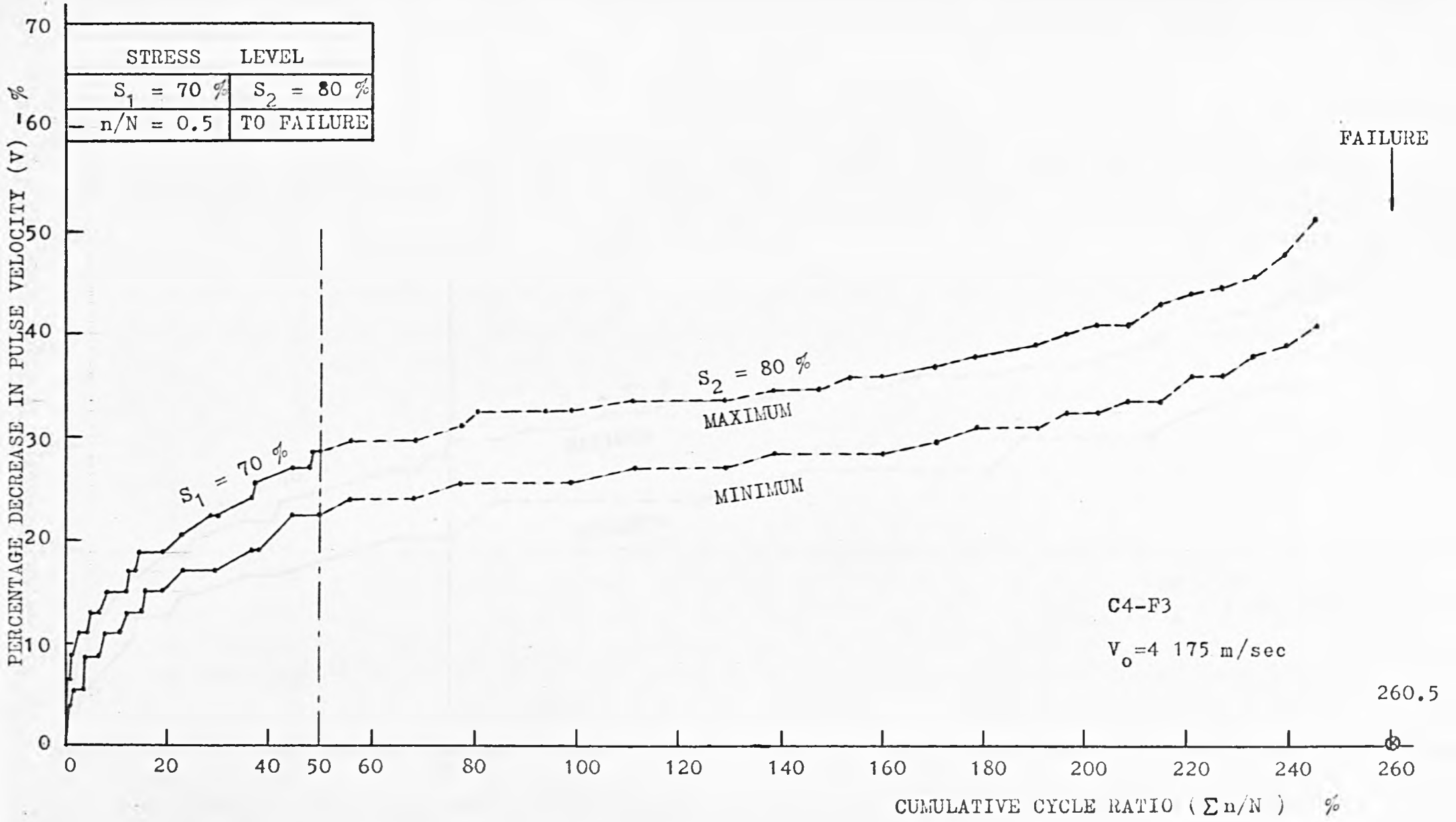

FIG. 9.10 VARIATION OF V WITH Σn/N OF A SPECIMEN UNDER PROGRAMME 2

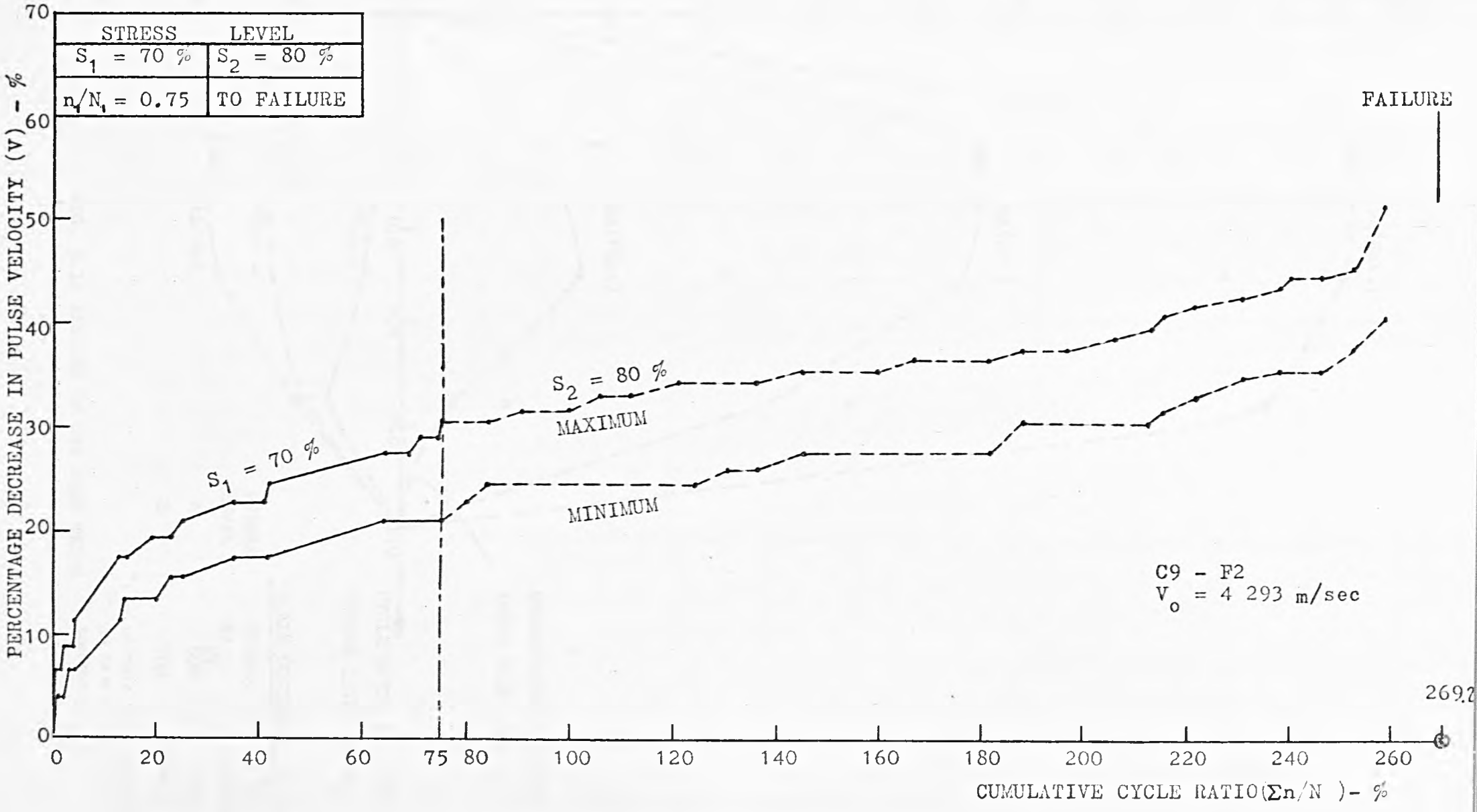

FIG. 9.11 VARIATION OF V WITH $\Sigma n/N$ OF A SPECIMEN UNDER PROGRAMME 2

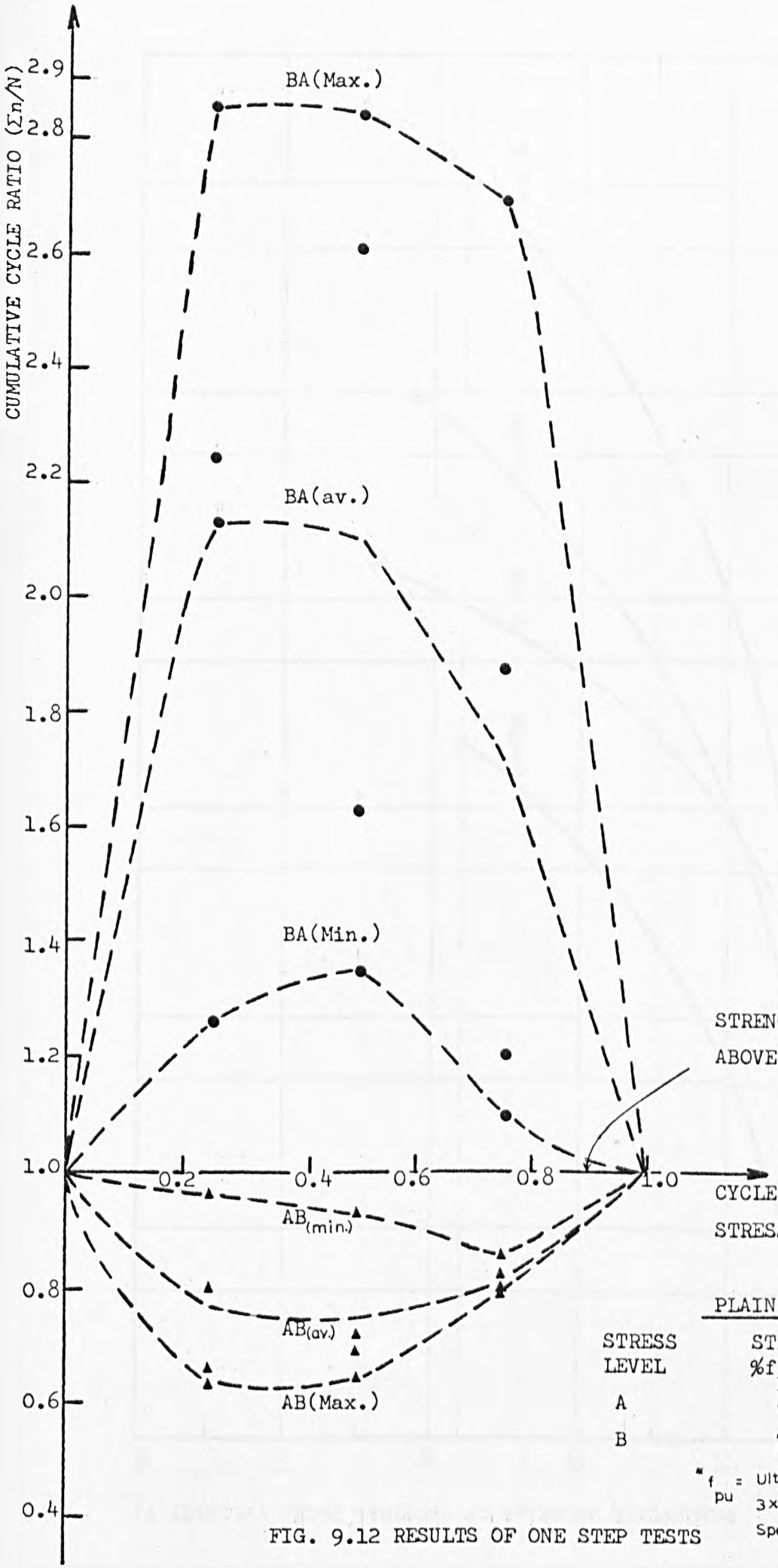

PLAIN CONCRETE, f^{*}_{pu} = 35.02 N/mm²

STRESS LEVEL	STRESS %f_{pu}	TOTAL LIFE (CYCLES)
A	80%	1632
B	70%	97486

* f_{pu} = Ultimate Static Strength of 3 x 3 x 8 in (76.2 x 76.2 x 203.2 mm) Specimens

FIG. 9.12 RESULTS OF ONE STEP TESTS

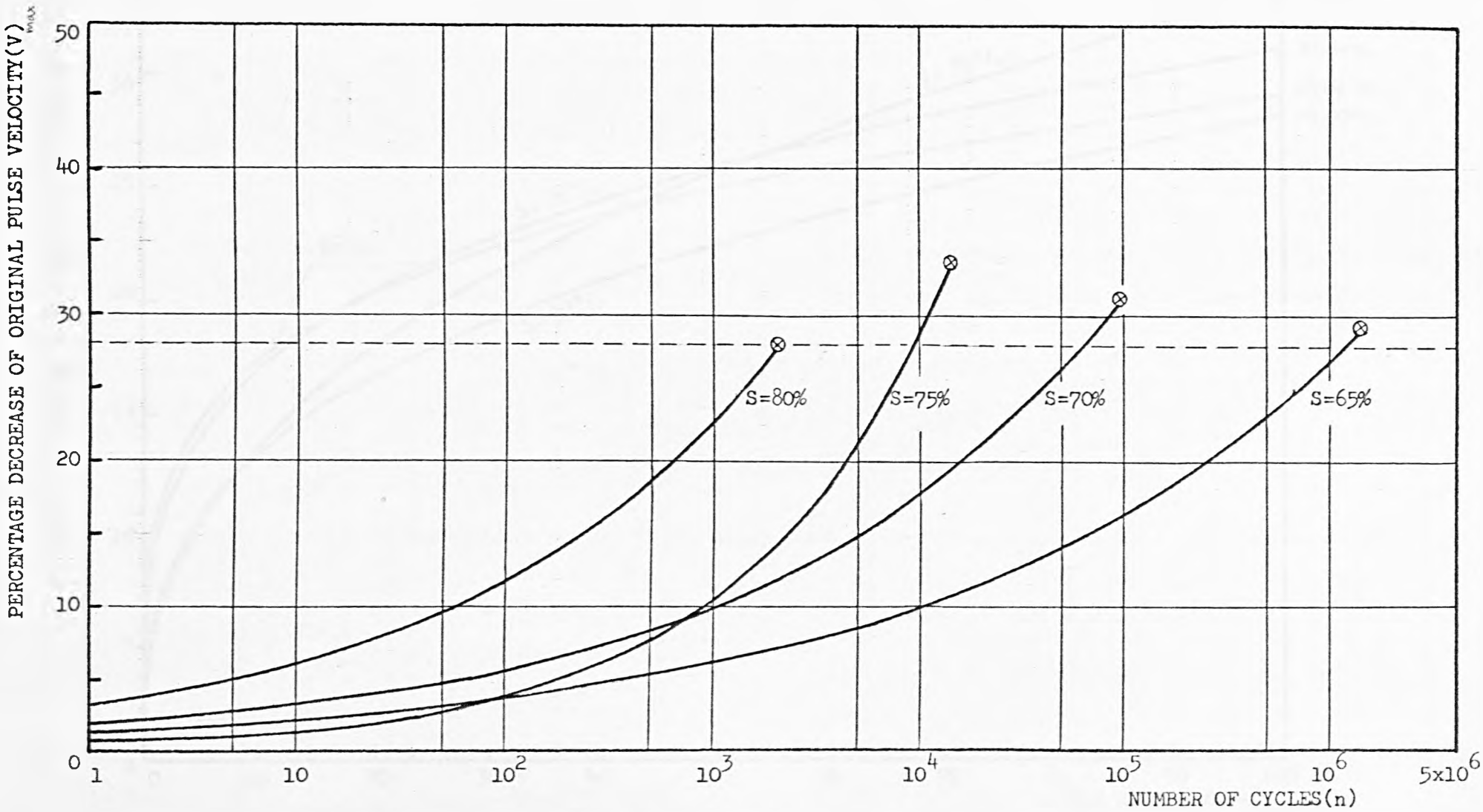

FIG. 9.13 VARIATION OF V_{max} WITH n DERIVED FROM TRIAL 1.2(b)

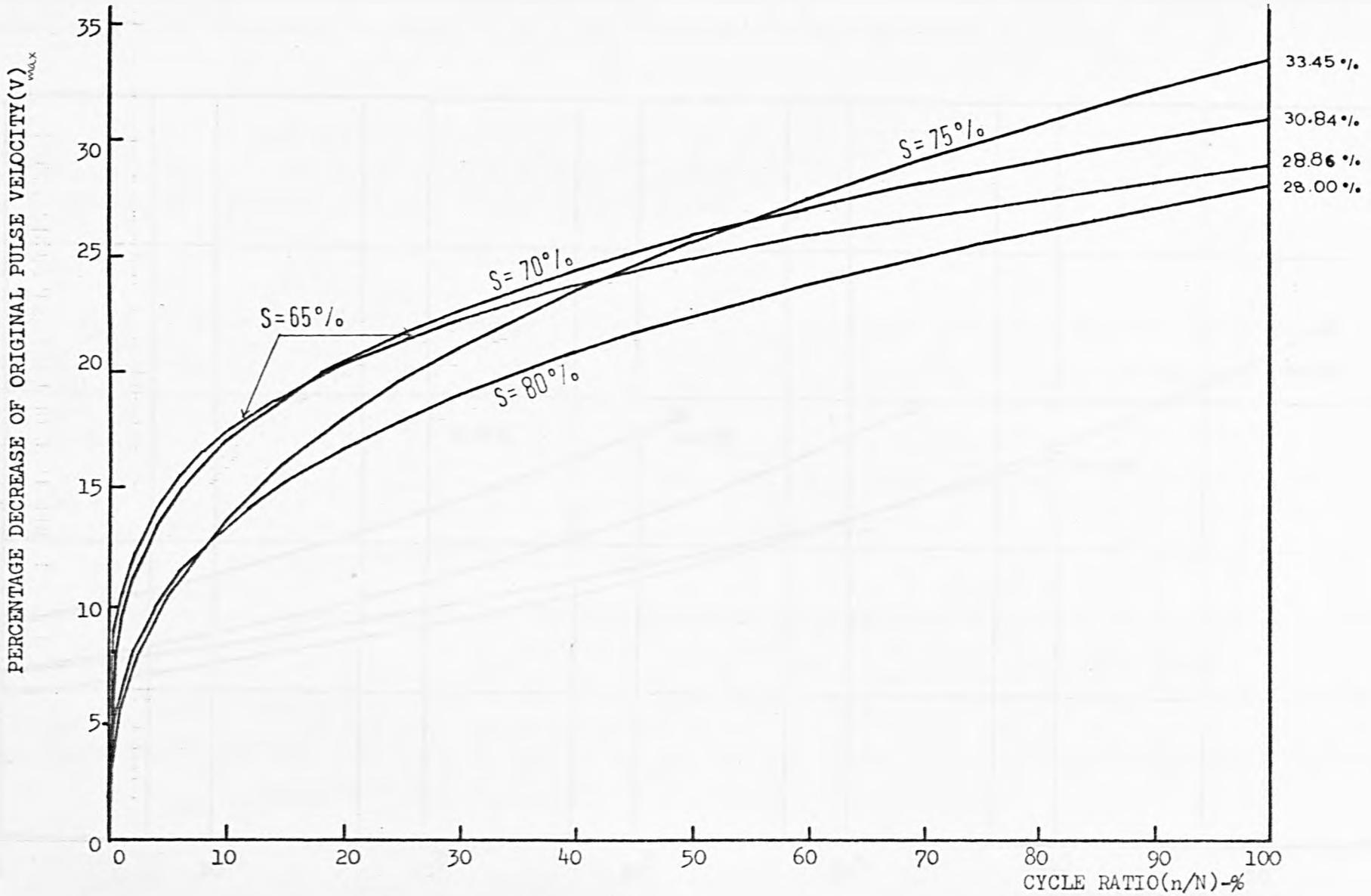

FIG. 9.14 VARIATION OF V_{max} WITH n/N DERIVED FROM TRIAL 1.2(b)

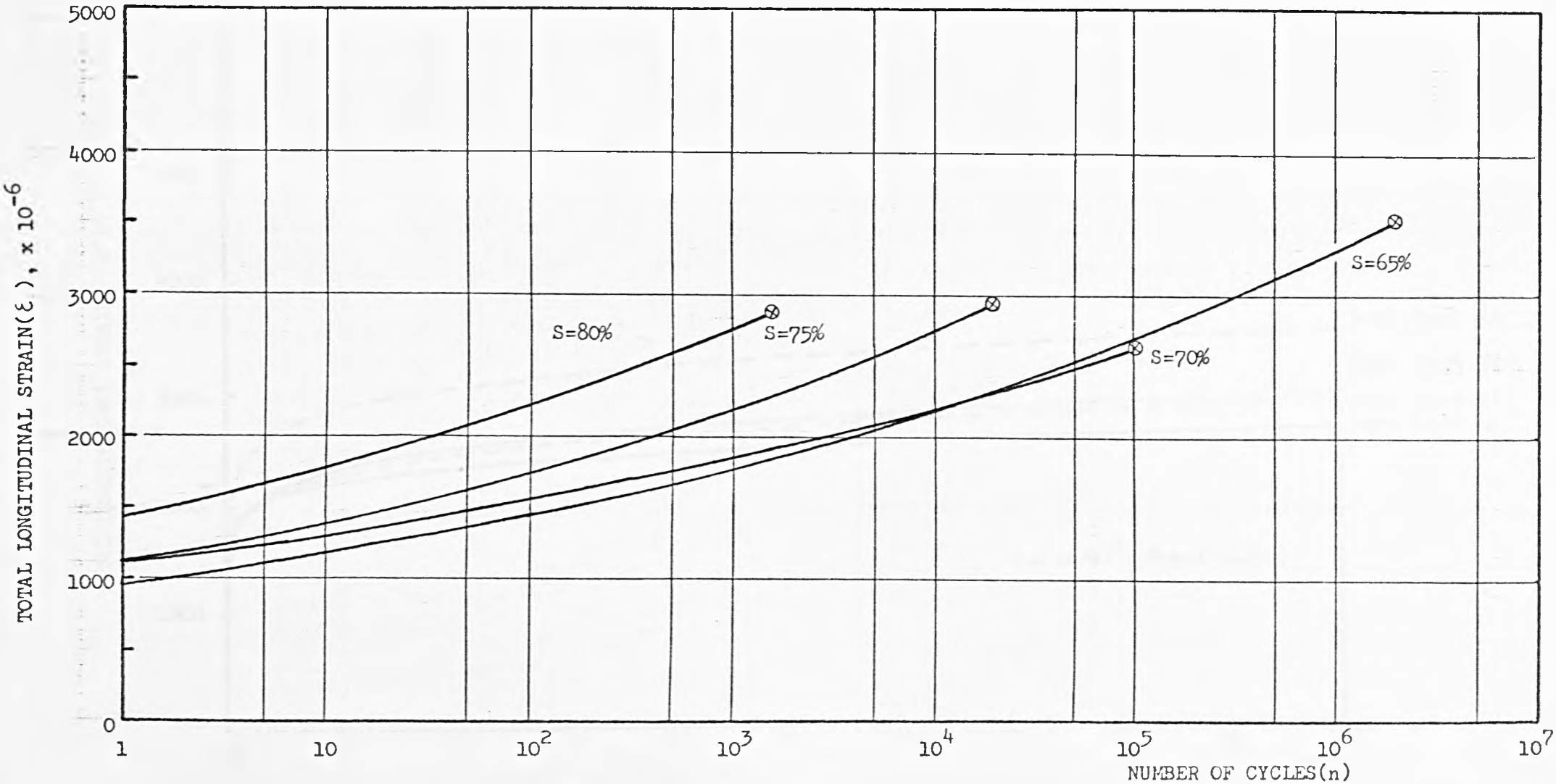

FIG. 9.15 VARIATION OF ε WITH n DERIVED FROM TRIAL 1.2(a)

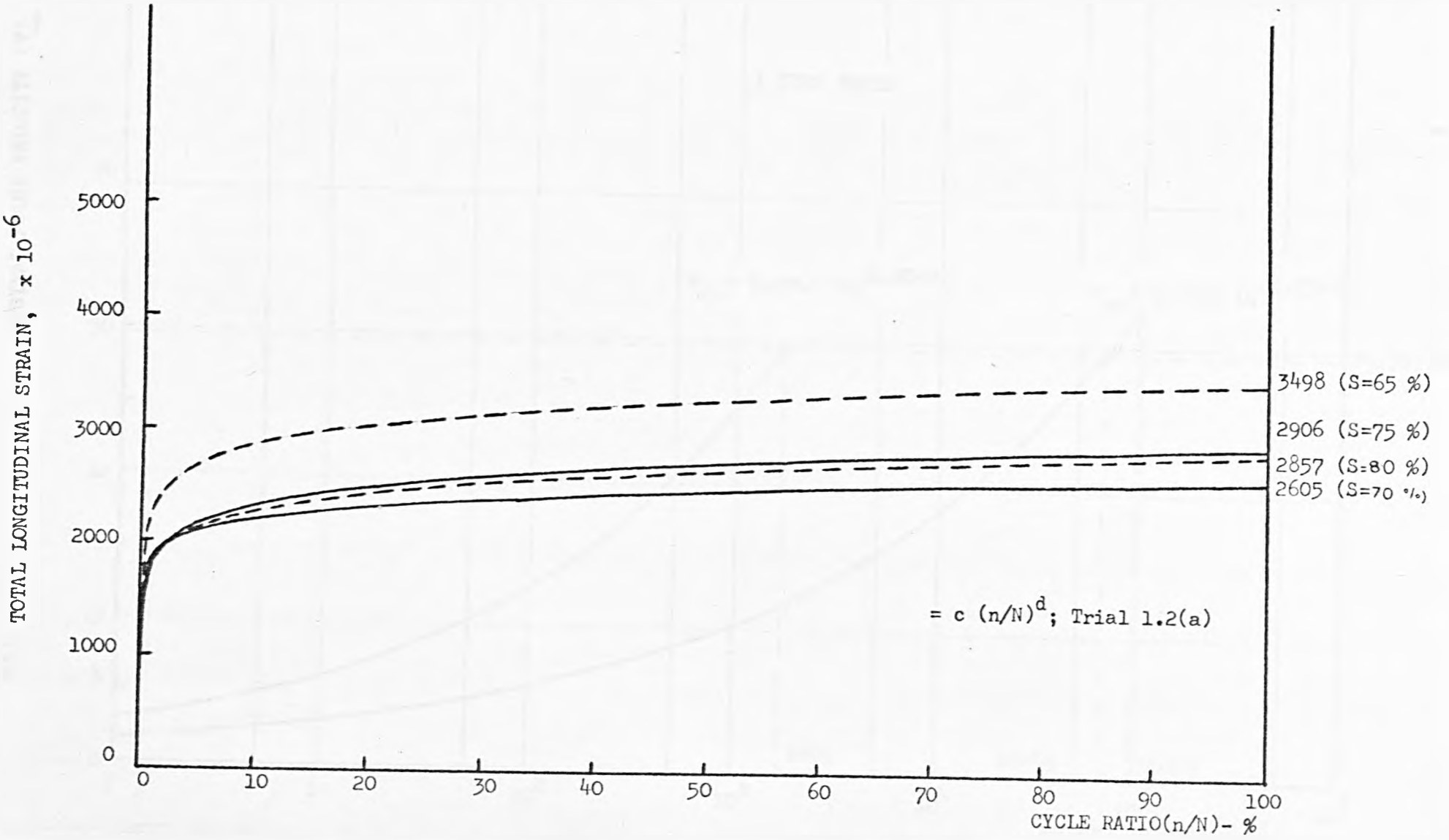

FIG. 9.16 VARIATION OF TOTAL STRAIN WITH n/N DERIVED FROM TRAIL 1.2(a)

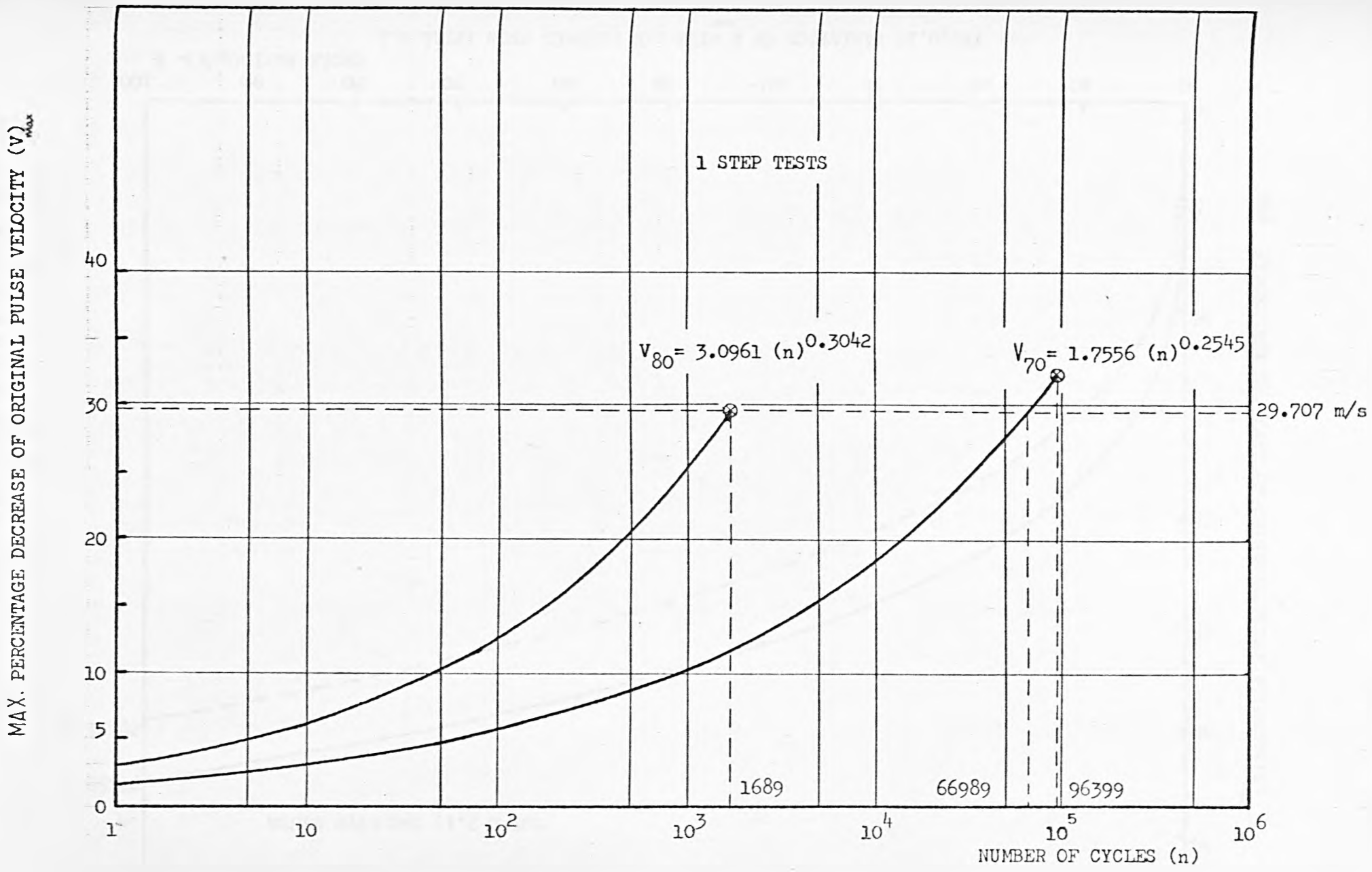

FIG. 9.17 VARIATION OF V_{max} WITH n DERIVED FROM TRIAL 2.1

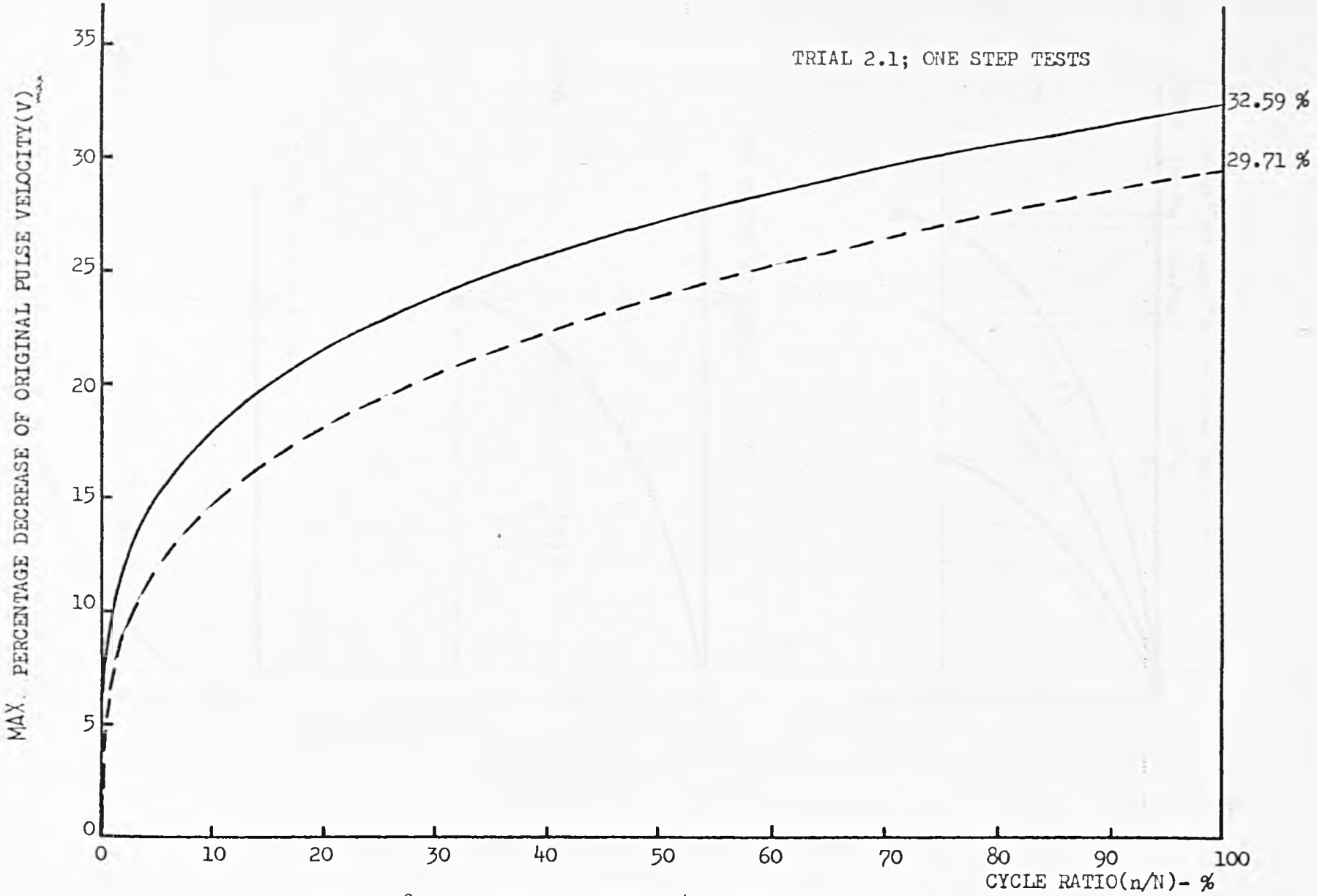

FIG.9.18 VARIATION OF V_{max} WITH n/N DERIVED FROM TRIAL 2.1

V = PERCENTAGE DECREASE OF ORIGINAL PULSE VELOCITY (MAX).

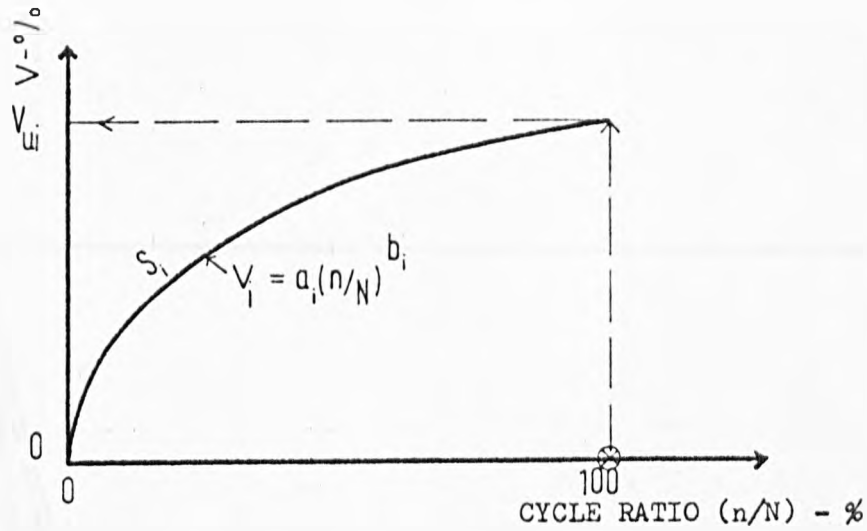

9.19.a

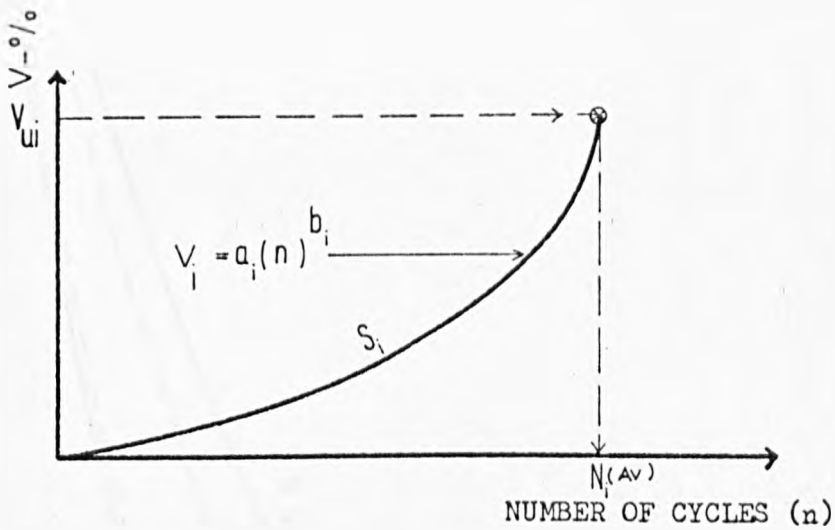

9.19.b

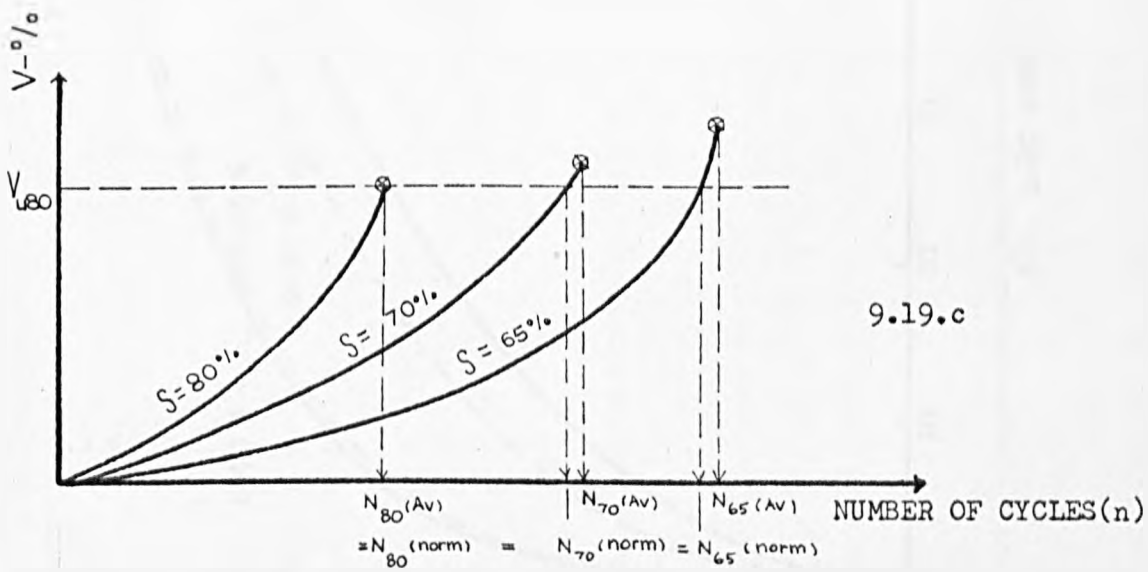

9.19.c

FIG. 9.19 STEPS IN ANALYSIS OF STRESS DEPENDENCE

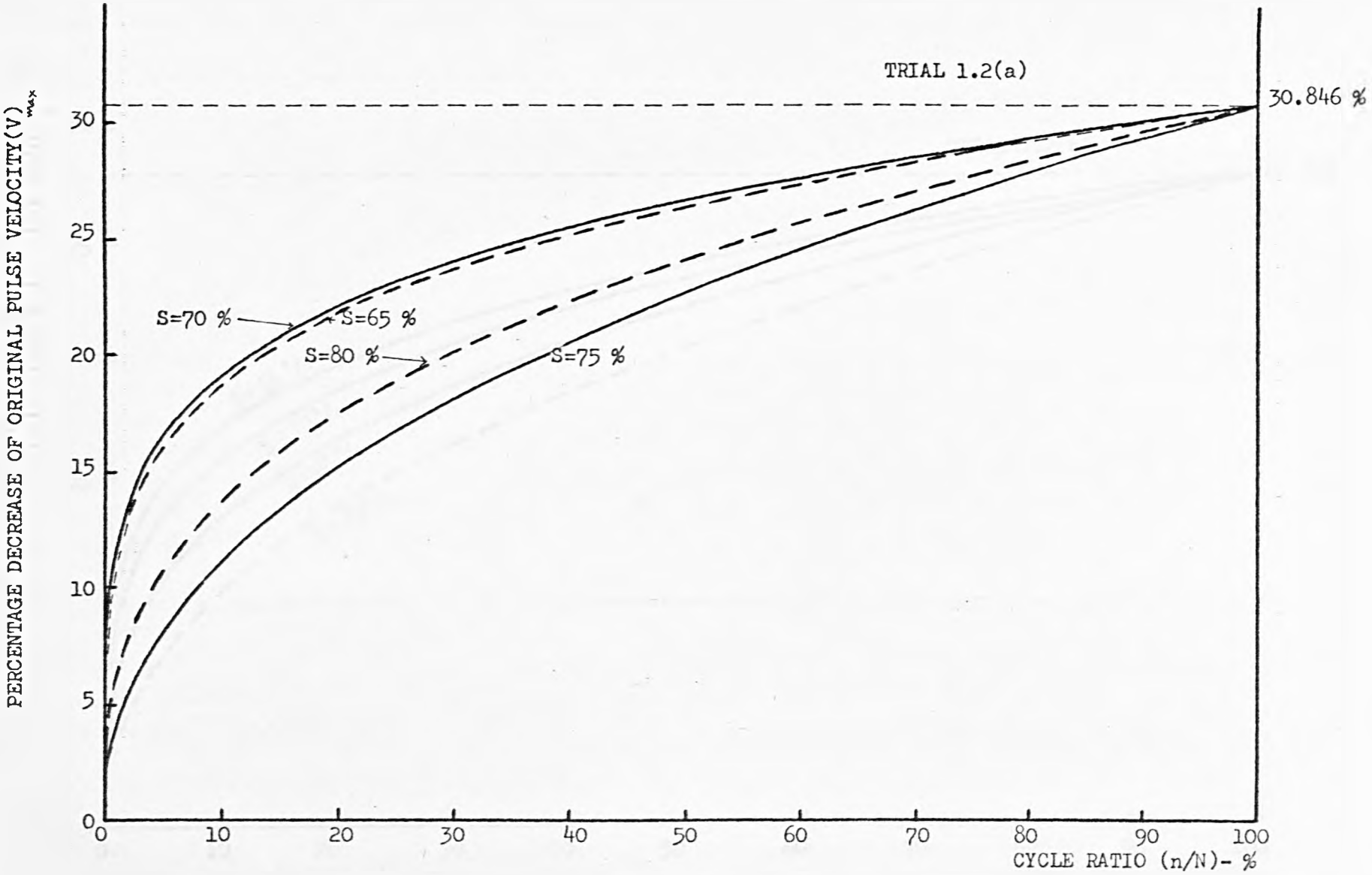

FIG. 9.20 NORMALISED DAMAGE(V_{max})-CYCLE RATIO RELATIONSHIP

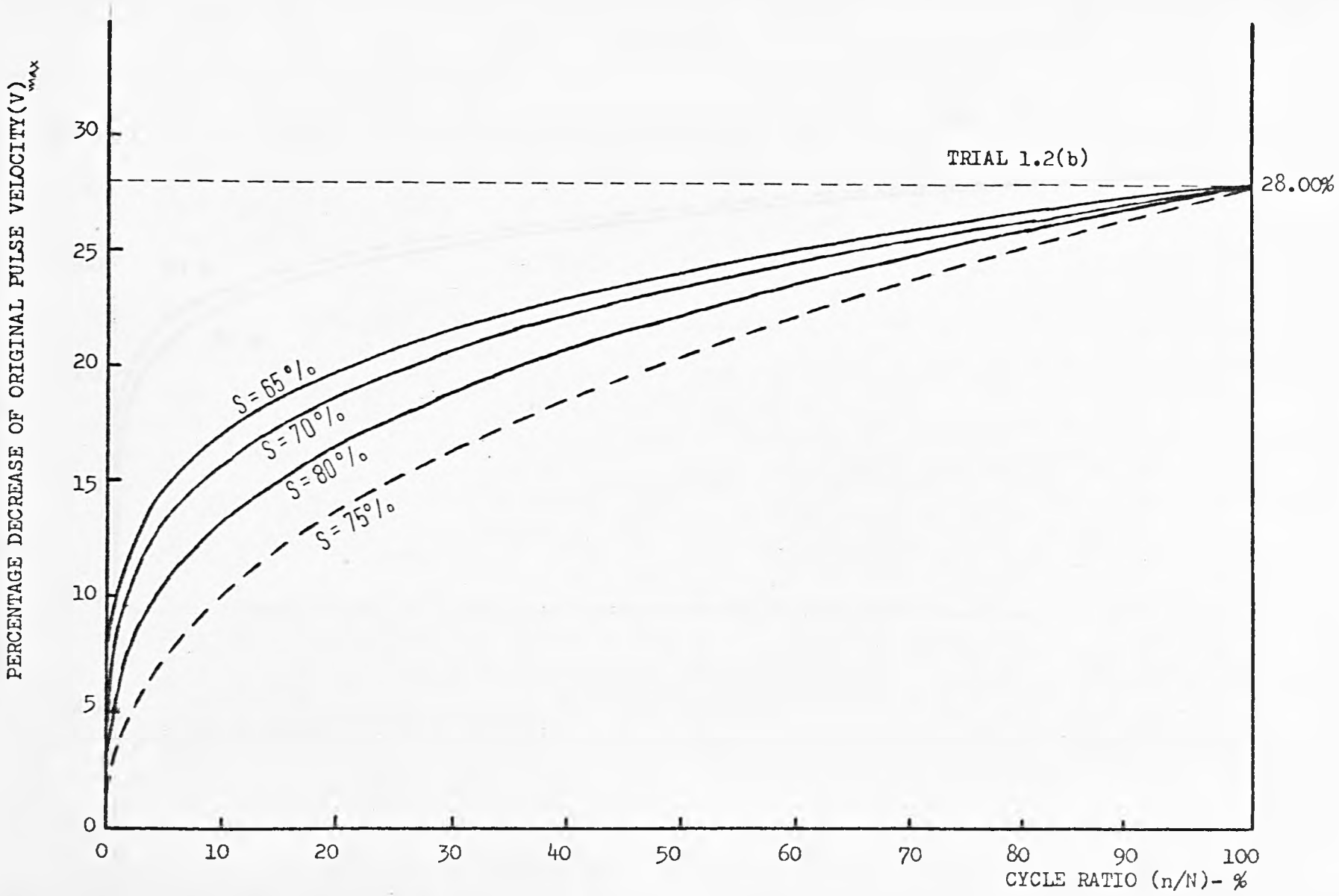

FIG. 9.21 NORMALISED DAMAGE$(V)_{max}$ - CYCLE RATIO RELATIONSHIP

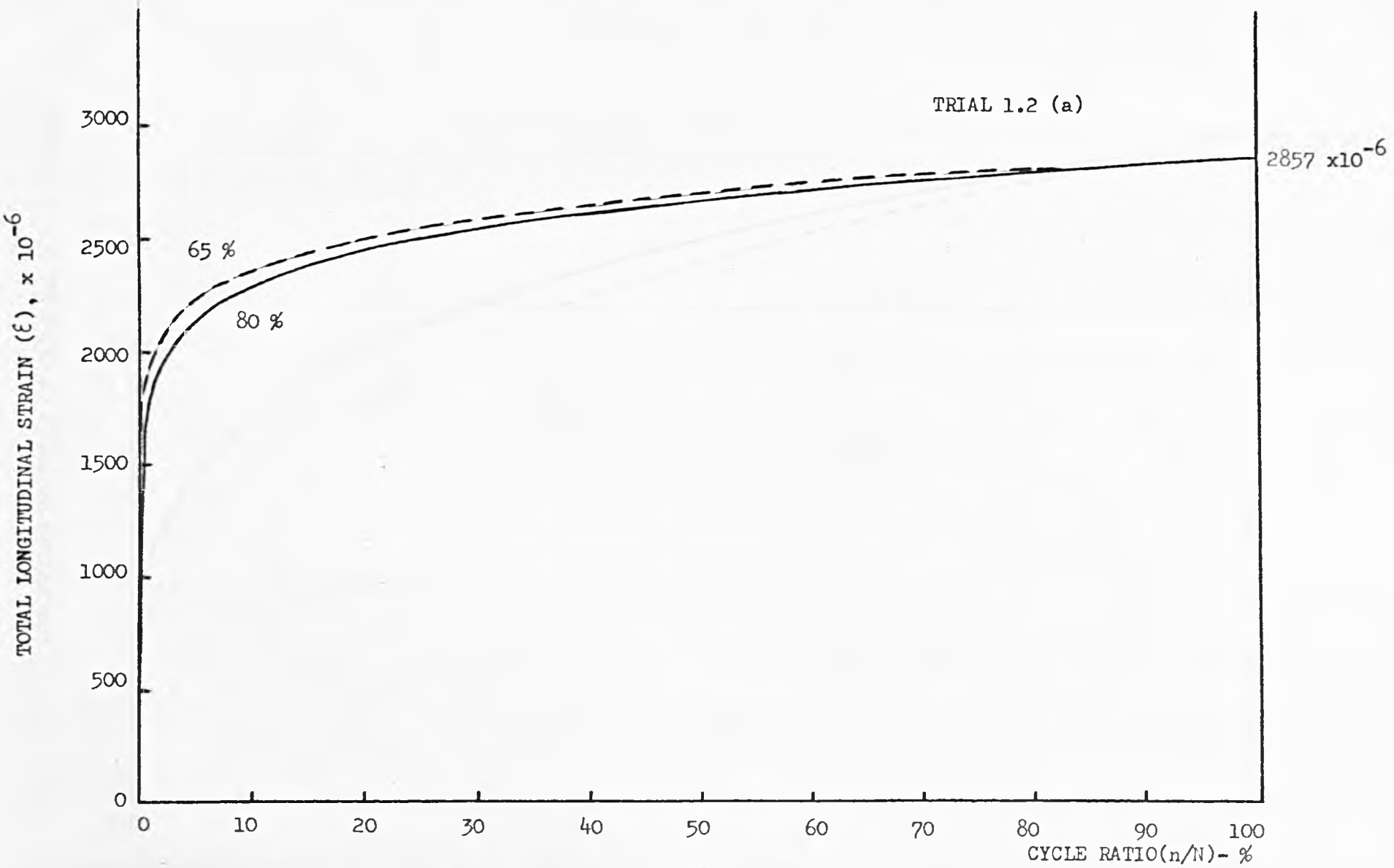

FIG. 9.22 NORMALISED DAMAGE(ε)- CYCLE RATIO RELATIONSHIP

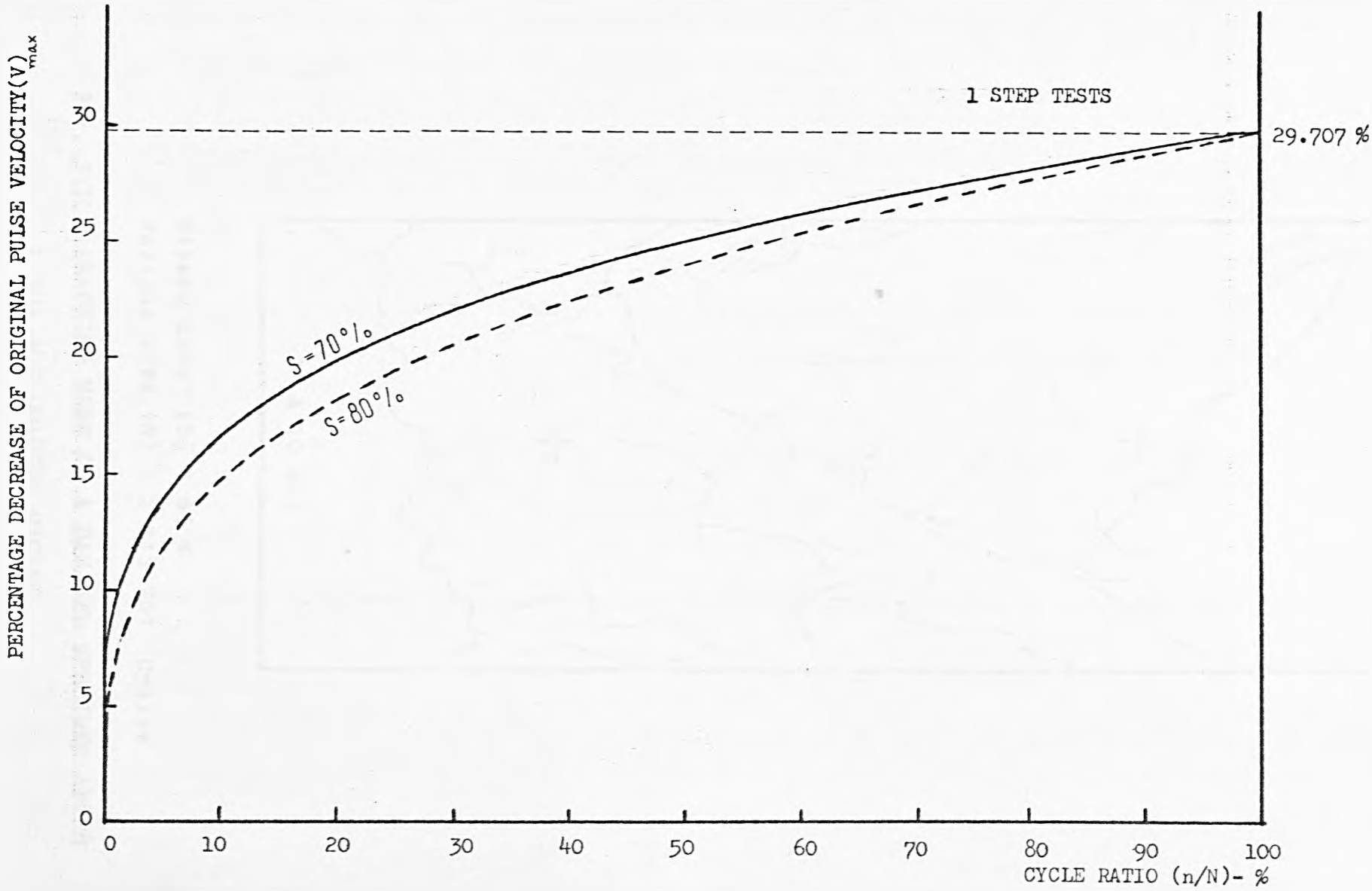

FIG. 9.23 NORMALISED DAMAGE(V_{max}) — CYCLE RATIO RELATIONSHIP

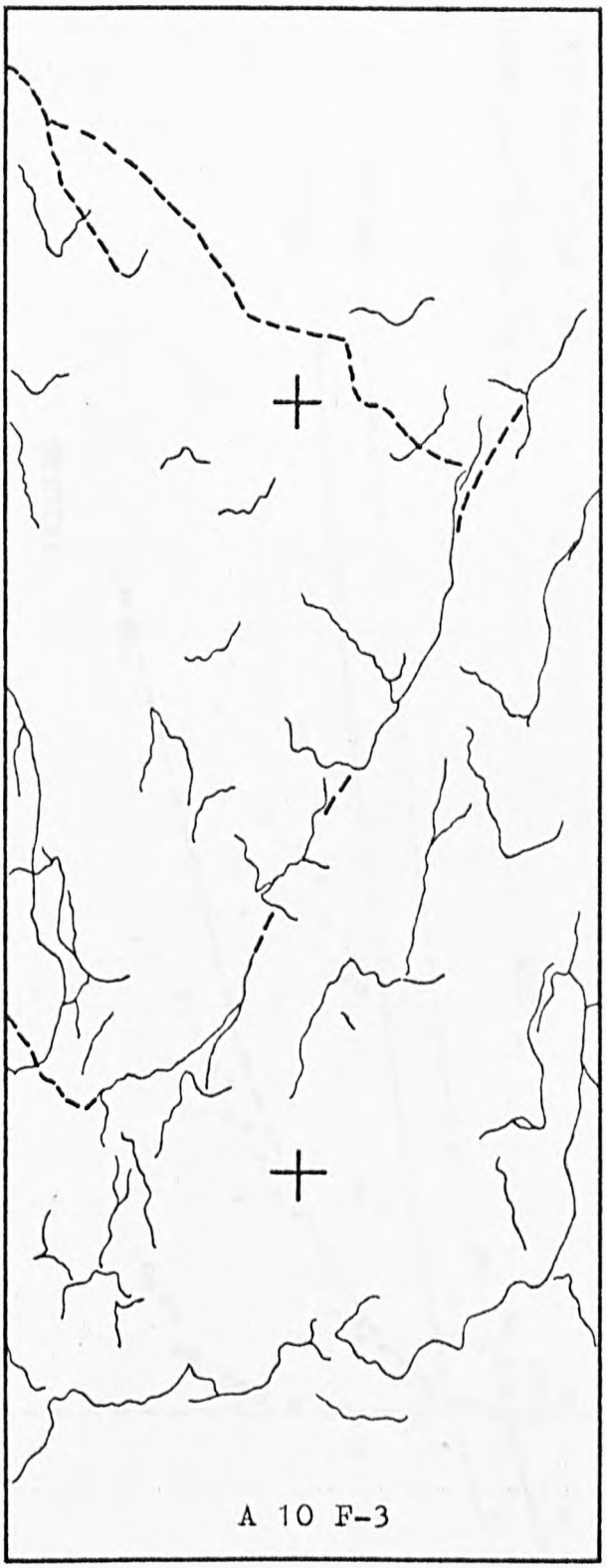

Stress Level (S) : 65 %
Fatigue Life (N) : 2 113 707 Cycles

FIG. 9.24 CRACKING MODE OF A DAMAGED SPECIMEN AFTER 1 804 400 LOADING CYCLES.

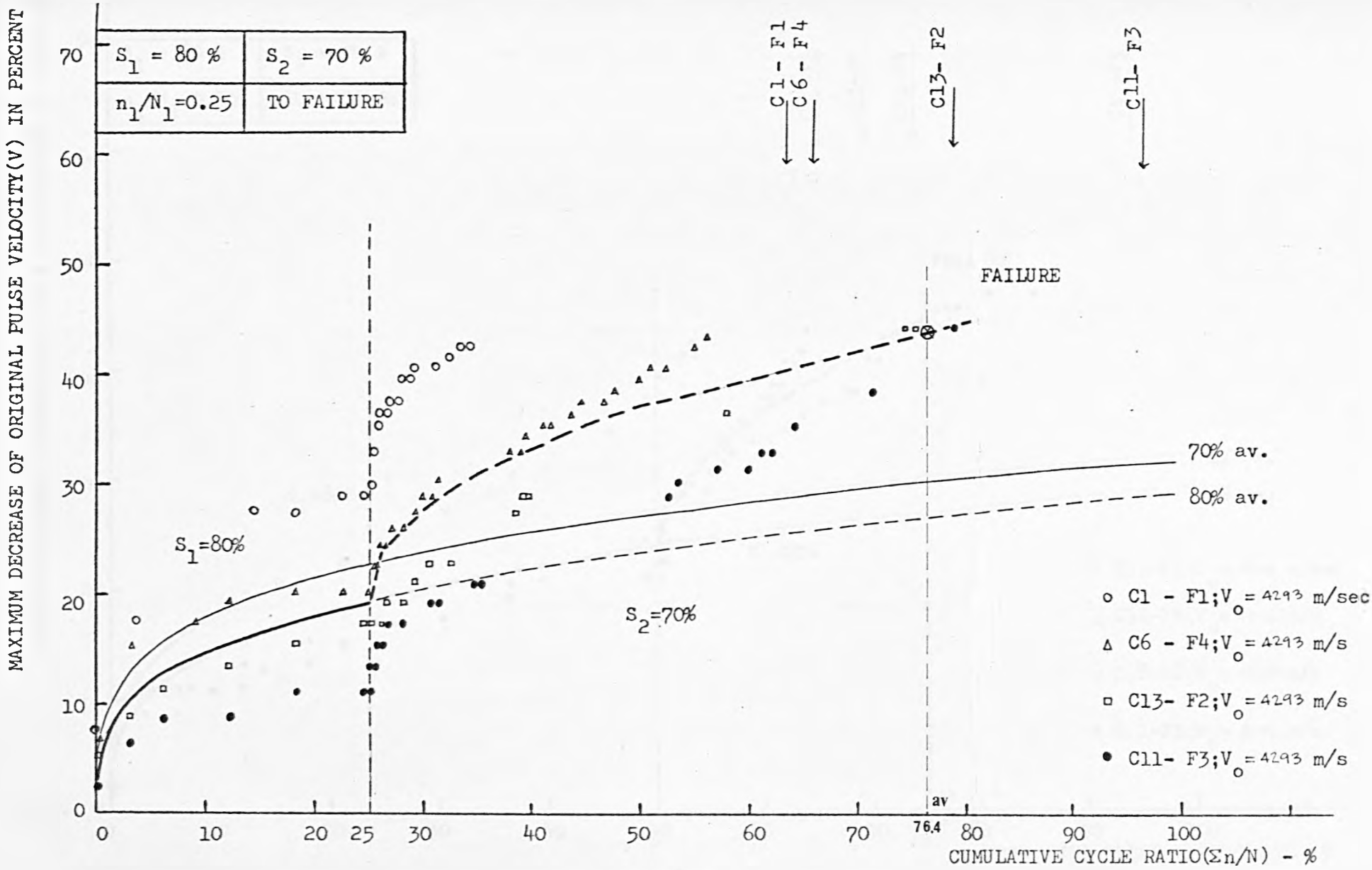

FIG. 9.25 VARIATION OF V_2 DUE TO S_2 OF ALL SPECIMENS UNDER LOADING PROGRAMME 1 ($S_1 > S_2$) AFTER n_1/N_1=0.25

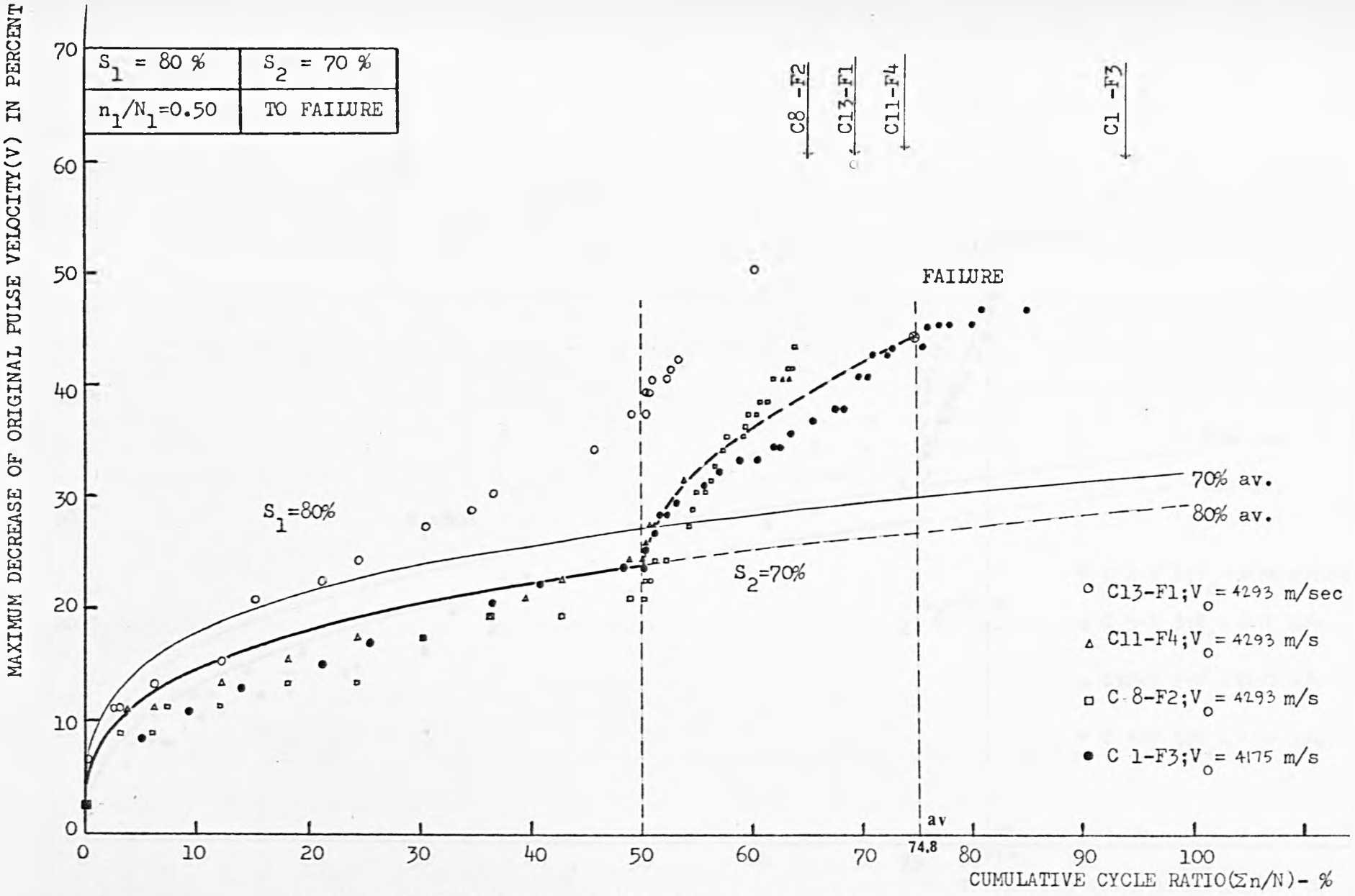

FIG. 9. 26 VARIATION OF V_2 DUE TO S_2 OF ALL SPECIMENS UNDER LOADING PROGRAMME 1
($S_1 > S_2$) AFTER n_1/N_1= 0.50

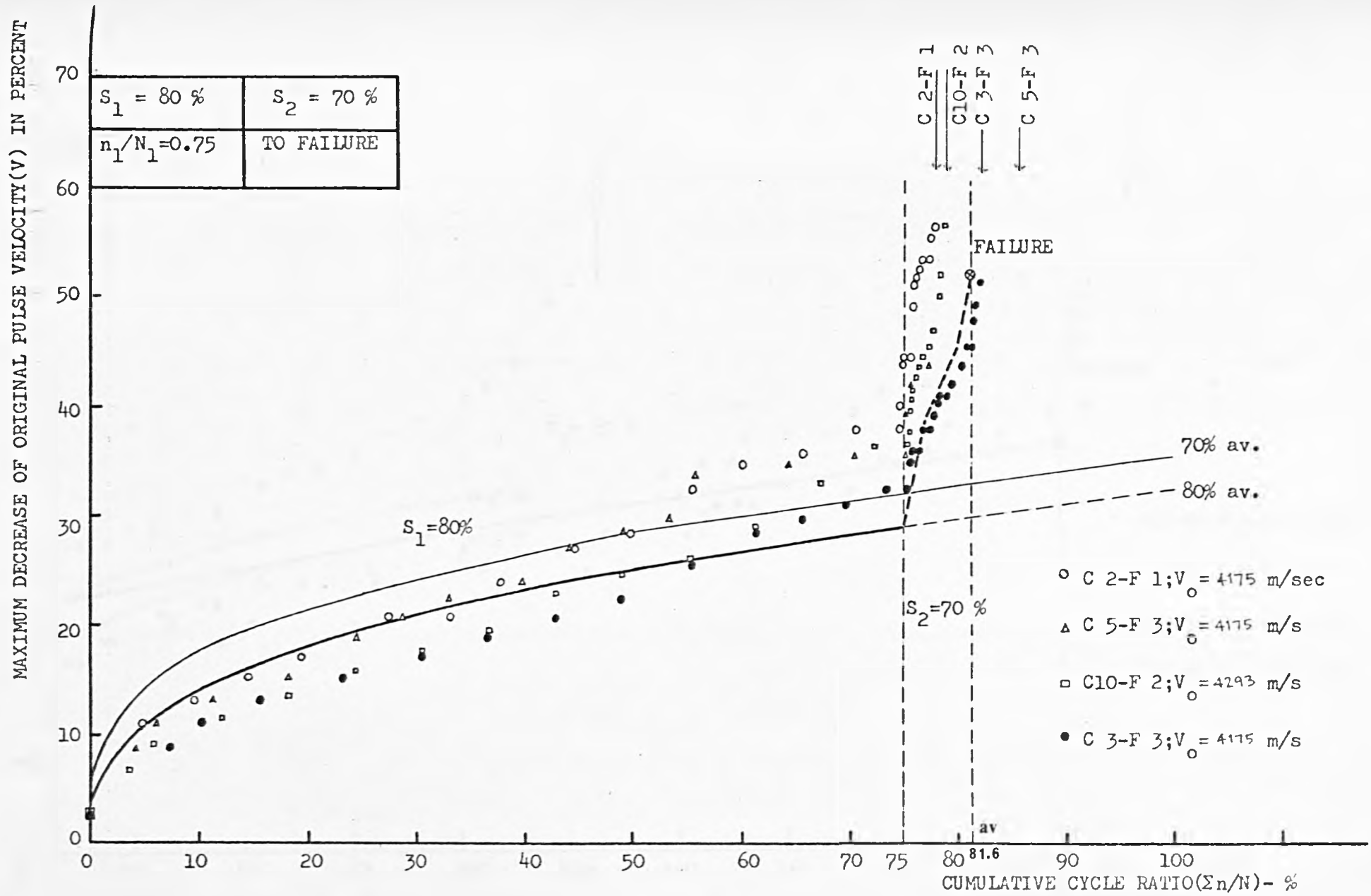

FIG. 9. 27 VARIATION OF V_2 DUE TO S_2 OF ALL SPECIMENS UNDER LOADING PROGRAMME 1 ($S_1 > S_2$) AFTER n_1/N_1= 0.75

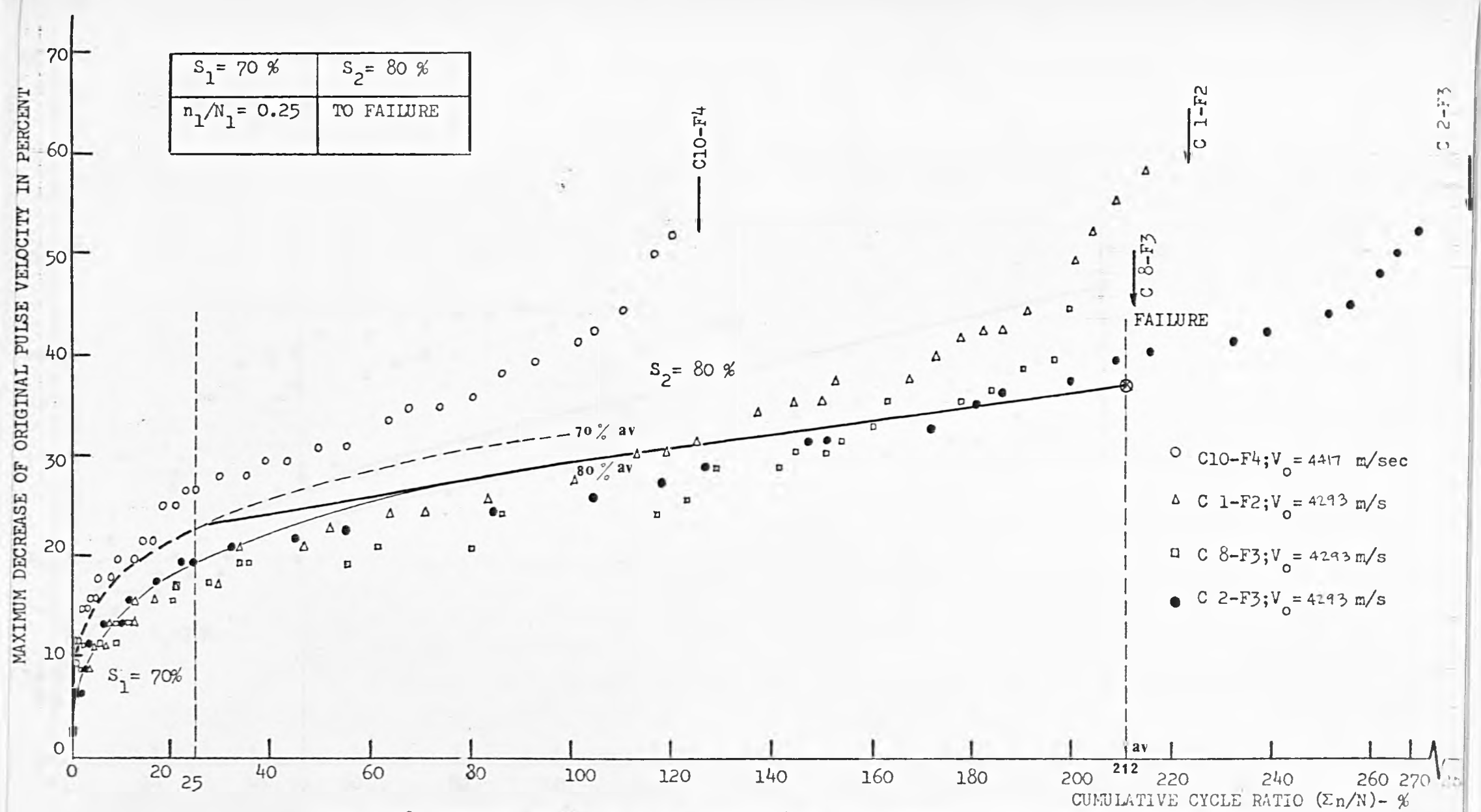

FIG. 9.28 VARIATION OF V_2 DUE TO S_2 WITH Σ n/N OF ALL SPECIMENS UNDER LOADING PROGRAMME 2 ($S_1 < S_2$) AFTER n_1/N_1= 0.25

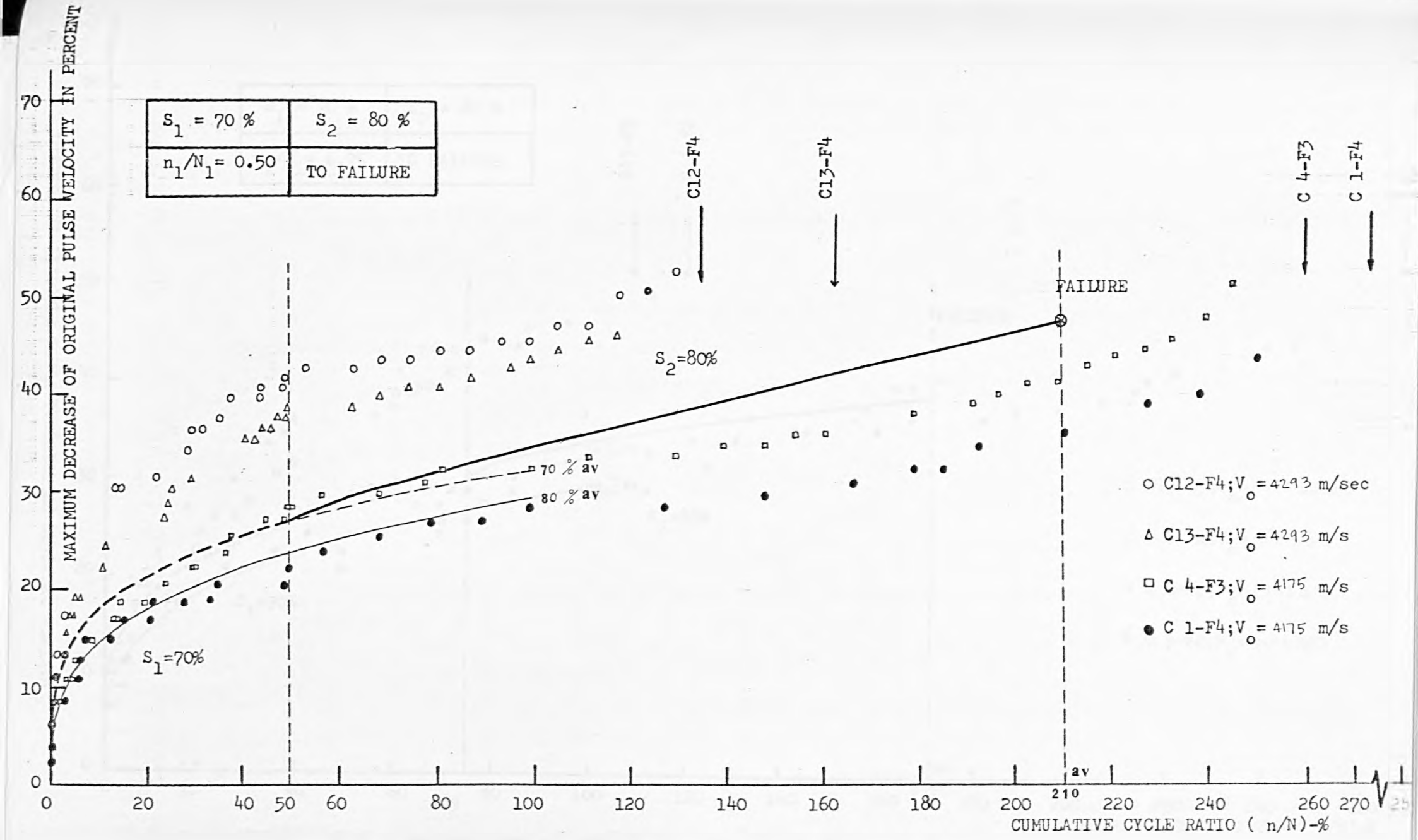

FIG. 9.29 VARIATION OF V_2 DUE TO S_2 WITH n/N OF ALL SPECIMENS UNDER LOADING PROGRAMME 2 (S_1 S_2) AFTER n_1/N_1 = 0.50

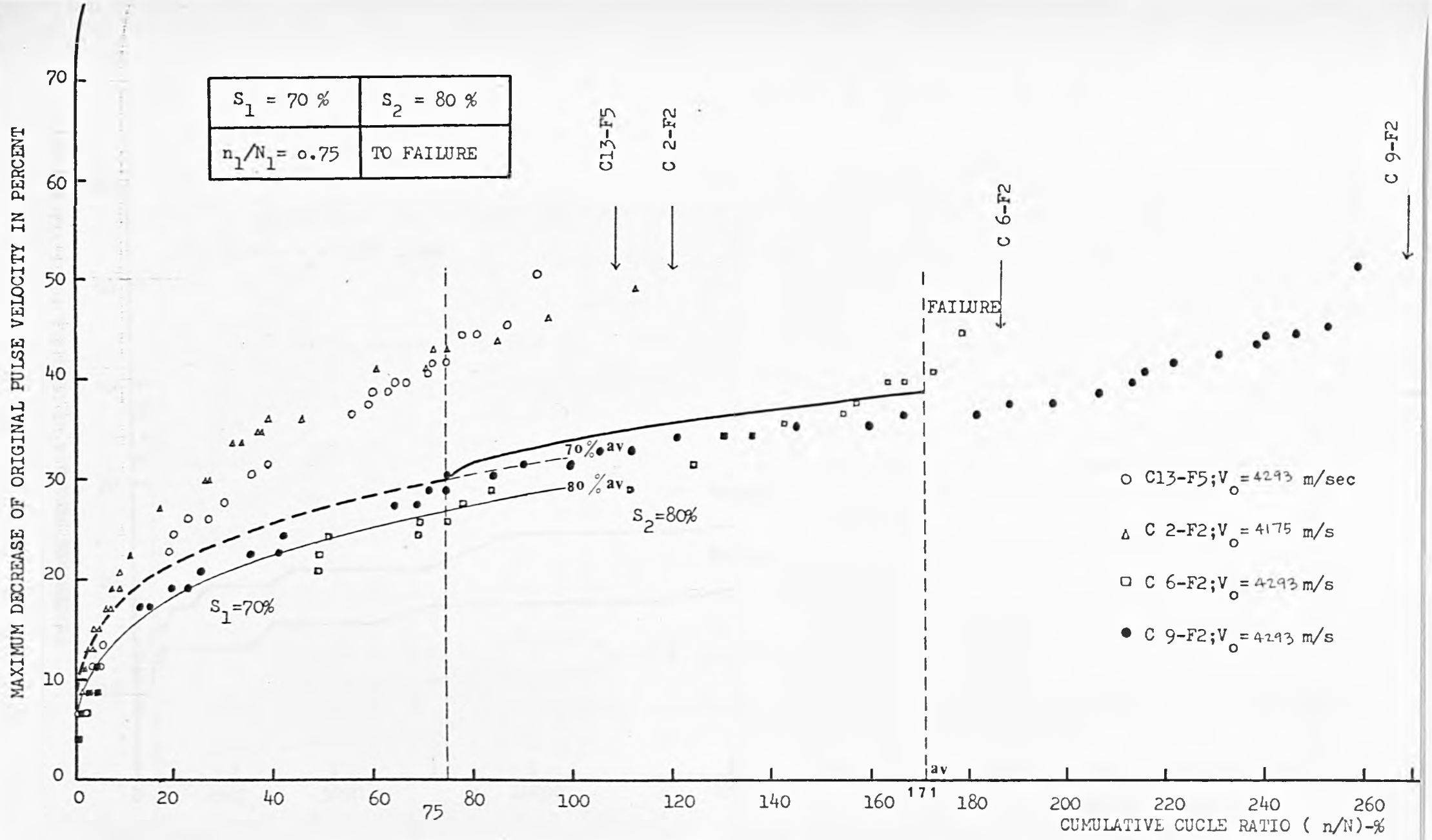

FIG. 9.30 VARIATION OF V_2 DUE TO S_2 WITH n/N OF ALL SPECIMENS UNDER LOADING PROGRAMME 2 (S_1 S_2) AFTER n_1/N_1=0.75

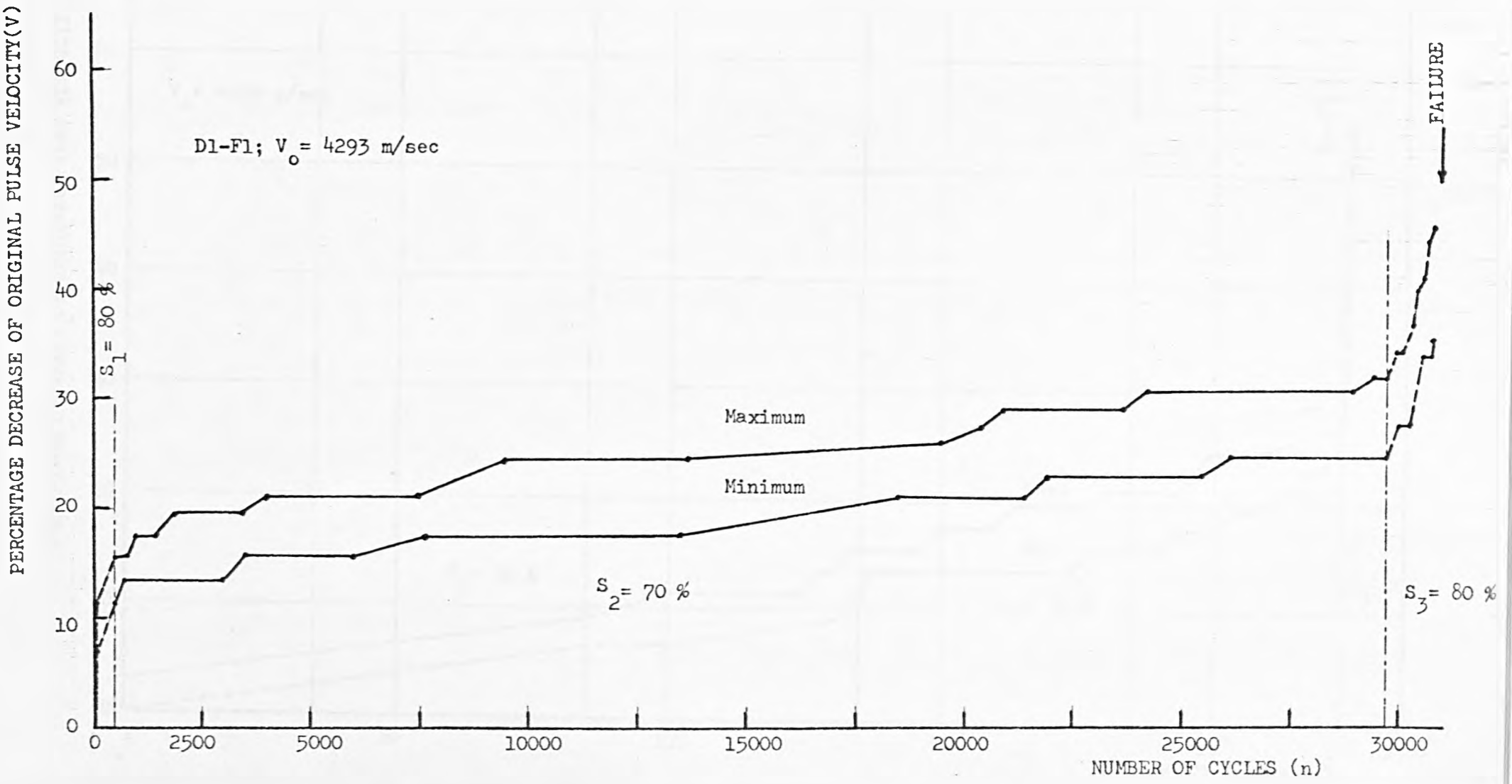

FIG. 10.1 VARIATION OF V WITH n OF A SPECIMEN SUBJECTED TO LOADING PROGRAMME 3

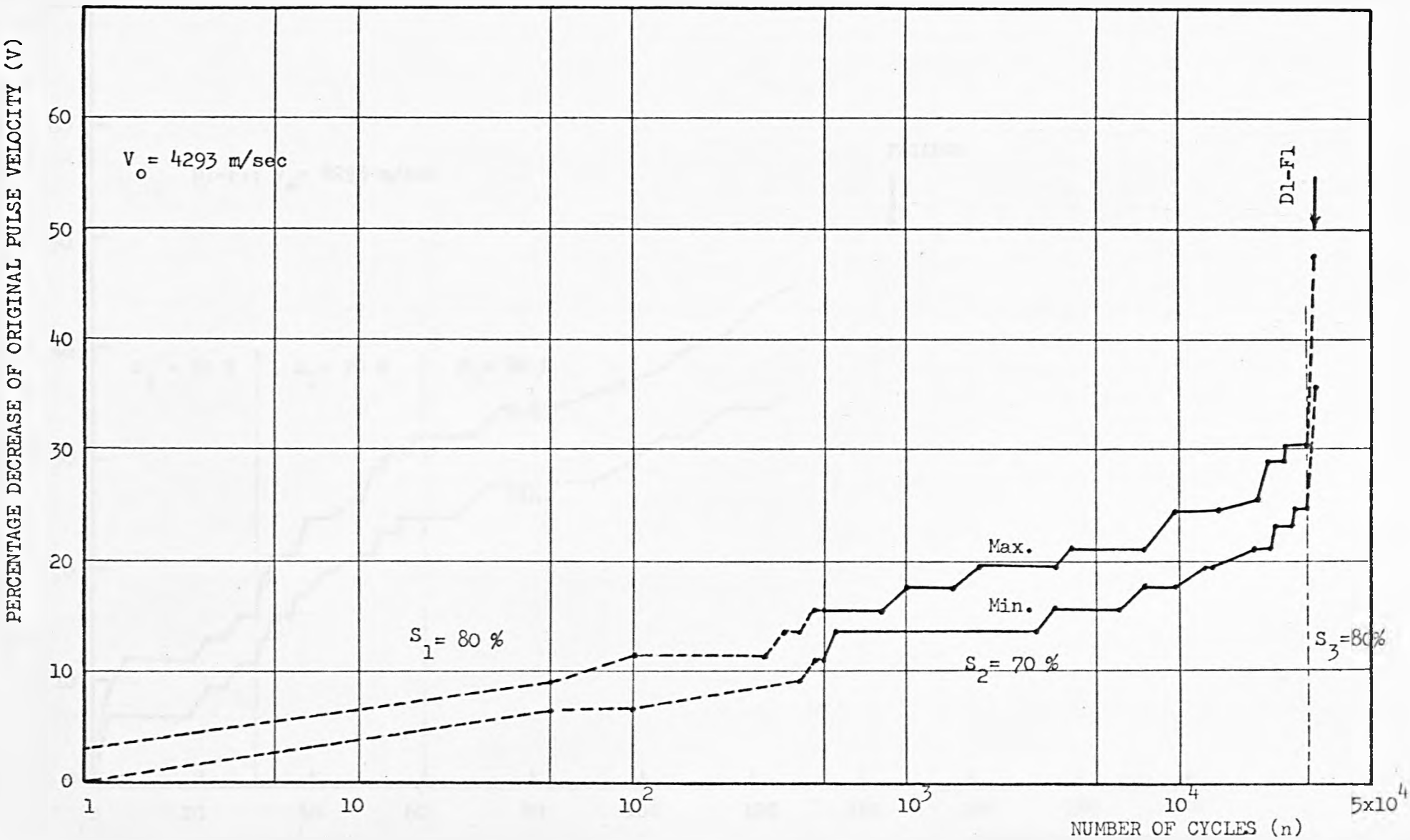

FIG. 10.2 VARIATION OF V WITH n OF A SPECIMEN SUBJECTED TO LOADONG PROGRAMME 3

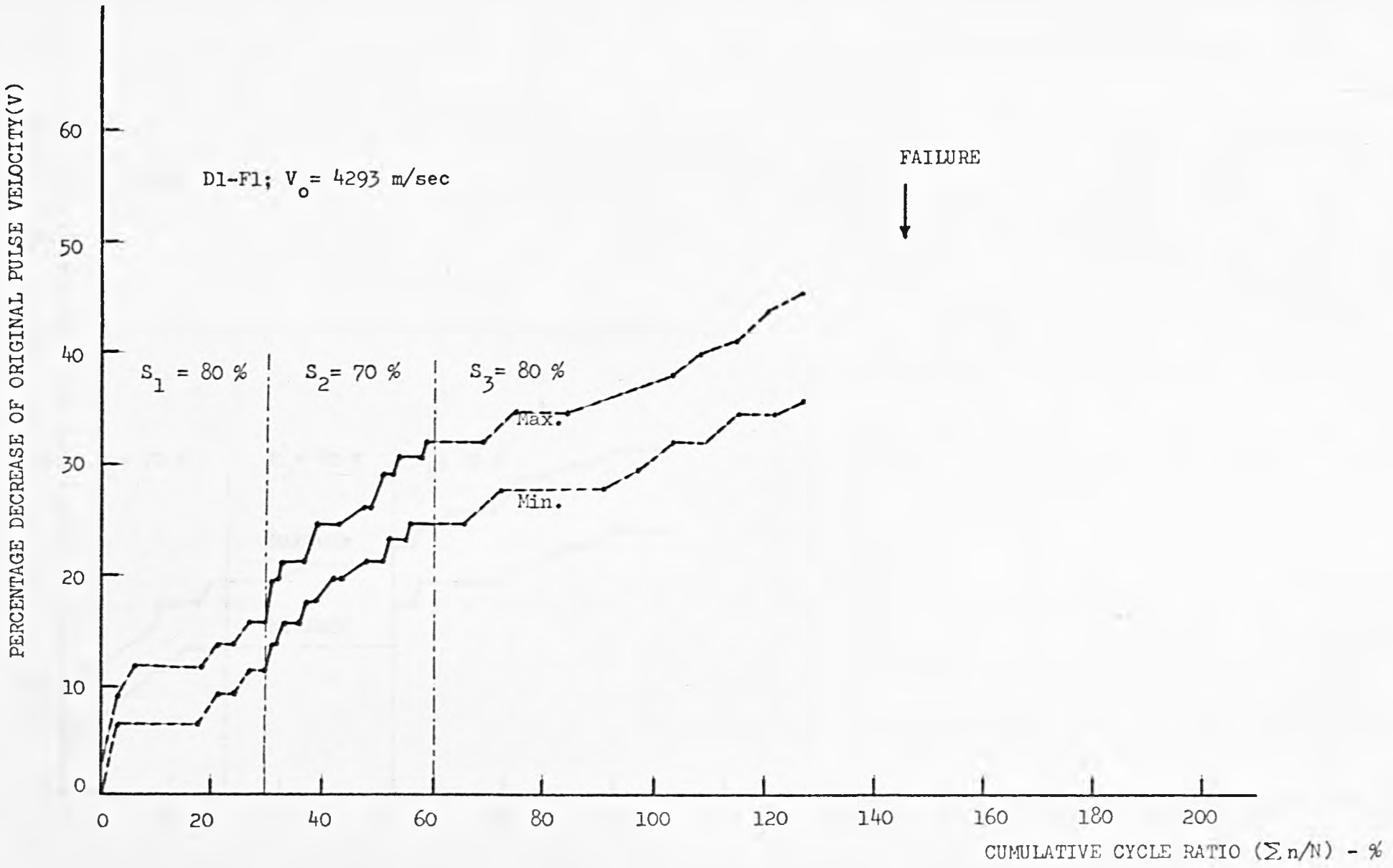

FIG. 10. 3 VARIATION OF V WITH $\sum n/N$ OF A SPECIMEN SUBJECTED TO LOADING PROGRAMME 3

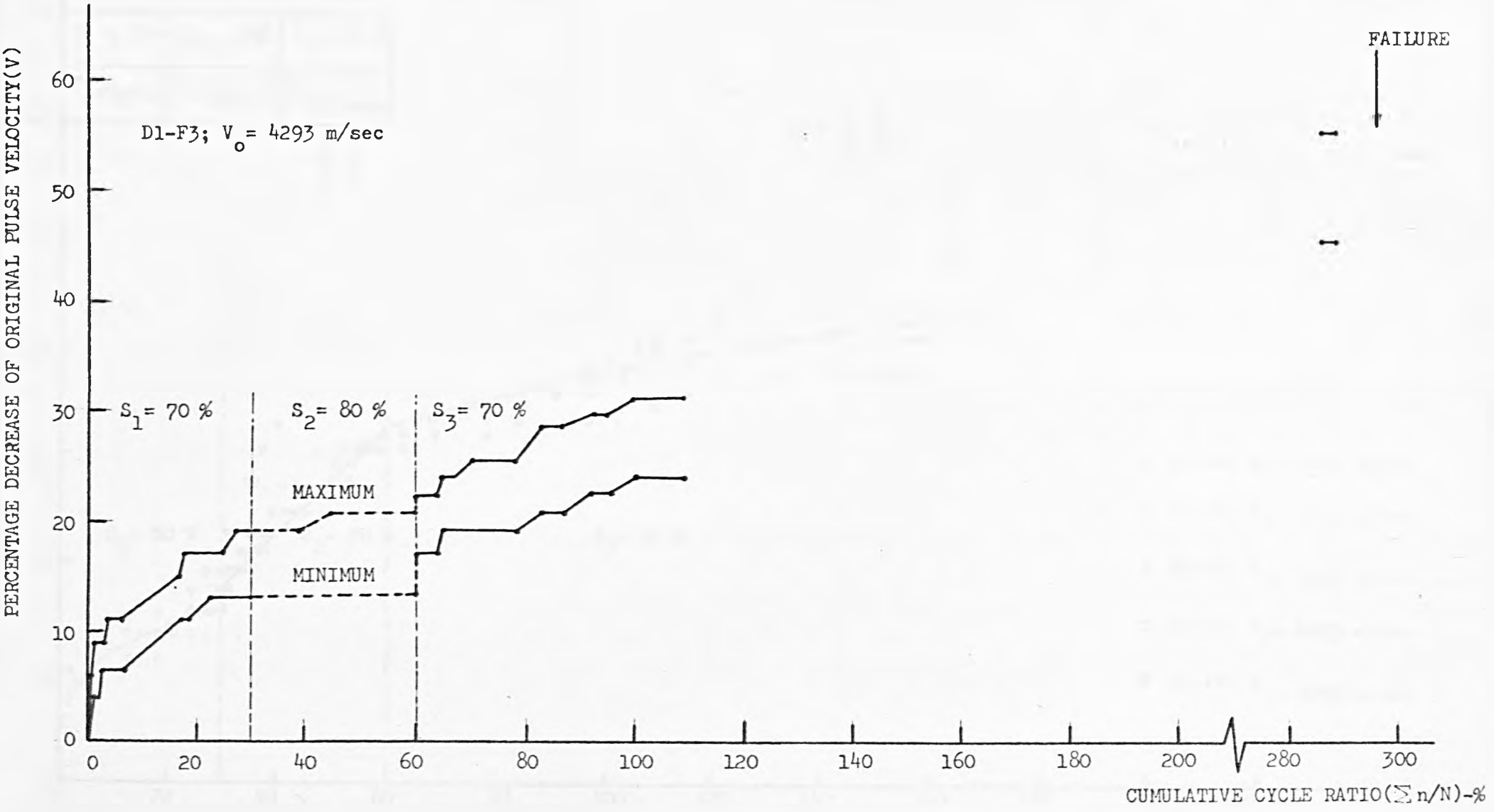

FIG. 10.4 VARIATION OF V WITH $\sum$ n/N OF A SPECIMEN SUBJECTED TO LOADING PROGRAMME 4

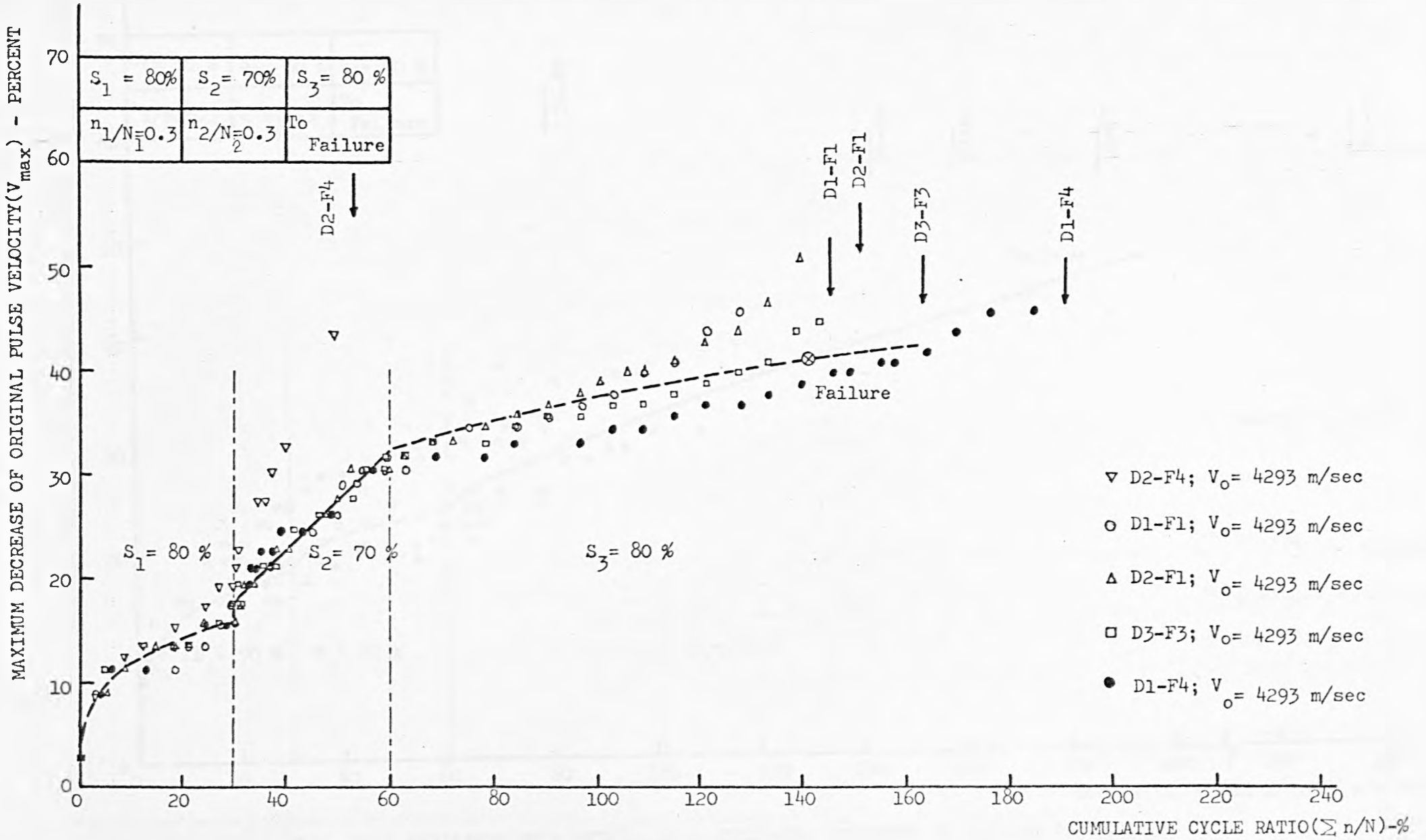

FIG. 10.5 VARIATION OF V_{max} WITH $\sum n/N$ OF SPECIMENS SUBJECTED TO LOADING PROGRAMME 3

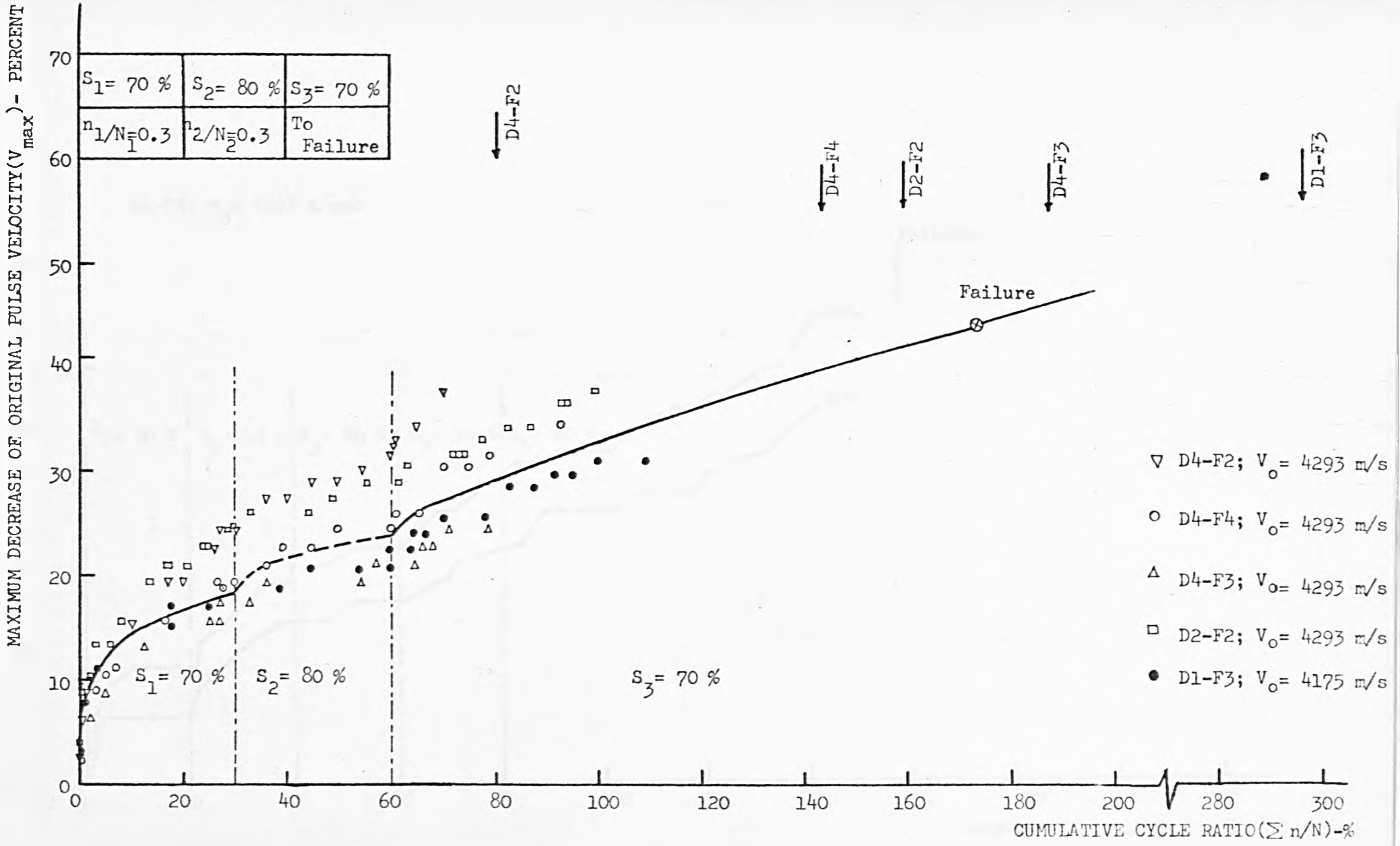

FIG. 10.6 VARIATION OF V WITH$\sum$ n/N OF SPECIMENS SUBJECTED TO LOADING PROGRAMME 4

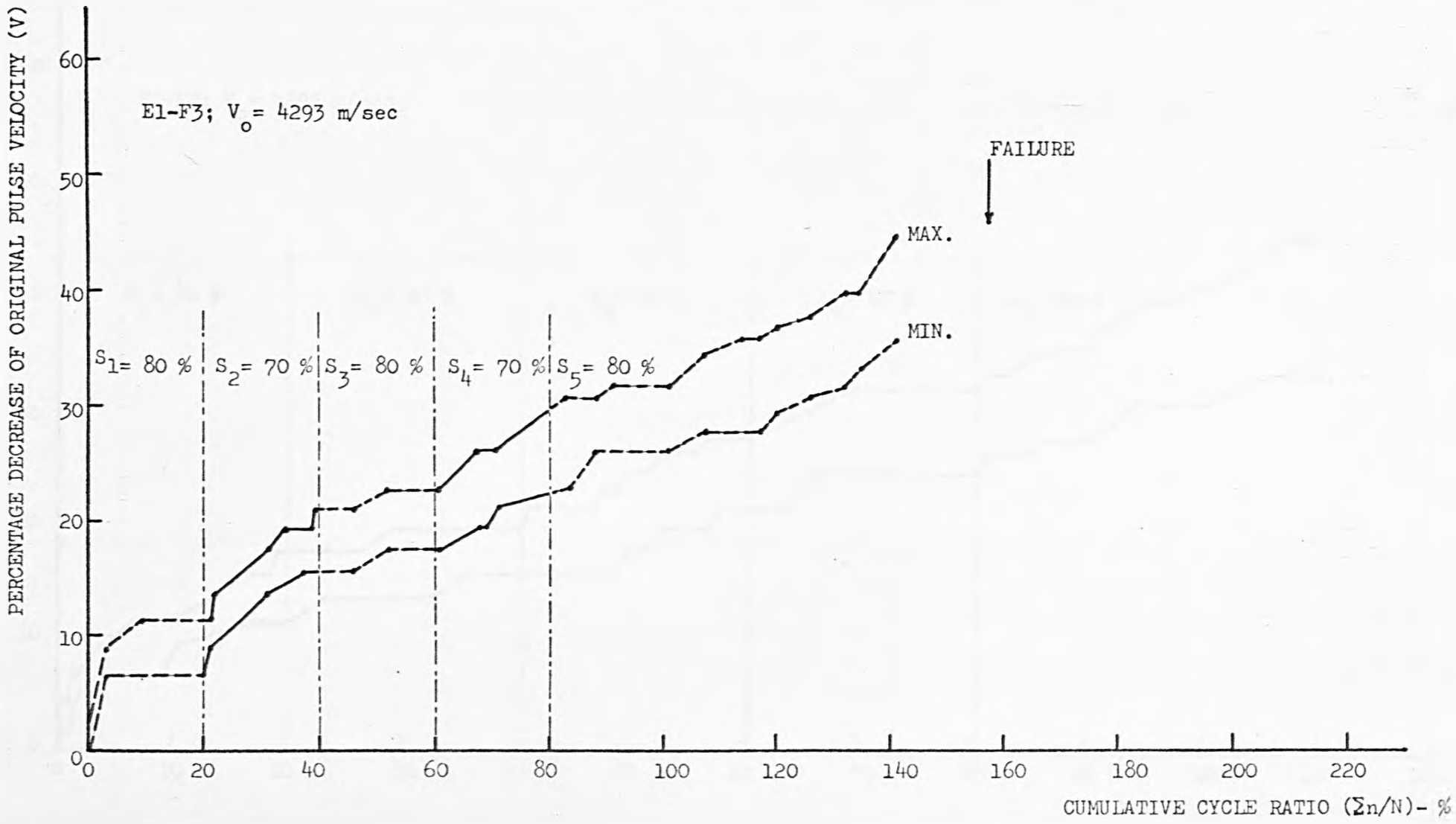

FIG. 10.7 VARIATION OF V WITH Σ n/N OF A SPECIMEN SUBJECTED TO LOADING PROGRAMME 5

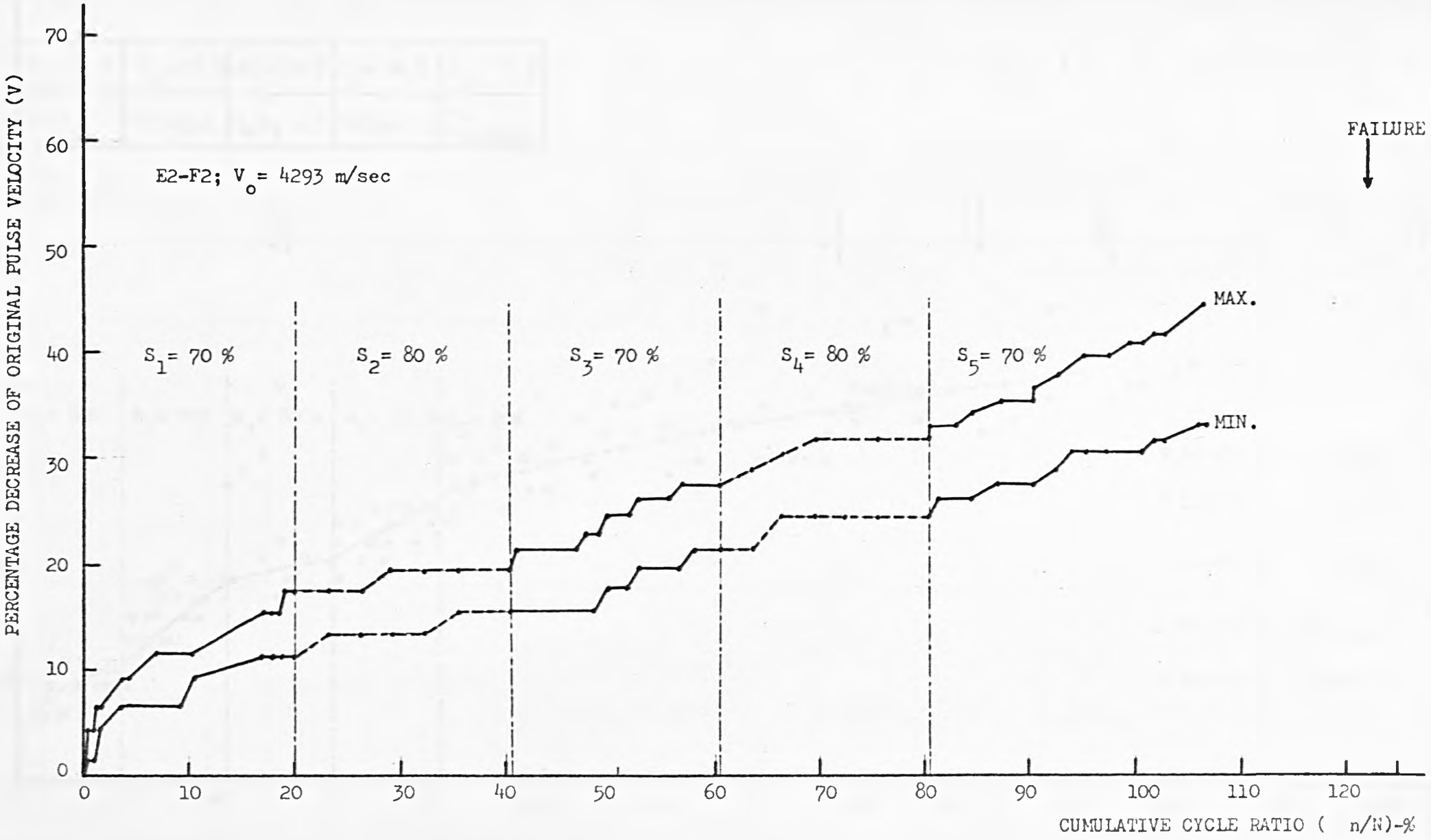

FIG. 10.8 VARIATION OF V WITH n/N OF A SPECIMEN SUBJECTED TO LOADING PROGRAMME 6

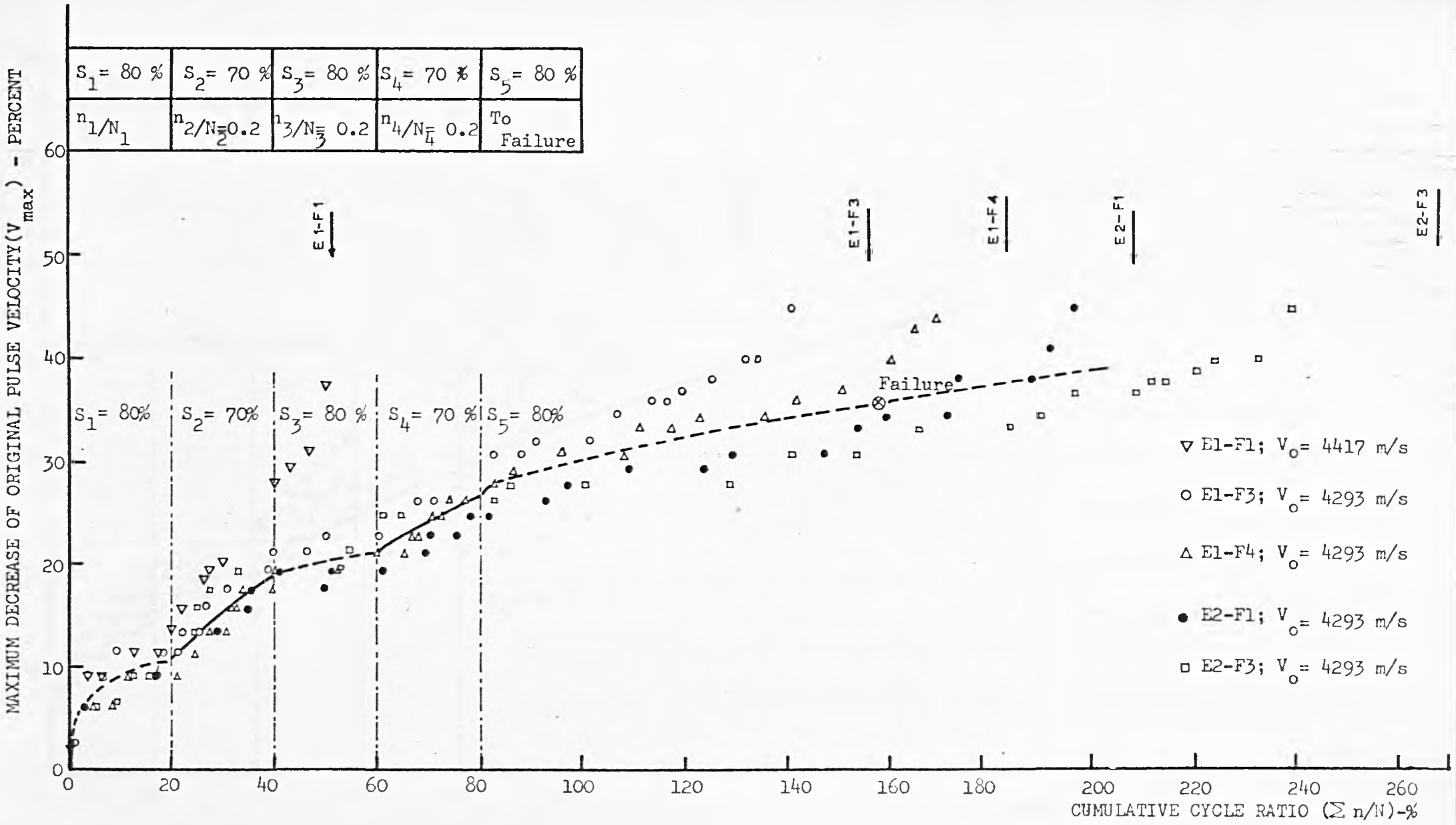

FIG.10.9 VARIATION OF V_{max} WITH Σn/N OF SPECIMENS SUBJECTED TO LOADING PROGRAMME 5

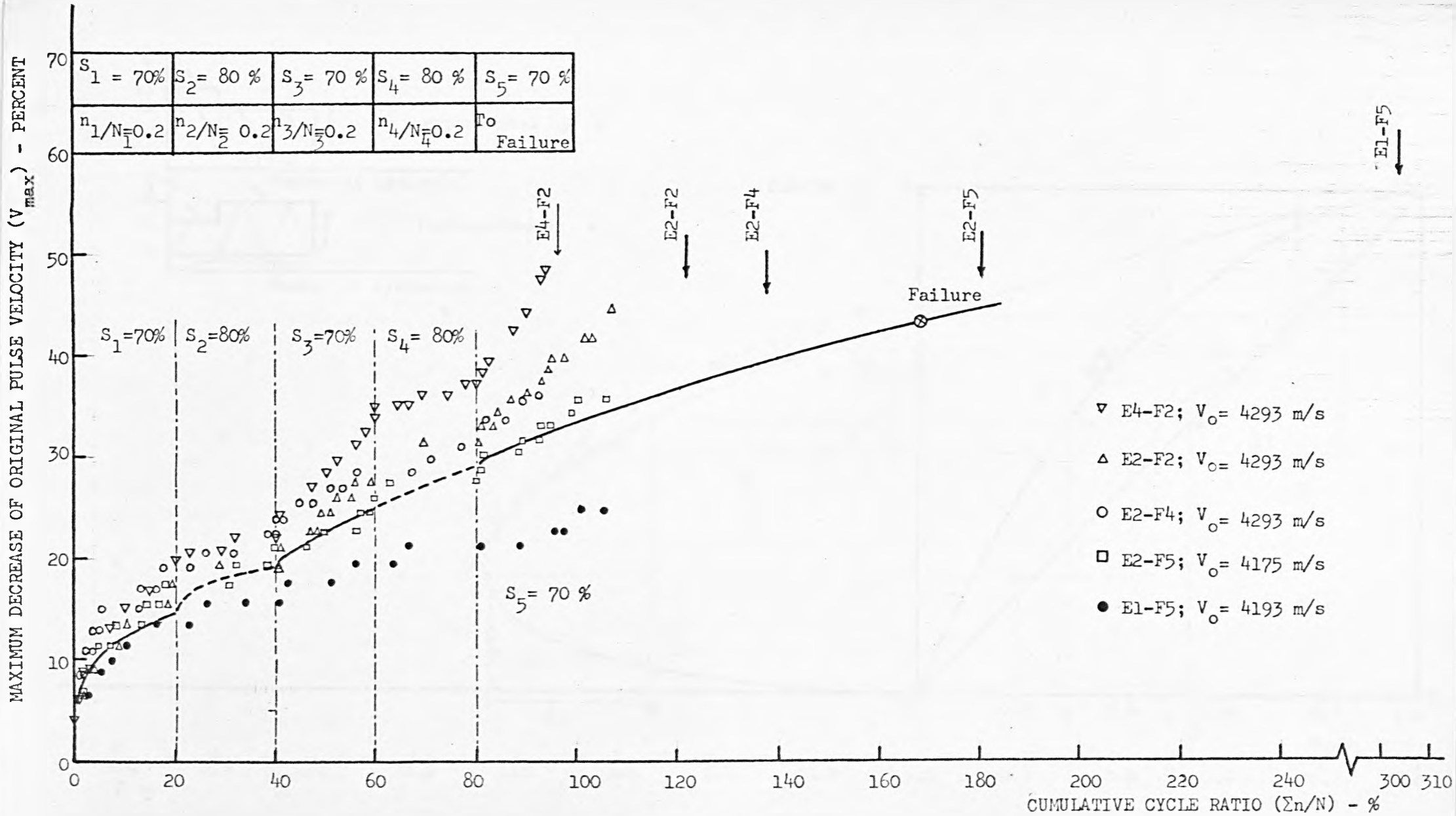

FIG. 10.10 VARIATION OF V_{max} WITH $\Sigma n/N$ OF SPECIMENS SUBJECTED TO LOADING PROGRAMME 6

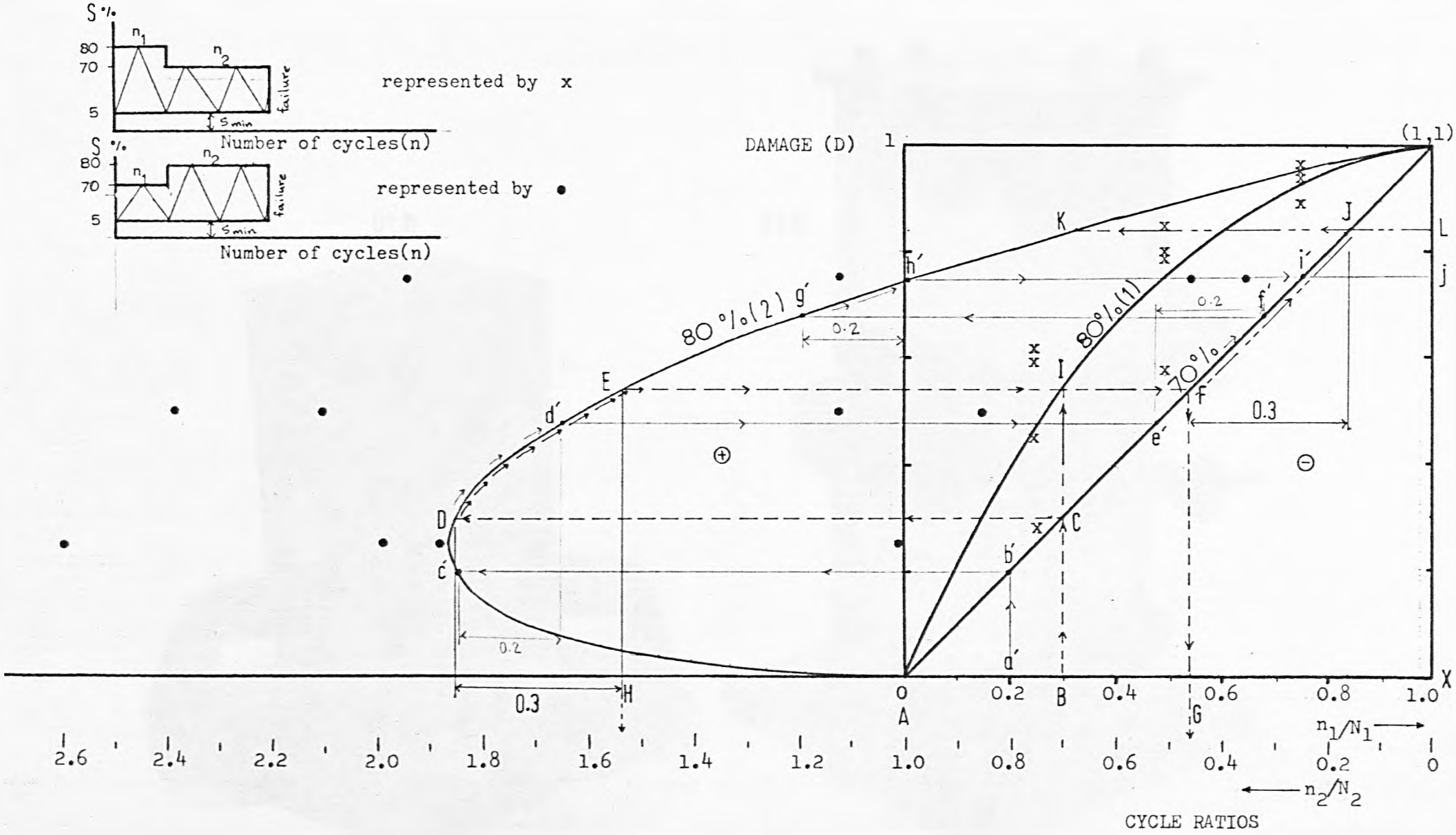

FIG. 11.1 CONCEPTUAL DAMAGE - CYCLE RATIO RELATIONSHIPS (FROM ONE STEP TESTS)

OLD

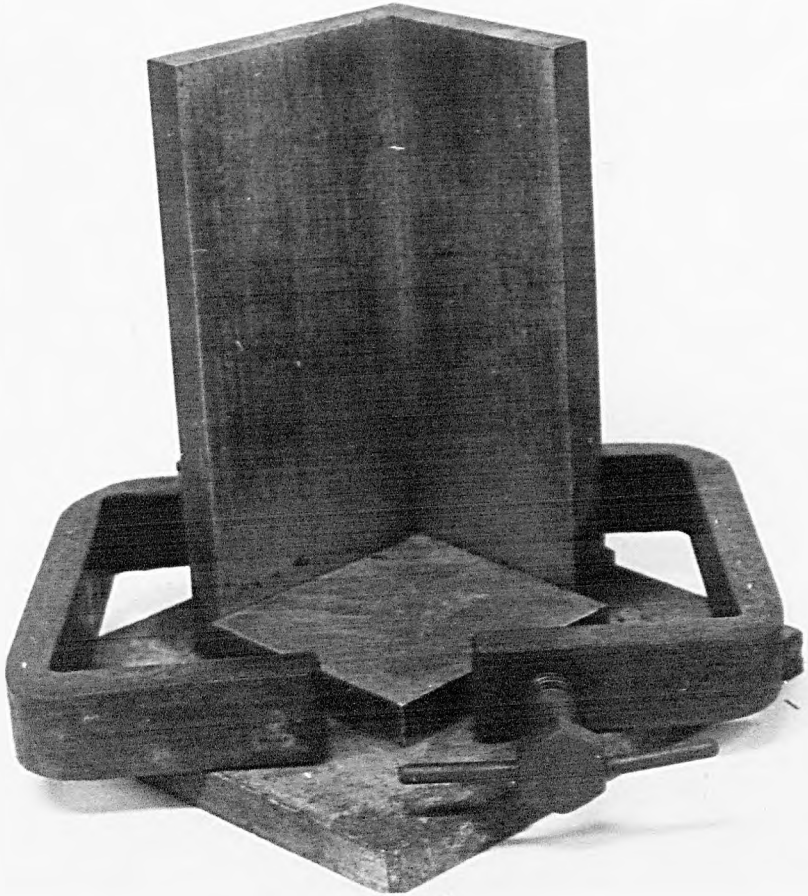

1(a)

NEW

1(b)

PLATE 1 JIG AND CAPPING ARRANGEMENTS.

A. "PUNDIT" instrument

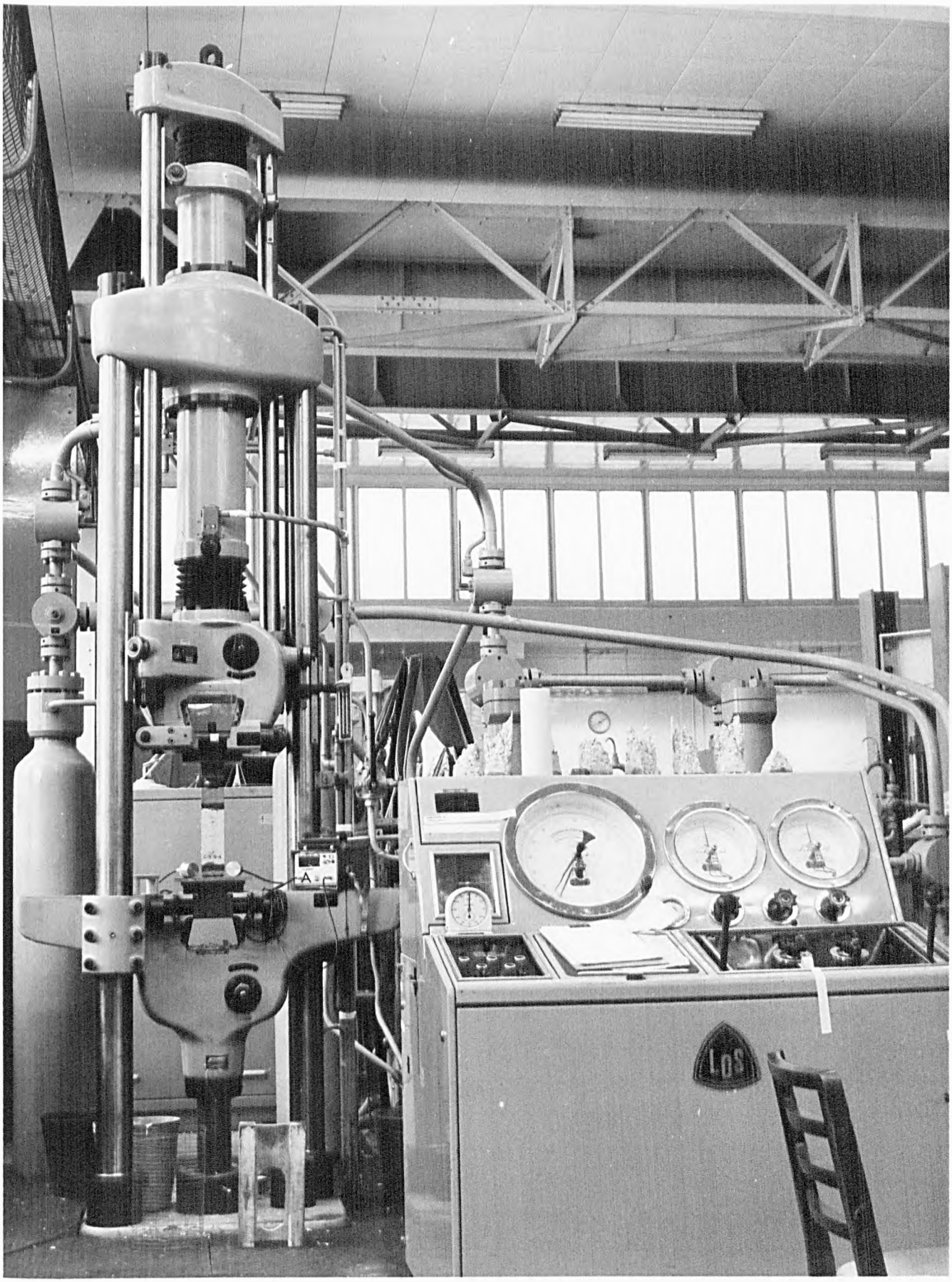

PLATE 2. LOS. FATIGUE TESTING MACHINE.

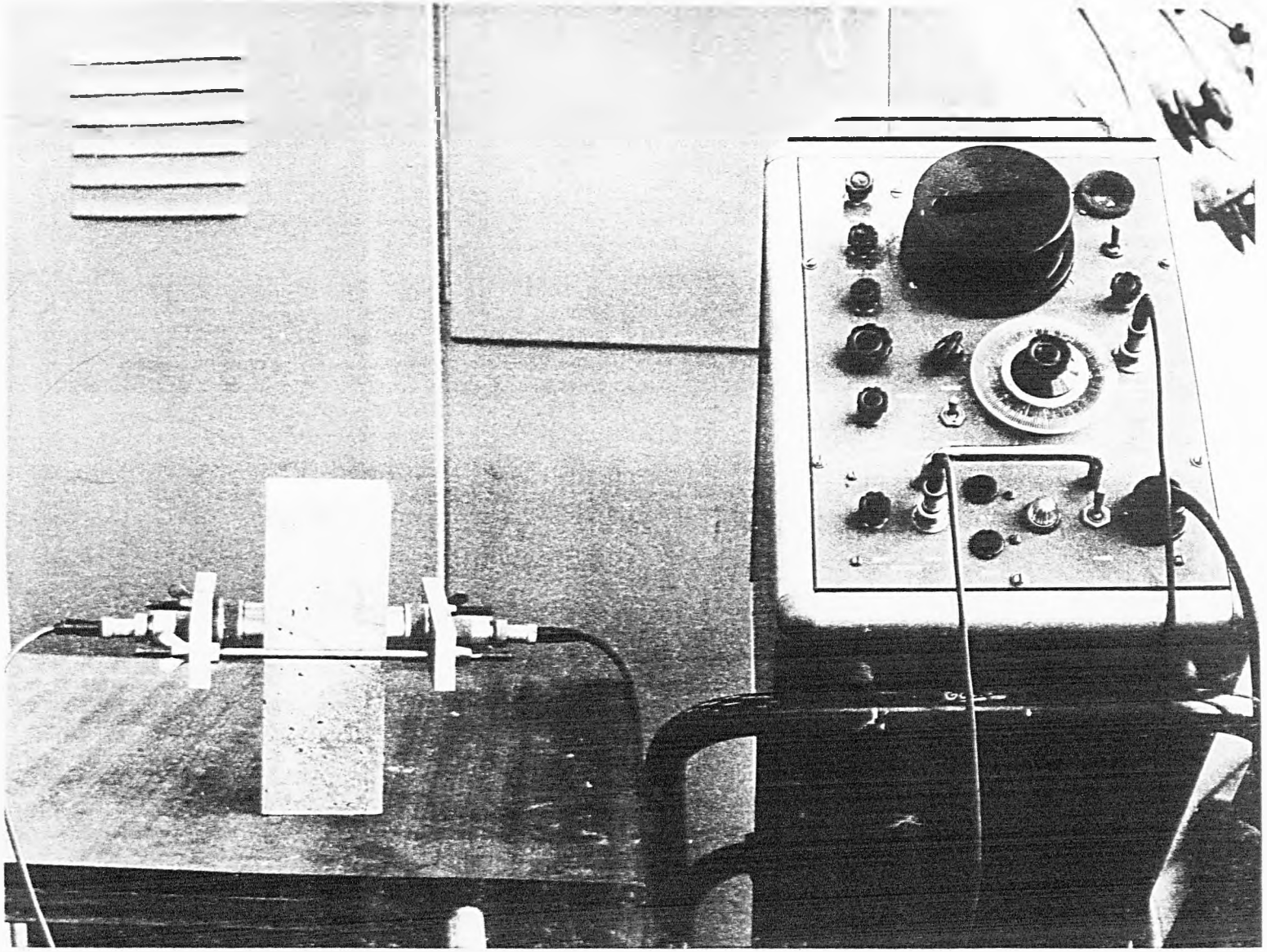

Plate 3 Cawkell Ultrasonic Material Tester

PLATE 4. FATIGUE FRACTURE MODE IN HIGHLY STRESSED SPECIMENS.

PLATE 5. FATIGUE FRACTURE MODE IN LOW STRESSED SPECIMENS.

PLATE 6. CRACKING PATTERNS IN STATIC SPECIMEN.

PLATE 7. FAILURE MODE IN FATIGUE SPECIMEN.

PLATE 8. FAILURE MODE IN FATIGUE SPECIMEN.